

2011

Stratigraphy and Palaeoenvironment of the Paleocene/Eocene boundary interval in the Indus Basin, Pakistan

Hanif, Muhammad

<http://hdl.handle.net/10026.1/865>

<http://dx.doi.org/10.24382/1607>

University of Plymouth

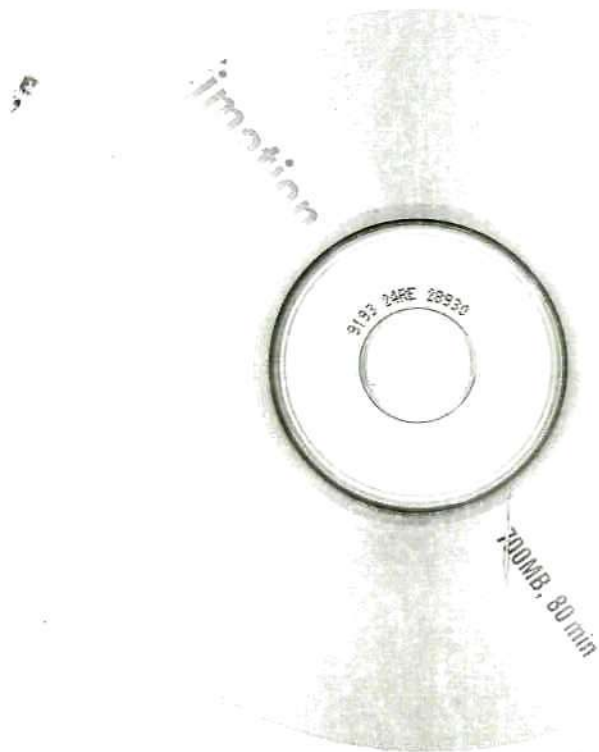
All content in PEARL is protected by copyright law. Author manuscripts are made available in accordance with publisher policies. Please cite only the published version using the details provided on the item record or document. In the absence of an open licence (e.g. Creative Commons), permissions for further reuse of content should be sought from the publisher or author.

**Stratigraphy and Palaeoenvironment
of the Paleocene/Eocene boundary
interval in the Indus Basin, Pakistan**

Muhammad Hanif

PhD

2011



Muhammad Hanif

**Stratigraphy and Palaeoenvironment of the Paleocene/Eocene boundary
interval in the Indus Basin, Pakistan**

by

Muhammad Hanif

A thesis submitted to the University of Plymouth
in partial fulfilment for the degree of

DOCTOR OF PHILOSOPHY

School of Geography, Earth and Environmental Sciences
Faculty of Science & Technology

02 August, 2011

This copy of the thesis has been supplied on condition that anyone who consults it is understood to recognise that its copyright rests with its author and that no quotation from the thesis and no information derived from it may be published without the author's prior consent.

Abstract

Muhammad Hanif

Stratigraphy and Paleoenvironment of the Paleocene/Eocene boundary interval in the Indus Basin, Pakistan

Marine sedimentary sections across the Paleocene/Eocene (P/E) boundary interval are preserved in the Patala Formation (Upper Indus Basin) and Dungan Formation (Lower Indus Basin), Pakistan. The P/E interval of the Patala Formation is composed of limestone and shale inter-beds indicating deposition on a carbonate platform. The analysis of larger foraminifera across the P/E interval from the Patala Formation (Kala Chitta Ranges), allows the recognition of the Larger Foraminiferal Turnover (LFT). The Larger Foraminiferal Turnover (LFT) observed in the Patala Formation is associated with the PETM (Paleocene Eocene Thermal Maximum) global climatic event and allows the recognition of the P/E boundary in shallow water carbonates of the Indus Basin. This turnover is already reported from other Tethyan sections and from the Salt Range (Upper Indus Basin), Pakistan. The recognition of the LFT allows the inter-basinal and intra-basinal correlation of the P/E interval of the shallow carbonates of the Indus Basin, Pakistan. The available literature on the Paleocene-Eocene Patala and Dungan formations is used to review the planktonic foraminiferal biostratigraphy of the P/E interval. The planktonic foraminiferal zones in the P/E interval of the Indus Basin are identified and reviewed in the light of new international zonations. The planktonic foraminiferal content of the Dungan Formation allows its correlation with the Laki Formation of Rajasthan (India).

Four dinoflagellate zones in the P/E interval of the Rakhi Nala section (Lower Indus Basin) are identified and correlated with international and regional zonations. The quantitative analysis of the dinoflagellate cyst assemblages together with geochemical data (i.e., carbon isotopes (organic only), C/N ratio, TOC, carbonate content) is used to reconstruct the palaeoenvironment across the P/E interval. The dinocyst assemblages in general, and the abundance of *Apectodinium* spp. in particular, indicate the warmer surface water conditions of the global PETM event. The dinocyst assemblages allow the local correlation of the Dungan Formation (part) of the Sulaiman Range with the Patala Formation (part) of the Upper Indus Basin and global correlation of the Zone Pak-DV with the *Apectodinium* acme Zone of the Northern and Southern hemispheres.

The carbon isotopic excursion (CIE) associated with PETM is now globally used to identify the P/E boundary. The CIE in total organic carbon (i.e., $\delta^{13}\text{C}_{\text{TOC}} = -28.9\text{‰}$) and total fine fraction organics (i.e., $\delta^{13}\text{C}_{\text{FF}} = 26.4\text{‰}$) from the Indus Basin is reported for the first time. This CIE record from the Indus Basin is compared with other Tethyan sections from Egypt and Uzbekistan and is also compared with the global sections from USA (Northern hemisphere) and from New Zealand (Southern hemisphere).

Contents

Abstract	i
Contents	ii
List of Figures and Tables	vii
List of Plates	xviii
Acknowledgements	xxiv
Author's Declaration	xxv
Chapter 1 Introduction	1
1.1 Introduction	1
1.2 This study	4
1.2.1 Foraminifera	10
1.2.2 Dinoflagellates	13
1.2.3 Organic Geochemistry	15
1.2.4 Carbonate content	19
1.3 Aims of Research	20
1.3.1 Objectives	20
1.3.2 Study Locations	21
Chapter 2 Methodology	23
2.1 Preparation of dinocyst slides	25
2.2 Foraminiferal analysis	27
2.2.1 Preparation	28
2.3 Stable Isotopic Analysis	33
2.3.1 Preparation	33
2.3.2 Instrumentation	35

2.4	Total organic carbon	37
Chapter 3	Introduction to the lithostratigraphy and the “field geology”	40
3.1	Introduction	40
3.2	Lithostratigraphy	42
3.2.1	Salt Range, Punjab (Upper Indus Basin)	42
3.2.2	Sulaiman depositional province, Punjab (Lower Indus Basin)	49
Chapter 4	Late Paleocene-early Eocene foraminiferal biostratigraphy: A review	61
4.1	Introduction	61
4.2	Planktonic foraminiferal biostratigraphy	63
4.2.1	Zone P3	63
4.2.2	Zone P4	64
4.2.3	Zone P5, E1 and E2	65
4.2.4	Zone E3	66
4.2.5	Zone E4	66
4.2.6	Zone E5	69
4.3	The P/E boundary interval and its intra-basinal correlation (Lower Indus Basin)	69
4.4	Larger foraminiferal biostratigraphy	72
4.4.1.	Shallow Benthonic Zone 4 (SBZ4)	77
4.4.2.	Shallow Benthonic Zones 5/6 (SBZ5/6)	78
4.5	Faunal turnovers in the Indus Basin and global	81

	correlation.	
4.6	Depositional environment across the P/E interval	82
4.6.1	<i>Miscellanea</i> micro-bioclastic wacke-packstone	83
4.6.2	<i>Nummulites</i> peloidal wacke-packstone	83
4.6.3	Interpretation	84
Chapter 5	Stratigraphy and palaeoenvironmental assessment of the Paleocene/Eocene boundary interval (Dungan Formation), Indus Basin Pakistan.	136
5.1	Introduction	136
5.2	Materials and Methods	137
5.3	Dinocyst Zonation	140
5.3.1	The Pak-DIV Zone	140
5.3.2	The Pak-DV Zone	141
5.3.3	The Pak-DVI Zone	141
5.3.4	The Pak-DVII Zone	142
5.4	Local correlation	142
5.5	Global correlation	142
5.6	Dinocyst assemblages and palaeoenvironment	144
5.6.1	Interval Td30 - Td33	144
5.6.2	Interval Td33 - Td37	147
5.6.3	Interval Td37 - Td43	150
5.6.4	Interval Td43-Td50	152
5.7	Interpretation of the peridinioid dinocyst complexes	153

5.8	Discussion	154
5.8.1	Palaeoproductivity	154
5.8.2	Palaeotemperature	157
5.8.3	Palaeosalinity	159
5.8.4	Other palaeoenvironmental inferences	160
5.9	Conclusions	165
Chapter 6	Paleocene-Eocene carbon isotope excursion in organic carbon from Indus Basin, Pakistan	178
6.1	Introduction	178
6.2	Material and Methods	182
6.3	Results	183
6.3.1	Biostratigraphy	183
6.3.2	Stable isotopes	184
6.3.3	<i>Apectodinium</i>	193
6.3.4	Carbonate content	193
6.4	Discussion	193
6.4.1	Comparison with previous studies	191
6.4.2	Environmental precursors to carbon isotopic excursion	194
6.4.3	$\delta^{13}\text{C}$ gradient and palaeoceanographic inferences	198
6.5	Conclusion	201
Chapter 7	Synthesis	202
7.1	Introduction	202

7.2	Chemo- and biostratigraphical calibration of the P/E boundary	202
7.2.1	Stable isotope stratigraphy	205
7.2.2	Calcareous nannofossils	205
7.2.3	Dinoflagellates	206
7.2.4	Planktonic foraminifera	208
7.2.5	Smaller benthonic foraminifera	209
7.2.6	Larger benthonic foraminifera	210
7.3	Integrated stratigraphy	212
7.4	Palaeoenvironment of the P/E boundary interval	214
7.5	Conclusions	218
	References	222
Appendix 1	Taxonomic notes on foraminifera and table of foraminiferal composition (in percent)	294
Appendix 2	List of dinocyst species, taxonomic notes on dinocyst and geochemical data.	306
Appendix 3	Stable isotope data of the carbonate fraction (bulk and fine fraction) from the Rakhi Nala section, Indus Basin (Pakistan).	314
Appendix 4	Samples collected from Indus Basin, Pakistan.	321

List of Figures and Tables

Chapter 1

- Figure 1.1 Paleogene time scale produced through a software called PAST (available at <http://folk.uio.no/ohammer/past/>). (1) Berggren et al. (1995), (2) Berggren & Pearson (2005). Asterisk (*) indicates continuation of NP8. 5
- Figure 1.2 Showing $\delta^{18}\text{O}$ and $\delta^{13}\text{C}$ curves and associated climatic, tectonic and biotic events for the past 70 Ma (after Zachos et al., 2001). 6
- Figure 1.3 High resolution biostratigraphy of the *Morozovella velascoensis* Zone and its subzones in the light of previous literature, bases of blue arrows indicate lowest (arrows pointing upward) and highest (arrows pointing downward) occurrences. 7
- Figure 1.4 Geological map of Pakistan showing field locations and main geological features; A- Chak Dalla and Kali Dilli sections (Kala Chitta Range), B- Rakhi Nala section (Sulaiman Range), MKT- Main Karakoram Thrust, MMT- Main Mantle Thrust and MBT- Main Boundary Thrust, SRT- Salt Range Thrust. 22

Chapter 2

Table 2.1	Comparision between the Stouge & Boyce (1983) disaggregation technique and the technique of Lirer (2000, text-figure 1).	34
Table 2.2	Times of dipping in acetic acid and of the Ultrasonic cleaner treatment for different studied lithologies (Lirer, 2000, text-figure 2).	34
Table 2.3	The amount of sample analysed for stable isotopes (fine fraction carbonate) and the carbonate weight percent.	39

Chapter 3

Figure 3.1	Geological map of Pakistan showing main geological features; MKT- Main Karakoram Thrust, MMT- Main Mantle Thrust, MBT- Main Boundary Thrust, SRT- Salt Range Thrust. N. B. Colours of the different units are simply to identify the regions discussed in the text. Green coloured area indicates Karakoram Block.	43
Figure 3.2	Generalized Cenozoic stratigraphy of the Upper Indus Basin; yellow coloured areas with vertical bars indicate hiatus (after Shah, 1977); Fm = Formation, LSt = Limestone.	50
Figure 3.3	Generalized Paleocene-Eocene stratigraphy of the Salt Range (Upper Indus Basin),	51

Fm = Formation, Lst = Limestone.

- Figure 3.4 Generalized stratigraphic succession in the eastern Sulaiman Fold Belt, the lithological log is diagrammatic (after Hemphil & Kidwai, 1973). 57
- Figure 3.5 Cenozoic lithostratigraphic correlation of previous workers, yellow colour indicates late Paleocene-early Eocene formations (modified after Warraich, 2000). 58

Chapter 4

- Figure 4.1 Planktonic foraminiferal and nannofossil zones for the late Paleocene - early Eocene of the Indus Basin. Biostratigraphical data are compiled from various sections of the Indus Basin; e.g., Samanta (1973), Dorreen (1974), Kothe et al. (1988) Afzal (1997), Warraich & Natori (1997), Warraich et al. (2000). Planktonic foraminiferal zones of the Indus Basin correspond to the zones of Berggren & Pearson (2005). P-Zones = Planktonic foraminiferal zones of Berggren & Pearson (2005). NP-Zones = Calcareous nannoplankton zones of Martini (1971), Chronostratigraphy of Berggren et al. (1995) with modifications of Berggren & Pearson (2005). 67
- Figure 4.2 Measured columnar section along the Rakhi Nala showing lithology, sample locations 68

and biostratigraphical distribution of the recorded planktonic foraminifera. The yellow coloured area indicates an interval with no foraminifera, and vertical green bars indicate lowest and highest occurrences of the important planktonic foraminiferal species reported by Warraich et al. (2000). The area under the red rectangle shows the Paleocene/Eocene interval planktonic foraminiferal zones. Red horizontal arrow shows the position of P5/E1 boundary based on BFEE of Warraich et al. (2000).

- Figure 4.3** Map showing locations of the Tanot-1 Well, 75
 Jaisalmer Basin, Rajasthan (India) and the Rakhi Nala section, Sulaiman Range, Lower Indus Basin, Pakistan (modified after Kalia & Kinisto, 2006)
- Figure 4.4** Summary of the faunal events (LFT- Larger 76
 Foraminiferal Turnover; BFEE - Benthonic Foraminiferal Extinction Event; PFET- Planktonic Foraminiferal Excursion Taxa) and lithostratigraphic correlation of the P/E boundary interval, Indus Basin.
- Figure 4.5** Palaeogeographical map showing the 79
 locations of the PFET (Planktonic Foraminiferal Excursion Taxa) worldwide (red circles) and Indus Basin (red square) after Hay et al. (1999).

(ODSN plate tectonic reconstruction service
<http://WWW.odsn.de/odsn/services/paleomap/paleomap.html>).

Figure 4.6 Correlation of the Paleocene/Eocene interval 80
shallow benthonic foraminiferal zones of the Upper
Indus Basin with other Tethyan zones. A = Top of the
Zone SRX1 and base of the Zone SRX2 represented by
the lowest occurrences (LO's) of *Nummulites deserti*,
N. thalicus, *Assilina spinosa*, *A. dandotica* and *A.*
prisca (Afzal, 1997), B = Zonal boundary of the
SRX2/SRX3 zones represented by the simultaneous
highest occurrences (HO's) of *Miscellanea miscella*, *M.*
stampi and *Lockhartia haimei* (Afzal, 1997), C= The
overlapping top boundary of the SRX2 and SRX3 of
Afzal (1997) and SBZ5/6 of Scheibner & Speijer (2009)
represented by the highest occurrence (HO) of the
Alveolina cucumiformis (Afzal, 1997; Scheibner &
Speijer, 2009), F = The total range of the *Alveolina*
cucumiformis (Hottinger, 1960; Scheibner & Speijer,
2009), D = The highest occurrence (HO) of
Glomalveolina primaeva, SBZ3 (Hottinger, 1960; Serra-
Kiel et al., 1998; Scheibner & Speijer, 2009), E =
Glomalveolina levis total range (Hottinger, 1960) as
well as *Hottingerina lukasi* total range, an index
species of SBZ4 (Drobne, 1975; Serra-Kiel et al., 1998;
Scheibner & Speijer, 2009), red line = LFT.

- Figure 4.7A** Columnar section of the Patala Shale Formation, 86
Kali Dilli Section, Kala Chitta Range (Upper Indus
Basin) showing sample location, lithological
description and microfacies distribution.
- Figure 4.7B** Larger foraminiferal distribution in the 87
SBZ4 Zone, Patala Shale Formation, Kali Dilli Section,
Kala Chitta Range (Upper Indus Basin).
- Figure 4.8A** Columnar section of the Margala Hill Limestone 88
Formation, Chak Dalla Section, Kala Chitta Range
(Upper Indus Basin) showing sample location,
lithological description and microfacies distribution.
- Figure 4.8B** Larger foraminiferal distribution in the 89
SBZ5 Zone, Margala Hill Limestone Formation, Chak
Dalla Section, Kala Chitta Range (Upper Indus Basin).

Chapter 5

- Figure 5.1** Map showing (a) location of the Rakhi Nala 138
section (i.e., red circle) Sulaiman Range, Indus
Basin, and (b) detailed map of the Rakhi Nala
section. The sky blue coloured line in map
(a) shows the coastline.
- Figure 5.2** Palaeolatitudinal map of the studied 139
area showing the location of the Indus Basin
during late Paleocene - early Eocene (ODSN plate
tectonic reconstruction service

<http://www.odsn.de/odsn/services/>

[paleomap/paleomap.html](http://www.odsn.de/odsn/services/paleomap/paleomap.html)).

- Figure 5.3** Dinoflagellate zones intra-basinal correlation 145
of the Indus Basin. Nanno= Nannoplankton, Dino =
Dinocyst, LO = lowest occurrence. The red line
indicates Paleocene Eocene boundary, CIE = Carbon
Isotopic Excursion.
- Figure 5.4** Global correlation of the dinoflagellate zone 146
Pak-DV from Indus Basin, Pakistan. Nanno=
Nannoplankton. Orange coloured area indicates global
correlation of the Zone Pak-DV with D5a and with the
bases of *Apectodinium homomorphum*, *A. augustum*
and P6b zones.
- Figure 5.5A** Dinoflagellate cyst composition (in percent) 148
and $\delta^{13}\text{C}_{\text{FF}}$ results from Rakhi Nala Section,
Sulaiman Range, Lower Indus Basin, Pakistan.
The red line indicates Paleocene/Eocene boundary,
FF = Fine fraction organic.
- Figure 5.5B** Dinocyst zones, lithological log, 149
 $\delta^{13}\text{C}_{\text{FF}}$ curve and sea level curve (= Onshore
(*Homotryblium*+*Polysphaeridium*)/Offshore
(*Spiniferites* association). Sea level curve for Rakhi
Nala represents dominantly offshore conditions with
minor sea level fluctuations, only sample Td43 shows
either a sea level drop (regression) or an increased

transportation of the coastal element to an open marine depositional environment.

- Figure 5.6** Planktonic foraminiferal composition 166
(in percent) from the Rakhi Nala section, Sulaiman Range, Lower Indus Basin (Pakistan). Yellow coloured area marks an interval barren of foraminifera. Red line indicates the Paleocene/Eocene boundary.
- Figure 5.7** Palaeobathymetric ranges of species 167
modified by Speijer (1994) after Van Morkhoven et al. (1986).
- Figure 5.8** Ranges of key benthonic foraminifera 168
(after Warraich, 2000).
- Figure 5.9** The distribution of benthonic foraminifera 169
recorded in the Paleocene - Eocene interval, Dungan Formation, Rakhi Nala section, Lower Indus Basin (Pakistan). The yellow coloured area indicates interval barren of foraminifera. Red line indicates the Paleocene/Eocene boundary.

Chapter 6

- Figure 6.1** The columnar section of the uppermost 185
140m of the Dungan Formation from the Rakhi Nala section, Sulaiman Range, Indus Basin (Pakistan).

- Figure 6.2A Lithological, stable isotope and *Apectodinium* data from the Rakhi Nala section and its comparison with other global sections. The area between red dotted lines show the onset of CIE in the Rakhi Nala, section, Sulaiman Range, Indus Basin (Pakistan). Curves have been correlated based on the isotope data. 186
- Figure 6.2B Lithological and stable isotopic data from the Rakhi Nala section and its comparison with other Tethyan sections. Area between dotted red lines indicates the onset of CIE in the Rakhi Nala, Indus Basin (Pakistan). Curves have been correlated based on the isotope data. 187
- Figure 6.3 Showing C/N data plotted against isotopic trends, TOC= Total organic carbon, FF= Fine fraction organic. 190
- Figure 6.4 Correlation of $\delta^{18}\text{O}$ (‰ VPDB) and $\delta^{13}\text{C}$ (‰ VPDB) values from the fine fraction carbonate (<63 μm) in the Rakhi Nala section, Pakistan. 191
- Table 6.1 Sample numbers, lithology, colour, TOC (%), Carbonate (%), *Apectodinium* (%), and stable isotopic results from the Rakhi Nala section; bold values show the Carbon Isotopic Excursion (CIE) . 192

Figure 6.5A $\delta^{13}\text{C}$ (‰ VPDB) versus total organic carbon (TOC % wt) for the Rakhi Nala section
Pre- CIE and CIE values have been separated. 195

Figure 6.5B $\delta^{13}\text{C}$ (‰ VPDB) versus total organic carbon (TOC % wt.) for the Rakhi Nala section, pre-CIE and CIE values are collated. 196

Chapter 7

Figure 7.1 Paleocene - Eocene correlation of deep and shallow waters biostratigraphical schemes in the Tethyan realm; LFT- Larger Foraminiferal Turnover, PETM - Paleocene Eocene Thermal Maximum, CIE - Carbon Isotopic Excursion, P Zone - Planktonic foraminiferal zones, NP Zone - Nannoplankton zones, B Zone - Bathyal benthonic foraminiferal zones, SB Zone - Shallow benthonic foraminiferal zones (After Scheibner & Speijer, 2009). 204

Figure 7.2 The different biostratigraphical schemes, lithology and carbon isotope data of the Dungan Formation, Rakhi Nala section, Sulaiman Range - Lower Indus Basin). B - zones = Bathyal benthonic zones of Berggren & Miller (1989), D - Zone = Dinoflagellate zones (This study) and P- Zones = Planktonic foraminifera zones of Berggren & Pearson 213

(2005). The area between the red dotted lines shows the onset of the CIE.

Figure 7.3 The Larger Foraminiferal Turnover (LFT) in the Chichali Pass section (i.e., replacement of Paleocene taxa such as *Ranikothalia* and *Lockhartia* by Eocene taxa such as *Nummulites*), SRX-4 is missing due to absence of larger foraminifera in interval between SRX-3 and SRX-5 (Modified after Afzal, 1997); B- Zones= Larger foraminiferal zones, AC Zone = *Alveolina cucumiformis* Zone. 215

Figure 7.4 Lithological log and biostratigraphical subdivision of the succession at Dungan Hill, together with the stratigraphical distribution of selected larger foraminiferal taxa (Modified after White, 1989); Ap (*Alveolina primaeva* Zone), Alc (*Alveolina levis-Alveolina cucumiformis* Zone), Ae (*Alveolina ellipsoidalis* Zone), Am (*Alveolina moussoulensis* Zone). LFT = Larger Foraminiferal Turnover. 216

List of Plates

Chapter 3

- Plate 3.1 Field photographs of the Pab Sandstone and Dungan Formation, Rakhi Nala section. 59
- Plate 3.2 Field photographs of the Dungan and Shaheed Ghat formations, Rakhi Nala section. 60

Chapter 4

- Plate 4.1 Photomicrographs of the Dungan Formation, Rakhi Nala section. 92
- Plate 4.1 (continued) Photomicrographs of the Dungan Formation, Rakhi Nala section. 93
- Plate 4.2 Planktonic foraminifera from the P/E boundary interval Dungan Formation, Rakhi Nala, Sulaiman Range, Lower Indus Basin. 95
- Plate 4.3 Planktonic foraminifera from P/E boundary interval Dungan Formation, Rakhi Nala, Sulaiman Range, Lower Indus Basin. 97
- Plate 4.4 Planktonic foraminifera from P/E boundary interval Dungan Formation, Rakhi Nala, Sulaiman Range, Lower Indus Basin. 99
- Plate 4.5 Larger foraminifera from Paleocene - Eocene Lockhart, Patala and Margala Hill Limestone formations of the Kalli Dilli and Dalla sections, Kala Chitta Ranges, Upper Indus Basin. 105

Plate 4.6	Larger foraminifera from Paleocene – Eocene Lockhart, Patala and Margala Hill Limestone formations of the Kalli Dilli and Dalla sections, Kala Chitta Ranges, Upper Indus Basin.	106
Plate 4.7	Larger foraminifera from Paleocene - Eocene Lockhart, Patala and Margala Hill Limestone formations of the Kalli Dilli and Dalla sections, Kala Chitta Ranges, Upper Indus Basin.	107
Plate 4.8	Larger foraminifera from Paleocene - Eocene Lockhart, Patala and Margala Hill Limestone formations of the Kalli Dilli and Dalla sections, Kala Chitta Ranges, Upper Indus Basin.	108
Plate 4.9	Larger foraminifera from Paleocene - Eocene Lockhart, Patala and Margala Hill Limestone formations of the Kalli Dilli and Dalla sections, Kala Chitta Ranges, Upper Indus Basin.	109
Plate 4.10	Larger foraminifera from Paleocene - Eocene Lockhart, Patala and Margala Hill Limestone formations of the Kalli Dilli and Dalla sections, Kala Chitta Ranges, Upper Indus Basin.	110
Plate 4.11	Larger foraminifera from Paleocene - Eocene Lockhart, Patala and Margala Hill Limestone formations of the Kalli Dilli and Dalla sections, Kala Chitta Ranges, Upper Indus Basin.	111

Plate 4.12	Larger foraminifera from Paleocene - Eocene Lockhart, Patala and Margala Hill Limestone formations of the Kalli Dilli and Dalla sections, Kala Chitta Ranges, Upper Indus Basin.	112
Plate 4.13	Larger foraminifera from Paleocene - Eocene Lockhart, Patala and Margala Hill Limestone formations of the Kalli Dilli and Dalla sections, Kala Chitta Ranges, Upper Indus Basin.	113
Plate 4.14	Larger foraminifera from Paleocene - Eocene Lockhart, Patala and Margala Hill Limestone formations of the Kalli Dilli and Dalla sections, Kala Chitta Ranges, Upper Indus Basin.	114
Plate 4.15	Larger foraminifera from Paleocene - Eocene Lockhart, Patala and Margala Hill Limestone formations of the Kalli Dilli and Dalla sections, Kala Chitta Ranges, Upper Indus Basin.	115
Plate 4.16	Larger foraminifera from Paleocene - Eocene Lockhart, Patala and Margala Hill Limestone formations of the Kalli Dilli and Dalla sections, Kala Chitta Ranges, Upper Indus Basin.	116
Plate 4.17	Larger foraminifera from Paleocene - Eocene Lockhart, Patala and Margala Hill Limestone formations of the Kalli Dilli and Dalla sections, Kala Chitta Ranges, Upper Indus Basin.	117

Plate 4.18	Larger foraminifera from Paleocene - Eocene Lockhart, Patala and Margala Hill Limestone formations of the Kalli Dilli and Dalla sections, Kala Chitta Ranges, Upper Indus Basin.	118
Plate 4.19	Showing Larger Foraminiferal Turnover from Paleocene <i>Ranikothalia / Miscellanea</i> - dominated assemblages (Fig. B) to Eocene <i>Nummulites</i> - dominated assemblages (Fig. A).	120
Plate 4.20	<i>Miscellanea</i> micro-bioclastic wacke-packstone microfacies from late Paleocene Patala Shale Formation of the Kala Chitta Range, Upper Indus Basin.	122
Plate 4.21	<i>Miscellanea</i> micro-bioclastic wacke-packstone microfacies from late Paleocene Patala Shale Formation of the Kala Chitta Range, Upper Indus Basin.	123
Plate 4.22	<i>Miscellanea</i> micro-bioclastic wacke-packstone microfacies from late Paleocene Patala Shale Formation of the Kala Chitta Range, Upper Indus Basin.	124
Plate 4.23	<i>Miscellanea</i> micro-bioclastic wacke-packstone microfacies from late Paleocene Patala Shale Formation of the Kala Chitta Range, Upper Indus Basin.	125
Plate 4.24	<i>Miscellanea</i> micro-bioclastic wacke-packstone microfacies from late Paleocene Patala Shale Formation of the Kala Chitta Range, Upper Indus Basin.	126

- Plate 4.25 *Miscellanea* micro-bioclastic wacke-packstone 127
microfacies from late Paleocene Patala Shale
Formation of the Kala Chitta Range, Upper Indus Basin.
- Plate 4.26 *Miscellanea* micro-bioclastic wacke-packstone 128
microfacies from late Paleocene Patala Shale
Formation of the Kala Chitta Range, Upper Indus Basin.
- Plate 4.27 *Nummulites* peloidal wacke-packstone microfacies 130
from early Eocene Margala Hill Limestone Formation
of the Kala Chitta Range, Upper Indus Basin.
- Plate 4.28 *Nummulites* peloidal wacke-packstone microfacies 131
from early Eocene Margala Hill Limestone Formation
of the Kala Chitta Range, Upper Indus Basin.
- Plate 4.29 *Nummulites* peloidal wacke-packstone microfacies 132
from early Eocene Margala Hill Limestone Formation
of the Kala Chitta Range, Upper Indus Basin.
- Plate 4.30 *Nummulites* peloidal wacke-packstone microfacies 133
from early Eocene Margala Hill Limestone Formation
of the Kala Chitta Range, Upper Indus Basin.
- Plate 4.31 *Nummulites* peloidal wacke-packstone microfacies 134
from early Eocene Margala Hill Limestone Formation
of the Kala Chitta Range, Upper Indus Basin.
- Plate 4.32 *Nummulites* peloidal wacke-packstone microfacies 135
from early Eocene Margala Hill Limestone Formation
of the Kala Chitta Range, Upper Indus Basin.

Chapter 5

Plate 5.1	Dinoflagellate cyst assemblages.	170
Plate 5.2	Dinoflagellate cyst assemblages.	172
Plate 5.3	Dinoflagellate cyst assemblages.	174
Plate 5.4	Benthonic foraminifera from the P/E boundary interval, Dungan Formation, Rakhi Nala, Sulaiman Range, Lower Indus Basin.	177

Acknowledgements

I am grateful to Almighty Allah, who bestowed me with the ability to successfully complete this research work and present my thesis.

I would like to thank my supervisors Professor Malcolm Hart and Dr Stephen Grimes, for all their help and support over the last few years. Thanks also to Professor Melanie Leng who supported my work at the NERC Isotope Laboratories and helped greatly with the analysis of materials, and Prof. Muhammad Tahir Shah who helped me to run the LOI analysis at the Geochemistry Laboratory, National Centre of Excellence in Geology, University of Peshawar.

Thanks to all the technicians who have also helped so much as without them this work would certainly not have been completed.

Thanks also to all at the SEM unit, University of Plymouth, for their patience and fantastic help in photographing my specimens.

I would also like to thank the support of my fellow postgraduate students particularly Emehmed Alfandi and Professor Kevin Taylor of Manchester Metropolitan University.

To Dr Meriel Fitzpatrick, Dr Jodie Fisher and all the staff of the SoGEES.

And most importantly to my parents, sisters and brothers, particularly to Tariq (brother) who supported me during my field work.

Above all, I thank my wife Basmina and my son Muhammad Ezekiel Hanif for missing my company during the time when I was abroad. The moral support of Basmina, was the most inspiring element during this exhaustive study without which it would have not been possible to complete this huge task.

AUTHOR'S DECLARATION

At no time during the registration for the degree of Doctor of Philosophy has the author been registered for any other University award without prior agreement of the Graduate Committee.

This study was financed with the aid of Faculty Development Programme of Higher Education Commission, Pakistan for the National Centre of Excellence in Geology, University of Peshawar, Pakistan.

A programme of advanced study was undertaken, which included training in micropalaeontological, palynological, isotopic and geochemical analytical techniques. Most of the work was undertaken at University of Plymouth, UK, some of the analysis were done at the NERC Isotope Geosciences Laboratory, UK, and at the Geochemistry Laboratory of the National Centre of Excellence in Geology, University of Peshawar, Pakistan.

Word count of main body of thesis: 36,909

Signed:



Date: 02 August 2011

Chapter 1: Introduction

1.1. Introduction

The Earth experienced climatic variations from a warm 'greenhouse' to a cooler 'icehouse' world during the Paleogene (Zachos et al., 2001). The Paleocene (65 to ~55 Ma) was a time of great environmental change, within both the marine and terrestrial realms and represents a period of significant perturbation and punctuated biotic changes, bounded by two important events in Earth history; initiated by the Cretaceous/Paleogene extinction event at the base and culminating in the Paleocene Eocene Thermal Maximum (PETM). This warming phase started in the mid-Paleocene (~59Ma) following the perturbation at the K/Pg boundary and ended in a hyperthermal event now known as the Paleocene Eocene Thermal Maximum. A timescale for the Paleocene-Eocene is shown in **Figure 1.1**.

The PETM is a brief, but extreme and rapid global warming event superimposed on the overall warming trend of the Paleocene (Kennett & Stott, 1991). A negative carbon isotopic excursion (CIE) marks the onset of the PETM (Kennett & Stott, 1991; Zachos et al., 2001). Evidence for the warming is observed in marine and terrestrial basins around the world (e.g., Kennett & Stott 1991; Thomas et al., 2002; Sluijs et al., 2006). The PETM occurred at 55.5 Ma (Gradstein et al., 2004) and is associated with a number of other events (**Fig. 1.2**).

Climatic events:

- 9-10°C rise in high latitude Sea Surface Temperature (SST);
- 4-5°C rise in deep sea and equatorial SST (Zachos et al., 2003; Tripathi & Elderfield, 2005); and
- 5°C rise on land (Wing et al., 2005).

Tectonic events:

- North Atlantic rifting and volcanism (Lawver et al., 1998); and
- India-Asia collision (Copeland, 1997).

Biotic events:

- Deep sea benthonic foraminiferal extinction (Thomas, 1990a,b; Thomas et al., 2002);
- Acme of the planktonic foraminiferal genus *Acarinina* (Arenillas & Molina, 1996; Kelly et al., 1998), with the dominance of *Morozovella* and the absence of *Subbotina* during the excursion (Petruzzo, 2007);
- Distinctive assemblages of calcareous nannoplankton (Bralower, 2002);
- Acme of the dinocyst *Apectodinium* (Crouch et al., 2001);
- Rapid radiation of mammals on land (Koch et al., 1992);
- Shallow water benthonic foraminiferal extinction and repopulation (Speijer et al., 1997); and
- Turnover of larger foraminifera on the Tethyan shelf (Orue-Etxebarria et al., 2001).

A number of palaeoceanographic changes associated with the PETM have been reported worldwide. These include changes in oceanic circulation such as the shift in the site of deep water formation from the southern hemisphere to the northern hemisphere (e.g., Kennett & Stott, 1991; Nunes & Norris, 2006).

Increased productivity is recorded along the southern margin of Tethys, and the upwelling of low oxygen intermediate water into the epicontinental basin led to increased biological productivity and anoxia at the sea floor before and during the PETM (Speijer & Schmitz, 1998; Speijer & Wagner, 2002). The epicontinental basins bordering the Tethys appear to have been particularly prone to severe oxygen deficiency during the PETM. A total organic carbon

(TOC) rich sapropel unit <1 m thick has been recorded in numerous localities over a large area between the Crimea and Uzbekistan (northern Tethyan margin) by Gavriliv et al. (1997). Similarly, Speijer et al. (1997) found dark sapropelic beds, with micropaleontological indications for anoxia, in association with a benthic extinction event in localities in Turkmenistan (northern Tethys) and Egypt (Southern Tethys). Speijer & Wagner (2002) referred to these deposits as black shales.

The PETM has been the focus of interest in recent years as this event is considered to be a close analogue to future global warming (Pancost et al., 2007; Zeebe et al., 2009). The *Morozovella velascoensis* Zone of Berggren et al. (1995) is the host zone for the PETM (the Paleocene/Eocene boundary interval). As a result of this, therefore, a large amount of high resolution biostratigraphical data from Tethyan and global sections have been produced in recent years across this interval (**Fig. 1.3**). Bolli (1966) described this zone as the *Globorotalia velascoensis* Zone and defined it as the interval between the last occurrences of *Globorotalia pseudomenardii* (below) and *Globorotalia velascoensis* (above). Stainforth et al. (1975) retained the existing name and definition although Blow (1979) redefined it by dividing it into two zones (P6 and P7) based on the lowest occurrence of *Acarinina berggreni*. It was named the *Morozovella velascoensis* Zone by Toumarkine & Luterbacher (1985). They defined it as the interval between the last appearance of *Planorotalites pseudomenardii* (below) and the highest occurrence of *M. velascoensis* (above). Canudo & Molina (1992) divided this zone into two zones based on the lowest occurrence of *Pseudohastigerina wilcoxensis*. These are the *Morozovella aequa* Zone below the lowest occurrence of *P. wilcoxensis* and the *P. wilcoxensis* Zone above the lowest occurrence of *P. wilcoxensis*. Later,

Berggren et al. (1995) retained the name given by Toumarkine & Luterbacher (1985) and, in addition, called it P5 and defined it as the interval between the last occurrence of *G. pseudomenardii* (below) and the highest occurrence of *M. velascoensis* (above). Molina et al. (1999) provided a high resolution biostratigraphy of the *M. velascoensis* Zone of Toumarkine & Luterbacher (1985) and they divided it into five subzones. Berggren & Pearson (2005), based on high resolution biostratigraphic data, have divided it into three zones (**Fig. 1.3**).

1.2. This Study

In a comparable situation to the extensive epicontinental basins on the southern margin of the Tethys, the Indus Basin on the north western margin of the Indian Plate provides excellent opportunities for faunal and geochemical studies, allowing the evaluation of the relations between the trophic regimes and their biota and the improvement of the stratigraphic resolution in the area. The Indus Basin can be subdivided into three depositional provinces:

- The Potwar-Kohat depositional province (Upper Indus Basin);
- The Sulaiman depositional province (Lower Indus Basin); and
- The Kirther depositional province (Lower Indus Basin).

The Potwar-Kohat depositional province is separated from the rest of the Indus Basin by a west-northwest-trending positive axis which extends from the Indian shield through the Kirana-Sargodha Hills up to the Khisor Range. The Sulaiman depositional province is also separated from the Kirther province in the south by

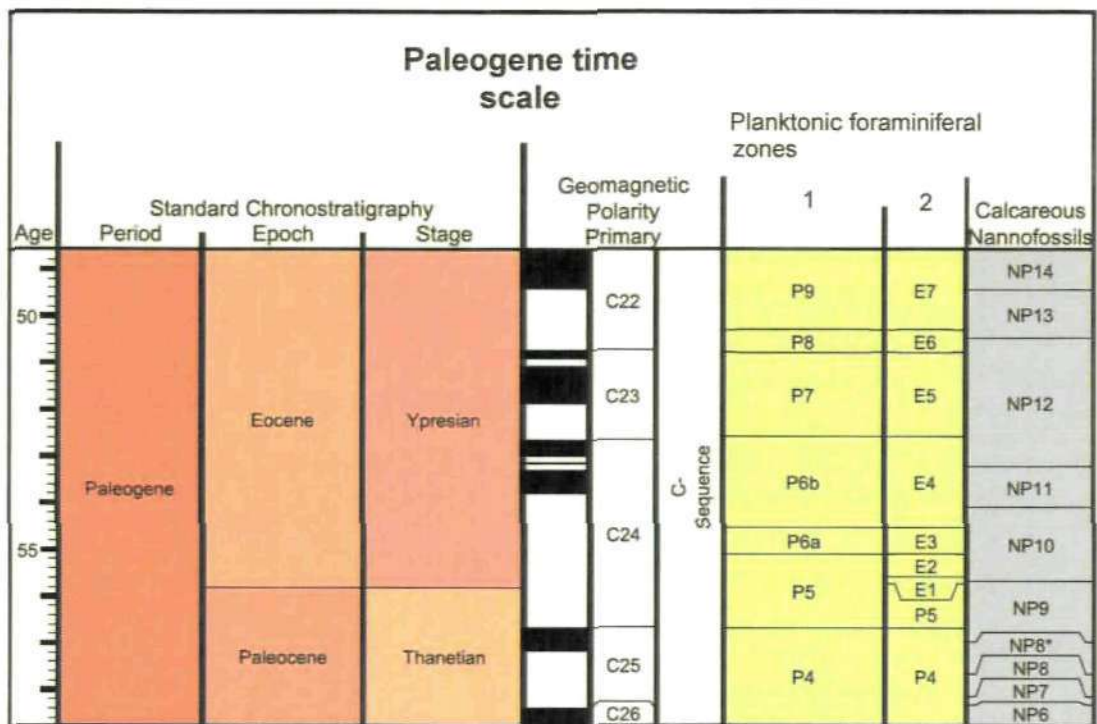


Fig.1.1: Paleogene time scale produced through a software called PAST (available at <http://folk.uio.no/ohammer/past/>). (1) Berggren et al. (1995), (2) Berggren & Pearson (2005). Asterisk (*) indicates continuation of NP8.

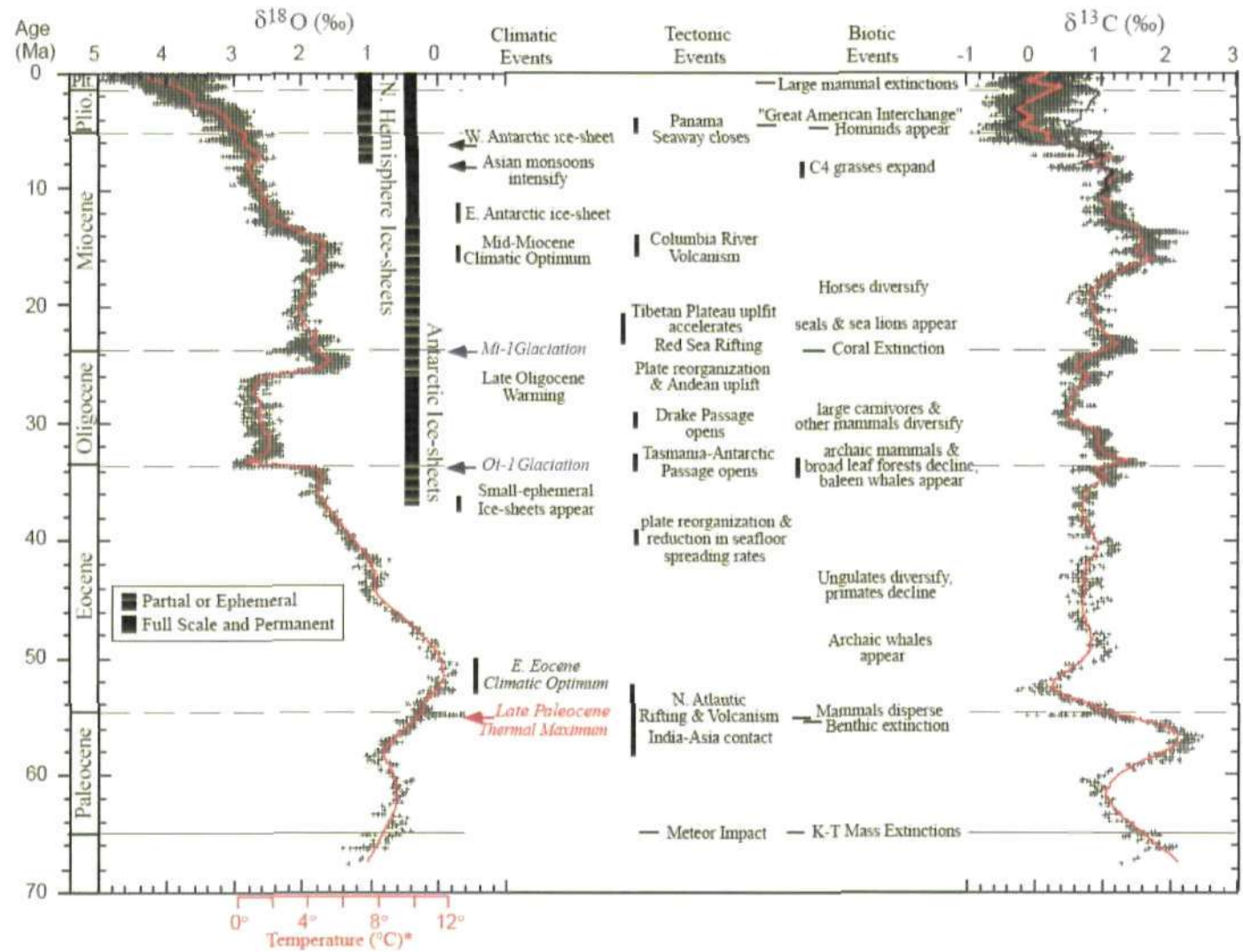


Fig. 1.2: Showing $\delta^{18}\text{O}$ and $\delta^{13}\text{C}$ curves and associated climatic, tectonic and biotic events for the past 70 Ma (after Zachos et al., 2001).

Age	Datum events	Bolli (1966) Stainforth et al. (1975)	Blow (1979)	Toumarkine & Luterbacher (1985)	Canudo & Molina (1992)	Berggren et al. (1995)	Molina et al. (1999)		Berggren et al. (2003)		Berggren & Pearson (2005)			
							Zones	Subzones	Zones	Subzones				
Ypresian	<i>M. velascoensis</i>	<i>Globorotalia subbotinae</i>	<i>Globorotalia (A.) wilcoxensis berggreni</i> P7	<i>Morozovella edgari</i>	<i>Pseudohastigerina wilcoxensis</i>	<i>M. velascoensis-M. formosa</i>	<i>Morozovella subbotinae</i>	<i>Morozovella edgari</i>			<i>Morozovella marginodentata</i> PRZ			
	<i>Ps. wilcoxensis</i>	<i>Globorotalia velascoensis</i>		<i>Morozovella velascoensis</i>		<i>Morozovella velascoensis</i> P5	<i>Morozovella velascoensis</i>	<i>Pseudohastigerina wilcoxensis</i>	<i>Pseudohastigerina wilcoxensis</i>	<i>Pseudohastigerina wilcoxensis</i>	P5c	<i>Pseudohastigerina wilcoxensis</i> Concurrent-range Zone E2		
	<i>A. sibaiaensis</i>				<i>Acarinina sibaiaensis</i>								P5b	<i>A. sibaiaensis</i> Lowest-Occurrence E1
	<i>I. laevigata</i>				<i>A. berggreni</i>								P5a	<i>Morozovella velascoensis</i> PRZ P5
<i>A. berggreni</i>	<i>Morozovella gracilis</i>													
Thanetian	<i>M. gracilis</i>	<i>Globorotalia pseudomenardii</i>	<i>Globorot. (M.) subbotinae subbotinae-Globorot. (M.) velascoensis acuta</i> P6	<i>Planorotalites pseudomen.</i>	<i>Planorotalites pseudomen.</i>	<i>A. soldadoensis</i> <i>G. pseudomena.</i> P4c	<i>Luterbach. Pseudomenardii</i>	<i>Muricoglob. Soldadoensis</i>		<i>A. soldadoensis/G. pseudomena.</i> P4c				
	<i>L. pseudomenardii</i>													

Fig. 1.3: High resolution biostratigraphy of the *Morozovella velascoensis* Zone and its subzones in the light of previous literature, bases of blue arrows indicate lowest (arrows pointing upward) and highest (arrows pointing downward) occurrences.

the sub-surface high called the Jacobabad High. Numerous well-exposed outcrops yielding well preserved microfossils are easily accessible in several localities. In addition to surface exposures, data regarding the sub-surface is available in the public domain as a result of the increasing hydrocarbon exploration activities in the Indus Basin.

Cenozoic marine sequences deposited in the Tethys Ocean before its demise, as a result of the collision between the Indo-Pakistan and Eurasian Plates, are well exposed throughout the Indus Basin. Cenozoic sedimentary records in the Indus Basin exhibit a change from Paleocene-Eocene marine sequences to non-marine littoral and terrestrial molasse-type deposits during the Neogene and Quaternary. In the Sulaiman Range, and in the Baluchistan Ophiolite and Thrust Belt, the Cenozoic-Mesozoic contact changes from an angular unconformity between the Paleocene and older units, to a disconformity and overlap in the Kohat-Potwar-Salt Range region (Raza et al., 1989; Gee & Gee, 1989). In the Lower Indus Basin, the contact between the Paleocene and the Cretaceous is disconformable (Williams, 1959) although it is transitional in places according to the Hunting Survey Corporation Ltd (1961). The non-marine Chitarwata Formation unconformably rests on the Paleogene marine strata (Kazmi, 1995). This marine Paleogene sequence consists of four formations which are, in ascending order, the Dungan, Shaheed Ghat, Baska and Kirther formations (see **Fig 3.5**, Chapter 3). In the Upper Indus Basin both the lower and upper boundaries of the Paleogene are unconformable (Shah, 1977). The Paleogene sequence consists of the following formations in ascending order: Paleocene; Hangu, Lockhart, Patala and Eocene; Nammal, Sakesar, Chorgali (see **Fig 3.3**, Chapter 3).

The stratigraphy of the fossiliferous Paleogene sediments of the Indus Basin, as it is represented in Pakistan, has been a subject of research since the late nineteenth century. The early studies have provided a detailed record of the lithology, biostratigraphy and palaeoenvironments (Wynne, 1872, 1874; Blanford, 1880; Davies, 1927; Davies & Pinfold, 1937; Eames, 1952; Haque, 1956; Nagapa, 1959; Hunting Survey Corporation, 1960; Latif, 1961, 1964, 1970; Hemphill & Kidwai, 1973; Fatmi, 1974; Middlemiss, 1986). This earlier work was compiled and published by the Geological Survey of Pakistan (GSP) (Shah, 1977) and, more recently, by Afzal et al. (2009). Since deep water to open marine sequences of early Cretaceous to late Eocene age are widely and excellently exposed in the Kirther and Sulaiman Ranges (Lower Indus Basin) there have been a number of studies of the Paleogene planktonic foraminifera (Haque, 1956, 1959; Latif, 1961, 1964; Samanta, 1973; Dorreen, 1974; Warraich et al., 2000). In the Salt Range (Upper Indus Basin) the frequent interfingering of both shallow and open marine sediments during the Paleogene offers an excellent opportunity to study the microfossils (including foraminifera, calcareous nannoplankton and dinoflagellates) in a wide spectrum of palaeoenvironments. This opportunity has been exploited in a number of previous studies (Davies & Pinfold, 1937; Haque, 1956; Köthe et al., 1988; Gibson, 1990; Weiss, 1988, 1993; Afzal & Von Daniels, 1991; Ashraf & Bhatti, 1991; Bybell & Self-Trail, 1993; Afzal, 1997). As a result of these publications a large amount of biostratigraphical and lithostratigraphical data are available for the Paleogene and, in particular, for the Paleocene/Eocene boundary interval of the Indus Basin. However, not enough work has been done in the area of palaeoenvironmental analysis using a multiple proxies approach including geochemical work (particularly stable isotopes). Therefore, a multiple proxy

approach is needed for better palaeoenvironmental interpretations and improved biostratigraphical resolution. This study is, therefore, an integrated attempt to improve the resolution and review (where needed) the planktonic foraminiferal and dinoflagellate biostratigraphy, the palaeoenvironmental interpretation across the Paleocene/Eocene boundary interval, and the correlation of this record from the Indus Basin with other Tethyan and global sections.

Since no proxy is truly sensitive to only one environmental parameter, for the most reliable reconstructions, a multi-proxy approach is preferable. This procedure should reduce the potential for misinterpretation. In this research a multi-proxy approach has been applied. Most other modern authors use multi-proxy data sets and so this makes comparison easier and more reliable.

1.2.1. Foraminifera

The aim of the foraminiferal investigation was to interpret the palaeoenvironment and biostratigraphy of the Paleocene/Eocene boundary interval. A number of factors related to the state of the water column generally control the evolution, diversification and extinction of planktonic foraminifera. Such factors are primarily associated with stratification within the water column, variations in the trophic structure and vertical temperature and density gradients (Leckie et al., 1998; Hart, 1999; Price & Hart, 2002; Keller, 2002; Keller & Pardo 2004; Coccioni & Luciani, 2004). High diversity assemblages in the modern ocean are typically seen within a well stratified water column, with normal salinity and nutrient content (Coccioni & Luciani, 2004). Depth stratification provides distinct biotic and physical environments in which stable ecological niches can be filled, and potentially competing species are separated (Lipps,

1979; Hemleben et al., 1989). The structure of foraminiferal assemblages will change with different nutrient conditions. Unstable eutrophic conditions are formed by increased nutrient influx which favours opportunistic (r-selected) species. These species are typically small in size and characterized by fast reproduction. A reduction in nutrient influx however will lead to more stable oligotrophic conditions favouring more specialised (K-selected) species. These species are larger in size and have much lower reproductive potential and longer life spans (MacArthur & Wilson, 1967; Hottinger, 1982, 1983; Scheibner et al., 2005). The intermediate species between two extremes are r/K, adopted to mesotrophic environments have a range of trophic strategies (Coccioni & Luciani, 2004). The abundance, diversity and morphology of Paleocene-Eocene planktonic and benthonic foraminifera provide information on the state of the water column and ecological niches filled.

Murray (2006) describes five broad groups of benthonic foraminiferal applications and these are;

- 1) Biostratigraphy;
- 2) Interpretation of palaeoenvironmental analysis
- 3) Interpretation of specific details of environments or processes such as palaeoproductivity, low oxygen, seasonal stratification of the water column, etc. (palaeoceanography);
- 4) A proxy for natural environmental change (e.g., sea level, climate); and
- 5) Monitoring of changes induced by the activities of man.

According to Murray (2006), benthonic foraminifera are the only important benthonic group of organisms for recording the history of events on the sea floor in a broad spectrum of environments from the intertidal zone to hadal

depths. Benthonic foraminifera have been used to interpret past bottom conditions such as bottom-water masses, presence/absence of an oxygen minimum zone (OMZ), currents, methane seeps, Aragonite Compensation Depth (ACD) and Calcite Compensation Depth (CCD) and their associated lysoclines. They have also been used for interpreting surface productivity; i.e., flux of organic material from the sea surface.

During the PETM benthonic foraminifera suffered a severe extinction (e.g., Tjalsma & Lohmann, 1983; Thomas, 1990a, b; Pak & Miller, 1992; Ortiz, 1995; Speijer, 1994). In a large number of previous studies this group of foraminifera, with the aid of other proxies, has been used as one of the basic tools in the reconstruction of the palaeoenvironments across the PETM. Although the deep sea has been the main focus of such studies, attempts have also been made at the interpretation of shallow marine environments and it has been shown that the benthonic foraminifera are an equally important proxy in the palaeoenvironmental reconstruction of shallow waters.

An enormous amount of research is devoted to studies of the application of foraminifera to palaeoenvironmental and environmental interpretation. Foraminifera are principally divided into benthonic (living within or on the sea floor) and planktonic (living in the water column). The benthonic foraminifera are used to reconstruct the bottom conditions while planktonic foraminifera are used as a proxy for surface water and water column conditions. Foraminifera are present in a broad spectrum of marine environments, ranging from coastal marshes to abyssal plains. As the distribution of foraminifera is controlled by a number of factors (i.e., nutrients and oxygen availability, temperature, salinity and pH) their presence/absence can be used to interpret the palaeoenvironments of geological successions. In addition to

palaeoenvironmental interpretation the foraminifera have been extensively used in biostratigraphy. Their fossilization potential is high, explaining their extensive use in the fossil record.

1.2.2. *Dinoflagellates*

The single-celled dinoflagellates are predominantly marine, eukaryotic plankton that typically occur as motile cells in surface waters, sometimes in astonishing concentrations called 'red tides' (e.g., Fensome et al., 1996a). They are characterized by having a variety of nutritional strategies. The lifestyles of most dinoflagellates are autotrophic but many have an heterotrophic lifestyle and may rank among the zooplankton. Some dinoflagellates produce preservable organic-walled hypnozygotic resting cysts (dinocysts) as a part of their often-complex life-cycle. In addition, (mainly vegetative) calcareous and siliceous cysts are known. The cyst part of the dinoflagellate life cycle is usually associated with sexual reproduction and is induced by particular surface water parameters, predominantly seasonal nutrient depletion, that only prevails for a brief period (Taylor, 1987). Typically, the motile stage does not preserve, but organic dinocysts are found from the late Triassic onwards (e.g., MacRae et al., 1996).

The dinoflagellates, together with diatoms and coccolithophorids, are amongst the most prominent marine primary producers in the oceans today and they play an important role in the global carbon cycle (e.g., Brasier, 1985). Moreover, they were probably an important factor in the development of coral reef systems; the ecological success of scleractinian corals since the Triassic was probably a direct result of their acquisition of dinoflagellate symbionts, which allowed them to exploit nutrient-poor environments (Trench, 1987).

Dinoflagellate symbionts are also known from some groups of extant and fossil planktonic foraminifera (e.g., Bé & Hutson, 1977; Spero, 1987). Over the past decades, the importance of dinocyst analysis has been increasingly recognized in hydrocarbon exploration where dinocyst biostratigraphy has now emerged as a routine tool (see, for example, Stover et al., 1996 and Williams et al., 2004, for a summary of existing Triassic to Neogene dinocyst biozonations). In many oil and gas provinces, such as the Paleogene of the North Sea Basin, they have yielded a higher stratigraphical resolution than calcareous microfossils (e.g., Gradstein et al., 1992). Remains of dinoflagellates are also major components of petroleum source rocks (Ayres et al., 1982) due to their ability to store lipids (Bold, 1973; Horner, 1985).

The organic-walled dinocysts have been increasingly employed as sensitive (palaeo-) environmental indicators over the past 30 years (e.g., Downie et al., 1971; Wall et al., 1977; Mudie & Harland, 1996; Dale, 1996; Pross et al., 2004; Prauss, 2009). The organic walled cyst-producing dinoflagellates are known to be highly sensitive to even small changes in surface water characteristics (e.g., Turon, 1981; Harland, 1983; de Vernal & Mudie, 1992; Harland & Long, 1996; Dale, 1996, 2001; Rochon et al., 1999; Targarona et al., 2000; Boessenkool et al., 2001; Marret & Scourse, 2002; Sangiorgi et al., 2002, 2003; Matthiessen et al., 2005). A wealth of Paleogene dinocyst data are available from recent ocean drilling (e.g., in the Southern Ocean) boosting more integrated, multidisciplinary studies and interpretations (Brinkhuis et al., 2003a,b; Sluijs et al., 2003; Röhl et al., 2004a, b; Schellenberg et al., 2004; Williams et al., 2004; Huber et al., 2004; Stickley et al., 2004; van Simaey et al., 2005). These and other recent research have led to

considerable progress in Paleogene dinocyst palaeoecology in the last twenty years.

For palaeoenvironmental studies the dinoflagellate cysts (= dinocysts) preserved in sediments provide the most important information. The high-resistant cysts have a great preservation potential. This group has been successfully adopted in a number of research projects of the reconstruction of sea-surface productivity, sea level change and temperature. Changes in productivity are thought to influence the ratio between the heterotrophic protoperidinioid and the autotrophic gonyaulacoid dinocysts (Harland, 1973; Almogi-Labin et al., 1993). The peridinioid/gonyaulacoid ratio may, therefore, be a good approximation of a palaeoproductivity signal in the fossil record, although Prauss (2009) and references therein have highlighted the problems involved with use of the ratio. Dinocyst preservation is, however, extremely sensitive to oxygen availability. The organic-walled dinocysts are neither affected by chemical dissolution nor by secondary mineralization and, therefore, offer a most reliable and promising tool for biostratigraphy in carbonate poor areas. This research attempts to interpret the palaeoenvironment by quantitative analysis of the dinocysts as well as use them as a tool for biostratigraphy and correlation.

1.2.3. Organic Geochemistry

Carbon isotopes relate to the amount of dissolved inorganic carbon (DIC) in seawater, which is maintained relatively near to zero (relative to the Vienna Pee Dee Belemnite (VPDB) international standard), balanced by the influx of carbon from terrestrial weathering, volcanic sources, oxidation of organic matter, and the output through the production of marine carbonates and burial of organic

matter (Berger & Vincent, 1986; Marshall, 1992). Typically there is not a large variation in the amount of DIC in the ocean. A gradient of $\delta^{13}\text{C}$ values is, however, seen through the water column (Berger & Vincent, 1986; Marshall, 1992). This is related to ocean productivity. Organic matter is predominantly composed of light carbon and, therefore, has very negative $\delta^{13}\text{C}$ values. Removal of organic carbon from the oceanic reservoir renders surface waters relatively enriched in $\delta^{13}\text{C}$ (Berger & Vincent 1986; Marshall 1992). As the organic matter moves down through the water column to the sea floor, it begins to break down and is oxidised, returning the light carbon back into the ocean waters. The surface waters, therefore, often show more positive $\delta^{13}\text{C}$ values than deeper in the water column and at the sea floor, and the more enhanced the productivity, the more pronounced this difference in surface and deep water $\delta^{13}\text{C}$ values becomes. Organisms, such as foraminifera, are thought to precipitate their tests in equilibrium with the isotopic composition of the water (e.g., Fairbanks et al., 1980; Savin et al., 1985).

Oxygen isotopes are similarly related to the oxygen isotope composition of the water (related to salinity) and, importantly, the temperature of the water mass. Globally, the oxygen isotope value of seawater is predominantly controlled by the amount of polar ice. Polar ice preferentially takes up the lighter ^{16}O , leaving global ocean waters enriched in the heavier ^{18}O and this results in more positive $\delta^{18}\text{O}$ values of the global ocean waters (e.g., Kennett & Stott, 1990). At times such as the PETM, when it is believed that there may have been no polar ice, the ocean waters were enriched with the lighter ^{16}O and more negative values are seen (e.g., Kennett & Stott, 1991). Similar to the carbon isotopes, the calcium carbonate tests of foraminifera and calcareous nanofossils may precipitate in equilibrium with the oxygen isotope value of the

seawater. Any values from a calcite test that differs from the equilibrium value of its ambient water shows fractionation or disequilibrium, expressed as $\Delta\delta^{18}\text{O}$ and $\Delta\delta^{13}\text{C}$ (Murray 1991).

This disequilibrium is caused by life processes collectively known as vital effects. These are:

1. Uptake of metabolic CO_2 during calcification;
2. Growth or calcification rate;
3. Physiological changes with ontogeny;
4. Kinetic isotope effects in the transport of carbonate ions to the site of calcification
5. Photosynthetic activity of symbionts; and
6. Diagenesis

Variations in the proportion of $^{13}\text{C}/^{12}\text{C}$ in biogenic carbonates are due to:

1. Global and regional changes in surface-water productivity;
2. Different water masses and circulation patterns;
3. Vital effects; and
4. Microhabitat effects.

Hence, assuming little or no 'vital effects' in the foraminifera, the planktonic foraminifera living in the water column record the isotopic composition of the surface waters while benthic foraminifera record the isotopic composition at the bottom of the water column. Isotopic data, and their comparison from these foraminifera, provides valuable information on water column productivity, thermal

stratification and water mass circulation. Whole-rock samples are primarily composed of calcareous nannofossils with a minor component of planktonic and benthonic foraminiferal fragments and can be used as a proxy to determine $\delta^{13}\text{C}$ trends for the general surface water conditions (Charisi & Schmitz, 1995, 1998). In nearshore settings in particular, variation in the isotopic composition of water can be caused by variations in evaporation and precipitation and/or freshwater runoff.

Diagenesis can cause large changes in the primary isotopic signal. The original isotope values of the carbonate become overprinted by recrystallisation of the original sediment and its components, in an environment different from that in which it originally formed. The amount of diagenesis depends on the type of sediments and their diagenetic history related, for instance, to burial depth and rate. Diagenesis can occur early (e.g., on the sea floor) or in shallow burial, or much later at depth. These different mechanisms have a differing effect on the isotope signals, but all will overprint any original isotope signal. All samples were assessed for diagenesis using scanning electron microscopy and thin section analysis. The foraminifera in all samples were found to be diagenetically altered and unsuitable for isotopic analysis.

The reconstruction of productivity patterns is of great interest because of the important links to current patterns, mixing of water masses, wind, the global carbon cycle and biogeography. Productivity is often reflected in the flux of carbon into the sediment. Generally speaking, there is a relationship between productivity in surface waters and organic carbon accumulation in the underlying sediments (Sarnthein et al., 1992). Below the central gyres, the deserts of the ocean, the organic carbon content in sediments is extremely low. In upwelling areas, the organic carbon content of the sediments can be

extremely high. From this observation it may be expected that, at any one place, a change in the content of the sediment organic carbon indicates a change in productivity through time (Wefer et al., 1999).

One marker for the fertility of sub-surface waters (that is, nutrient availability) is the carbon isotope ratio within the water ($^{13}\text{C}/^{12}\text{C}$, expressed as $\delta^{13}\text{C}$). Further information about the terrestrial portion is provided by the C/N ratios. Values between 7.0 and 9.0 are considered to indicate marine and those >15 are assumed to be of terrestrial origin. Uncertainties in the end member values, when using these methods of identifying the proportion of terrigenous carbon, result in semi-quantitative estimates only (Wefer et al., 1999). This research utilizes a number of organic geochemical proxies as a tool to reconstruct palaeoenvironment. These include TOC (total organic carbon), $\delta^{13}\text{C}_{\text{TOC}}$ (total organic carbon) and $\delta^{13}\text{C}_{\text{FF}}$ (total fine fraction organic carbon) isotopes and C/N ratios.

1.2.4. Carbonate content

The carbonate content is predominantly constituted of biogenic components, and this may add information on variations in palaeoproductivity. In the ocean and above the continental slopes, the carbonate production is dominated by phytoplankton and zooplankton, whereas in near shore environments benthonic organisms are the major sources (Rühlemann et al., 1999). In shallow water settings the terrestrial input also plays an important role. Low carbonate values can indicate an increased terrigenous component. In arid areas, the deep weathering of exposed rocks is of importance and low carbonate sediments might result due to the transportation of the weathered terrigenous material to the basin (El Kammar & El Kammar, 1996). Carbonate content together with

planktonic foraminiferal numbers and planktonic/benthonic ratio of the sediments can be used to estimate carbonate dissolution (Guasti & Speijer, 2007; see discussion on foraminifera in Chapter 4).

1.3. Aims of Research

This research aims to assess the palaeoenvironmental changes across the Paleocene-Eocene transition, to improve the resolution and review (where needed) the foraminiferal and dinoflagellate biostratigraphy, and provide new information on the stable isotope stratigraphy.

1.3.1. Objectives

In order to deliver on the aims of this research the following objectives are important and have been addressed:

- Study geological succession in the Indus Basin across the P/E transition;
- Foraminiferal analysis to determine the palaeoenvironment and review the biostratigraphy;
- Dinocyst biostratigraphical analysis of the previously unzoned P/E boundary interval from the Sulaiman Range (Lower Indus Basin) and provide a correlation to the existing dinocyst zones of the Upper Indus Basin and other Tethyan and global sections;
- Quantitative dinocyst and geochemical analyses (i.e., carbonate content, TOC and C/N ratios) to interpret palaeoenvironmental changes across the P/E boundary interval; and
- Stable carbon isotope analysis (i.e., $\delta^{13}\text{C}_{\text{TOC}}$ (total organic carbon) and $\delta^{13}\text{C}_{\text{FF}}$ (total fine fraction organic carbon)) of the P/E transition and provide a comparison of the isotope data from the Indus Basin with other Tethyan and global sections.

1.3.2. Study Locations

In order to achieve the above mentioned objectives, samples and data from the following areas of the Indus Basin have been collected; Sulaiman Ranges (Lower Indus Basin), Kala Chitta Range (Upper Indus Basin) (**Fig. 1.4**).

Sulaiman Range (Lower Indus Basin)

Rakhi Nala (29°59' N and 70° 03' E) exhibits undisturbed and very well exposed Paleocene-Eocene marine successions. This section is easily accessible by means of the Dera Ghazi Khan-Quetta road. It lies on the easternmost flank of the Sulaiman Range. All four Paleogene formations are typically exposed in this section.

Kala Chitta Range (Upper Indus Basin)

The Kala Chitta Range forms the northern edge of the Potwar Sub-basin (Upper Indus Basin). It merges laterally towards the east into the Hazara Mountains and Margala Hills and westwards into the Samana Range. The range lies between latitudes 33° 30' and 34°N and longitudes 72° and 72° 45'E. The stratigraphical sections from where the samples were collected are linked by metalled, unmetalled and fair weather roads accessible by four-wheel drive vehicle. Sections of the Paleocene and Eocene rocks were measured at the following two localities;

- Chak Dalla section: latitude 33° 39' 56.2"N; longitude 72° 23' 41.3" E
- Kali Dilli section: latitude 33° 39' 9.4"N; longitude 72° 18' 20"E

The Chak Dalla section is located in a gorge north of Sakhi Zinda Pir Rest House. The gorge exposes a section of the Lockhart Limestone Formation and the Patala Shale Formation.

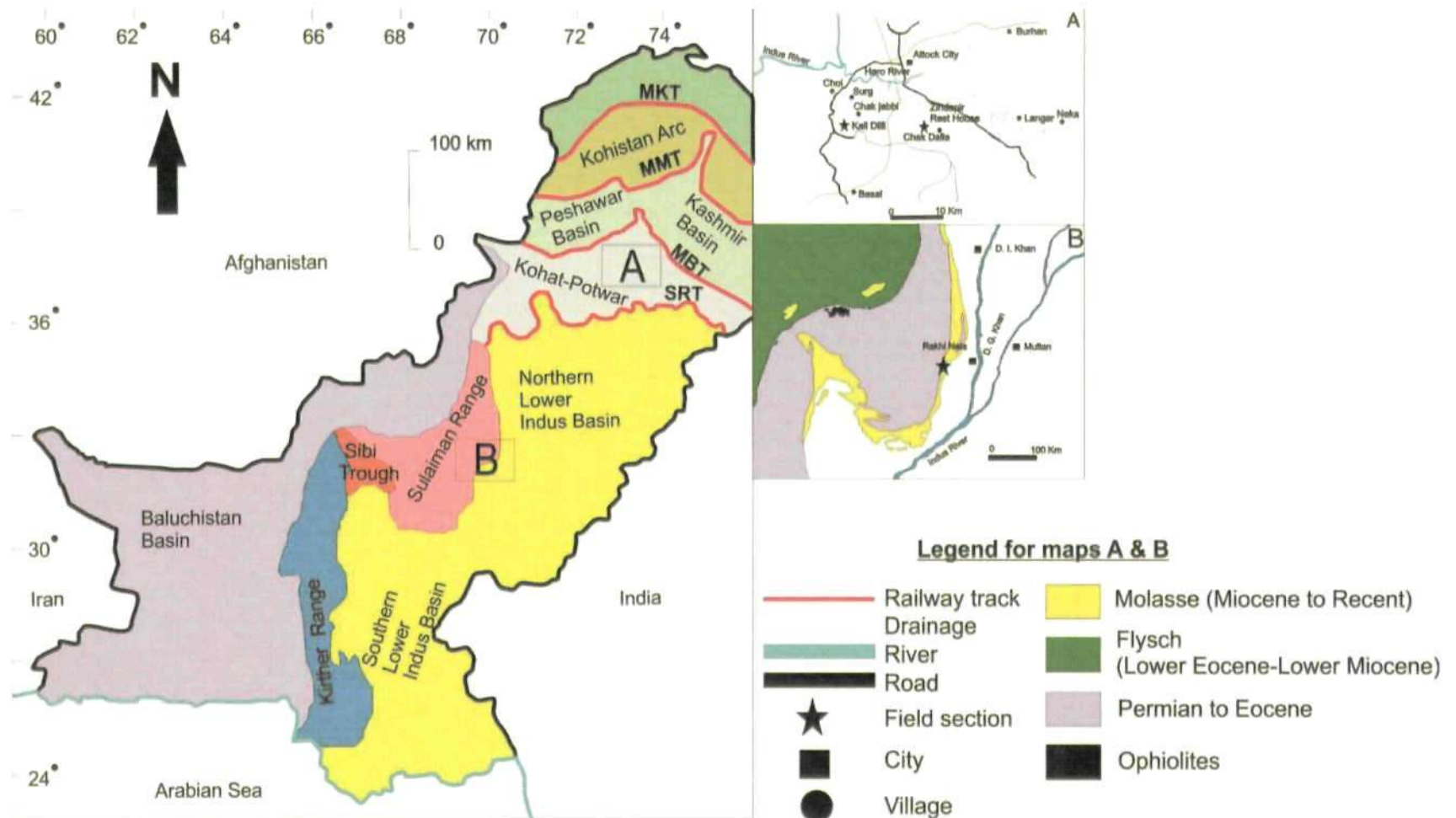


Fig. 1.4: Geological map of Pakistan showing field locations and main geological features; **A-** Chak Dalla and Kali Dilli sections (Kala Chitta Range), **B-** Rakhli Nala section (Sulaiman Range), **MKT-** Main Karakoram Thrust, **MMT-** Main Mantle Thrust and **MBT-** Main Boundary Thrust, **SRT-** Salt Range Thrust.

Chapter 2: Methodology

This chapter describes the methods used to process and analyse the samples used in this research. Over 200 samples were collected during the field work from sections in the Indus Basin, Pakistan.

Sampling in the Indus Basin was undertaken in November 2007 and November 2008. It is clear from the literature that the P/E boundary in the Indus Basin lies in the upper-most part of the Dungan Formation (Lower Indus Basin) and the Patala Formation (Upper Indus Basin) (e.g., Afzal, 1997; Warraich et al., 2000). Therefore, these two formations were the target for sample collection in this research. In order to ensure un-weathered rock sample collection, the weathered surface material was removed before collecting a sample. A fine sample interval (e.g., 25-50 cm) was used across the expected P/E boundary. Coarser sample intervals of 1-5 m and >5 m were used elsewhere with additional samples taken of any new lithologies which would be missed by this sample spacing. Samples were systematically labelled (e.g., **Td-1**, T represents Tertiary, d represents the Dungan Formation and 1 represents the sample number) and transported to the University of Plymouth for processing and analysis. Some of the samples were thin sectioned at National Centre of Excellence in Geology, University of Peshawar.

The following methods were adopted to achieve the objectives of this research (see **Section 1.3.1** Chapter 1 for objectives);

- Planktonic and smaller benthonic foraminifera were obtained from lithologies; i.e., mainly clays and silts by using white spirit method (see

Section 2.2.1 for details). A representative assemblage of the species present was obtained by picking >300 (where possible) specimens per sample. Foraminifera were identified using the following literature; Haque (1956, 1959), LeRoy (1953), Samanta (1973), Berggren & Aubert (1975), Aubert & Berggren (1976), Tjalsma & Lohmann (1983), Van Morkhoven et al. (1986), Kaminski et al. (1989), Speijer (1994), Afzal (1997) and Warraich et al. (2000). The planktonic/benthonic ratio was determined and key planktonic genera were calculated as percentages. Representative specimens were photographed in the Electron Microscopy Centre at the University of Plymouth, UK.

- Thin sections were prepared from strongly lithified lithologies (i.e., limestone) to study the larger benthonic foraminifera and other sedimentological features (see **Section 2.2.1** for details). Key genera were identified following the work of Schaub (1981), Adams (1988), White (1989), Al-Sayigh (1998), Hottinger (2009) and Haynes et al. (2010). The representative specimens were photographed using the petrographic microscope facility at the Manchester Metropolitan University, UK.
- Dinocyst slides were prepared following the standard techniques (see **Section 2.1.1** for details), >200 specimens per sample were counted. Key genera were calculated as percentages and the data were plotted against the stratigraphic section. The dinocyst genera were identified using the work of Davey et al. (1966), Wilson & Clowes (1980), Jan du Chêne & Adediran (1984), Köthe et al. (1988), Bujak & Brinkhuis (1998),

Iakovleva et al. (2001), Iakovleva & Kulkova (2003) and Sluijs & Brinkhuis (2009).

- Stable carbon isotope analysis i.e., $\delta^{13}\text{C}_{\text{TOC}}$ (total organic carbon) and $\delta^{13}\text{C}_{\text{FF}}$ (total fine fraction organic carbon) were performed using a Carlo Erba 1500 EA online to a VG TripleTrap plus a secondary cryogenic trap in the mass spectrometer (see **Section 2.3.2** for details). The isotope data were plotted against the stratigraphic section.
- The total organic carbon (TOC) and C/N ratios were determined using a Carlo Erba 1500 elemental analyser.
- The carbonate content and total organic carbon (TOC) were determined by using the loss on ignition (LOI) method. The data were calculated in percentages (see **Section 2.4** for details).

2.1. Preparation of dinocyst slides

Analysis of the dinocyst assemblage has been carried out on a selection of 63 samples collected from the Rakhi Nala section (see **Figure 1.4** from Chapter 1). Sample intervals of 25-50 cm were used for the uppermost part of the Dungan Formation (see **Figure 5.1** from Chapter 5). These samples were selected from, and across, a foraminiferal barren interval. The aim of the dinocyst investigation was to interpret the biostratigraphy and palaeoenvironment of this interval. The samples were processed at *Geotechniques Research* by Jonah Chitolie using the standard palynological processing methodology (hydrochloric acid followed by hydrofluoric acid for demineralisation). Oxidation was not deemed necessary

because of the well-preserved nature of the palynomorphs. The detailed procedure adopted for these samples is described as follows (Chitolie, *pers. comm.*).

Samples were cleaned of surface contamination by scraping the outer layers with a stainless steel scalpel (for hard rocks), or by brushing with a dry nylon toothbrush (for soft rocks). Some pieces were too small to be cleaned by these methods. Samples were oven-dried at 100°C for approximately ten hours. After weighing (carbonate-rich samples weighed 50-118 g; clay samples weighed 5-8 g), the samples were placed in glass beakers (2 litre beakers for the chalk and 1 litre for the clay) and 100 ml of distilled water added to each sample, followed by a small amount of 50% hydrochloric acid, with any reaction being allowed to subside before the addition of more acid. The carbonate-rich samples foamed due to their high reactivity. After being washed through a 15µm sieve with filtered tap water, the residues were returned to the glass beakers where concentrated hydrochloric acid was added to eliminate un-dissolved carbonate. After further washing, the samples were placed in 250 ml polypropylene beakers and 50% hydrofluoric acid was added and left overnight. Samples were then washed through a 15µm polyester sieve.

The recovered residues, in almost all of the samples, contained well preserved palynomorphs, some of which were transparent. Oxidation was not, therefore, deemed necessary. All residues were examined before mounting and any that were found to contain calcium fluoride precipitate were treated with 50% hydrochloric acid and heated at 80°C for approximately one hour. The residues were divided in two, with one part stained using Bismark brown R.

For each sample two glass coverslips were cleaned and placed on a warm plate. A small amount of residue was placed in a vial and mixed with polyvinyl acetate. The residue was pipetted onto the coverslip and left to dry. A small amount of Elvacite was used as the mounting medium and was placed on each slide and then inverted onto the coverslip. Elvacite is made by dissolving 20g of Elvacite 2044 resin (a trade name for methacrylate resin) in 35 ml of xylene. The slides were kept in a fume hood over night and then placed in a drying oven at 80°C for two hours.

For all samples, a minimum of 200 dinocysts (where possible) were counted and the entire slide was scanned for the presence of additional age diagnostic taxa. Photomicrographs were taken using the digital photomicroscope facilities at the University of Plymouth.

2.2. Foraminiferal analysis

Foraminiferal analysis has been carried out on a selection of over 100 samples. In order to analyse the samples for foraminifera, each sample was processed, according to the rock type (i.e., limestones were thin sectioned; clays and silts were disaggregated), to liberate the foraminifera and differentiate the species. Where it was not possible to break down the sediments, thin sections were made in order to determine foraminifera and the relative abundance of the assemblages in the samples. Liberated foraminifera were utilised for the determination of both biostratigraphy and palaeoenvironmental change.

2.2.1. Preparation

White Spirit Method

Sample composed of clays and silts were processed using the white spirit method of Brasier (1980). According to this process samples were broken down into $<1\text{cm}^3$ fragments, dried in an oven overnight at $\sim 40^\circ\text{C}$, cooled and weighed. The sample fragments were then placed in beakers in a fume cupboard and white spirit was poured onto each sample. Samples were covered with the white spirit and the effectiveness checked visually (air bubbles seen leaving the rocks). While soaking was taking place the bowls were covered in 'cling-film' to contain vapour and placed in a fume cupboard. The samples were left until they were completely saturated; the time of saturation varied from 30 minutes to 8 hours depending on the porosity and type of lithology. In order to achieve full absorption, the samples were kept in white spirit for 8 hours. Upon saturation the excess white spirit was removed and hot water was poured onto the samples until covered. The samples were then allowed to break down, being gently and intermittently stirred throughout the process. Once breakdown was completed the samples were thoroughly washed over a $63\ \mu\text{m}$ sieve to remove any residue of the white spirit and wash out the finer clay and silt. A portion of the $<63\ \mu\text{m}$ sample was collected for geochemical analysis. The $>63\ \mu\text{m}$ portion was washed, collected, dried in a cool oven and weighed. The residues were then placed in sample storage tubes prior to analysis.

Cold acetolysis Method

The "cold acetolysis" method of Lirer (2000) has been applied in a number of studies (e.g., Fornaciari et al., 2007; Luciani et al., 2007; Coccioni et al., 2004)

to disaggregate strongly lithified samples where standard methods are not successful in disaggregation. Luciani et al. (2007) tested this method against standard methods and found no differences in the assemblage composition obtained from these two different methods.

According to previous workers this method is very effective in the disaggregation of highly lithified rocks in a short time. Some argue that it can also be used to “clean” samples processed by other methods making microscope work easier. Lirer (2000) applied this method on Tertiary sediments of the central and southern Apennines (Italy) and found it very effective and useful. This method uses cold digestion with highly concentrated acetic acid. Similar techniques (but with diluted acetic acid) are commonly used to disaggregate conodonts from samples (**Table-2.1**).

According to the “cold acetolysis” technique the strongly lithified samples are broken down into small fragments of about 5mm in diameter. The small size of the samples will increase the surface area and will allow the acetic acid to react faster. A solution called “ethanoic acid” CH_3COOH (80% acetic acid and 20% H_2O) is prepared. The small fragments of sample are then placed in a glass beaker and are covered with ethanoic solution in such a way that the level of solution remains 2cm higher than the sample fragments. This solution slowly disaggregates the rock. In order to avoid any damage to the fossil content, Lirer (2000) recommended a continuous check while the samples are in the solution. In cases where the amount of acetic acid is not sufficient to cover the rock fragments, the sample may harden by absorbing all the acetic acid. In such cases it is sufficient to place the sample into an ultrasonic cleaner to dissolve it. The time of disaggregation varies with different rock types (**Table-2.2**). The time

of disaggregation for each sample is decided according to its type and strongly lithified samples are allowed to stay in the solution for a relatively longer period of time. Regular checks should be made until the disaggregation is completed.

On completion of reaction the samples are immediately removed from the solution to prevent etching of the foraminifera by the prolonged contact with the acid. The samples are then washed over a 63 μ m sieve with abundant deionised water to collect the residue and eliminate any remaining acid from the sample. If the residue still contains inorganic matter and the foraminifera are not completely clean, the residue is dipped again in a beaker containing water diluted Desogen and is placed into an ultrasonic cleaner for one to two hours (**Table-2.2**). After thorough washing (care is taken to prevent the contact between skin and the residue) the sample is dried overnight at <40 $^{\circ}$ C, cooled and dry sieved on a 63 μ m sieve. After weighing the samples are then placed in specimen tubes to get them ready for analysis.

This method was tested in this study but was not found as useful as described in previous works. It was also costly both in terms of time and expense compare to white spirit method. The foraminifera obtained through this method were found to be etched by acid reaction. The white spirit method was, therefore, used for the material from the Indus Basin.

Thin Sections

Lithified sedimentary rocks which could not be processed with the above methods were thin sectioned in order to analyse their foraminiferal components as well as their sedimentological characteristics. Selected samples were cut into

billets using the cutter machine. These billets were then mounted on the glass slides using the "magic fast" and ground down using a grinding machine. They were then polished with the help of abrasive powder. This grinding powder, which is silicon carbide powder, is available in different sizes; i.e., 100, 220, 400, 600, 800, and 1000. By using a combination of these powders the specimen is polished to a very thin size (i.e., 30 micron and >30micron in carbonate rocks) suitable for microscopic examination.

Picking

Care was taken in picking a representative measure of the fauna from a sample in order to ensure unbiased analysis of all samples. There is no absolutely standard method adopted by every worker but it is obvious from existing literature that a number of variables such as sieve size, splitting sample into fractions and number of individuals per sample (the figure of 300 or 301 is often quoted as a minimum) must be decided in developing a picking rationale and these variables depend on the nature of sediment, foraminiferal assemblages and purpose of study (e.g., biostratigraphy and palaeoenvironment).

Most of the previous work done on Tethyan sediments used >100 μ m (mostly 125-500 μ m) fraction size for the analysis of foraminifera: e.g., Speijer et al. (1996), Kouwenhoven et al. (1997), Speijer et al. (1997), Speijer & Schmitz (1998), El-Dawy (2001) and Orue-Etxebarria et al. (2001). In this study the >63 μ m residue was sieved and picked at two different sieve sizes: i.e., 63-125 μ m and 125-630 μ m. The smaller fraction was only scanned for age

diagnostic foraminifera and important palaeoenvironmental indicators. This small fraction provided a better spectrum of potential indicator species and larger assemblages (>300 specimens) were produced. When using a larger sieve size small but potentially important environmental indicator species may be lost especially within the stressed marine conditions of the P-E transition (Ortiz 1995; Alegret et al., 2005) and may create artificial barren intervals in samples dominated by small sized species. This is particularly important for clay rich sediment with rare foraminifera (Fisher, 2006).

Each sample was examined on a gridded tray and >300 specimens were picked to obtain a representative assemblage of the species present. Phelger (1960) suggested that 301 specimens provide sufficient accuracy for most quantitative studies.

Methods of analysis

The foraminifera were identified using the works of LeRoy (1953), Samanta (1973), Berggren & Aubert (1975), Aubert & Berggren (1976), Tjalsma & Lohmann (1983), Van Morkhoven et al. (1986), Kaminski et al. (1989), White (1989), Speijer (1994), Afzal (1997) and Warraich et al. (2000). Counts of key genera were calculated as percentages. Foraminifera in the thin section were photographed using a petrographic microscope and scanning electron microscopy was undertaken utilizing the facilities of the Electron Microscopy Centre at the University of Plymouth, UK.

2.3. Stable Isotopic Analysis

In order to gain isotopic information on the whole water column, $\delta^{13}\text{C}$ and $\delta^{18}\text{O}$ analyses were carried out on both bulk and fine fraction (<63 μm) specimens of carbonate and organic components of the samples.

2.3.1. Preparation

Bulk isotopic analysis

For samples that had been processed for foraminiferal analysis, bulk isotope analysis was carried out on the fine (<63 μm) fraction of the sediment samples. This fraction was chosen over ground homogenised whole rock samples in order to control the source of the carbonate in the sediment being analysed and, therefore, the part of the water column that the isotope results represent. The <63 μm fraction was collected during the processing of the samples for foraminiferal analysis. Following the breakdown of sediments as outlined above, a portion of the <63 μm fraction can be collected as the samples are washed over a 63 μm sieve to collect the coarser foraminiferal portion. In the <63 μm size fraction carbonate allochems such as shell fragments and foraminifera found in the coarser fractions, can be kept to a minimum. Therefore, the results from the fine fraction are thought to represent the isotopic composition of the surface waters. The fine fraction samples were collected in a basin placed below the 63 μm sieve. As a lot of water was also collected the samples were filtered through filter paper in order to remove the water and the samples were then placed in an oven at 40°C overnight until dry. Once dried the samples were

Stouge & Boyce (1983)	Lirer (2000)
1) dilution of acetic acid made up of 10-15% of CH ₃ COOH and 90-85% H ₂ O	1) dilution of acetic acid made up of 80% of CH ₃ COOH and 20% of H ₂ O
2) disaggregation time at least 1 week to obtain the first results	2) disaggregation time at least 2 hours
3) change of acid at least 2-3 times	3) no change of acid
4) to keep the sample in a plastic or polyethylene bucket	4) to keep the sample in a beaker to continuously check the disaggregation
5) no ultrasonic cleaner	5) use of ultrasonic cleaner
6) size of fragments about 5cm in diameter	6) size of fragments about 5mm in diameter

Table-2.1: Comparison between the Stouge & Boyce (1983) disaggregation technique and the technique of Lirer (2000, text-figure 1).

Lithologies	<u>Time/hour Acetic acid</u>	<u>Time/hour ultrasonic cleaner</u>
fine-grained clacarenite	at least 10	at least 2-3
calcilutite	5-7	1 to 2
marly-limestone	5	1 to 2
marly-limestone	2-3	1 to 2
shaly-marl	2	1 to 2

Table-2.2: Times of dipping in acetic acid and of the ultrasonic cleaner treatment for different studied lithologies (Lirer, 2000, text-figure 2).

removed from the beakers and ground in an agate pestle and mortar to homogenize the sediment ready for analysis. The samples were then weighed and placed in small sample bags to await analysis.

Organic isotopic analysis

After crushing and forming a powder by using an agate pestle and mortar, the bulk samples and the <63 μ m fractions obtained during the processing of the samples for foraminiferal analysis were de-carbonated using 10% HCL and neutralised by repeated washing with distilled and deionised water before organic carbon isotope analysis. The bulk de-carbonated samples dominantly represent the complete organic components present both in the water column and on the sea floor. The <63 μ m de-carbonated fraction represents the organic component of the water column.

2.3.2. Instrumentation

In order to analyse the isotopic composition of the bulk carbonate, fine fraction carbonate, bulk organic and fine fraction organic a number of different mass spectrometers were used. A brief outline of the instruments used in this study is given below.

Isotope methods for carbonate analysis

Initially the $\delta^{13}\text{C}$ and $\delta^{18}\text{O}$ analyses on the fine fraction carbonate from the Rakhi Nala section were undertaken at the University of Plymouth. Due to the variation in carbonate content in the samples, the amount of sediment for analysis was calculated according to the carbonate content present in the

samples (**Table-2.3**). The samples were reacted with 100% phosphoric acid at 90°C. The evolved CO₂ was analysed on a GV Instruments Isoprime Mass Spectrometer with a Gilson Multiflow carbonate auto-sampler. The results were calibrated against Vienna Pee Dee Beleminte (VPDB) using the international standard NBS-19 (National Bureau of Standards 19; $\delta^{13}\text{C}=1.95\text{‰}$, $\delta^{18}\text{O}=-2.20\text{‰}$). Reproducibility of replicate analyses for both $\delta^{13}\text{C}$ and $\delta^{18}\text{O}$ was better than 0.2‰.

Due to the low carbonate content of some of the samples there was a need to use sample masses above those recommended for the technique. As a result of the excess mass there was an incomplete reaction with the acid, which led to fractionation of the isotopes.

In order to confirm the results from the University of Plymouth Mass spectrometer, oxygen and carbon isotope analyses on the same fine fraction carbonate were undertaken at the Natural Environment Research Council (NERC) Isotope Geosciences Laboratory at the British Geological Survey in Keyworth, UK. Each sample was analysed using standard offline vacuum methods (McCrea, 1950) on a dual inlet stable isotope mass spectrometer.

Isotope methods for organic analysis

The organic carbon content of the samples was measured using a Carlo Erba 1500 elemental analyser at the NERC Isotope Geosciences Laboratories (NIGL) at Keyworth (UK). Acetanilide was used as the calibration standard. Samples were weighed into tin capsules. Replicate analyses indicated a precision of $\pm 0.1\%$ in well-mixed samples (1 Standard Deviation, SD).

The organic carbon $^{13}\text{C}/^{12}\text{C}$ analyses were performed at NIGL using a Carlo Erba 1500 EA online to a VG TripleTrap plus a secondary cryogenic trap in the mass spectrometer for these very low carbon values were calculated to the VPDB scale using a within-run laboratory standard (BROC1) calibrated against NBS 19 and NBS 22. Replicate analysis of well-mixed standards indicated a precision of $\pm <0.1\%$ (1 SD).

2.4. Total organic carbon; Loss on ignition method

Total Organic Carbon (TOC) analysis was carried out at the National Centre of Excellence in Geology (NCEG), University of Peshawar, Pakistan. Samples were analysed for TOC using the loss on ignition (LOI) method. This method is commonly used to estimate the organic and carbon content of sediments (e.g., Dean, 1974; Bengtsson & Enell, 1986). Around 200-500mg of sediment was placed in weighed crucibles. The sediment was then weighed and dried in an oven overnight at 105°C. Once dried and cooled they were weighed again to determine the dry weight. Samples were then placed in a muffle furnace at a temperature of 550°C for two hours. At this temperature any organic matter in the sediment will become oxidized to carbon dioxide and ash. The samples were then removed from the furnace, cooled and weighed again. The amount of organic matter can then be calculated as a weight percent using the weight loss measured. The samples were then returned to the furnace at a temperature of 950°C for four hours to determine the weight percent of carbonate in the sample. At 950°C the carbonate in the samples will release carbon dioxide. Once removed from the furnace the samples were again cooled and weighed to

determine the weight loss and weight percent of carbonate in the samples. The concentrations of calcium carbonate were calculated for all samples by using (% weight of inorganic carbon x 8.33). Dean (1974) evaluated the method and concluded it was a fast, effective and inexpensive method of determining the carbonate and organic content of sediments. However, Dean (1974) indicates that the method may not be as good for clay-poor sediments and notes that various losses of salts, structural water and inorganic carbon can occur. Bengtsson & Enell (1986) warn that clay may lose structural water during LOI and, according to Ball (1964), this can occur at temperatures as low as 500°C, causing a weight loss of up to 20% in clay minerals.

When the TOC for isotopic analysis was also calculated at the NERC Isotope Geosciences Laboratories (NIGL) at Keyworth (UK), using Carlo Erba 1500 elemental analyser as mentioned earlier, the weight percentages of organic carbon were found to be much higher in the LOI method. This was thought to be due to the high clay content of the sediments and the presence of interstitial waters.

Td sample	Carbonate Wt%	Approx weight for <63 μm $\delta^{13}\text{C}$			
		1st run	2nd run	3rd run	4th run
30	10.2	2.0	2.0		
31	10.7	1.9	1.9	1.9	
32		2.0	2.0	2.0	
33	11.2	1.8	1.8		
34	14.8	1.4	1.4	1.4	
35	2.5	7.9	15.8		
36	2.1	9.4	18.8	18.8	18.8
37	2.2	9.1	18.2	36.4	37.0
38	2.8	7.1	14.2	28.4	14.2
39	6.1	3.3	3.3	3.3	
40	8.4	2.4	2.4	2.4	
41	12.0	1.7	1.7	1.7	
42	17.1	1.2	1.2		
43	18.8	1.1	1.1	1.1	
44	16.2	1.2	1.2		
45	16.6	1.2	1.2		
46	24.8	0.8	0.8	0.8	
47	17.6	1.1	1.1		
48	13.4	1.5	1.5	1.5	
49		2.0	2.0	2.0	
50		2.0	2.0	1.5	
51		2.0	1.0	1.0	
52		2.0	2.0	10.0	20.0
53		2.0	2.0	10.0	10.0
54		2.0	6.0	10.0	10.0
55		2.0	6.0	10.0	15.0
56		2.0	6.0	10.0	20.0
57		2.0	6.0	10.0	20.0
58		2.0	6.0	10.0	30.0
59		2.0	6.0	10.0	

Table-2.3: The amount of sample analysed for stable isotopes (fine fraction carbonate) and the carbonate weight percent.

Chapter 3: Introduction to the lithostratigraphy and the “field geology”

3.1. Introduction

The geological history of the terrain covered by Pakistan is very complex as it is situated along the contact between the Indo-Pakistan and the Eurasian Plates. The depositional history of the Indo-Pakistan Plate, along with volcanic events, pre- and post-collision events and accretion of the Arabian Plate are reflected in the stratigraphic succession exposed in Pakistan. Sedimentary sequences that range from Precambrian to Recent were deposited along the western wedge of the Indian Shield.

The Tethys Ocean occupied the region between the southern margin of the Eurasian Plate and north of the Indo-Pakistan Plate. This ocean closed gradually as a result of the northward movement of the Indo-Pakistan Plate and several microplates lying in-between were attached to the Eurasian Plate, along with the sedimentary sequences of the Indo-Pakistan Plate (Bender, 1995). In the Pakistani Himalayas, the Eurasian Plate is separated by the Main Karakoram Thrust (MKT) in the north and the Indo-Pakistan Plate by the Main Mantle Thrust (MMT) in the south of the famous Kohistan Island Arc (Tahirkheli et al., 1979). The Sulaiman and Kirther ranges lie in a transpressional zone on the northwest and west respectively resulting from the collision between the India and Afghan Blocks (e.g., Banks & Warburton, 1986; Humayon et al., 1991; Jadoon, 1991; Jadoon et al., 1992; Davies & Lillie, 1994; Warraich et al., 1995) (Fig. 3.1).

The Mesozoic to Paleogene sedimentary sequence is widely exposed along the northwestern margin of the Indus Basin of the Indian subcontinent,

central Pakistan. This is the sedimentary cover of the Indo-Pakistan Plate that was folded during the continent-to-continent collision with the Eurasian Plate and which formed several fold and thrust belts such as the Kirther, Sulaiman and Salt ranges. These sediments were deposited in the Tethys Ocean that once covered the region between the southern margin of the Eurasian Plate and the north of the Indo-Pakistan Plate (e.g., Banks & Warburton, 1986; Humayon et al., 1991; Jadoon, 1991; Jadoon et al., 1992; Davies & Lillie, 1994; Warraich et al., 1995; Beck et al., 1995; Robinson et al., 2000) . These sediments are exposed along the Kirther, Sulaiman and Salt ranges which are seen from south to north in Pakistan. The Indus Basin can be subdivided into three depositional provinces:

- a. The Potwar-Kohat depositional province (Upper Indus Basin);
- b. The Sulaiman depositional province (Lower Indus Basin); and
- c. The Kirther depositional province (Lower Indus Basin).

The Potwar-Kohat depositional province is separated from the rest of the Indus Basin by a west-northwest-trending positive axis which extends from the Indian Shield through the Kirana-Sargodha Hills. The Khisor Range, where Paleocene rocks are absent, may be the surface expression of this axial trend. The Paleocene rocks of this province consist, in ascending order, of the Hangu, Lockhart and Patala formations (**Figs 3.2, 3.3**). The Paleocene rocks gradually thin southeastwards toward the eastern end of the Salt Range, suggesting a shoreward shallowing of the sea during Paleocene time (Gibson, 1990).

The Sulaiman depositional province is also separated from the Kirther province in the south by the sub-surface high known as the Jacobabad High. The Paleogene sequence of the Sulaiman Range consists of the Paleocene-

Eocene Dungan Formation, the early Eocene Shaheed Ghat and Baska formations, and the mid-late Eocene Kirther Formation, all of which overlie the Mesozoic marine shelf sediments (**Figs 3.4, 3.5**). The Paleogene fauna reported from the Dungan Formation include abundant tropical and sub-tropical indicators, suggesting a habitat of tropical-subtropical Tethyan waters (Warraich et al., 2000).

The Kirther depositional province is comparable in size to the Sulaiman province; both are more than three times as large as the Potwar-Kohat province (**Fig. 3.1**). The Paleocene sequence of the Kirther province consists of the Ranikot Group which includes (in ascending order) the Khadro, Bara and Lakhra formations. The Lakhra Formation of this province can be correlated with the Patala Formation of the Potwar-Kohat depositional province and with the upper part of the Dungan Formation of the Sulaiman province.

3.2. Lithostratigraphy

3.2.1. Salt Range, Punjab (Upper Indus Basin)

For many years the Upper Indus Basin has been a centre of geological and palaeontological activities as a result of the oil producing Potwar depression. Around this depression a number of geological elements are found. In the north, it is surrounded by the Kala Chitta Range and Margala Hills and on the southern side by the Salt Range (**Fig. 3.1**). The name Salt Range is derived from the occurrence of gigantic deposits of rock salt embedded in the bright red marls of the Precambrian, stratigraphically known as the "Salt Range Formation" (formerly "Punjab Saline Series"). The Salt Range is essentially an

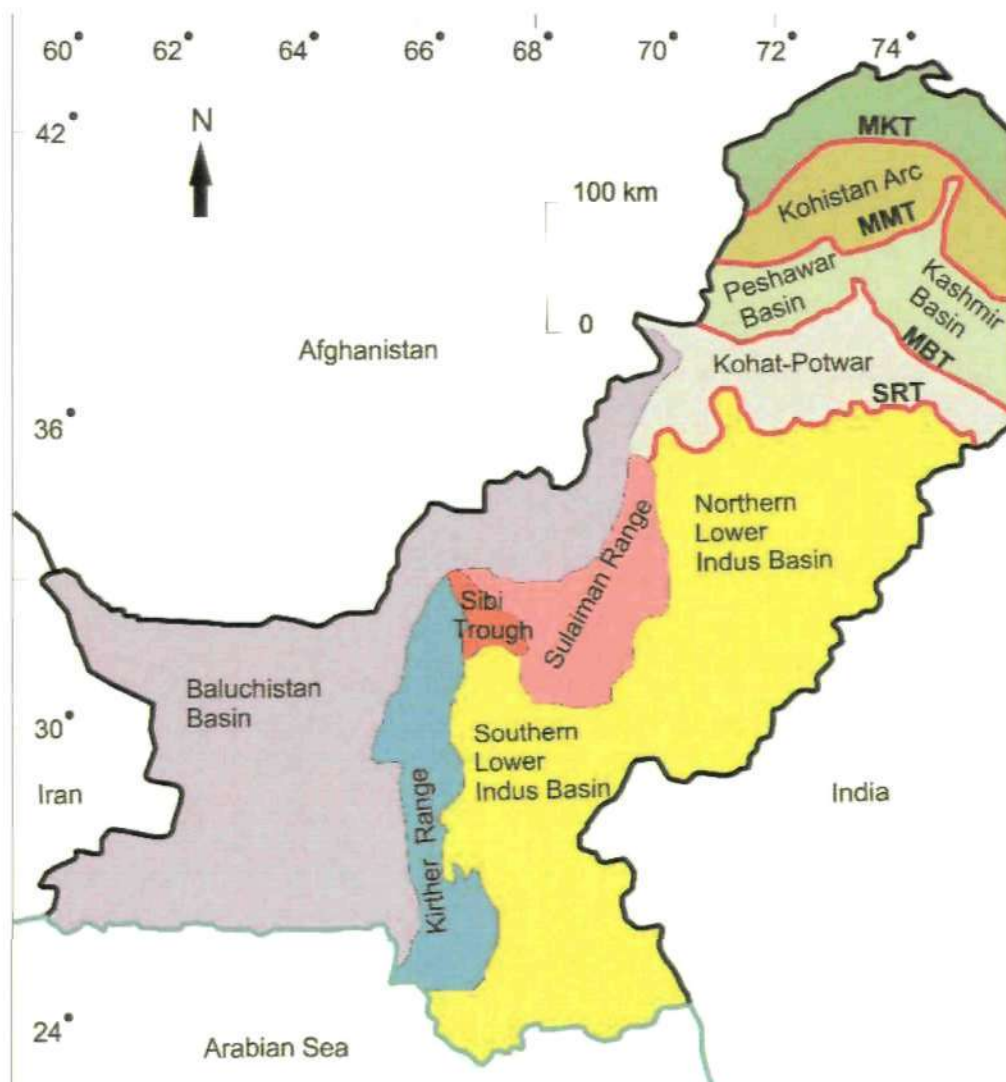


Fig. 3.1: Geological map of Pakistan showing main geological features; **MKT**- Main Karakoram Thrust, **MMT**- Main Mantle Thrust, **MBT**- Main Boundary Thrust, **SRT**- Salt Range Thrust. N. B. Colours of the different units are simply to identify the regions discussed in the text. Green coloured area indicates Karakoram Block.

E-W trending, elongated narrow mountain belt deeply cut by the River Indus near Kalabagh, from where it takes a sharp turn, like a hair-pin bend, running in almost a N-S direction (**Fig. 3.1**). It has a great variety of geological features for which it is rightly known as the "Field Museum of Geology" where strata from the Permian to Cenozoic are richly fossiliferous, contain diagnostic faunas and are almost completely exposed due to a lack of vegetation (**Fig. 3.2**). Apart from the easily available road-side geology, there are some prominent gorges which provide fantastic locations for the study of the Pre-Cenozoic and Cenozoic sedimentary succession.

Pioneer palaeontological investigations sub-divided the lower Cenozoic sediments into three time-rock units; i.e., the Ranikot Group, Kirther Series and Laki Series (Blandford, 1876). Later a six fold sub-division for the lower Cenozoic sediments was introduced (Davies, 1935; Pinfold, 1939). As they are *Nummulites*-bearing both the Ranikot and Laki sediments were previously considered to be of Early Eocene age (e.g., Blandford, 1876; Noetling, 1903; Pinfold, 1939; Davies, 1935). Further palaeontological research has suggested that the Ranikot Beds are, in fact, Paleocene in age (Haque, 1956; Adams, 1970). For all practical purposes therefore, the lithological boundary between the (Paleocene) Ranikot Beds and the (Eocene) Laki Series (i.e., the currently recognised contact between the Patala and Nammal formations) throughout the Upper Indus Basin was used to mark the Paleocene/Eocene boundary. This was considered concomitant with the extinction level of the larger foraminifera *Miscellanea miscella* and *Lockhartia haimei* (Adams, 1970). Within the succession of deeper marine strata, where this group of fossils was completely missing, only the lithological boundary between Patala and Nammal formations

was used to mark this boundary. In some areas the placing of the lithological boundary is, in itself, controversial. Some workers have placed the Paleocene/Eocene boundary within the lower part of overlying Nammal Formation (Haque, 1956).

Subsequently, the dating of these rocks through the use of other groups of fossils (i.e., planktonic foraminifera, calcareous nannoplankton and dinoflagellates) opened a new approach. Using these groups of fossils, the Paleocene/Eocene boundary was placed within the lower part of the Patala Formation in the Khairabad area (i.e., at the highest occurrence (HO) of *Morozovella velascoensis* and/or lowest occurrence (LO) of *Acarinina wilcoxensis berggreni* and LO of *Tribrachiatus bramlettei* (Weiss, 1988, 1993; Kothe et al., 1988; Afzal & von Daniels, 1991). The placing of this boundary is still controversial (see Gibson, 1990). As a result of these biostratigraphical investigations, it was recognised that a major facies change may exist in this area. In such an area, where a major facies change from very shallow water to deep marine occurs, demarcation of the Paleocene/Eocene boundary is not a simple task especially in the situation like the Indus Basin where the Paleocene/Eocene boundary has not been officially defined. Therefore, a more suitable criteria is needed to be worked out to define this boundary for the Salt Range.

Lockhart Limestone Formation

Shah (1977) reported that the Lockhart Limestone was named by Davies (1930) from exposures near Fort Lockhart, about 5 miles west of the border of the Kohat quadrangle. Meissner et al. (1974, 1975), Wells (1984) and Pivnik (1992)

studied the lithofacies relationships of the Lockhart Limestone Formation and interpreted the unit as being deposited in a Paleocene shallow marine environment prior to the collision between India and Asia. According to Afzal (1997) the uppermost beds are fossiliferous, medium to dark brownish grey, cliff forming, nodular limestones containing abundant foraminifera, bivalves, gastropods, echinoid fragments, bryozoans, ostracods, corals and algae. This fossil assemblage is indicative of a shallow marine environment (carbonate platform). Shah (1977) correlated the formation with the Bara Formation and the lower parts of the Dungan and Rakhshani formations of the Lower Indus Basin. Only the top-most bed yielded the planktonic foraminifera that reflect a very brief and short term sea level rise (Afzal, 1997).

Wells (1984) and Yeats & Hussain (1987) considered its deposition was in a Paleocene-Eocene foreland basin. The Lockhart Limestone weathers, in places, into rounded nodules and is brecciated (as was observed by Davies, 1930) in its lower part near Fort Lockhart.

The lithological characteristics of the Lockhart Limestone Formation and the presence of larger and smaller benthonic foraminifera suggest that the unit was deposited in an high energy, shallow marine environment (Shafique, 2001). The following larger benthonic foraminifera are reported; *Miscellanea miscella*, *Rotalia trochidiformis*, *Lockhartia haimi*, *L. conica*, *Operculina patalensis*, *O. jiwani*, *O. salsa*, *Redmodina henningtoni* and *Discocyclina ranikotensis*. The smaller benthic foraminifera are represented by *Cibicides alleni*, *Cribogloborotalia challinori* and *Anomalina* spp. On the basis of this assemblage Middle to Late Paleocene age has been assigned to the Lockhart Formation

(Afzal, 1997). It is also noted that "The formation conformably and transitionally overlies and underlies the Hangu Formation and Patala Formation respectively" (Shah, 1977).

Patala Shale Formation

The term Patala Formation was formalized by the Stratigraphic Committee of Pakistan for the Patala Shale of Davies & Pinfold (1937) and its usage was extended to other parts of the Kohat-Potwar and Hazara areas. According to Shah (1977) the formation includes the Tarkhobi Shales of Eames (1952a, b), part of the Hill Limestone of Wynne (1872) and Cotter (1933), part of the Nummulitic Formation of Waagen & Wynne (1872), part of the Nummulitic Series of Middlemiss (1896) and the Kuzagali Shale of Latif (1970).

This formation in the Salt Range area comprises dark greenish grey, selenite-bearing (probably the result of weathering) and in places carbonaceous and calcareous shales and marl. There are subordinate white to light grey and nodular limestone and yellowish brown calcareous sandstone (Shah, 1977).

The lower part of the Patala Shale Formation is a dark grey to brownish grey shale, in places gypsiferous, with common layers of medium grey, thin, nodular limestone. The middle unit is composed of dark brownish grey shale with very thin beds of claystone, sandstone and limestone. The middle unit is in places glauconite bearing. The lower and middle parts are rich in larger foraminifera. Other important constituents are ostracods, bivalves, corals, fish teeth, echinoid fragments, algae, bryozoans, etc. The top of the formation is marked by a thin layer of dark, rusty brown, sandy, fossiliferous, ledge-forming

limestone. This limestone ledge is overlain by dark grey to black shale, rich in planktonic, smaller and larger foraminifera (Afzal, 1997). The Patala Shale Formation has a transitional lower contact with the Lockhart Limestone Formation (Porth & Raza, 1990; Kothe et al., 1988). The lower-most part of the Patala Shale Formation indicates an environment representing the deeper part of a shelf with an open marine influx. The remainder of the lower portion indicates a restricted marine lagoonal environment. The middle and upper part of the formation suggest a deepening of the environment (Afzal, 1997). Based on the fauna recovered from Patala Shale Formation, it has been assigned a late Paleocene and early Eocene age (Gibson, 1990) and is correlated with the Dungan Formation of the Sulaiman province. According to Shah (1977) "the Patala Formation is conformably and transitionally overlain by the Nammal Formation in the Salt Range, the Panoba Shale in the Kohat area and the Margala Hill Limestone in the Hazara and Kala Chitta areas".

Nammal Formation

According to Shah (1977) the term Nammal Formation has been formally accepted by the Stratigraphic Committee of Pakistan for the Nammal Limestone and Shale of Gee (in Fermor, 1935) and Nammal Marl of Danilchik & Shah (1967) occurring in the Salt and Trans-Indus ranges. The Nammal Gorge section in the Salt Range is the type section for the Nammal Formation (Shah, 1977).

The Nammal Formation consists of alternations of shale (grey to olive green) and limestone (light grey to bluish grey and argillaceous in places) and it has a lower contact with the Patala Shale Formation and an upper contact with

the Sakesar Limestone Formation with both the contacts being transitional (Shah, 1977). The lower part of the Nammal Formation is predominantly light olive-grey to bluish-grey marl with light to medium grey, thin to medium bedded limestone. The upper part is light bluish grey, medium bedded, cliff-forming limestone; both upper and lower parts are rich in planktonic and smaller benthonic foraminifera. The lower part indicates deep inner to middle shelf environments, while the upper part of the formation is suggestive of an inner shelf environment (Afzal, 1997).

3.2.2. Sulaiman depositional province, Punjab (Lower Indus Basin)

The Sulaiman depositional province extends south-southwest from the Khisor Range to the town of Quetta. The Sulaiman depositional province is separated from the Kirther depositional province by the Jacobabad sub-surface high in the south while, to the north, it is separated from the Kohat-Potwar depositional province by the Kirana-Sargodha Hills which are a surface exposure of the Indian Shield. The Sulaiman Range is a broad fold and thrust belt of the Himalayan Mountains. It has a lobe shape along with the Kirther Range and was formed as a result of the oblique collision of the Indo-Pakistan Plate with the Afghan Block in a transpressional zone on the northwest and western margin of the Indo-Pakistan Plate (Yeats & Lawrence, 1984). The Sulaiman Range is bordered by an ophiolite and flysch belt on the western side, whereas it forms the continuation of the Kirther Range around the tight arc of the Sibi Trough, where it is separated by a broad fold overlain by the alluvial deposits of the Indus River system in the east (**Fig. 3.1**).

Age		Upper Indus Basin																	
		Sub Basins and Formations																	
		Salt Range and Potwar						Kohat											
Quaternary	Pleistocene	Lei Conglomerate																	
Tertiary	Pliocene	Siwaliks Group	Soan Fm																
			Dhok Pathan Fm																
			Nagri Fm																
	Miocene	Rawalpindi Group	Chinji Fm																
			Kamlial Fm																
	Oligocene	Unconformity	Murree Fm																
	Eocene	Charat Group							Kohat Fm										
									Kuldana Fm										
									Chorgali Fm			Jatta Gypsum			Bahadur Khel Salt				
Sakesar LSt									Shekhan Fm										
Nammal Fm									Panoba Shale										
Paleocene										Patala Fm									
	Lockhart Fm																		
	Hangu Fm																		

Fig.3.2: Generalized Cenozoic stratigraphy of the Upper Indus Basin; yellow coloured areas with vertical bars indicate hiatus (after Shah, 1977); **Fm** = Formation, **LSt** = Limestone.

Age	Blandford (1876)	Noetting (1903)	Pinfold (1934)	Davies (1935)	Haque (1956), Naggap (1959), Adams (1970)	Shah (1977)	Afzal (1997)								
Eocene	Kirther Series	Kirther Series	Kirther Series		Kirther Series		Kirther Series	Chorgali Formation	Chorgali Fm						
			Laki Series	Bhadrar Beds	Laki Series	Bhadrar Beds				Laki Series	Bhadrar Beds				
				Sakesar Lst		Sakesar Limestone									
		Nammal Lst and Shale		Nammal Lst and Shale											
		Laki Series	Patala Shale	Laki Series	Khairabad Lst (Lockhart Lst)	Laki Series	Laki Series	Sakesar Lst	Sakesar Formation	Sakesar Fm					
			Dak Pass Beds (Hangu Fm)		Nammal Lst and Shale										
	Ranikot Group		Ranikot Group		Ranikot Group						Ranikot Group	Laki Series	Nammal Lst and Shale	Nammal Formation	Nammal Fm
		Lockhart Fm													
	Ranikot Group	Ranikot Group	Ranikot Group	Ranikot Group	Laki Series	Ranikot Group	Patala Fm (Patala Shale)	Patala Fm	Patala Fm						
Lockhart Fm															
Hangu Fm															
Paleocene					Ranikot Group	Lockhart Lst (Khairabad Lst)	Lockhart Fm	Lockhart Fm							
						Hangu Fm (Dak Pass Beds)	Hangu Fm	Hangu Fm							

Fig.3.3: Generalized Paleocene-Eocene stratigraphy of the Salt Range (Upper Indus Basin), **Fm** = Formation, **Lst** = Limestone

Previous work on the Sulaiman Range has resulted in a great deal of published literature. Warraich & Natori (1997) compiled and summarized the existing and some very old literature. They reported that Blandford (1883), Oldham (1890), Davies (1939), Pinfold (1939) and Eames (1952b) had produced some basic stratigraphical work, whereas Shah (1977; 1987; 1990) has compiled an updated stratigraphy. Hemphill & Kadwai (1973) did the initial mapping in the northern Sulaiman Range while the Hunting Survey of Pakistan completed the major reconnaissance mapping. Sarwar & Dejong (1979), Banks & Warburton (1986), Lillie et al. (1989), Jadoon et al. (1992; 1993), Jadoon (1991, 1992), Humayaon et al. (1991), Warraich et al. (1995), Jones (1997), Warwick et al. (1998) and Warraich et al. (2000) have discussed the structural and tectonic development and stratigraphy of the different parts of the Sulaiman Range.

The end of the Mesozoic is marked by a period of emergence in parts of Pakistan. The Cenozoic rocks, therefore, have an unconformable lower contact with older units and the same is reported from the Sulaiman Range by the Hunting Survey Corporation Ltd (1961). Cenozoic rocks were deposited in a broad sea that gradually narrowed and retreated southwards with the passage of time to occupy its present position as the Arabian Sea. The rocks of the Cenozoic exhibit a variation in thickness and lithology in different areas. However, the Paleocene and Eocene sediments are mainly limestone and siltstone/mudstone whereas the younger sediments are dominantly sandstone, siltstone and mudstone (Warraich et al., 2000). The Paleocene sediments are almost entirely representative of marine environments. The Eocene succession consists of limestone, calcareous shale with subordinate sandstone and conglomerate. Locally red beds, gypsum, anhydrite, salt and coal are also

found and described in different parts of the Indus Basin (Warraich & Natori, 1997). Towards the end of the Paleocene, there was a partial emergence followed by submergence in the early Eocene when the sea inundated major parts of Pakistan. Nagappa (1959) has reported a short-lived regression at the end of the early Eocene as a result of which evaporites were formed in the Kohat area. This regression affected a large area, including Kohat, the Southern Indus Basin, the Axial Belt and Baluchistan.

Pab Sandstone Formation

The term Pab Sandstone was introduced by Vredenburg (1906), the name being derived from Pab Range in the Kirther depositional province (Shah, 1977). The formation typically comprises white, cream or brown quartzose sandstone which weathers yellow brown and is medium to coarse grained. The bedding is thick to massive and shows sedimentary structures such as cross-stratification. Marls and argillaceous limestone are found intercalated with the sandstones in places (Shah, 1977; Warraich & Natori, 1997).

Dungan Limestone Formation

The name Dungan Limestone was introduced by Oldham (1890) to a thick limestone succession between the Parh limestone and the Ghazij Formation in the Dungan Hills of the Sulaiman province. Williams (1959) renamed Dungan Limestone as Dungan Formation, and excluded the basal beds (his Fort Munro Limestone Member) which were found to have an unconformable relationship with the rest of the unit (Shah, 1977).

Shah (1977) redefined the Dungan Formation of Williams (1959) and included the Lower Rakhi Gaj Shales, Zinda Pir Shales and Zinda Pir Limestone (lower part) of Eames (1952a, b) and the Dungan Group (excluding the Moro Formation), the Dab Formation and the Karkh Group of the Hunting Survey Corporation Ltd (1961) (**Fig. 3.5**).

The Dungan Limestone Formation consists mainly of nodular to massive limestones with subordinate siltstone, marl, sandstone and limestone conglomerate. The limestone is dark grey to brown and cream white, weathering to brown, grey and buff yellow. The dark blue-grey, brown and olive siltstone, which weathers green, becomes dominant in the southern Sulaiman Range. The Dungan Limestone Formation is widely distributed in the Sulaiman Range. The lower contact of the Dungan Formation is unconformable and marks one of the major unconformities in the basin. The upper contact with the Ghazij Formation is reported to be conformable (Warraich & Natori, 1997). Rich fossiliferous assemblages of foraminifera, gastropods, bivalves and algae have been reported by the Hunting Survey Corporation Ltd. (1961), Latif (1961, 1964), Samanta (1973), Dorreen (1974), Kazmi (1988), Warraich & Natori (1997) and Warraich et al. (2000).

The late Paleocene- early Eocene Dungan Limestone Formation, which is the focus of the present study, is well exposed along the land sections of the Zinda Pir and Rakhi Nala areas and is unconformably underlain by the Cretaceous Pab Sandstone Formation and overlain by the Shaheed Ghat Formation of Eocene age (**Plates 3.1 & 3.2**).

Shaheed Ghat Mudstone Formation

Williams (1959) redefined the Ghazij Group of Oldham (1890) as the Ghazij Formation. Later, Shah (1977) incorporated the Shales and Alabaster, Rubbly Limestone, Green and Nodular Shales, Upper Rakhi Gaj Shales and Zinda Pir Limestone (upper part) of Eames (1952b), Chat beds of Nagappa (1959) and the Ghazij Shales, Tiyon Formation and the upper part of the Gidar Dhor Group of the Hunting Survey Corporation Ltd. (1961) in the definition of the Ghazij Formation (see Warraich & Natori, 1997). Shah (1987, 1990) has published a revised version of his stratigraphy in which he has replaced his Ghazij Formation with the "Ghazij Group" which consists of the following four formations; Baska Formation, Tol Formation, Drug Formation and Shaheed Ghat Formation. Warraich & Natori (1997) revised and re-described both the Shaheed Ghat and Drug formations of Shah (1990) as the Shaheed Ghat Formation. According to Warraich & Natori (1997) the lithology of the Shaheed Ghat Formation dominantly consists of green grey to olive green mudstone, gradually changing from siltstone to nodular siltstone to limestone from the base upwards. Warraich & Natori (1997) retained the Baska Formation of Shah (1977). Hence the Ghazij Group of Shah (1990), as redefined by Warraich & Natori (1997), consists of only two formations; the Shaheed Ghat and Baska formations.

Shah (1987, 1990) introduced the Shaheed Ghat Formation, including within it the Upper Rakhi Ghaj Shales and the Green and Nodular Shales of Eames (1952b), Ghazij Formation of Oldham (1890) and Rakhi Gaj Shale Member of Jamilddin et al. (1971). The Shaheed Ghat Formation is dominantly

composed of olive green, chocolate brown and grey coloured clays, with associated gypsum beds. Subordinate limestone and argillaceous limestone beds occur frequently and irregular calcite veins are described as common in the middle part of the formation (Warraich & Ogasawara, 2001). The age of the Shaheed Ghat Formation is described as Paleocene (Hunting Survey Corporation Ltd, 1961) to early Eocene (Eames, 1952a; Latif, 1964; Samanta, 1973; Warraich & Natori, 1997).

		Age	Thickness (m)	Formation	Lithological Description
Cenozoic		Pliocene and Pleistocene	1493	Chaudhwan Formation	Conglomerate with subordinate sandstone and claystone
		Upper Pliocene	1694	Litra Formation	Silty claystone with subordinate conglomerate and sandstone
		Pliocene	430	Vihawa Fm	Sandstone with subordinate sandy siltstone
		Oligocene Miocene	369	Chitarwata Fm	Shale with subordinate conglomerate and sandstone.
		Middle-Upper Eocene	735	Kirther Formation	Shale with subordinate marl and thick limestone interbeds
			189	Baska Shale	Claystone, bedded alabaster, gypsiferous limestone&marl
		Eocene	2743	Gahzij Formation	Shale with minor amounts of sandstone, conglomerate and limestone.
		Paleocene	190	Dungan Fm	Sandstone and shale in the south and limestone in the north

Fig.3.4: Generalized stratigraphic succession in the eastern Sulaiman Fold Belt; the lithological log is diagrammatic (after Hemphil & Kidwai, 1973).

Age		Sulaiman Range, Southern Indus Basin, Pakistan															
Cenozoic	Oligocene	Eames (1952b)		Shah (1977)		Kazmi (1995)	Warraich (1999)										
		Zinda Pir		Rakhi Nala		Siwalik Group	Chitarwata Formation	Chitarwata Formation									
	Eocene	Late	Pellatispira Beds	Pellatispira Beds	Kirther Formation	Darazinda Member	Darazinda Formation	Kirther Formation	Darazinda Member								
			Upper Chocolate Clays Passage Beds	Upper chocolate Clays Passage Beds						Pir Koh Ls & Marl Member	Pir Koh Limestone & Marl Formation	Pir Koh Limestone & Marl Member					
		White Marl Band	White Marl Band	Sirki Member									Domanda Formation	Sirki Member			
		Lower Chocolate Clays	Lower Chocolate Clays												Habibbrahi Limestone Member	Habibbrahi Limestone Formation	Habibbrahi Limestone Member
		Platy Limestone	Platy Limestone														
	Early	Shales with Alabaster Rubbly Limestone Green and nodular Shale Ghazij Shales Zinda Pir Limestone (Upper Part)	Shales with Alabaster Rubbly Limestone Green and nodular Shale Upper Rakhi Gaj Shales	Ghazij Formation	Ghazij Group	Drug Formation	Ghazij Group	Shaheed Ghat Formation									
									Zinda Pir Limestone (Lower Part)	Lower Rakhi Gaj Shales	Dungan Formation	Dunghan Formation	Dungan Formation				
	Paleocene	Late	Zinda Pir Shales	Zinda Pir Shales	Dungan Formation	Dungan Formation	Dungan Formation	Dungan Formation									
Pab Sandstone			Pab Sandstone	Pab Sandstone					Pab Sandstone	Pab Formation							
Maastrichtian		Pab Sandstone	Pab Sandstone	Pab Sandstone	Pab Sandstone	Pab Sandstone	Pab Formation										

Fig. 3.5: Cenozoic lithostratigraphic correlation of previous workers, yellow colour indicates late Paleocene-early Eocene formations (modified after Warraich, 2000)

Plate 3.1

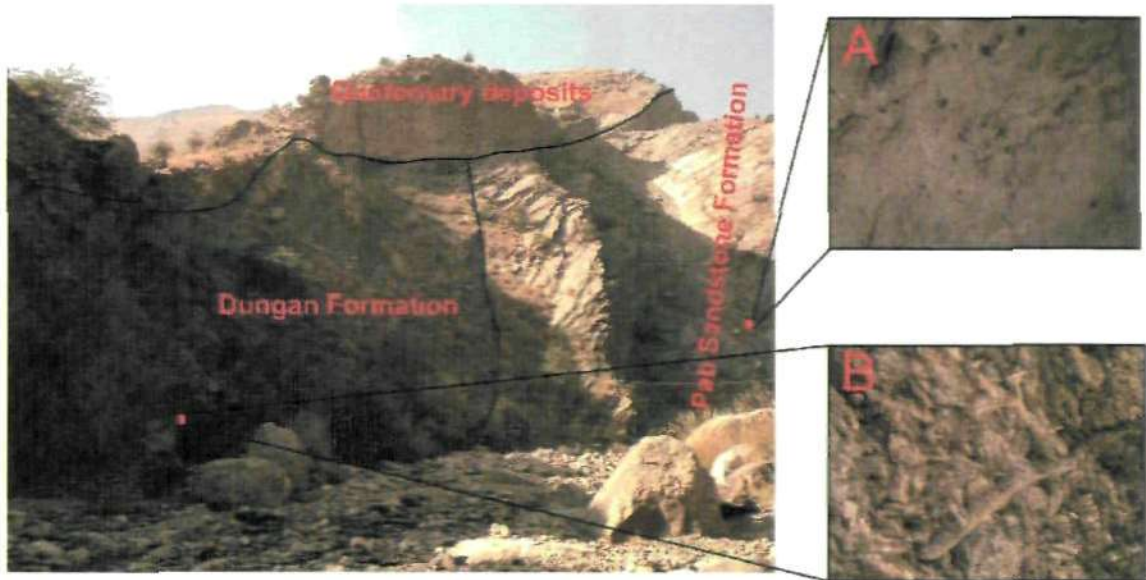


Fig.1: Camera facing west at the contact between Dungan Formation and Pab Sandstone Formation, Rakhi Nala (cliff height approximately 10 m), **A:** Showing quartzose sandstone of Pab Sandstone Formation (Cretaceous), **B:** Showing burrowed calcareous sandstone of Dungan Formation.



Fig.2: Left- Camera facing SW at the intra-formational faulted contact between burrowed calcareous sandstone (A) and Shale (B) of Dungan Formation, Rakhi Nala section (note figure for scale). **Right-** Camera facing East at the shale of the Dungan Formation, Rakhi Nala section (the strata visible is approximately 8 m thick).

Plate 3.2



Fig.1: Camera facing east at the black shale and thin limestone interbeds of the Dungan Formation, Rakhi Nala. Note the figures for scale.



Fig.2: Camera facing NE at the upper most part of the Dungan Formation, Rakhi Nala. Note the figure for scale.



Fig.3: Camera facing east at the Eocene Shaheed Ghat Formation, Rakhi Nala (approximate distance to the nearest point on main cliff is 5m).

Ch 4: Late Paleocene-early Eocene foraminiferal biostratigraphy: A review

4.1. Introduction

Biostratigraphical studies of the Paleogene planktonic foraminifera is thought to have originated in the Former Soviet Union (Berggren, 1960). In the mid-late 1930's (e.g., Glaessner, 1934, 1937a, b; Subbotina, 1934, 1936, 1939; Morozova, 1939) the importance of planktonic foraminifera in biostratigraphical studies had been realized as this group of foraminifera is cosmopolitan in nature and can be applied as a reliable biostratigraphical tool globally. Important biostratigraphical studies/reviews concerning at least part of the Paleogene were subsequently published by Subbotina (1953), Alimarina (1962, 1963), Leonov & Alimarina (1964), Shutskaya (1956, 1958, 1960a, b, 1970), Bolli (1957 a, b, 1966), Shutskaya et al. (1965), Krasheninnikov (1965, 1969), Berggren (1969), Krasheninnikov & Muzylev (1975), Stainforth et al. (1975), Blow (1979), Toumarkine & Luterbacher (1985).

The late Paleocene-early Eocene planktonic foraminiferal biostratigraphy has been improved in the last two decades, due to the great interest dedicated to the Paleocene Eocene Thermal Maximum (PETM) since its discovery by Kennett & Stott (1991). A number of planktonic foraminiferal biostratigraphic zonal schemes across the Paleocene/Eocene boundary have been proposed. These include the following tropical to subtropical planktonic foraminiferal biostratigraphical schemes; Canudo & Molina (1992), Berggren et al. (1995), Arenillas & Molina (1996), Berggren & Norris (1997), Pardo et al. (1999), Molina et al. (1999), Berggren & Ouda (2003), Berggren et al. (2003) and Berggren & Pearson (2005).

An attempt to improve the biostratigraphical resolution across the Paleocene/Eocene boundary has been made by Arenillas & Molina (1996). They proposed the *Igorina laevigata* Zone for the lower part of the *Morozovella velascoensis* Zone of Berggren et al. (1995). It was soon realized that this zone was not applicable as *I. laevigata* is a rare morphotype and may be a junior synonym of *Igornia albeari* (e.g., Blow, 1979; Berggren & Norris, 1997). Later Zone P5 of Berggren et al. (1995) was subdivided by Pardo et al. (1999). This subdivision was based on the Lowest Occurrence (LO) of *Acarinina sibaiaensis* and/or *Acarinina africana*. Following the work of Pardo et al. (1999), Molina et al. (1999) subdivided the *M. velascoensis* Zone of Berggren et al. (1995) into five subzones (see **Figure 1.3** in Chapter 1).

Berggren & Pearson (2005) proposed that the distinct and stratigraphically limited planktonic foraminifera "excursion taxa" are associated with the Carbon Isotope Excursion (CIE). These taxa are of great utility in identifying the Paleocene/Eocene boundary (e.g., Kelly et al., 1996, 1998) which lies within the middle part of Zone P5 of Berggren et al. (1995). Following the work of Pardo et al. (1999) and Molina et al. (1999), Berggren & Pearson (2005) divided Zone P5 of Berggren et al. (1995) based on the LO of one of the excursion taxa, *Acarinina sibaiaensis*. They also used the LO of *Pseudohastigerina wilcoxensis* to further subdivide the older Zone P5.

The Dungan Formation in the Lower Indus Basin and the Patala Formation in the Upper Indus Basin are of late Paleocene-early Eocene age on the basis of planktonic foraminiferal zones (see Latif, 1964; Samanta, 1973; Warraich & Natori, 1997; Gibson, 1990; Afzal, 1997; Warraich et al., 2000;

Shafique, 2001). The Dungan and Patala formations can be correlated and the nomenclature of the existing planktonic foraminiferal biostratigraphical zones of the Indus Basin can be reviewed (**Fig. 4.1**) using the late Paleocene-early Eocene planktonic foraminiferal zones P3 to E2 of Berggren & Pearson (2005). The late Paleocene-early Eocene successions in the Indus Basin also yield larger benthonic foraminifera which have been used in previous research (e.g., Afzal, 1997) to supplement the planktonic foraminiferal biostratigraphy (see **Fig. 4.6**). In order to avoid confusion created by the acronym 'LO' denoting both 'lowest' and 'last' occurrences in the literature the lowest (LO) and highest (HO) occurrences of palaeontological events are adopted here (after Berggren & Pearson, 2005) to define the limits of a biozone. They applied the first appearance datum (FAD) and last appearance datum (LAD) of palaeontological events to define time limits of a biochron (*sensu* Aubry, 1995). The Paleocene/Eocene notation of Berggren & Pearson (2005) is used in this research. The planktonic foraminifera recorded in the Rakhi Nala section are represented in **Plates 4.1-4.4** and their biostratigraphical distribution is shown in **Figure 4.2**. Taxonomic notes on foraminifera are provided in **Appendix 1**.

4.2. Planktonic foraminiferal biostratigraphy

4.2.1. Zone P3. *Morozovella angulata* Lowest-occurrence Zone

The planktonic foraminiferal zone P3 (i.e., *Morozovella angulata*-*Globanomalina pseudomenardii* zone of Berggren et al., 1995; Berggren & Norris, 1997 and of Olsson et al., 1999) from the Lower Indus Basin has been identified by Warraich et al. (2000). Following the convention that the nominate taxon should be present within the zone, Berggren & Pearson (2005), retaining the definition, re-

named the P3 zone as the '*Morozovella angulata* Lowest-occurrence Zone'. This zone was also subdivided by Berggren et al. (1995) as subzones P3a and P3b based on the LO of *Igorina albeari*. This subdivision was also followed by Berggren & Pearson (2005). However, because of the sporadic occurrence of *I. albeari* the LO of *Morozovella acuta* was used for this subdivision in the Lower Indus Basin. Berggren & Pearson (2005) adopted the recalibrated age of the *G. pseudomenardii* (FAD) as 59.4 Ma (after Berggren et al., 2000) instead of 59.2 Ma (after Berggren et al., 1995). The subzone P3a was modified after Berggren et al. (1995) and designated as the *M. angulata*-*M. acuta* Interval Subzone by Warraich et al. (2000) in the Lower Indus Basin. However, following Berggren & Pearson (2005) this subzone can be renamed as the *Igorina pusilla* Partial-Range Subzone. In order to avoid the use of *M. angulata* as the nominate taxon for both P3 and P3a, this subzone is redefined here as the partial range of *Igorina pusilla* between the LO of *M. angulata* and the LO of *M. acuta*. Similarly, the subzone P3b of Warraich et al. (2000) can be re-named and modified after Berggren & Pearson (2005) as the *M. acuta* Lowest-occurrence Subzone. The zone P3 is equivalent to the *G. angulata* Zone of Dorreen (1974) of the Kirther Range (Lower Indus Basin). Zone P3 is not reported from the Upper Indus Basin (Afzal, 1997).

4.2.2. Zone P4. *Globanomalina pseudomenardii* Taxon-range Zone

The name and definition of Zone P4 in the Lower Indus Basin follows Warraich et al. (2000). However, the nomenclature of its two-fold subdivision is revised. Due to the absence of *Parasubbotina variospira* the P4a/P4b subzonal boundary cannot be demarcated, although the P4b/P4c subzonal boundary can

be identified by *A. soldadoensis* (LO) as reported by Warraich et al. (2000). Therefore, the P4a and P4b jointly and P4c subzones of Berggren & Pearson (2005) are equivalent to the *Globanomalina pseudomenardii*-*Acarinina soldadoensis* Interval Subzone and the *Acarinina soldadoensis soldadoensis*/*Globanomalina pseudomenardii* Concurrent Range Subzone respectively of Warraich et al. (2000). In the Kirther Range (Lower Indus Basin) Zone P4 is equivalent to the lower part of the *G. velascoensis* Zone of Dorreen (1974). Zone P4 in the Upper Indus Basin can be established on the total range of the *Planorotalites pseudomenardii* (= *G. pseudomenardii*) following Afzal (1997). Similar to the Lower Indus Basin, only the P4b/P4c subzonal boundary in the Upper Indus Basin can be established, based on the *Muricoglobigerina soldadoensis* (LO) reported by Afzal (1997). Therefore, the subzones P4a and P4b of Berggren & Pearson (2005) are equivalent to the *P. pseudomenardii* Zone of Afzal (1997) and the P4c subzone of Berggren & Pearson (2005) is equivalent to the *Mg. soldadoensis* Zone of Afzal (1997).

4.2.3. Zone P5. (*Morozovella velascoensis* Partial-range Zone),

Zone E1. (*Acarinina sibaiaensis* Lowest-occurrence Zone) and

Zone E2. (*Pseudohastigerina wilcoxensis*/*Morozovella velascoensis*

Concurrent-range Zone)

Zone P5 of Warraich et al. (2000) in the Lower Indus Basin (Sulaiman Range) is revised following Berggren & Pearson (2005). Due to the absence of Planktonic Foraminiferal Excursion Taxa (PFET) such as *Acarinina africana*, *Acarinina sibaiaensis* and *Morozovella allisonensis* in the Lower Indus Basin, therefore,

the zonal boundary P5/E1 can only be recognized based on the onset of the Carbon Isotopic Excursion (CIE- see Chapters 5 & 6) and Benthonic Foraminiferal Extinction Event (BFEE- Warraich et al. (2000), see **Figure 4.2**). However, the zonal boundary E1/E2 is recognized based on the lowest occurrence (LO) of *P. wilcoxensis*. P5 and E1 together and E2 are, therefore, equivalent to the P5 (lower-middle) and P5 (upper) respectively of Warraich et al. (2000). In the Lower Indus Basin (Kirther Range) zones P5, E1 and E2 are equivalent to the *G. velascoensis* Zone of Dorreen (1974). In the Upper Indus Basin, due to the absence of PFET and the sporadic occurrence of *P. wilcoxensis*, neither the zonal boundary P5/E1 nor E1/E2 can be identified. Therefore, the P5, E1 and E2 of Berggren & Pearson (2005) are equivalent to the *Acarinina wilcoxensis berggreni* Zone (lower to middle) of Afzal (1997).

4.2.4. Zone E3. *Morozovella marginodentata* Partial-range Zone

The Eocene Planktonic Foraminiferal Zone E3 can be recognized in both the Lower and Upper Indus basins. This zone is equivalent to the P6 Zone (lower part up to the LO of *M. formosa*) of Warraich et al. (2000) in the Lower Indus Basin (Sulaiman Range) and to the *Globorotalia rex* (lower part) Zone of Dorreen (1974) in the Lower Indus Basin (Kirther Range) and to the *A. wilcoxensis berggreni* (upper) Zone of Afzal (1997).

4.2.5. Zone E4. *Morozovella Formosa* Lowest-Occurrence Zone

The Eocene Zone E4 is equivalent to the rest of the P6 Zone (from the LO of *Morozovella formosa*) of Warraich et al. (2000) in the lower Indus Basin (Sulaiman Range) and to the middle part of the *G. rex* Zone of Dorreen (1974)

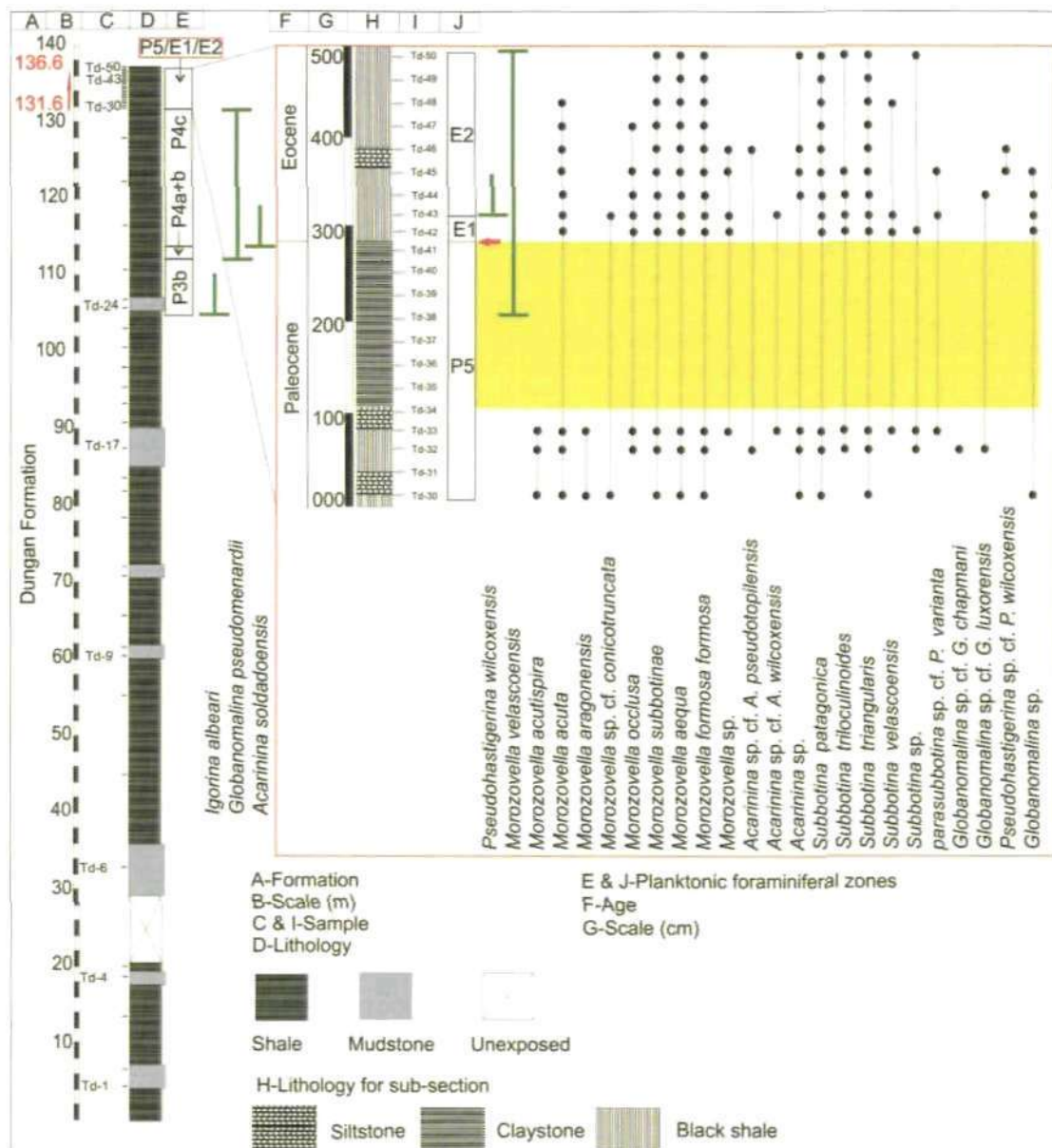


Fig. 4.2: Measured columnar section along the Rakhi Nala showing lithology, sample locations and biostratigraphical distribution of the recorded planktonic foraminifera. The yellow coloured area indicates an interval with no foraminifera, and vertical green bars indicate lowest and highest occurrences of the important planktonic foraminiferal species reported by Warraich et al. (2000). The area under the red rectangle shows the Paleocene/Eocene interval planktonic foraminiferal zones. Red horizontal arrow shows the position of P5/E1 boundary based on BFEE of Warraich et al. (2000).

in the Lower Indus Basin (Kirther Range) and to the *M. formosa* Zone of Afzal (1997) in the Upper Indus Basin.

4.2.6. Zone E5. *Morozovella aragonensis*/*Morozovella subbotinae*

Concurrent-range Zone

The Eocene Zone E5 is equivalent to the P7 Zone of Warraich et al. (2000) and P7, P8 of Warraich & Ogasawara (2001) in the Lower Indus Basin (Sulaiman Range) and to the upper part of *G. rex* Zone of Dorreen (1974) in the Lower Indus Basin (Kirther Range) and to the *M. aragonensis* Zone of Afzal (1997) in the Upper Indus Basin.

4.3. The P/E boundary interval and its intra-basinal correlation (Lower Indus Basin)

The Dungan Formation in the Lower Indus Basin, the Patala Formation in the Upper Indus Basin (see details in **Section 4.6**) and the Laki Formation of Rajasthan (India) contain the P/E boundary interval (**Fig. 4.4**). In order to reconstruct the depositional environment of marine sedimentary rocks, foraminifera have been widely used in a number of previous studies worldwide. For example, Grimsdale & van Morkhoven (1955), Smith (1955) & Ingle (1980) used the percentage of planktonic foraminifera to determine the distance to the shore. They noted that the plankton percentage increases from shelf to open ocean and exceeds 50% in the deeper environments of the outer shelf. A similar approach using the P/B ratio has been applied to modern patterns of planktonic and benthonic foraminiferal distributions by Gibson (1989) and the data obtained were compared with the results from Paleogene sediments. He found that the results derived from the P/B ratios are reliable and in accordance

with the palaeoenvironmental interpretations made from other methods. There are, however, a number of philosophical objections to the application of P/B ratios for palaeoenvironmental interpretation citing such things as 'differential dissolution or oxygen conditions' (e.g., Adelseck & Berger, 1975; Van der Zwaan et al., 1990; Murray, 1991). Despite these, Warraich (2000) has observed high P/B (98-99%) in association with high values of species richness and diversity in the Dungan Formation (Sulaiman Range). He suggested that the deposition of the Dungan Formation occurred in a deep marine environment. Furthermore, he noted that the westward thinning of the limestone interbeds indicated a westward dipping slope environment. A carbonate-rich turbidite facies exists in the lower part of the Dungan Formation, which hampers the identification of the early Paleocene planktonic foraminiferal zones (e.g., Samanta 1973; Warraich, 2000; Kalia & Kinsto, 2006; this study).

The neritic Paleogene sedimentary sequence in the Jaisalmer Basin (India) is the eastward extension of the Indus Basin. In the Jaisalmer Basin (**Fig. 4.3**) planktonic foraminiferal zones were described by Kalia and Kinsto (2006) for the late Paleocene-early Eocene succession in the Tanot-1 well. Similar to the lower part of the Dungan Formation of the Raki Nala succession in the Sulaiman Range, the lower part of their Ranikot Formation is composed of quartz sandstone and claystone and did not yield any planktonic foraminifera. The upper part of their Ranikot Formation is predominantly composed of marlstone and claystone with subordinate quartz sandstone. This upper part of the Ranikot Formation and the succeeding Laki Formation, which is composed of carbonate rocks, yielded the following planktonic foraminiferal zones; P4a, P4(b+c), *Globanomalina pseudomenardii-Acarinina sibaiyaensis* Interval

Subzone (P5a), *Acarinina sibaiaensis*-*Pseudohastigerina wilcoxensis* Interval Zone (P5b) and the *Pseudohastigerina wilcoxensis* -*Morozovella velascoensis* Concurrent range Zone (P5c).

According to Kalia and Kinoto (2006) the planktonic foraminiferal Zone P4 is composed of sandstone, claystone, siltstone, marl and limestone beds in the upper Ranikot Formation and lower Laki Formation of Rajasthan (India). This zone is dominantly represented by shale in the Sulaiman Range, Pakistan (**Fig. 4.2**). Zone P5 (equivalent to P5, E1 and E2) in Rajasthan is composed of claystone, quartz-sand, marl, limestone and shale (Kalia & Kinoto, 2006). In Sulaiman Range, the Zone P5 (equivalent to P5, E1 and E2) is composed of black shale, claystone and siltstone (**Fig. 4.2**). A claystone horizon, barren of foraminifera, is encountered in both Rajasthan (~3m thick according to Kalia & Kinoto, 2006) and the Indus Basin (~170cm thick according to this study, see **Fig. 4.2**). An interval immediately above this claystone horizon records the PFET in Rajasthan (Kalia & Kinoto, 2006). However, the P/E boundary (base of P5b of Kalia & Kinoto, 2006) is being placed at the base of this claystone horizon in Rajasthan (**Fig. 4.4**). The PFET are used to recognize the P/E boundary (**Fig. 4.5**) but these taxa are neither reported in the literature or have been encountered in the present study of the Indus Basin, Pakistan. The interval considered to represent the P/E boundary interval (as reported by Kalia & Kinoto, 2006) is barren of foraminifera. This interval is, therefore, suitable for the investigation of other microfossil groups (such as dinoflagellates) and other proxies (such as stable isotopes) which have been used to study the P/E boundary interval in the Indus basin (see Chapters 5 & 6 for details). During the late Paleocene and early Eocene the deposition of a dominantly limestone

facies in the Laki Formation in Rajasthan (India) represents a carbonate platform. The deposition of a dominantly planktonic foraminiferal shale and siltstone facies in the Dungan Formation (**Plate-4.1D & 4.1H**) of the Sulaiman Range (Pakistan) yields late Paleocene-early Eocene planktonic foraminifera (**Plates 4.2-4.4**) and represents deposition on a westward dipping slope under deep marine conditions. Therefore, by combining the results from both these areas, it can be suggested that during late Paleocene-early Eocene times deposition in the Indus Basin occurred in an east-west oriented basin. The Indian part of the Indus Basin in the east represents a shallow environment of deposition (e.g., Kalia & Kinsto, 2006; Rabha & Kalia, 2007; Bhandari, 2008), while the Sulaiman Range (in the west) represents an open marine environment of deposition.

4.4. Larger foraminiferal biostratigraphy

The upper Paleocene to lower Eocene Patala Formation (Upper Indus Basin) from which most of the fauna was recorded (see **Plates 4.5-4.18** and **Appendix-1**), mainly comprises an inter-bedded succession of shales and limestones and was deposited in a shallow marine shelf environment (Afzal, 1997). The Patala Formation is broadly equivalent to the Dungan Formation in the Lower Indus Basin (**Fig. 4.1**).

Different groups of Cenozoic larger foraminifera from the Indus Basin have been described and used to formulate zonal schemes in previous research (e.g., Nuttall, 1925, 1926; Davies & Pinfold, 1937; de Cizancourt, 1938; Gill, 1952, 1953; Smout, 1954; Smout & Haque, 1956; Haque, 1956;

Nagappa, 1959; Hottinger, 1960; Adams, 1970; Blondeau, 1972; Kureshy, 1978; Schaub, 1981; Weiss, 1988; Butt, 1989, 1991).

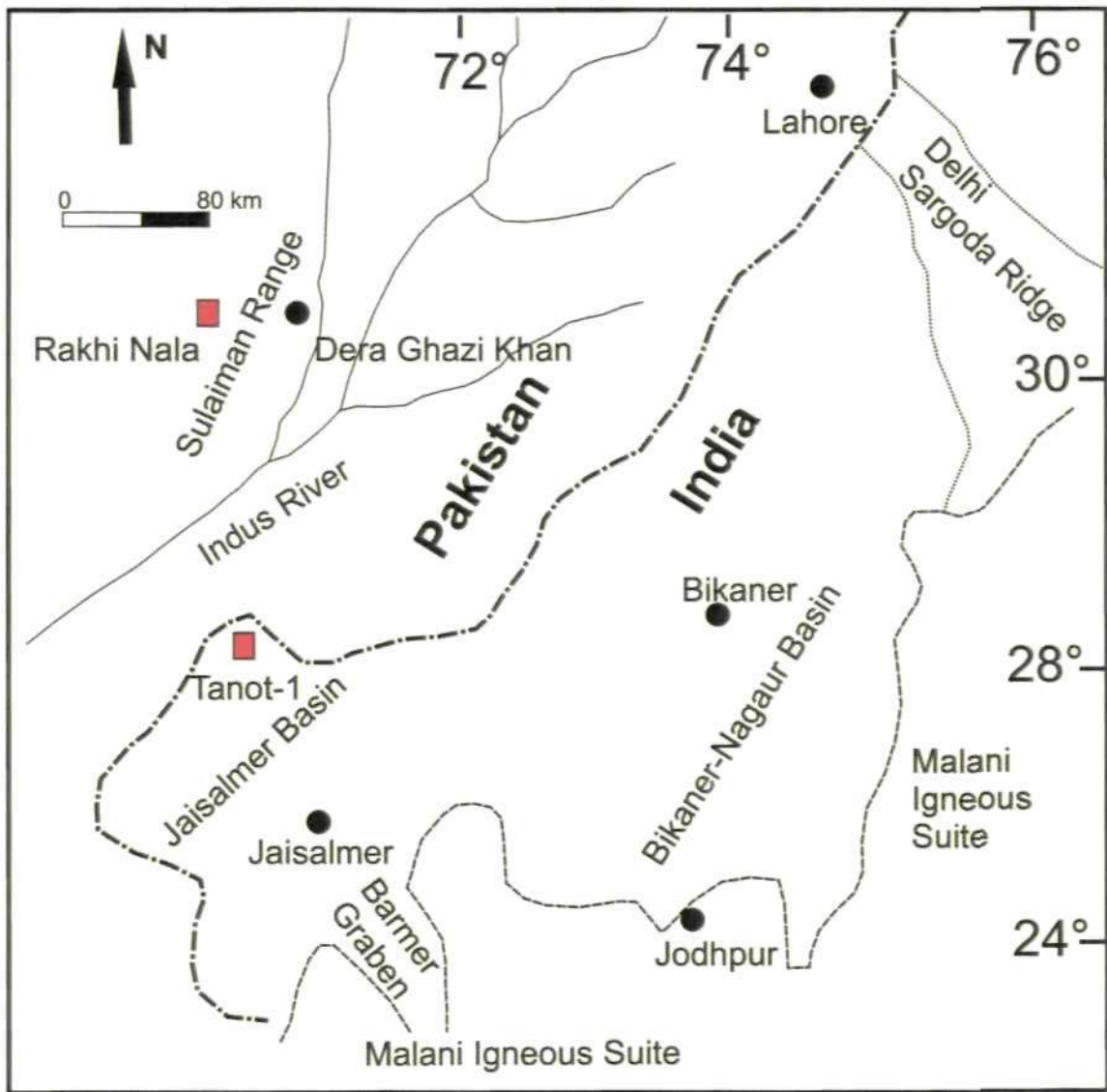
The upper Paleocene to lower Eocene sedimentary rocks in the Upper Indus Basin represent a shallow marine shelf environment of deposition where the foraminiferal assemblage is more readily controlled by the environment of deposition. The inter-fingering of larger foraminiferal dominated and planktonic foraminiferal dominated intervals hampers the development of a complete biostratigraphical scheme based on a single group of foraminifera (Afzal, 1997). Consequently, it becomes impossible to develop a complete biostratigraphic zonal scheme based exclusively on the larger foraminifera. Therefore, Afzal (1997) proposed a local zonation scheme for the Indus Basin. This local larger foraminiferal zonal scheme of Afzal (1997) is compared with other Tethyan schemes of Serra-Kiel et al. (1998), Scheibner et al. (2005) and Scheibner & Speijer (2009) (**Fig. 4.6**).

The Paleocene-Eocene interval and the position of the Paleocene/Eocene boundary are of major importance to this research. Therefore, only the late Paleocene to early Eocene larger foraminiferal biostratigraphy is reviewed according to the Tethyan larger foraminiferal biostratigraphic schemes (e.g., Hottinger, 1960; Serra-Kiel et al., 1998; Hottinger, 1998; Scheibner & Speijer, 2009).

An important event that occurred within the Paleocene/Eocene boundary interval is the Larger Foraminiferal Turnover (LFT). The LFT was first described by Hottinger & Schaub (1960) and is characterized by the start of adult dimorphism and large shell size in larger foraminifera (particularly the

nummulitids and alveolinids). The LFT marks the base of the Ilerdian, which is placed between zones SBZ5 and SBZ6 of Serra-Kiel et al., 1998 (Hottinger, 1998). Serra-Kiel et al. (1998) proposed a shallow waters benthonic zonal scheme for the Paleocene and Eocene but the position of the Paleocene/Eocene boundary remained uncertain. De Graciansky et al. (1998), on seismic evidence, placed the Paleocene/Eocene boundary in the middle part of the P5 Zone of Berggren et al. (1995), which is equivalent to the SBZ5/SBZ6 boundary of Serra-Kiel et al. (1998). Later, the Carbon Isotopic Excursion (CIE) has been accepted as a marker criterion (calibrated at 55 Ma by Norris & Röhl (2000) and re-calibrated by Gradstein et al. (2004) at 55.8 Ma) for the Paleocene/Eocene boundary (Aubry & Ouda, 2003). The CIE marks a significant global warming event (see Chapter 6 for details on the CIE). This CIE is detectable worldwide in both marine and terrestrial records. Therefore, this marker provided a base for correlation of the Paleocene/Eocene boundary across a wide range of depositional environments.

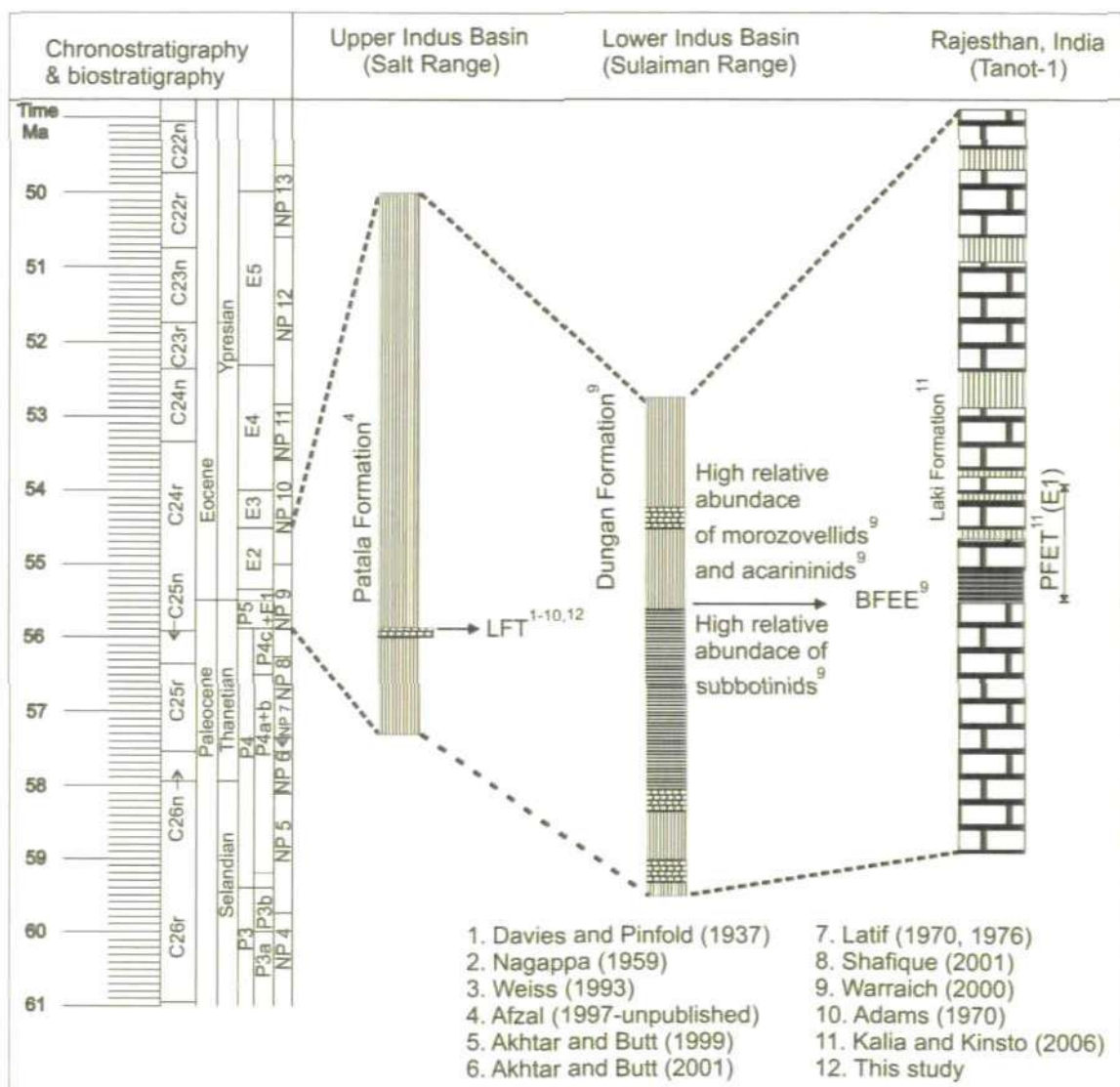
Recent research confirms the synchronicity of the LFT and the CIE (e.g., Orue-Etxebarria et al., 2001; Pujalte et al., 2003). The placement of the Paleocene/Eocene boundary at the SBZ4/SBZ5 boundary and its correlation with various planktonic and benthonic boundary markers is confirmed by Scheibner et al. (2005) and Scheibner & Speijer (2009).



Legend

- International boundary
- - - Inter-basinal boundary
- Geological boundary of Delhi Sarghoda Ridge
- River
- City
- Study site

Fig.4.3: Map showing locations of the Tanot-1 Well, Jaisalmer Basin, Rajasthan (India) and the Rakhi Nala section, Sulaiman Range, Lower Indus Basin, Pakistan (modified after Kalia & Kinisto, 2006).



 Siltstone
  Limestone
  Black shale
  Claystone

Fig.4.4: Summary of the faunal events (LFT- Larger Foraminiferal Turnover; BFE - Benthonic Foraminiferal Extinction Event; PFET- Planktonic Foraminiferal Extinction Taxa) and lithostratigraphical correlation of the P/E boundary interval, Indus Basin.

4.4.1. Shallow Benthonic Zone 4 (SBZ4)

The SRX-1 larger foraminiferal Zone of Afzal (1997) is the late Paleocene Zone in the Indus Basin. The base of this zone was not encountered by Afzal (1997) but the top is defined by the simultaneous Lowest Occurrences (LO's) of *Nummulites deserti*, *N. thalicus*, *Assilina spinosa*, *A. dandotica* and *A. prisca*. This zone is characterized by the complete absence of the genus *Nummulites*. The important larger foraminifera encountered by Afzal (1997) include *Miscellanea miscella*, *M. stampi*, *Lockhartia haimeii*, *Lockhartia* sp., *Ranikothalia sindensis*, *R. nuttalli*, *Rotalia* sp., *Operculina jiwani*, *O. subgranulosa* and *O. salsa*.

The SBZ4 Zone is equivalent to the *Glomalveolina levis* Zone of Hottinger (1960) and SBZ4 Zone of Serra-Kiel et al. (1998) and Scheibner & Speijer (2009) (Fig. 4.6). The SBZ4 larger benthonic foraminifera recorded in the present research is given in Figure 4.7B, and include; *Ranikothalia* sp. cf. *R. kohatica* (e.g., Plates 4.10A, 4.16C), *Ranikothalia* spp. (e.g., Plates 4.14A, 4.15D & 4.16B), *Lockhartia* spp. (e.g., Plates 4.8I, 4.11B, 4.13A, 4.15N & 4.16L), *Caudrina* sp. cf. *C. soldadensis* (e.g., Plates 4.14M & 4.18G), *Miscellanea* spp. (e.g., Plates 4.9S, 4.10D, 4.11O, 4.12A, 4.13D, 4.14G, 4.15C, 4.16P, 4.17A & 4.18B), *Assilina* sp. cf. *A. ranikoti* (e.g., Plates 4.8D, 4.9A & 4.11I), *Nummulitoides* sp. cf. *N. inaequilateralis* (e.g., Plates 4.11A, 4.12C, 4.13E & 4.18C), *Operculina* sp. cf. *O. hardiei* (e.g., Plate 4.9Q), *Operculina* spp. (e.g., Plates 4.10B, 4.14B & 4.16H).

4.4.2. Shallow Benthonic Zones 5/6 (SBZ5/6)

Scheibner & Speijer (2009) combined SBZ5/6 based on the co-occurrence of the index species of both biozones (**Fig. 4.6**). According to Hottinger (1960) the precursor biozones of SBZ5 and SBZ6 are the *Aleovlina cucumiformis* and *Alveolina ellipsoidalis* biozones, identified by the total ranges of *Alveolina cucumiformis* (junior synonym of *Alveolina vredenburgi*, Hottinger et al., 1998) and *Alveolina ellipsoidalis*, respectively. Based on the first appearance of true alveolinids characterized by an increase in size, flosculinisation, axial thickening and adult dimorphism (Hottinger, 1960), the larger foraminifera of this biozone can be very easily recognized (Scheibner & Speijer, 2009).

The SRX-2 & 3 zones of Afzal (1997) in the Indus Basin represent the SBZ4 and SBZ5/6 of Scheibner & Speijer (2009). The SRX-2 Zone is defined by the simultaneous LO's of *Nummulites deserti*, *N. thalicus*, *Assilina dandotica*, *A. spinosa* and *A. prisca* to the Highest Occurrence (HO) of *Alveolina vredenburgi* (= *Alveolina cucumiformis*). The SRX-3 Zone is defined by the simultaneous HO's of *Miscellanea miscella*, *M. stampi*, *Lockhartia haimei* to the simultaneous HO's of *Alveolina cucumiformis* and *Assilina dandotica*.

The larger foraminifera of SBZ5/6 encountered in this research is given in **Figure 4.8B**, and include; *Nummulites* spp. (e.g., **Plates 4.5A, 4.6E & 4.8N**), *Alveolina* spp. (e.g., **Plates 4.8A & 4.9M**), *Nummulites* sp. cf. *N. globulus* (e.g., **Plate 4.9I**), *Assilina* sp. (e.g., **Plate 4.10T**).

55.5 Ma Reconstruction

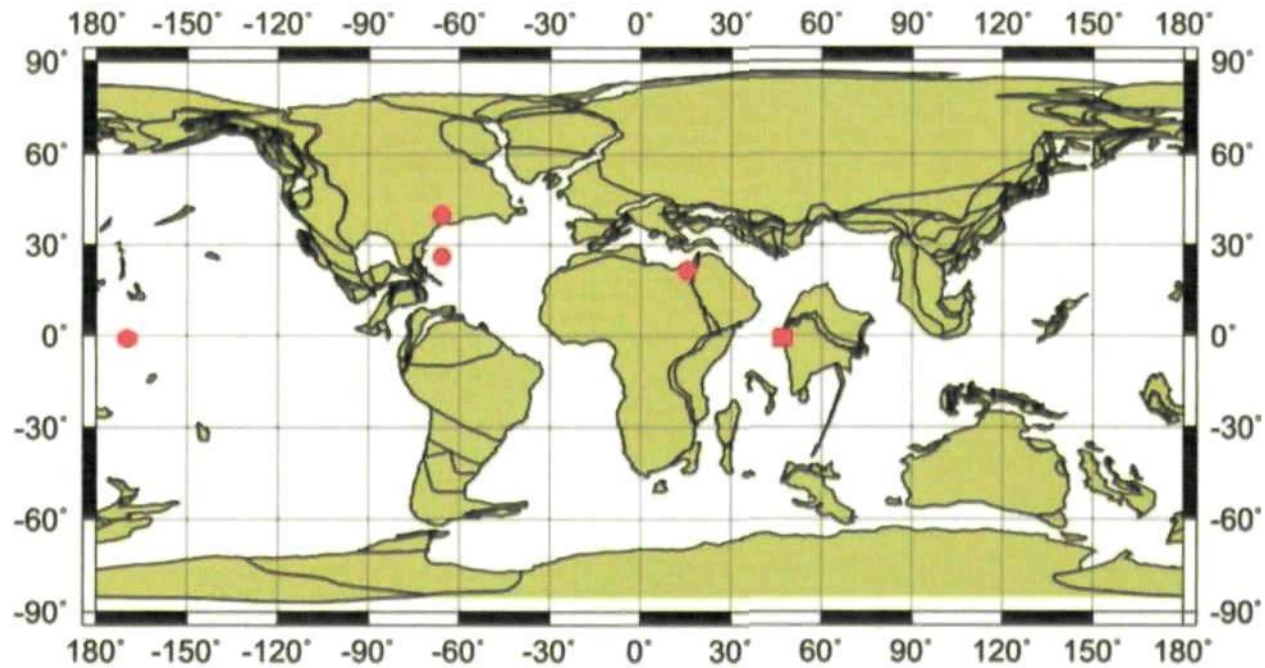


Fig.4.5: Palaeogeographical map showing the locations of the PFET (Planktonic Foraminiferal Excursion Taxa) worldwide (red circles) and Indus Basin (red square) after Hay et al. (1999) (ODSN plate tectonic reconstruction service <http://www.odsn.de/odsn/services/paleomap/paleomap.html>).

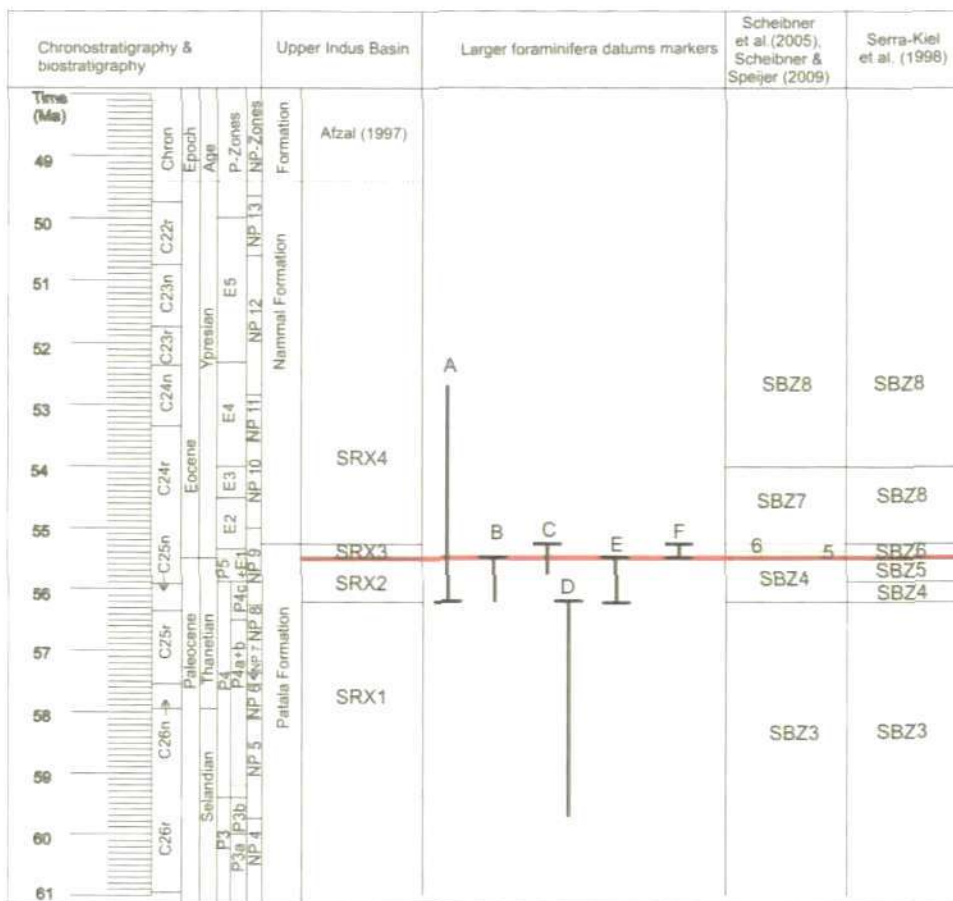


Fig. 4.6: Correlation of the Paleocene/Eocene interval shallow benthonic foraminiferal zones of the Upper Indus Basin with other Tethyan zones. **A** = Top of the Zone SRX1 and base of the Zone SRX2 represented by the lowest occurrences (LO's) of *Nummulites deserti*, *N. thalicus*, *Assilina spinosa*, *A. dandotica* and *A. prisca* (Afzal, 1997), **B** = Zonal boundary of the SRX2/SRX3 zones represented by the simultaneous highest occurrences (HO's) of *Miscellanea miscella*, *M. stampi* and *Lockhartia haimei* (Afzal, 1997), **C** = The overlapping top boundary of the SRX2 and SRX3 of Afzal (1997) and SBZ5/6 of Scheibner & Speijer (2009) represented by the highest occurrence (HO) of the *Alveolina cucumiformis* (Afzal, 1997; Scheibner & Speijer, 2009), **F** = The total range of the *Alveolina cucumiformis* (Hottinger, 1960; Scheibner & Speijer, 2009), **D** = The highest occurrence (HO) of *Glomalveolina primaeva*, SBZ3 (Hottinger, 1960; Serra-Kiel et al., 1998; Scheibner & Speijer, 2009), **E** = *Glomalveolina levis* total range (Hottinger, 1960) as well as *Hottingerina lukasi* total range, an index species of SBZ4 (Drobne, 1975; Serra-Kiel et al., 1998; Scheibner & Speijer, 2009), red line = LFT.

4.5. Faunal turnovers in the Indus Basin and global correlation

The famous late Paleocene-early Eocene event called the Paleocene-Eocene

Thermal Maximum (PETM) is associated with a number of biotic events. These are:

- An acme in the planktonic foraminifera genus *Acarinina* (Arenillas & Molina, 1996; Kelly et al., 1998), the dominance of morozovellids and an absence of subbotinids (Petrizzo, 2007);
- Distinctive assemblages of calcareous nannoplankton (Bralower, 2002);
- Acme of the dinoflagellate cyst *Apectodinium* (Crouch et al., 2001);
- Rapid radiation of mammals on land (Koch et al., 1992);
- Shallow benthonic foraminiferal extinction and repopulation (Speijer et al., 1997); and
- Larger Foraminiferal Turnovers on Tethyan shelves (Alegret et al., 2005).

Some of the PETM biotic events can be identified in the Indus Basin as reported in the previous literature. Based on such events, the P/E boundary interval of the Indus Basin can be correlated globally.

All larger foraminifera are extreme K-strategists; i.e., characterized by long individual lives and low reproductive potential. Following the work of Hottinger & Schuab (1960), Orue-Etxebarria et al. (2001) reported a larger foraminiferal turnover (LFT) characterized by a change in the nummulitid morphotypes at the base of Ilerdian stage which is nearly coeval with the Paleocene Eocene Thermal Maximum (PETM) in Spain. Similarly, from Egypt, Scheibner et al. (2005) reported the LFT within the planktonic foraminiferal Zone P5, predating the PETM by 300

k.y. Their LFT is characterized by the gradual disappearance of Paleocene taxa such as *Ranikothalia* and *Miscellanea* and the rise of *Nummulites* and *Alveolina*. A similar trend of LFT as that described by Scheibner et al. (2005) can be recognized in the Salt Range (Upper Indus Basin) based on the larger foraminiferal data reported in the literature (e.g., Afzal, 1997) as well as that observed in the Kala Chitta Ranges, Upper Indus Basin in this study (**Figs 4.4, 4.6 & Plate 4.19**).

The extinction of Velasco type fauna (Berggren & Aubert, 1975) in the middle of planktonic foraminiferal Zone P5 (at P5/E1 boundary) marks the Benthonic Foraminiferal Extinction Event (BFEE) in the Sulaiman Range, Indus Basin (**Fig. 4.4**). This BFEE is reported by Warraich (2000) from the work done by Dr Ritsu Nomura of Shimane University, Japan. Another biotic event associated with the PETM is the acme occurrence of the dinoflagellate cyst *Apectodinium* which is reported from the late Paleocene nannoplankton Zone NP9 prior to the Paleocene/Eocene boundary in the Upper Indus Basin (Kothe et al., 1988). The *Apectodinium* acme is regarded as an event associated with the P/E boundary in the previous literature. However, this acme is reported prior to the P/E boundary (e.g., Sluijs et al., 2007b) which is in accordance with the results from the Indus Basin (see detailed discussion in Chapters 5 & 6).

4.6. Depositional environment across the P/E interval (Upper Indus Basin)

The Patala Shale and Margala Hill Limestone (= Nammal Limestone Formation of the Salt Range) formations in the Kala Chitta Range represent upper Paleocene and lower Eocene successions respectively. The Patala Shale Formation was logged and sampled in the Kali Dilli Section (see **Figure 1.4** from Chapter 1 and **Figures 4.7A & 4.7B**). The Patala Shale Formation in the Kali Dilli Section contains limestone and shale inter-beds. Only the limestone samples were processed from

the Patala Shale Formation. Based on a petrographic analysis, and according to the classification of Dunham (1962), the following microfacies from the upper Paleocene Patala Shale Formation is recognized '*Miscellanea micro-bioclastic wacke-packstone*'

The Margala Hill Limestone Formation was logged and sampled in the Chak Dalla Section (see **Figure 1.4** from Chapter 1 and **Figures 4.8A & 4.8B**). The Margala Hill Limestone Formation is dominantly composed of limestone with minor shale inter-beds. Only the limestone samples were processed from the Margala Hill Limestone Formation. Based on a petrographic analysis and according to the classification of Dunham (1962), the following microfacies from the lower Eocene Margala Hill Limestone is recognized '*Nummulites Peloidal wacke-packstone*'

4.6.1. *Miscellanea micro-bioclastic wacke-packstone*

This facies contains the skeletal fragments of foraminifera and other microfossils (i.e., micro-bioclasts). The major allochem types are *Miscellanea* spp., *Nummulitoides* spp., *Ranikothalia* spp. and *Lockhartia* spp.. *Orbitolites* spp., *Alveolina* spp., bryozoans, dasyclad algae and other Miliolidae occur as minor constituents. Partial replacement of the allochems by spar is common in this microfacies.

4.6.2. *Nummulites Peloidal wacke-packstone*

The major allochem types of this microfacies are *Nummulites* spp., peloids and micro-bioclasts. Dasyclad algae, *Assilina* spp., *Alveolina* spp. and *Discocyclina* spp. occur as minor allochem types. Partial replacement of the allochems by spar is

common (e.g., **Plate 4.30A**). Calcite filled micro-fractures, cutting across the allochems in some samples, can be seen.

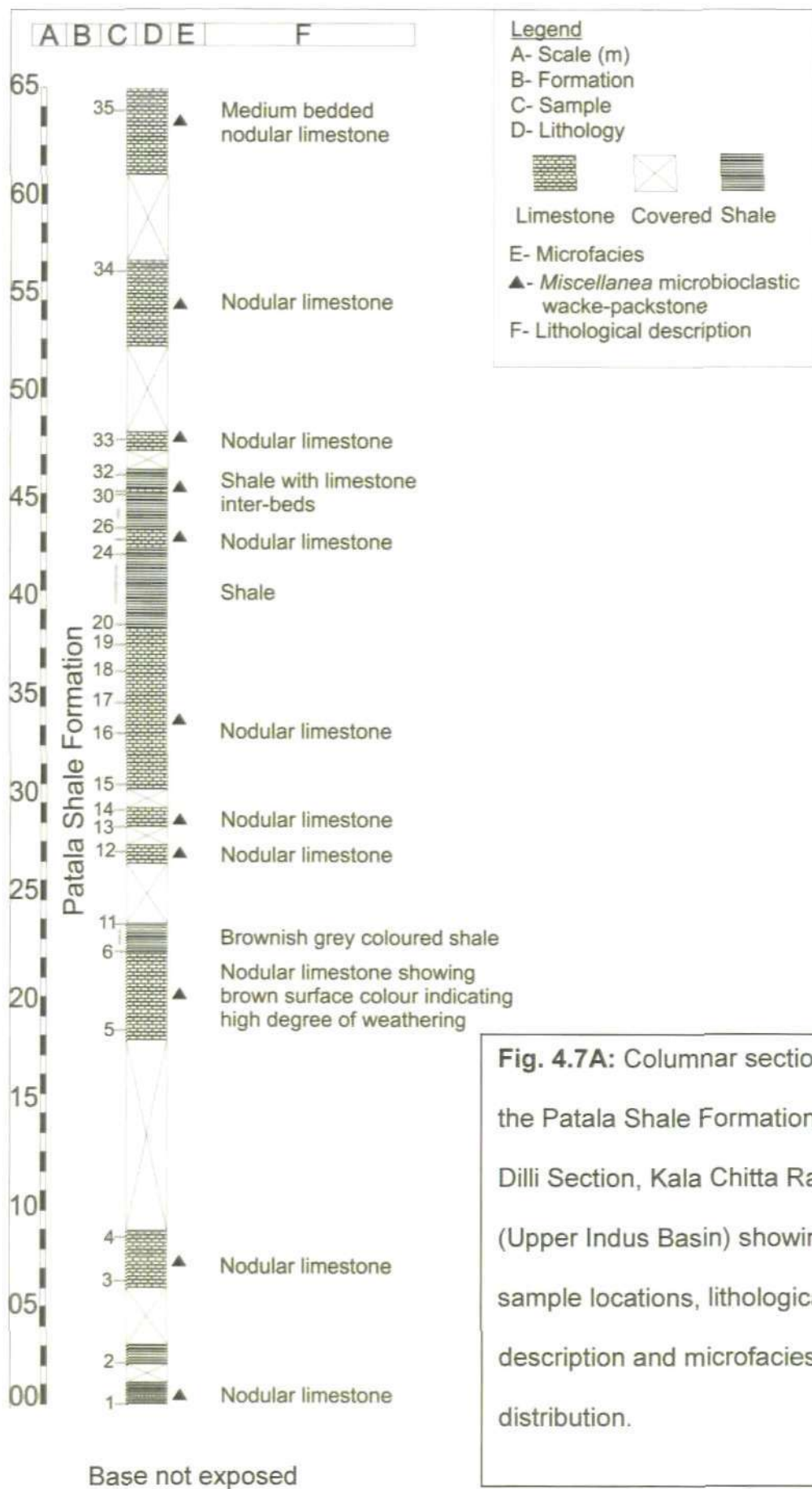
4.6.3. Interpretation

The abundant occurrence of larger foraminifera in both the Patala Shale and Margala Hill Limestone formations indicate that the environment of deposition was shallow marine across the Paleocene/Eocene interval of the Kala Chitta Range. The presence of lime mud as a matrix indicates a generally sub-tidal environment below fair-weather wave conditions. The partial replacement of allochems by spar and the presence of calcite filled micro-fractures in both microfacies indicate later phases of diagenesis. The common presence of micro-bioclasts in the microfacies of the Patala Shale Formation imply higher energy conditions and/or transportation of the bioclasts to the site of deposition.

According to Murray (1973) Miliolidae require salinity conditions higher than 32 ppt. Clarke et al. (1973), from the Persian Gulf, describe that the modern imperforate foraminifera (e.g., Miliolidae) are particularly common in protected embayments and lagoons. Therefore, the presence of Miliolidae in the upper Paleocene Patala Shale Formation implies higher salinity conditions.

The absence of Miliolidae and the presence of relatively more *Alveolina* spp. in the *Nummulites* peloidal wacke-packstone microfacies of the lower Eocene Margala Hill Limestone Formation indicate normal salinity conditions. Peloids are generally of diverse origin. Some that have regular outlines and good sorting are regarded as faecal pellets while others, which occur as a range of different shapes and sizes, are believed to be micritized skeletal fragments. These two different types of peloids indicate two different types of energy conditions. The peloids of

faecal origin can only be preserved in low energy sub-tidal conditions, while the peloids of micritized skeletal fragments origin may survive the higher energy conditions. The peloids present in association with other skeletal bio-clasts in the *Nummulites* peloidal wacke-packstone microfacies are believed to be of skeletal origin indicating higher energy conditions.



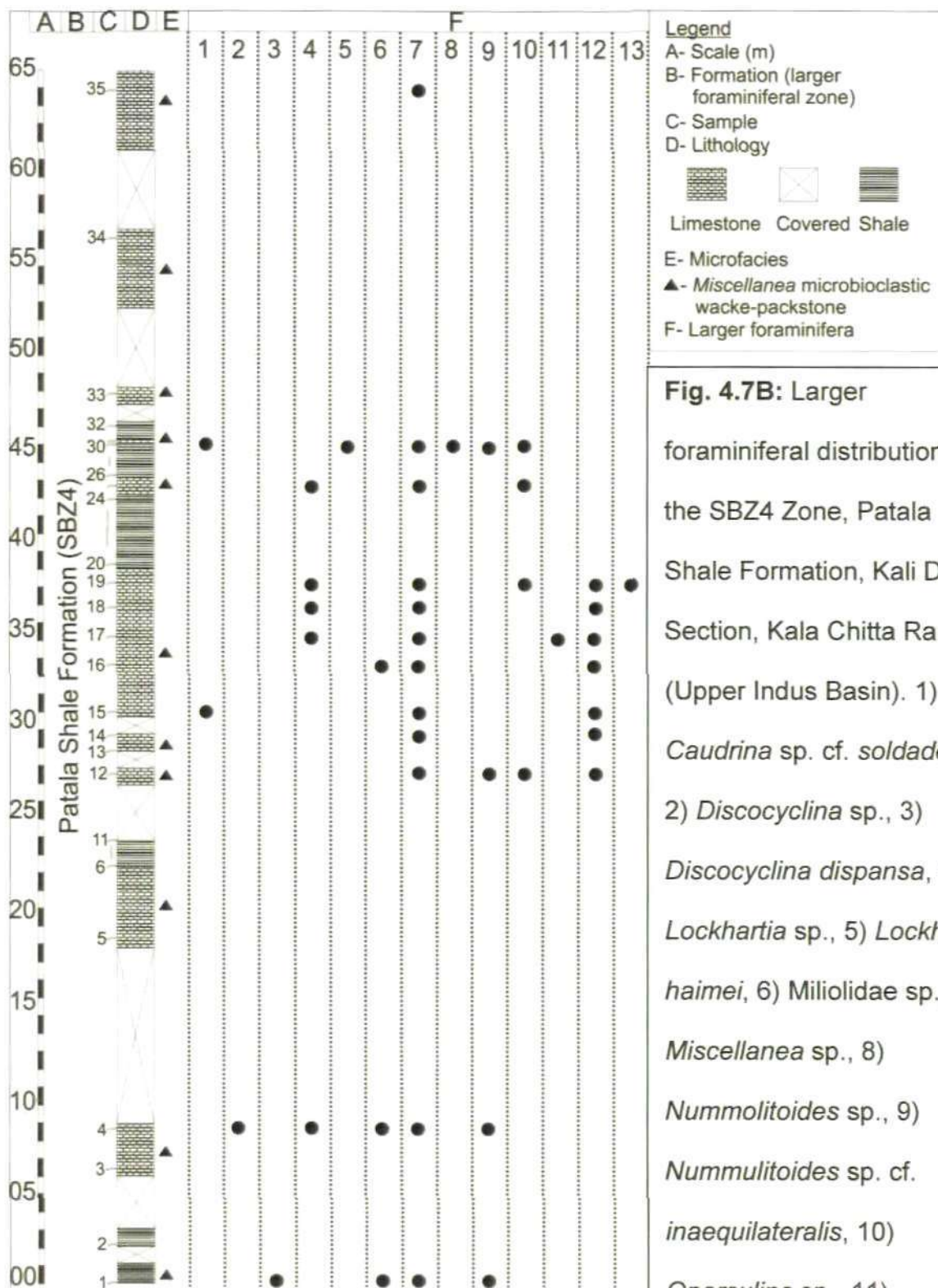


Fig. 4.7B: Larger foraminiferal distribution in the SBZ4 Zone, Patala Shale Formation, Kali Dilli Section, Kala Chitta Range (Upper Indus Basin). 1) *Caudrina* sp. cf. *soldadensis*, 2) *Discocyclina* sp., 3) *Discocyclina dispansa*, 4) *Lockhartia* sp., 5) *Lockhartia haimei*, 6) Miliolidae sp., 7) *Miscellanea* sp., 8) *Nummolitoides* sp., 9) *Nummulitoides* sp. cf. *inaequilateralis*, 10) *Operculina* sp., 11) *Orbitolites* sp., 12) *Ranikothalia* sp., 13) *Ranikothalia* sp. cf. *Kohatica*.

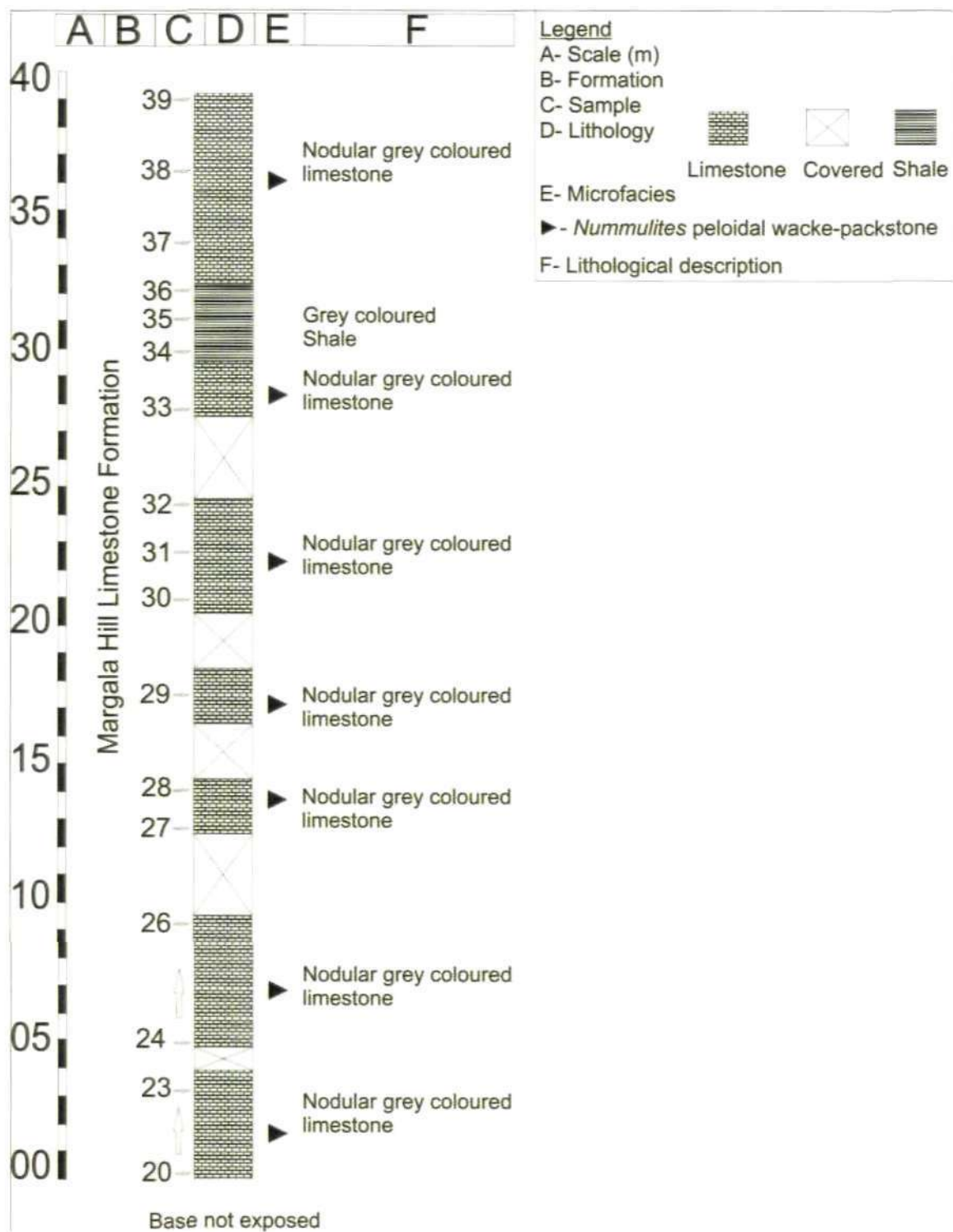


Fig. 4.8A: Columnar section of the Margala Hill Limestone Formation, Chak Dalla Section, Kala Chitta Range (Upper Indus Basin) showing sample location, lithological description and microfacies distribution.

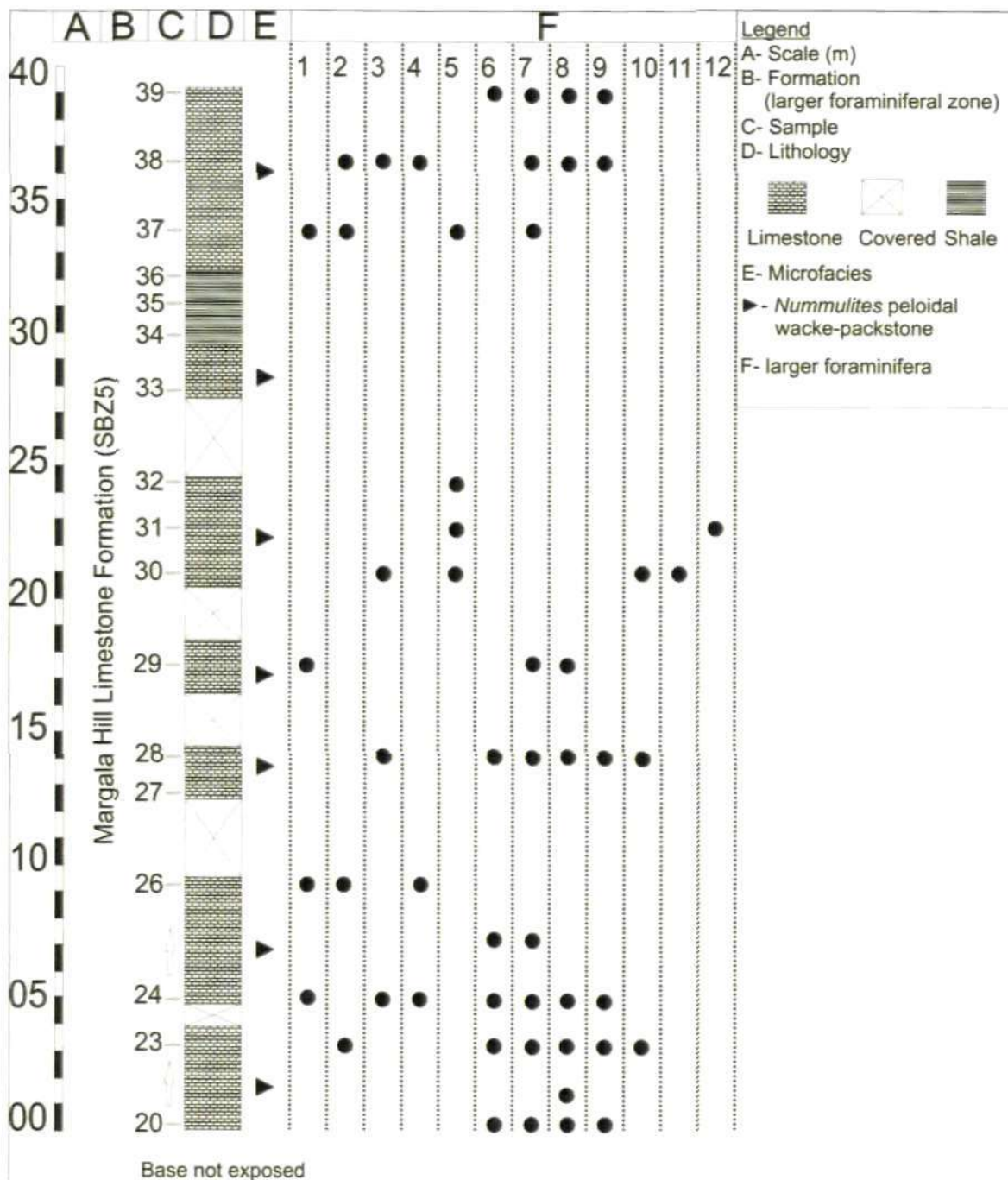


Fig. 4.8B: Larger foraminiferal distribution in the SBZ5 Zone, Margala Hill Limestone Formation, Chak Dalla Section, Kala Chitta Range (Upper Indus Basin).

- 1) *Alveolina* sp., 2) *Assilina* sp., 3) *Assilina* sp. cf. *ranikoti*, 4) *Lockhartia* sp., 5) *Miscellanea* sp., 6) *Nummulites* sp., 7) *Nummulites* sp. cf. *mammilatus*, 8) *Nummulites* sp. cf. *atacicus*, 9) *Nummulites globulus*, 10) *Operculina* sp., 11) *Operculina* sp. cf. *hardiei*, 12) *Palaeonummulites* sp.

Plate 4.1

Fig. A (Td17): Photomicrograph of lower part of the Dungan Formation at Rakhi Nala, Sulaiman Range, showing quartz sandstone facies devoid of any age diagnostic planktonic foraminifera.

Fig. B (Td9): Photomicrograph of lower part of the Dungan Formation at Rakhi Nala, Sulaiman Range, showing quartz sandstone facies, *Subbotina* (a) and *Morozovella* (b) species are present.

Fig. C (Td13): Photomicrograph of lower part of the Dungan Formation at Rakhi Nala, Sulaiman Range, representing mixed planktonic foraminifera quartz sandstone facies with dominant morozovellids.

Fig. D (Td34): Photomicrograph of upper part of the Dungan Formation at Rakhi Nala, Sulaiman Range, representing planktonic foraminiferal siltstone facies, *Morozovella* sp. cf. *M. aequa* (a) is present.

Fig. E (Td34): Photomicrograph of upper part of the Dungan Formation at Rakhi Nala, Sulaiman Range, representing planktonic foraminiferal siltstone facies, *Morozovella* sp. cf. *M. aequa* (a).

Fig. F (Td13): Photomicrograph of lower part of the Dungan Formation at Rakhi Nala, Sulaiman Range, representing mixed planktonic foraminifera quartz sandstone facies, *Morozovella* sp. cf. *M. gracilis* (a) is present.

Fig. G (Td31): Photomicrograph of upper part of the Dungan Formation at Rakhi Nala, Sulaiman Range, representing planktonic foraminiferal siltstone facies.

Fig. H (Td46): Photomicrograph of upper part of the Dungan Formation at Rakhi Nala, Sulaiman Range, representing planktonic foraminiferal siltstone facies, showing change in planktonic foraminiferal assemblages from morozovellid-dominated to subbotinid/acarininid-dominated assemblages.

Plate 4.1

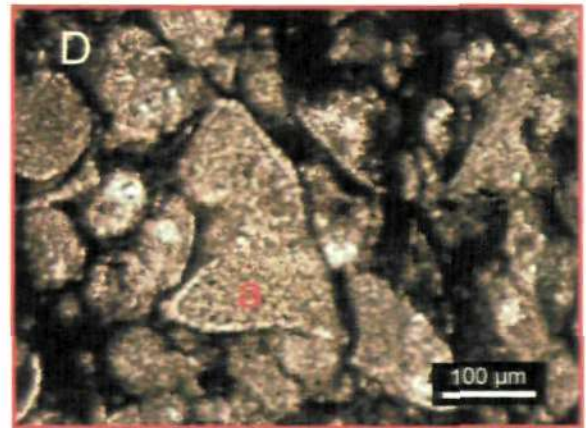
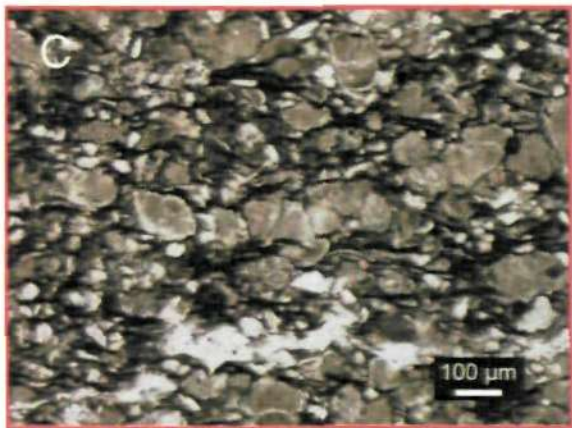
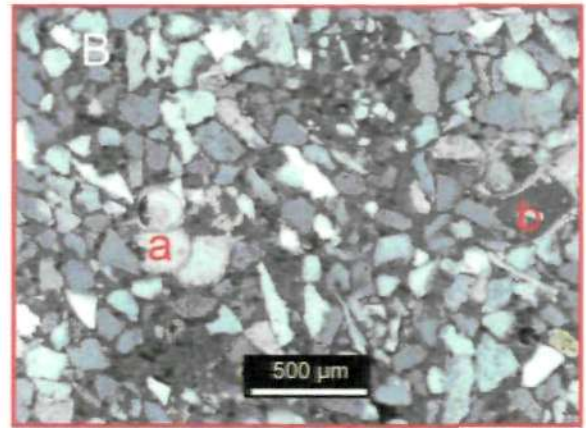
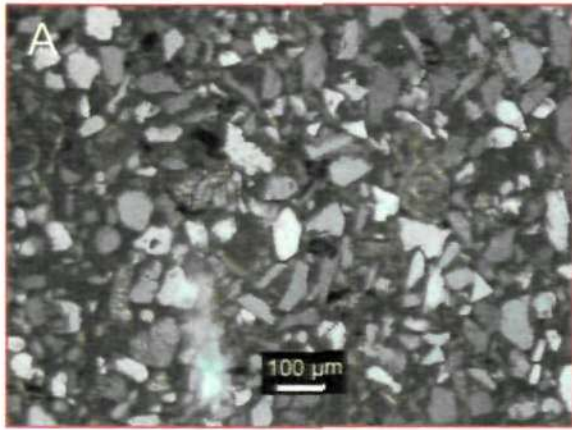
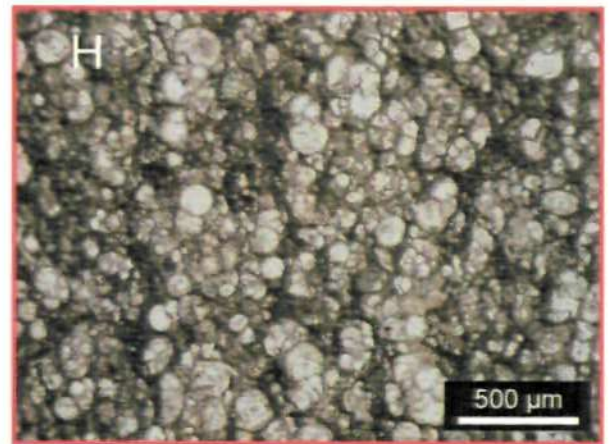
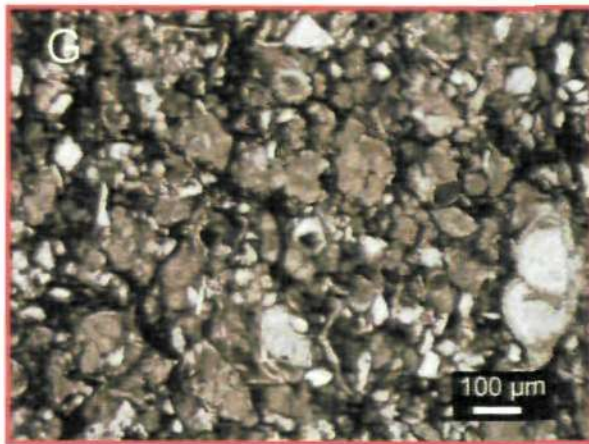
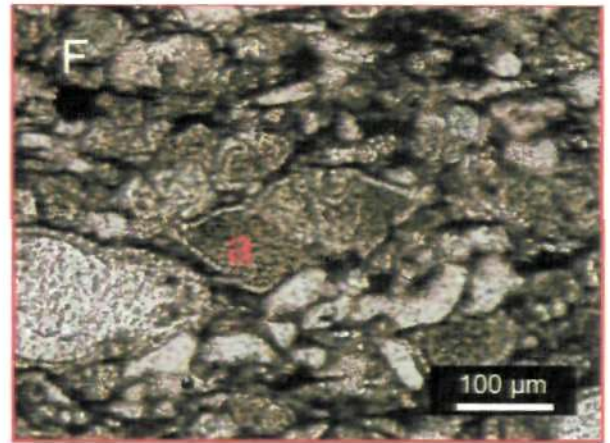
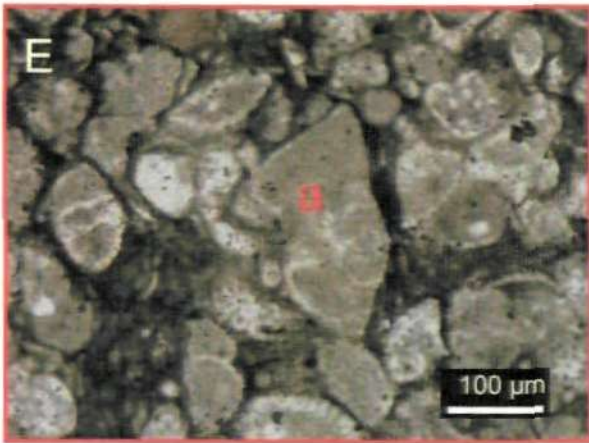


Plate 4.1 (continued)



Plates 4.2-4.4

Planktonic foraminifera from the Palaeocene/Eocene interval Dungan Formation, Rakhi Nala, Sulaiman Range, Lower Indus Basin.

Plate 4.2

A-I, K, M, O, P, S-X, Z-B1, D1 (Scale bar = 100µm), J, L, N, Q, R, Y, C1 (Scale bar = 50µm), (A)- *Acarinina* sp. cf. *A. wilcoxensis*, sample # (Td-33), (B)- *Acarinina* sp., (Td-30), (C)- *Acarinina* sp., (Td-50), (D)- *Acarinina* sp., (Td-50), (E)- *Acarinina* sp., (Td-50), (F)- *Acarinina* sp., cf. *A. pseudotopilensis* (Td-32), (G)- *Acarinina* sp., (Td-45), (H)- *Acarinina* sp., (Td-43), (I)- *Acarinina* sp. cf. *A. wilcoxensis*, (Td-43), (J)- *Acarinina* sp., (Td-44), (K)- *Acarinina* sp., (Td-44), (L)- *Acarinina* sp. cf. *A. wilcoxensis*, (Td-44), (M)- *Acarinina* sp., (Td-44), (N)- *Acarinina* sp., (Td-44), (O)- *Acarinina* sp., (Td-44), (P)- *Acarinina* sp., (Td-44), (Q)- *Acarinina* sp., (Td-44), (R)- *Globanomalina chapmani*, (Td-32), (S)- *Globanomalina* sp. cf. *G. chapmani*, (Td-32), (T)- *Pseudohastigerina* sp. cf. *P. wilcoxensis*, (Td-32), (U)- *Globanomalina* sp. cf. *G. chapmani*, (Td-32), (V)- *Globanomalina* sp., (Td-42), (W)- *Globanomalina* sp., (Td-42), (X)- *Pseudohastigerina* sp. cf. *P. wilcoxensis*, (Td-47), (Y)- *Globanomalina* sp., (Td-45), (Z)- *Globanomalina* sp., (Td-44), (A1)- *Globanomalina* sp., (Td-44), (B1)- *Globanomalina* sp. cf. *G. luxorensis*, (Td-44), (C1)- *Globanomalina* sp., (Td-44), (D1)- *Globanomalina* sp., (Td-45).

Plate 4.2

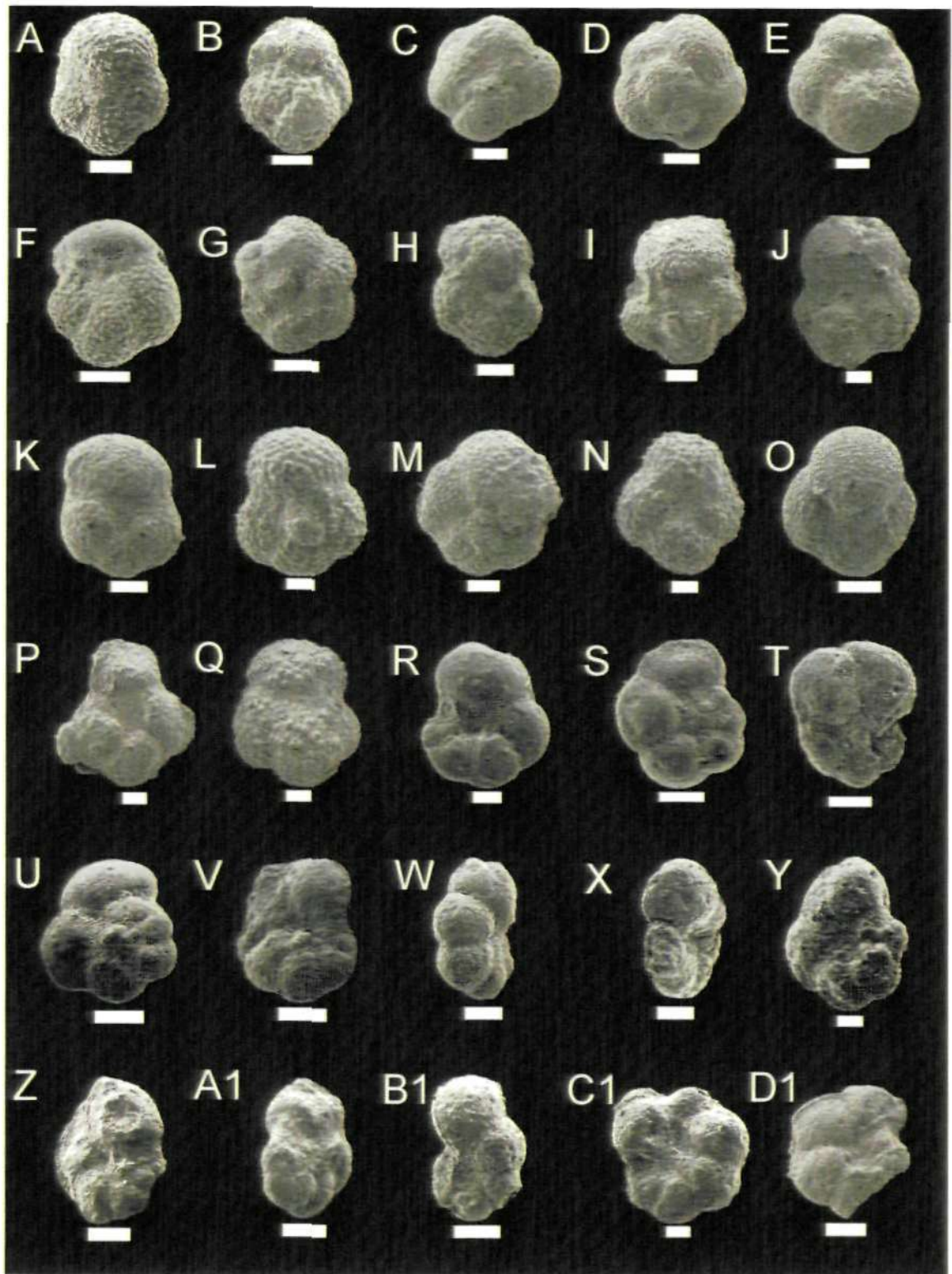


Plate 4.3

A-A1, C1, D1 (Scale bar= 100µm), B1 (Scale bar= 50µm), (A)- *Morozovella* sp. cf. *M. conicotruncata*, sample # (Td-43), (B)- *Morozovella* sp. cf. *M. formosa Formosa*, (Td-33), (C)- *Morozovella aragonensis*, (Td-33), (D, E, F)- *Morozovella acutispira*, (D-Td-33, E-Td-33, F-Td-33), (G)- *Morozovella aequa*, (Td-33), (H)- *Morozovella formosa formosa*, (Td-33), (I)- *Morozovella* sp. cf. *M. conicotruncata*, (Td-30), (J, K)- *Morozovella* sp. cf. *M. aragonensis*, (J-Td-30, K-Td-30), (L)- *Morozovella acutispira*, (Td-30), (M, N)- *Morozovella subbotinae*, (M-Td-48, N-Td-48), (O)- *Morozovella* sp., (Td-48), (P, Q, R)- *Morozovella aequa*, (P-Td-50, Q-Td-45, R-Td-45), (S)- *Morozovella subbotinae*, (Td-45), (T)- *Morozovella* sp., (Td-45), (U)- *Morozovella* sp., (Td-44), (V)- *Morozovella* sp., (Td-48), (W)- *Morozovella occlusa*, (Td-45), (X)- *Morozovella acuta*, (Td-47), (Y)- *Morozovella* sp., (Td-47), (Z)- *Morozovella acuta*, (Td-44), **A1. B1.** *Morozovella aequa*, (**C1**)- *Morozovella acuta*, (Td-32), (**D1**)- *Morozovella* sp. cf. *M. acutispira*, (Td-32).

Plate 4.3

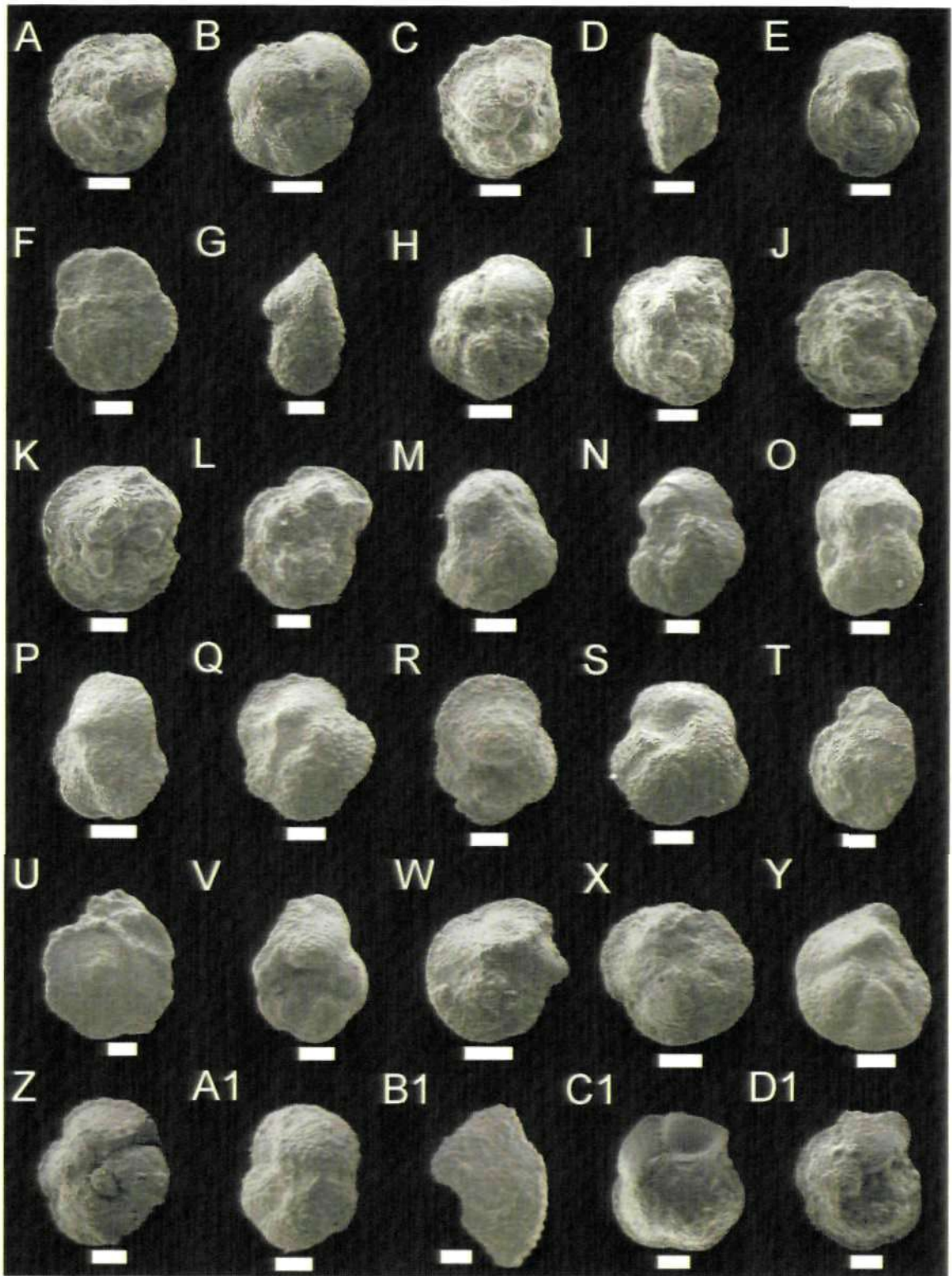
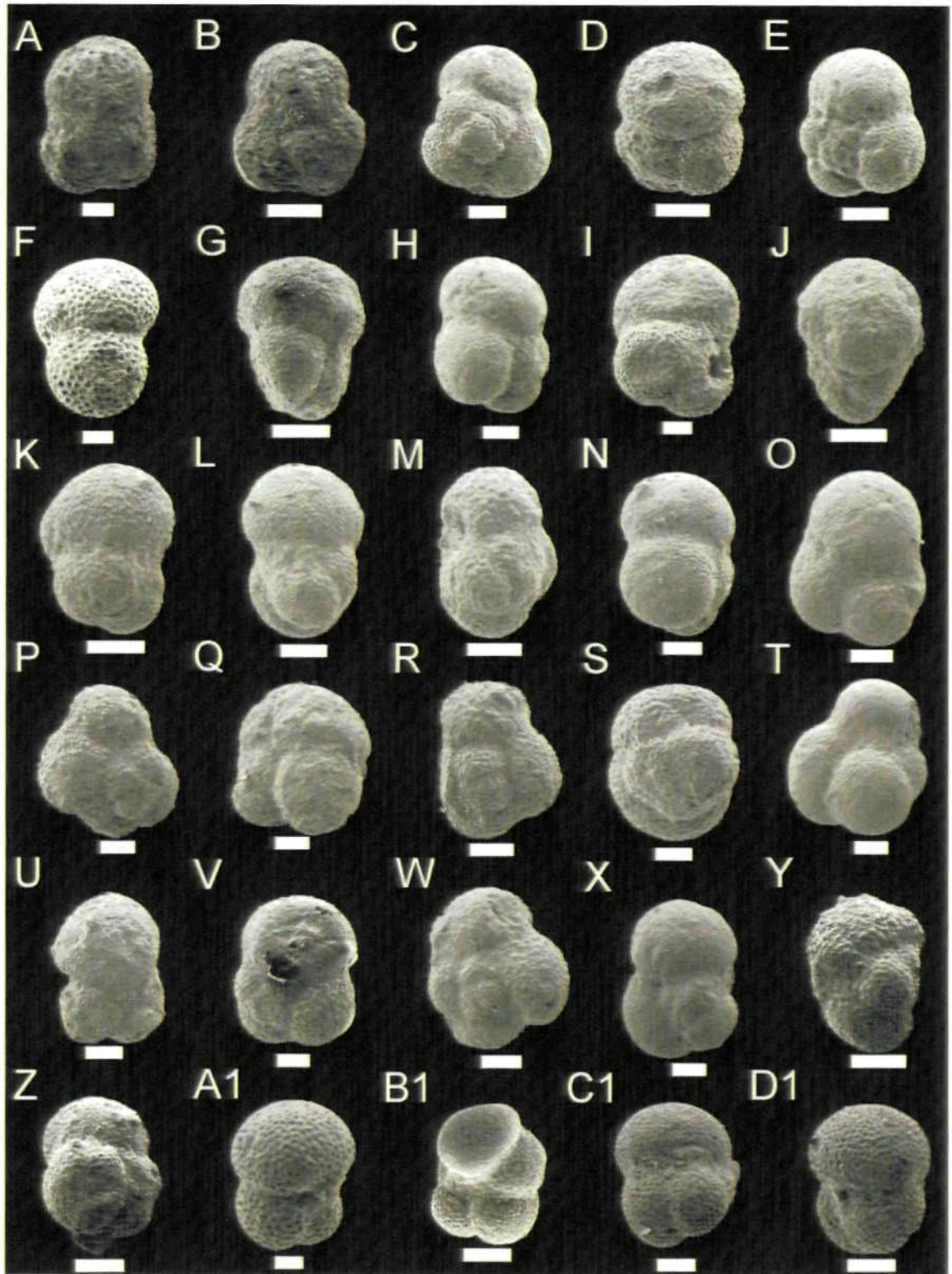


Plate 4.4

B-E, G, H, J-R, T, U, W, X, Y, Z, B1-D1 (Scale bar= 100µm), A, F, I, S, V, A1 (Scale bar = 50µm), (A)- *Subbotina triloculinoidea*, sample # (Td-43), (B, C)- *Subbotina triangularis*, (B-Td-43, C-Td-33), (D)- *Subbotina velascoensis*, (Td-33), (E)- *Subbotina triangularis*, (Td-33), (F)-*Subbotina triloculinoidea*, (Td-33), (G)- *Subbotina velascoensis*, (Td-48), (H)- *Subbotina triangularis*, (Td-50), (I)- *Subbotina* sp. cf. *S. triloculinoidea*, (Td-50), (J)- *Subbotina* sp., (Td-50), (K, L)- *Subbotina triloculinoidea*, (K-Td-50, L-Td-50), (M, N)- *Subbotina* sp. cf. *S. triangularis*, (M-Td-50, N-Td50), (O)- *Subbotina triangularis*, (Td-50), (P)- *Parasubbotina* sp. cf. *P. varianta*, (Td-43), (Q)- *Subbotina* sp. cf. *S. velascoensis*, (Td-43), (R)- *Subbotina* sp. cf. *S. triangularis*, (Td-44), (S)- *Subbotina* sp., (Td-48), (T)- *Subbotina* sp. cf. *S. patagonica*, (Td-50), (U, V)- *Subbotina* sp. cf. *S. triloculinoidea*, (U-Td-43, V-Td-44), (W)- *Parasubbotina* sp., (Td-45), (X)- *Subbotina triloculinoidea*, (Td-45), (Y)- *Subbotina* sp. cf. *S. velascoensis*, (Td-44), (Z)- *Subbotina* sp. cf. *S. patagonica*, (Td-44), (A1) *Subbotina triloculinoidea*, (Td-32), (B1)- *Parasubbotina* sp., (Td-33), (C1, D1)- *Subbotina triloculinoidea*, (C1-Td-45, D1-Td-50) .

Plate 4.4



Plates 4.5-4.18

Larger foraminifera from Paleocene - Eocene Lockhart, Patala and Margala Hill Limestone formations of the Kalli Dilli and Dalla sections, Kala Chitta Ranges (Fig.3.1), Upper Indus Basin. Sample numbers are given against each specimen, examples; d20= sample # 20 in Dalla section, kd1= sample # 1 in Kalli dilli section.

Plate 4.5

(A, B, D, F-L)- *Nummulites* spp., sample # (d20), (C, J, M)- *Nummulites* sp. cf. *N. mammilatus*, (d20), (E)- *Nummulites* sp. cf. *N. atacicus*, (d20), (N, O)- *Alveolina* spp., (d26).

Field of View (FOV) = 5.7 mm (Figs A, C-G, I, K-O); 2.7 mm (Figs A, B, H, J).

Plate 4.6

(O)- *Operculina* sp., (d23), (E, F, K, N)- *Nummulites* spp., (E, F- d20; K, N- d23), (R)- *Nummulites* sp. cf. *N. mammilatus*, (d23), (A, B, D, G, H, I, J, L)- *Nummulites* sp. cf. *N. atacicus*, (A, B, D- d20; G, H- d22; I, J, L- d23), (C, K, M)- *Nummulites* sp. cf. *N. globulus*, (C- d20; K, M- d23), (P, Q)- *Assilina* spp., (d23).

FOV = 5.7 mm (Figs B-I, K-R); 2.7 mm (Figs J, A).

Plate 4.7

(I, L, N)- *Nummulites* spp., (I, L- d23; N- d25), (A, B, C, G, M, O)- *Nummulites* sp. cf. *N. mammilatus*, (A, B, C, G, M- d23; O- d25), (D, E, H, K)- *Nummulites* sp. cf. *N. atacicus*, (d23), (F)- *Nummulites* sp. cf. *N. globulus*, (d23), (J)- *Assilina* sp., (d23).

FOV = 5.7 mm (Figs A-O); 2.7 mm (Fig. C).

Plate 4.8

(I, P)- *Lockhartia* spp., (I- d24; P- d26), (N)- *Nummulites* sp., (d24), (F)- *Nummulites* sp. cf. *N. mammilatus*, (d24), (B, E, G, H, J)- *Nummulites* sp. cf. *N. atacicus*, (d24), (K, L, M)- *Nummulites* sp. cf. *N. globulus*, (d24), (D)- *Assilina* sp. cf. *A. ranikoti* (Nuttall), (d24), (Q)- *Assilina* sp., (d26), (A, C, O)- *Alveolina* spp., (A, C- d24; O- d26).

FOV = 5.7 mm (Figs A, C-E, G, H, I, J, M, O-Q); 2.7 mm (Figs B, F, K, L, N).

Plate 4.9

(S)- *Miscellanea* sp., (d30), (B)- *Nummulites* sp., (d28), (Q)- *Operculina* sp. cf. *O. hardiei*, (d30), (D, E, N, O)- *Nummulites* sp. cf. *N. mammilatus*, (D, E- d28; N, O - d29), (C, F, G, H, K, P)- *Nummulites* sp. cf. *N. atacicus*, (C, F, G, H- d28; K, P- d29), (I)- *Nummulites* sp. cf. *N. globulus*, (d28), (A, R)- *Assilina* sp. cf. *A. ranikoti* (Nuttall), (A- d28; R- d30), (J)- *Operculina* sp., (d28), (L, M)- *Alveolina* spp., (d29).

FOV = 5.7 mm (Figs A, B, D-Q); 2.7 mm (Fig. C).

Plate 4.10

(D, E, F, G, I, K)- *Miscellanea* spp., (D, E, F, G- d31; I - d32; K- d37), (B)- *Operculina* sp., (d30), (M, P, S, U)- *Nummulites* sp. cf. *N. mammilatus*, (M- d37; P- d23; S, U- d38), (O)- *Nummulites* sp. cf. *N. atacicus*, (d23), (Q, R)- *Nummulites* sp. cf. *N. globulus*, (Q, R- d38), (J, T, V)- *Assilina* spp., (J- d37; T,

V- d38), (L)- *Alveolina* sp., (d37), (H)- *Palaeonummulites* sp., (d31), (A, C, N)-
Ranikothalia sp. cf. *R. Kohatica*, (A, C- d30; N- d37).

FOV = 5.7 mm (Figs A-R, T); 2.7 mm (Figs S, U, V).

Plate 4.11

(O, P)- *Miscellanea* spp., (kd1), (B, C)- *Lockhartia* spp., (d38), (G)- *Nummulites*
sp., (d39), (E, H)- *Nummulites* sp. cf. *N. mammilatus*, (E- d38; H- d39), (F, K, L,
M)- *Nummulites* sp. cf. *N. atacicus*, (F- d38; K, L, M- d39), (D, J, N)-
Nummulites sp. cf. *N. globulus*, (D- 38; J, N- d39), (I)- *Assilina* sp. cf. *A. ranikoti*
(Nuttall), (d38), (A)- *Nummulitoides* sp. cf. *N. inaequilateralis*, (d38).

FOV = 5.7 mm (Figs J-M, O); 2.7 mm (Figs A-I, N, P).

Plate 4.12

(A, B, D, E, F, I, L)- *Miscellanea* spp., (A, B, D, E, F, I- kd1; L- kd4), (H)-
Miliolidae, (kd1), (G)- *Discocyclusina dispansa*, (kd1), (C, J, K, M)- *Nummulitoides*
sp. cf. *N. inaequilateralis*, (C- kd1; J, K, M- kd4).

FOV = 5.7 mm (Figs A, C, E-M); 2.7 mm (Figs B, D).

Plate 4.13

(D, M)- *Miscellanea* sp., (D- kd4; M- kd12), (A, B, C)- *Lockhartia* spp., (kd4),
(J, K, L)- *Miliolidae*, (kd4), (E, F, H, N)- *Nummulitoides* sp. cf. *N.*
inaequilateralis, (E, F, H- kd4; N- kd12), (G, I)- *Discocyclusina* spp., (kd4).

FOV = 5.7 mm (Figs A-N).

Plate 4.14

(D, E, G, I, J)- *Miscellanea* spp., (D, E, G- kd14; I, J- kd15), (A, F, H, K, L)- *Ranikothalia* spp., (A- kd12; F- kd14; H, K, L- kd15), (M)- *Caudrina* sp. cf. *C. soldadensis*, (kd15), (B, C)- *Operculina* spp., (kd12).

FOV = 5.7 mm (Figs A-M).

Plate 4.15

(C, E, F, G, K, L, M, O, P)- *Miscellanea* spp., (C, E, F- kd16; G- kd17; K, L, M, O, P- kd18), (H, N)- *Lockhartia* spp., (H- kd17; N- kd18), (D, I, Q)- *Ranikothalia* spp., (D- kd16; I- kd17; Q- kd18), (A, B)- *Miliolidae* spp., (kd16), (J)- *Orbitolites* sp., (kd17).

FOV = 5.7mm (Figs C, G-Q); 2.7 mm (Figs A, B, D-F).

Plate 4.16

(A, E, F, G, I, J, K, N, O, P, Q, S)- *Miscellanea* spp., (A, E, F, G, I, J, K, N, O, P, Q- kd19; S- kd25), (L, R)- *Lockhartia* spp., (L- kd19; R- kd25), (B)- *Ranikothalia* sp., (kd19), (H)- *Operculina* sp., (kd19), (C, D, M)- *Ranikothalia* sp. cf. *R. kohatica*, (kd19).

FOV = 5.7 mm (Figs A-S).

Plate 4.17

(A, B, C, D, E, F, G, H, I, J, K, M, N, O, P, Q)- *Miscellanea* spp., (kd25), (L, R, S)- *Operculina* spp., (kd25).

FOV = 5.7 mm (Figs A-S).

Plate 4.18

(**B, H, K, L, M, N**)- *Miscellanea* spp., (B, H- kd30; K, L, M, N- kd35), (**E, I**)-
Nummulitoides spp., (kd30), (**G**)- *Caudrina* sp. cf. *C. soldadensis*, (kd30), (**C**)-
Nummulitoides sp. cf. *N. inaequilateralis*, (kd30), (**A, D, J**)- *Operculina* spp.,
(kd30), (**F**)- *Lockhartia haimei*, (kd30).

FOV = 5.7 mm (Figs A-N).

Plate 4.5

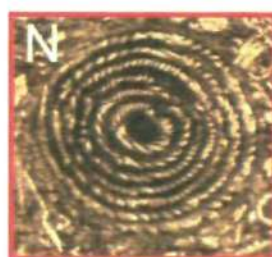
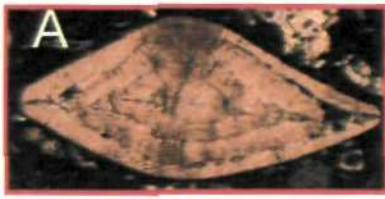


Plate 4.6

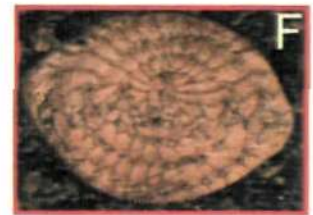
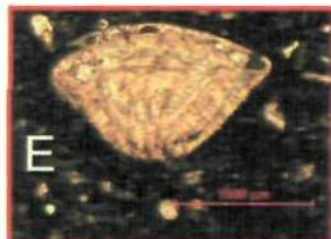


Plate 4.7

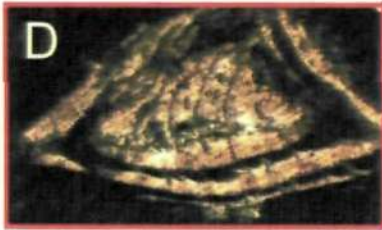


Plate 4.8

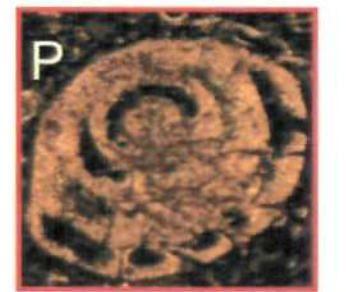
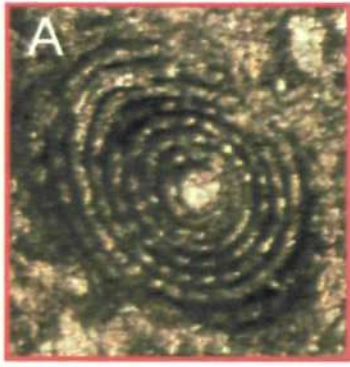


Plate 4.9

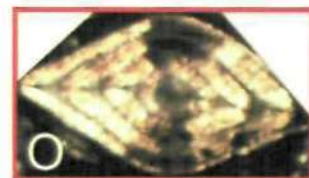
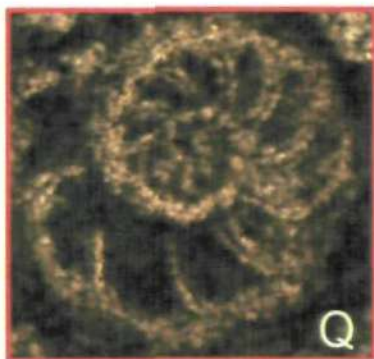
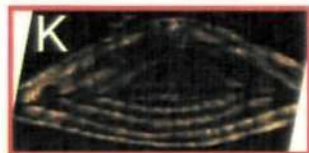
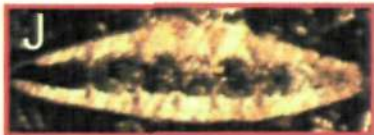


Plate 4.10

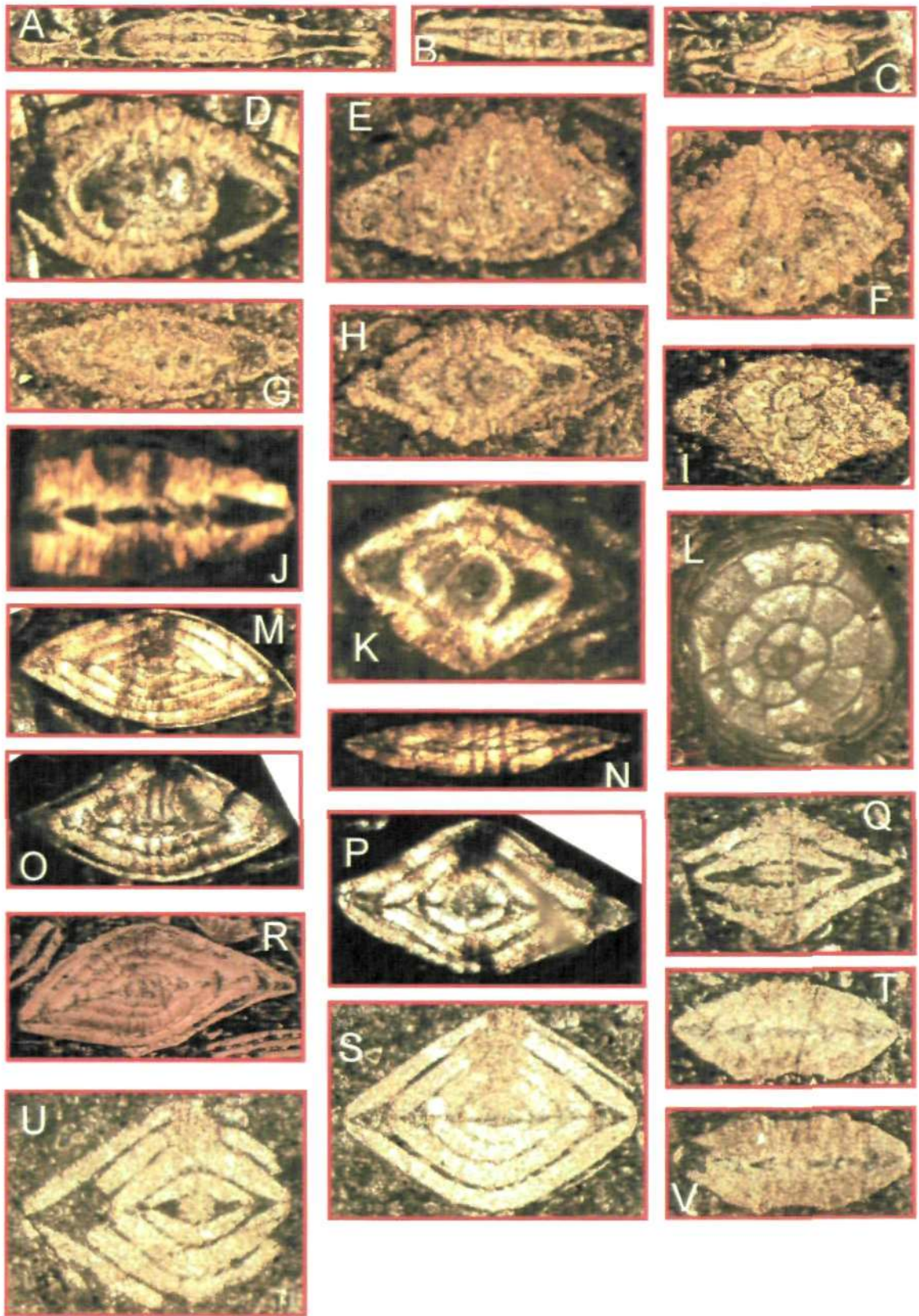


Plate 4.11

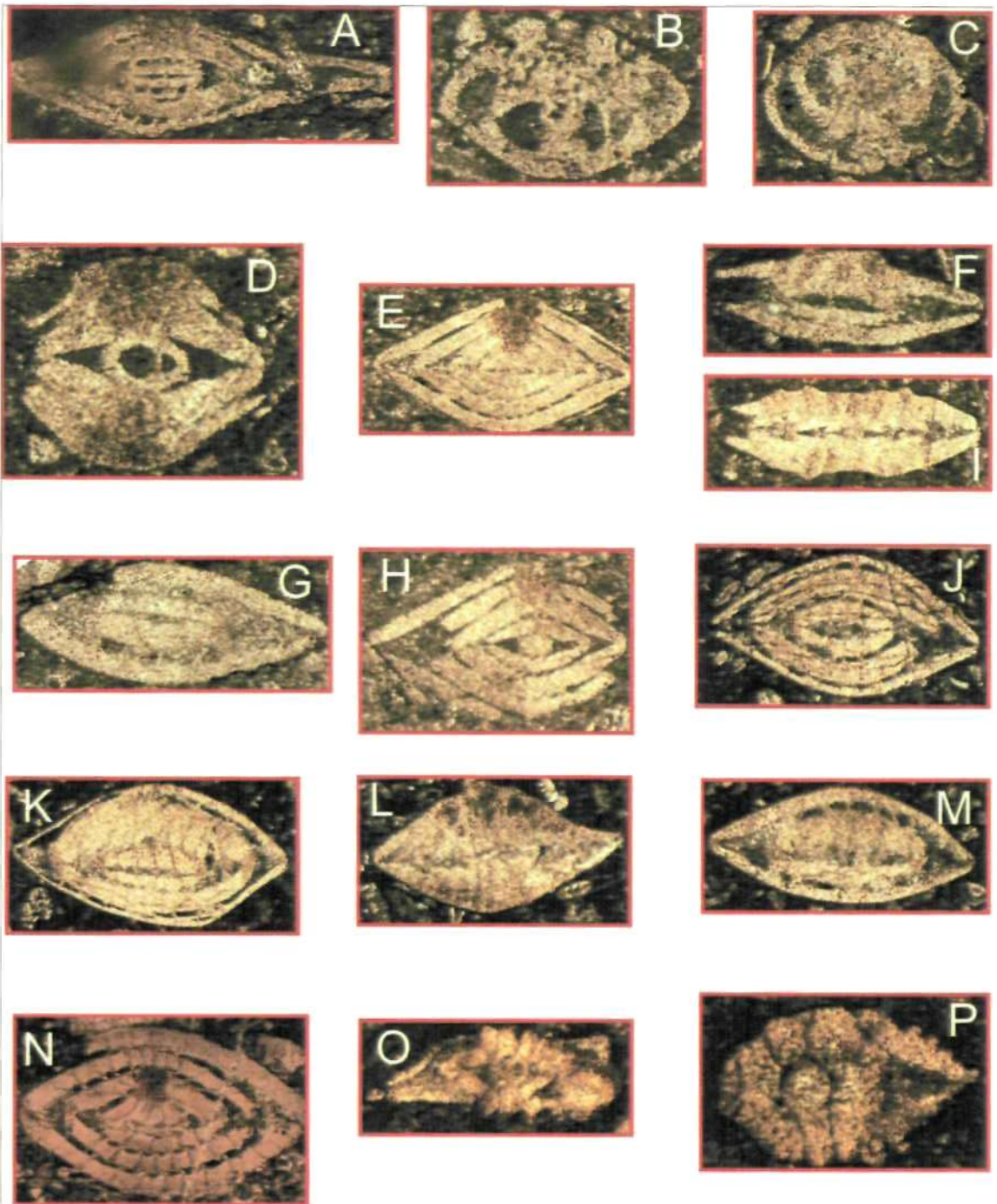


Plate 4.12

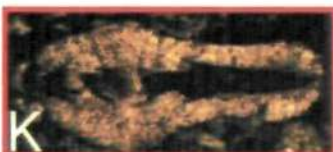
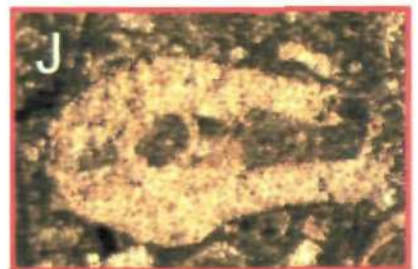
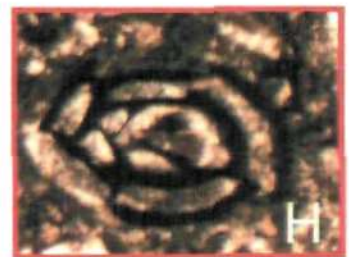
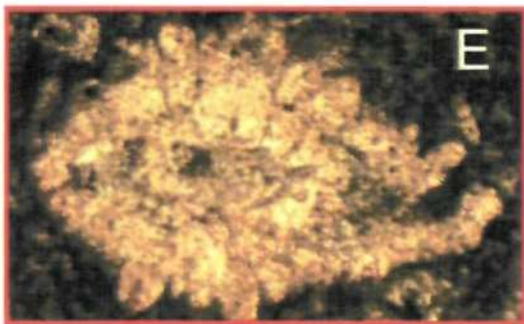
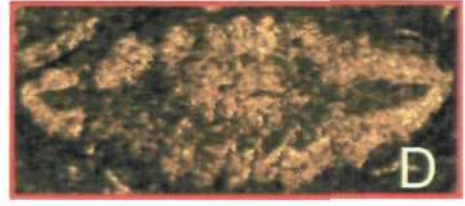
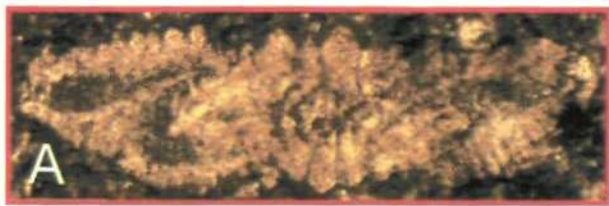


Plate 4.13

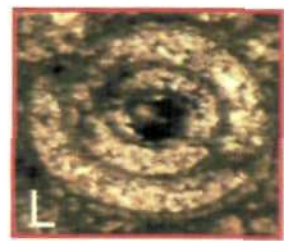
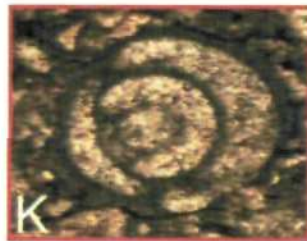
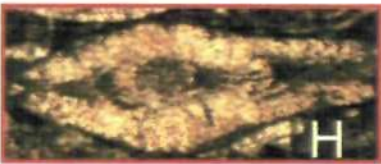
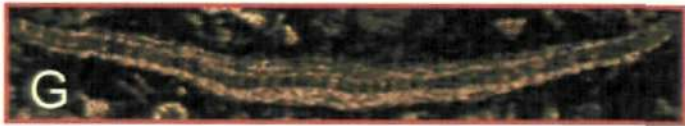
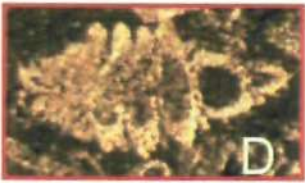
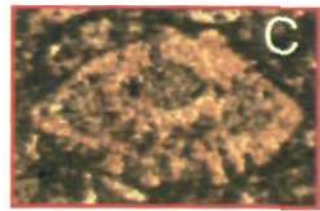
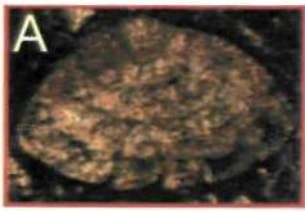


Plate 4.14

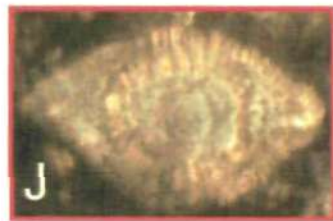
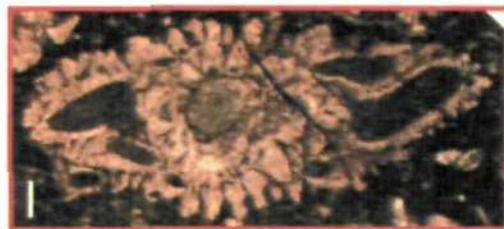
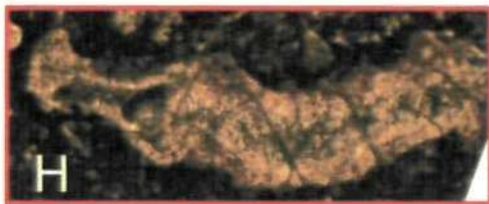


Plate 4.15

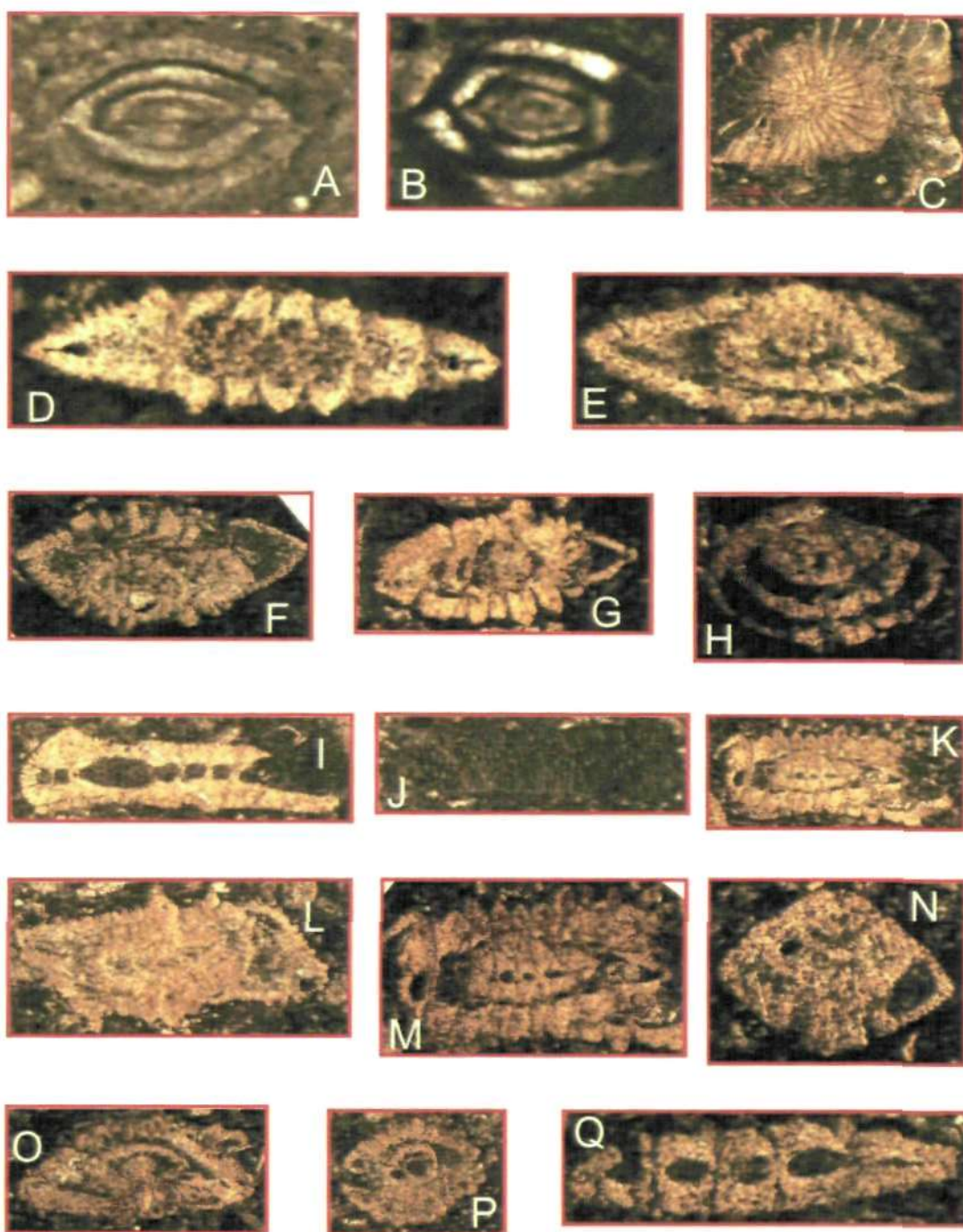


Plate 4.16

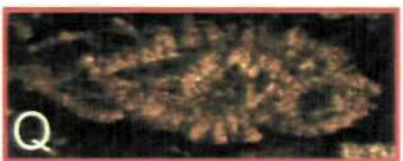
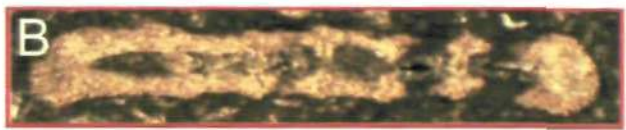


Plate 4.17

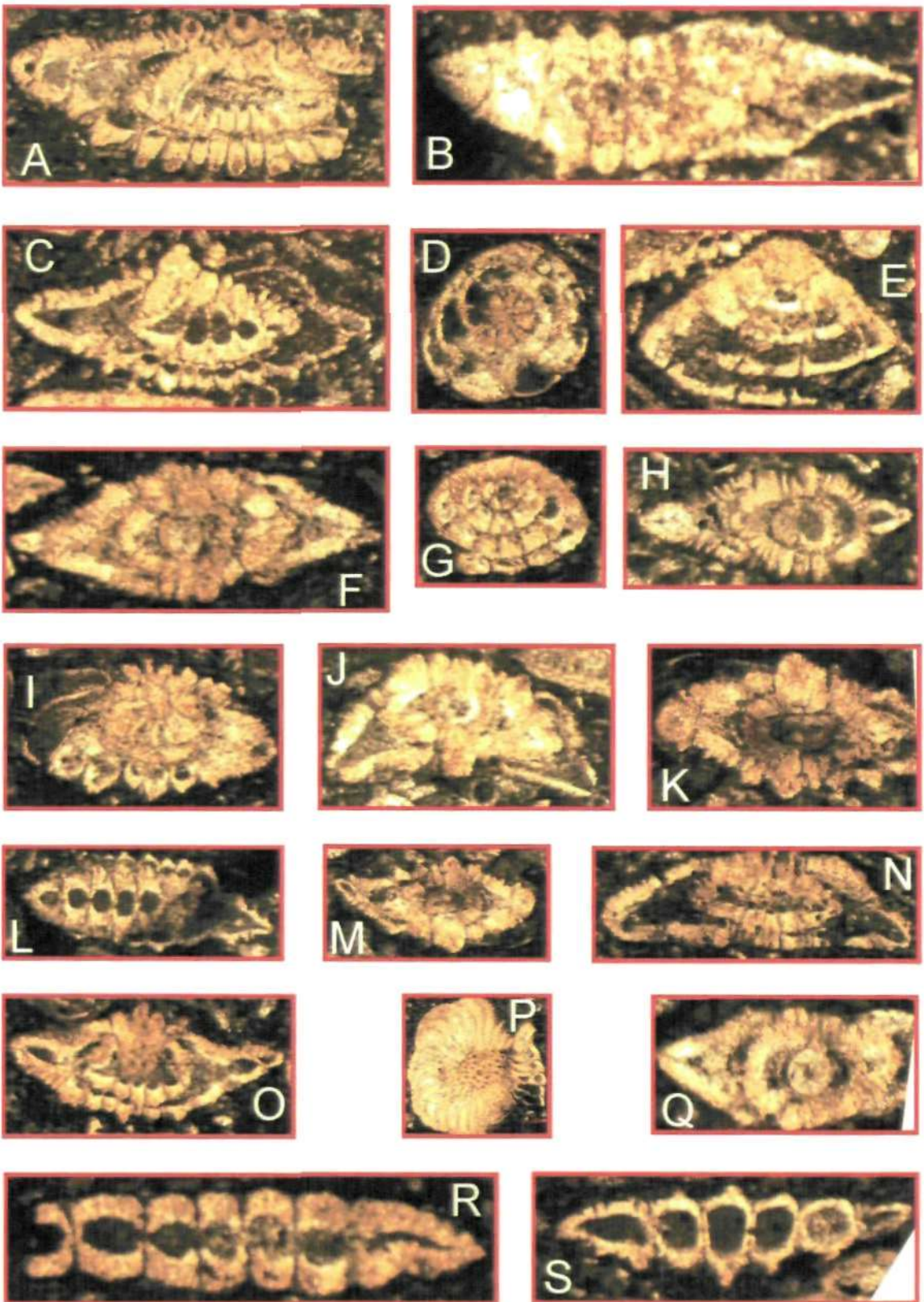


Plate 4.18

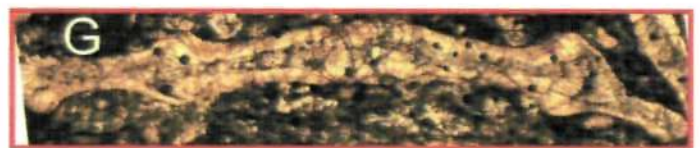
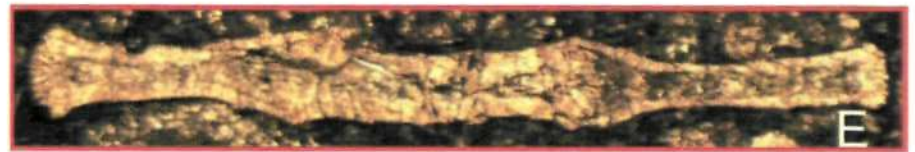
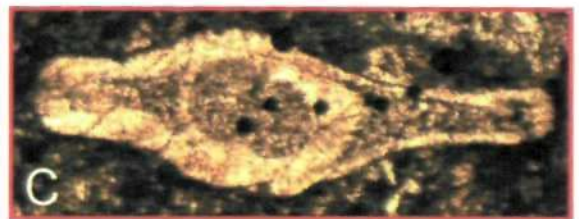


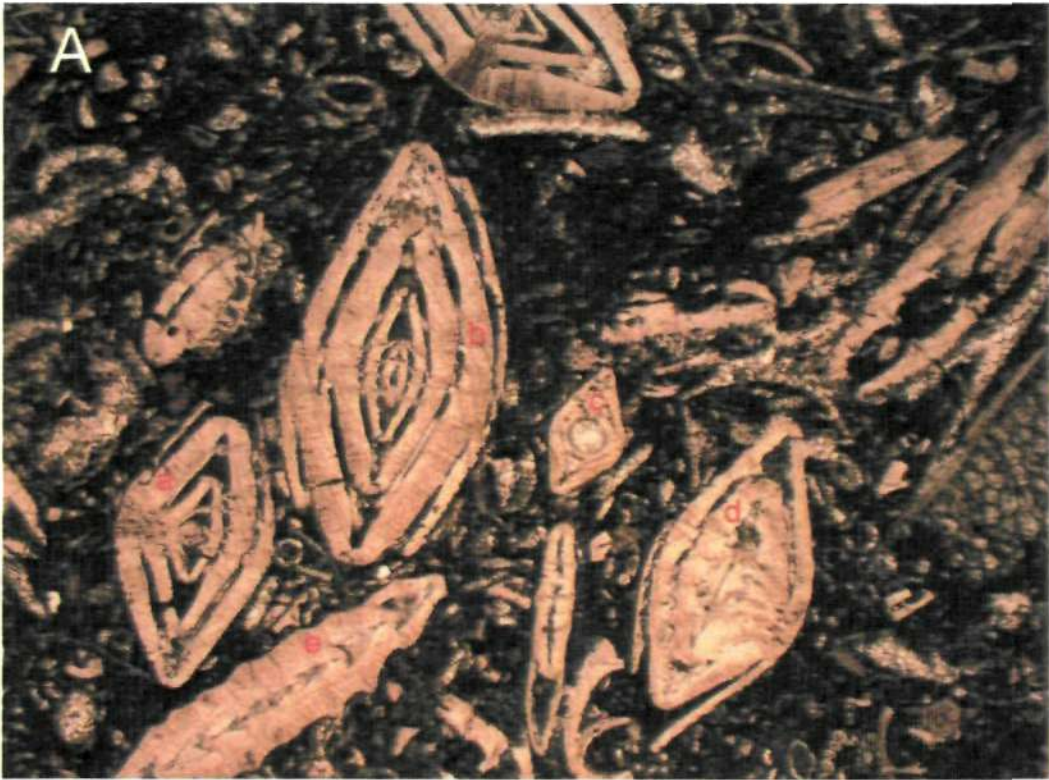
Plate 4.19

Showing Larger Foraminiferal Turnover from Paleocene *Ranikothalia* / *Miscellanea* - dominated assemblages (**Fig. B**) to Eocene *Nummulites*-dominated assemblages (**Fig. A**).

Fig. A: Eocene Margala Hill Limestone, Dalla section (= Nammal Limestone Formation of Salt Range) of the Kala Chitta Range, *Nummulites* spp. (a-d), *Assilina* sp. (e), **FOV**= 5.7 mm.

Fig. B: Paleocene Patala Formation of the, Kalli Dilli section, Kala Chitta Range, (a) *Nummulitoides* sp. (Haynes et al., 2010) (mistakenly identified as *Ranikothalia sindensis* by Butt (1991)), *Miscellanea* sp. (b), **FOV**= 5.7 mm.

Plate 4.19



FOV= 5.7 mm



FOV= 5.7 mm

Plates 4.20-4.26

Miscellanea micro-bioclastic wacke-packstone microfacies from upper Paleocene Patala Shale Formation of the Kalli Dilli section, Kala Chitta Range, Upper Indus Basin. FOV = 5.7 mm, 2.7 mm (Fig. 4.25B).

Fig. 4.20A: *Miscellanea* spp. (a), *Nummulitoides* sp. (b), *Lockhartia* spp.

Fig. 4.20B: *Miscellanea* sp. (a), bryozoans (b), coral (c).

Fig. 4.21A: *Miscellanea* sp. (a), Coral (b)

Fig. 4.21B: *Alveolina* sp. (a), calcite filled stylolite following the periphery of *Alveolina* sp. (b), *Nummulitoides* sp. (c).

Fig. 4.22A: *Miscellanea* sp. (a), *Ranikothalia* sp. (b), bioclast of *Ranikothalia* sp. (c).

Fig. 4.22B: *Orbitolites* sp. (a), *Discocyclina* sp. (b)

Fig. 4.23A: *Miscellanea* sp. (a), *Lockhartia* sp. (b), Calcite filled micro-fracture (c)

Fig. 4.23B: *Discocyclina* spp. (a), *Miscellanea* spp. (b), Miliolidae spp. (c)

Fig. 4.24A: *Ranikothalia* sp. (a), *Miscellanea* sp. (b)

Fig. 4.24B: *Ranikothalia* sp. (a), Miliolidae spp. (b), planktonic foraminiferid (c), fragment of dasyclad algae (d)

Fig. 4.25A: Unidentified larger foraminifera (a), *Ranikothalia* sp. (b), *Nummulitoides* sp. (c), *Miscellanea* sp. (d), Algae (e), dasyclad algae (f)

Fig. 4.25B: Unidentified larger foraminifera (a)

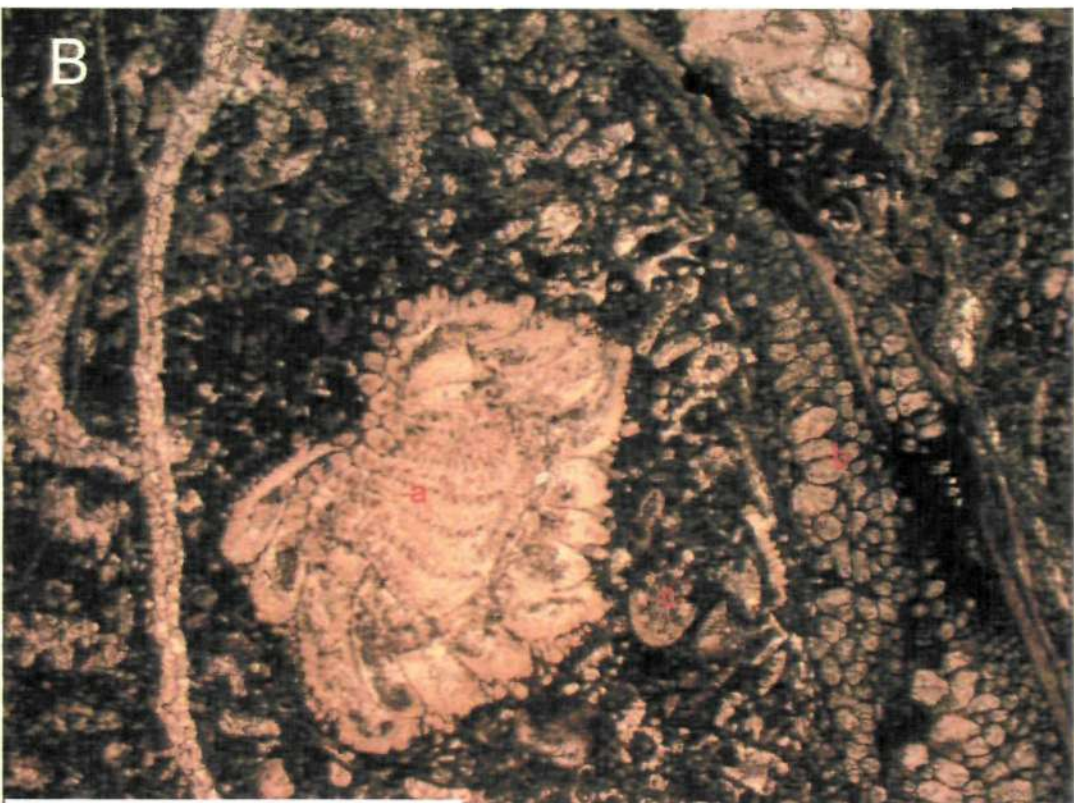
Fig. 4.26A: *Miscellanea* spp. (a), Miliolidae spp. (b), dasyclad algae (c)

Fig. 4.26B: *Miscellanea* spp. (a)

Plate 4.20

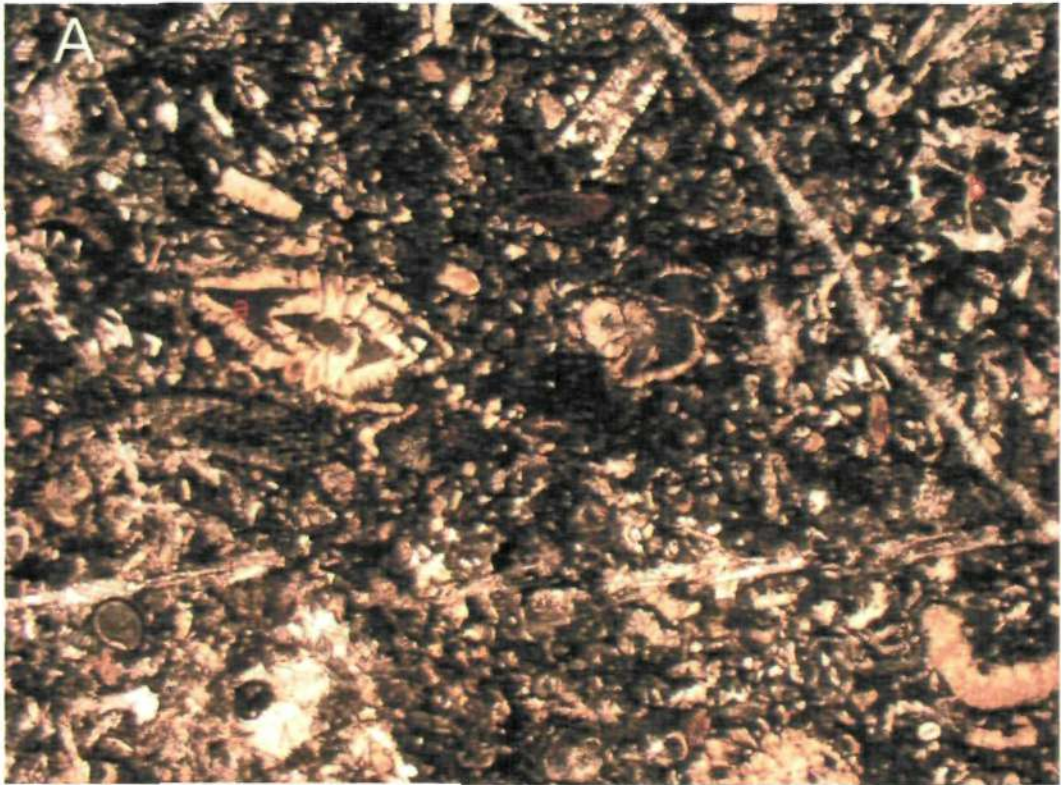


FOV= 5.7 mm

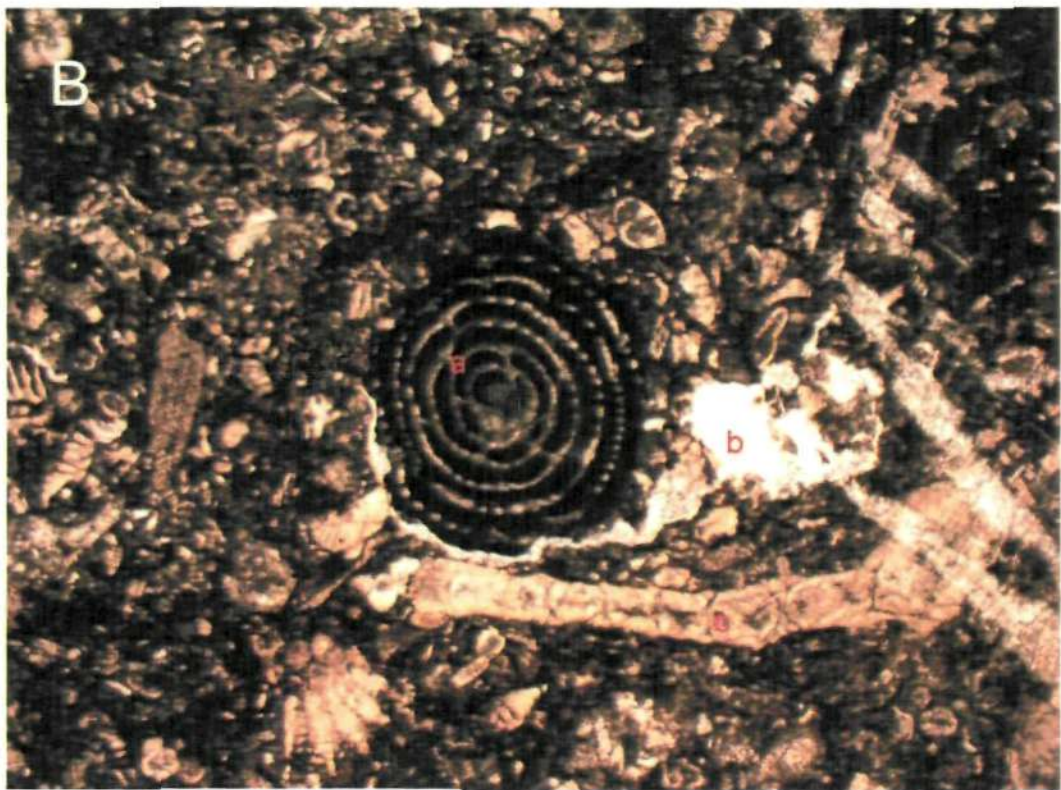


FOV= 5.7 mm

Plate 4.21



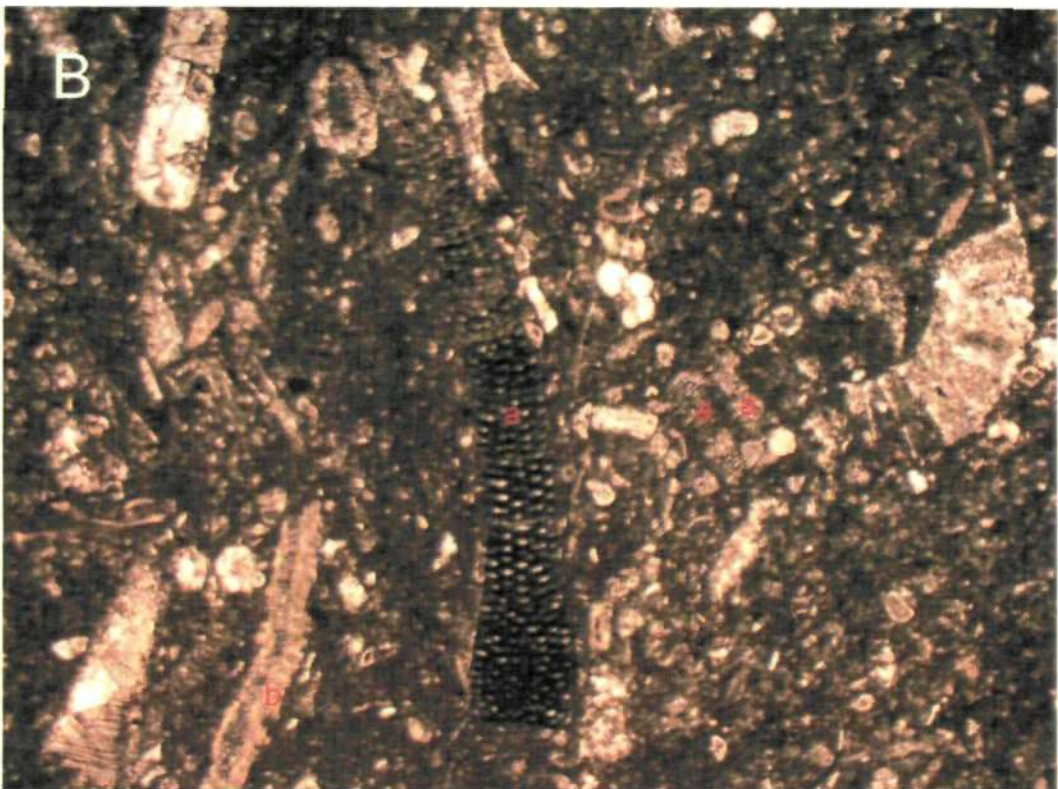
FOV= 5.7 mm



FOV= 5.7 mm

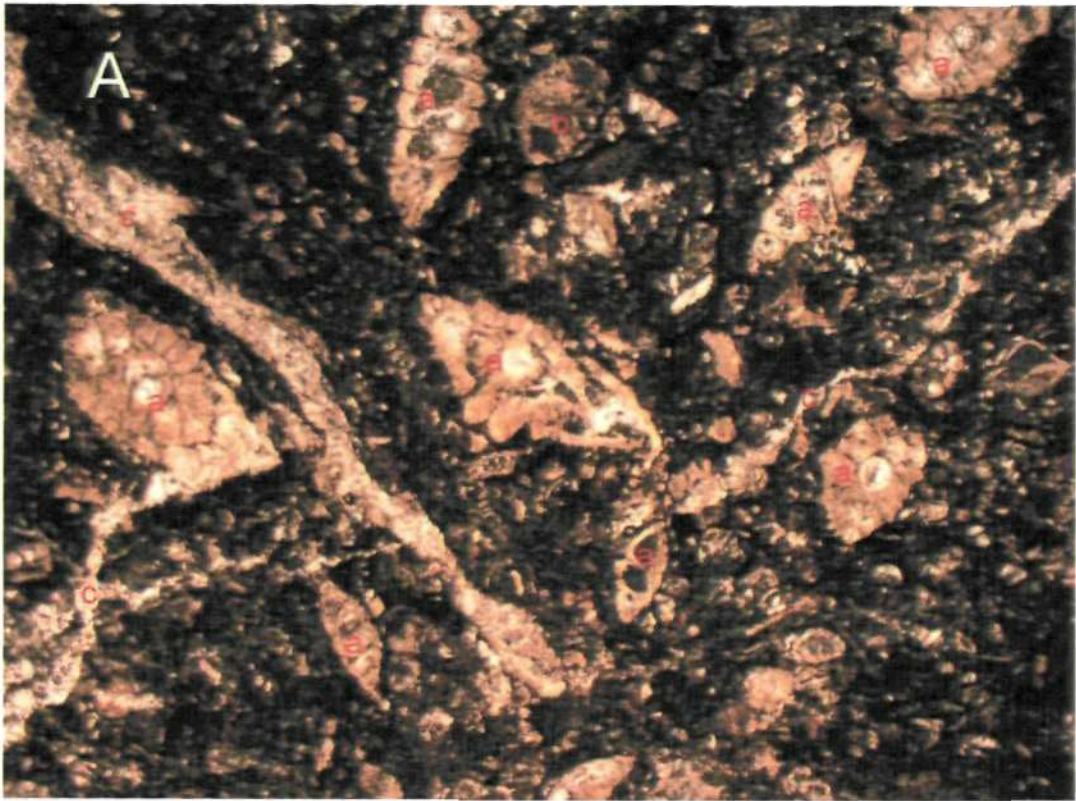


FOV= 5.7 mm

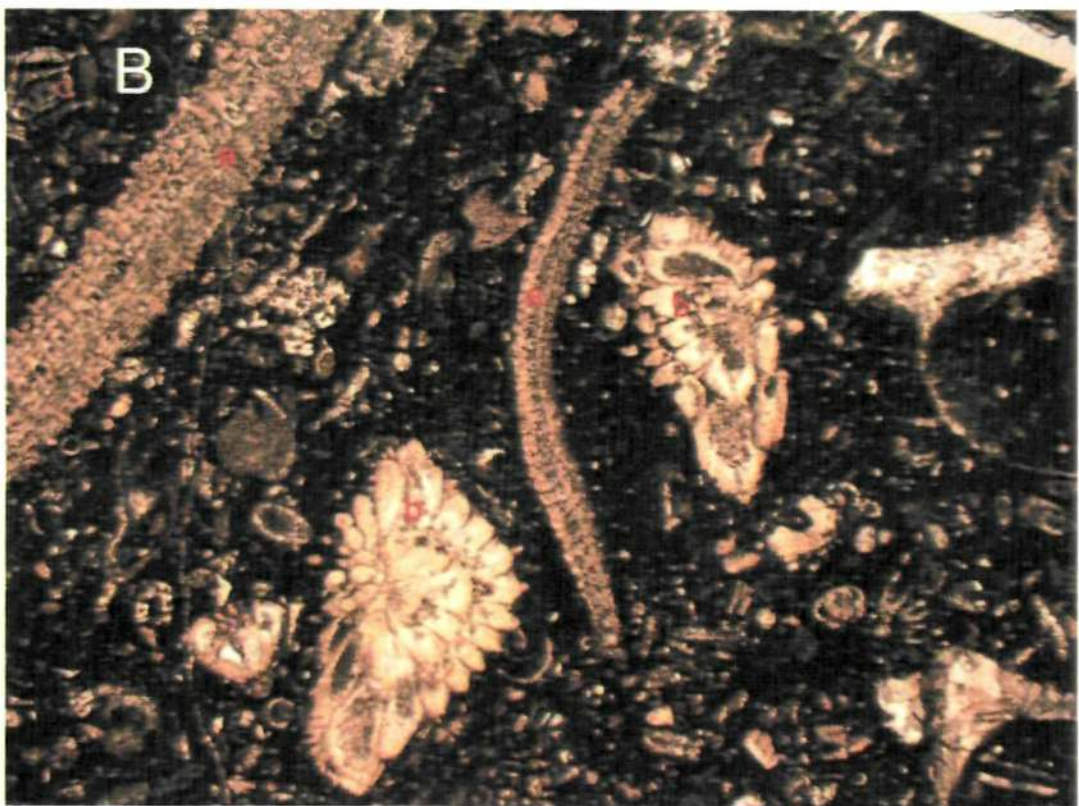


FOV= 5.7 mm

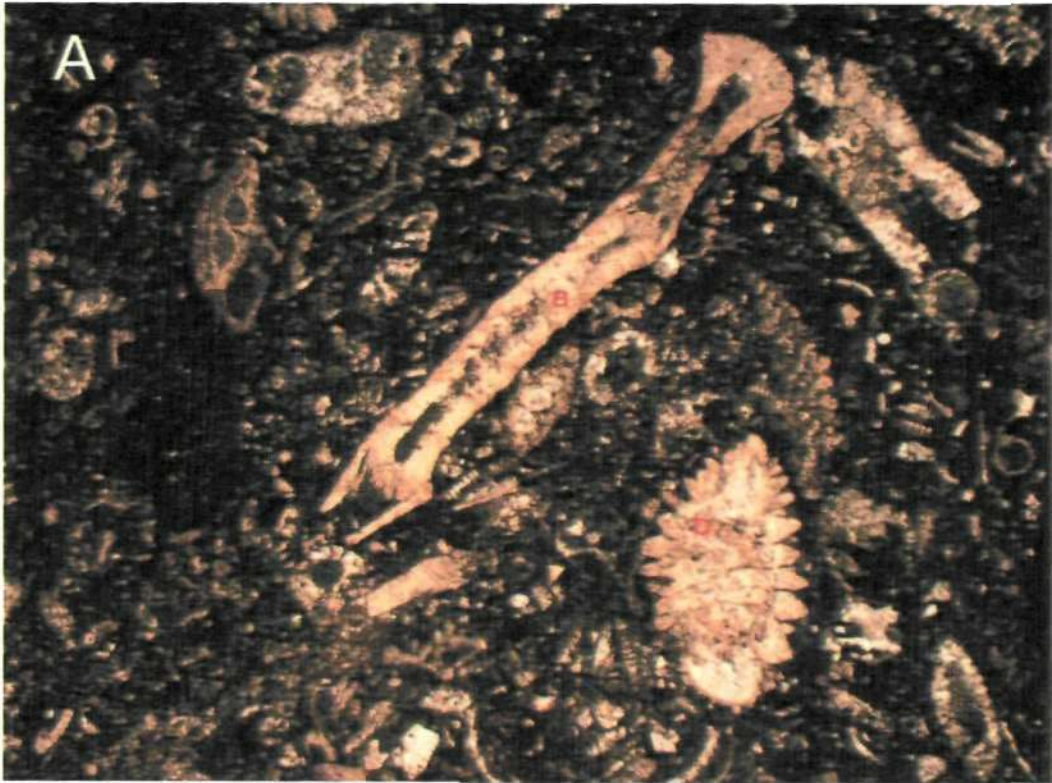
Plate 4.23



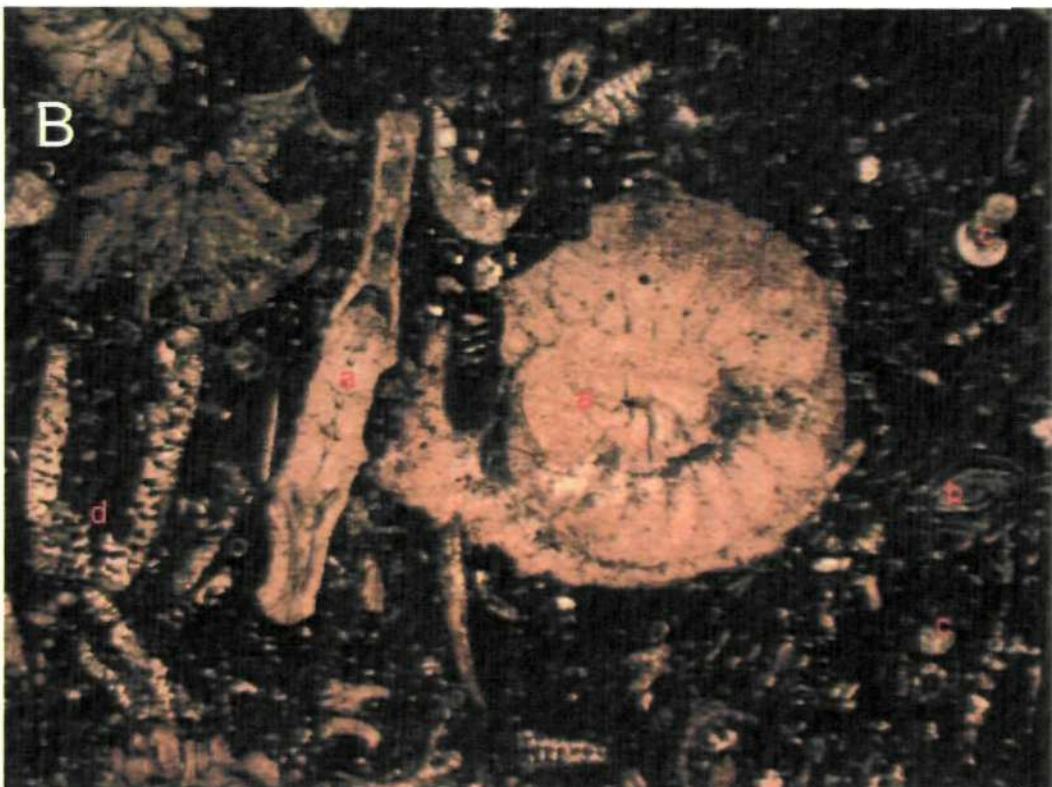
FOV= 5.7 mm



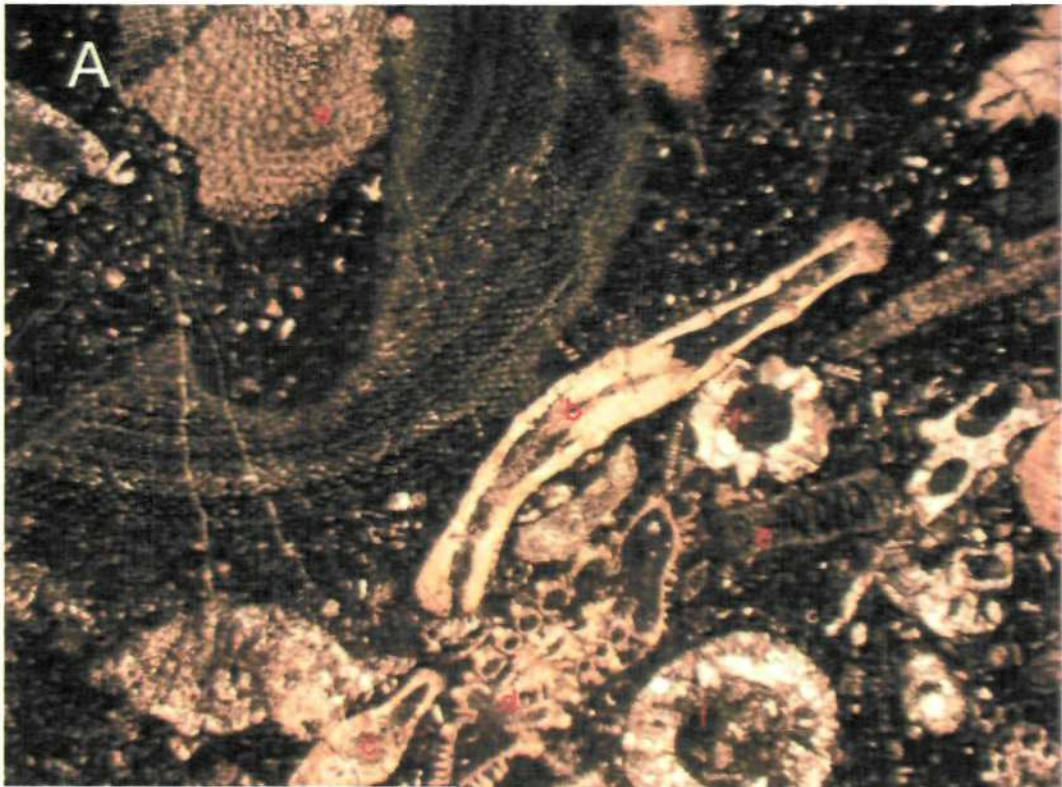
FOV= 5.7 mm



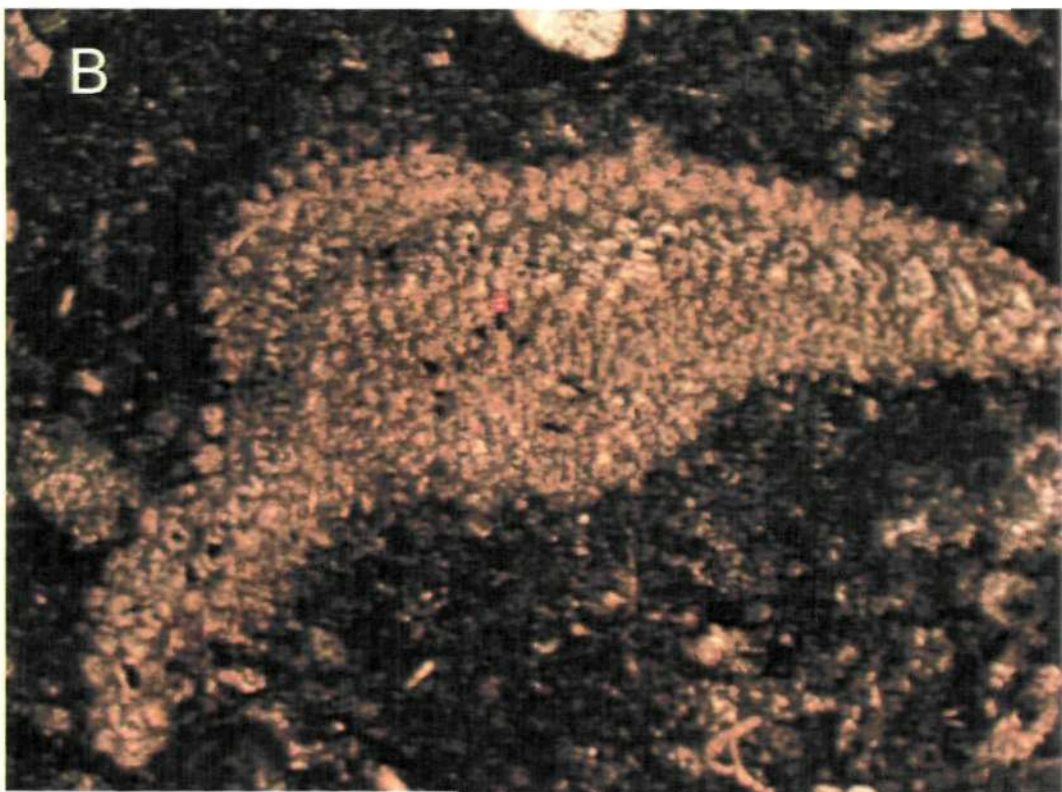
FOV= 5.7 mm



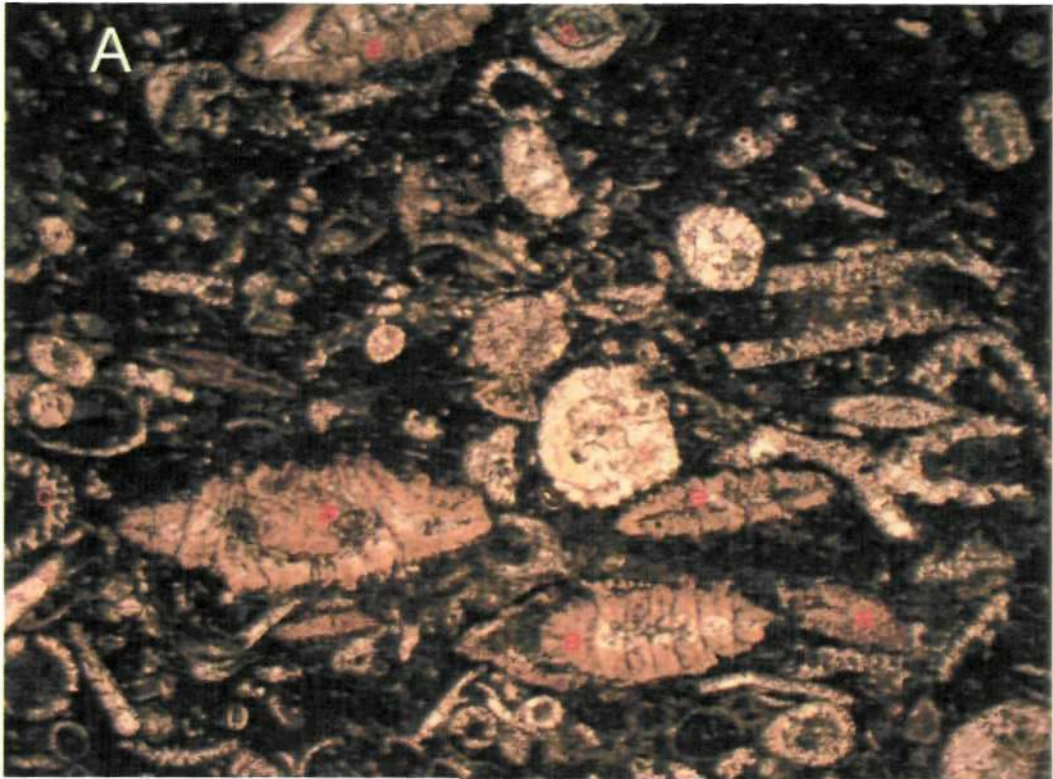
FOV= 5.7 mm



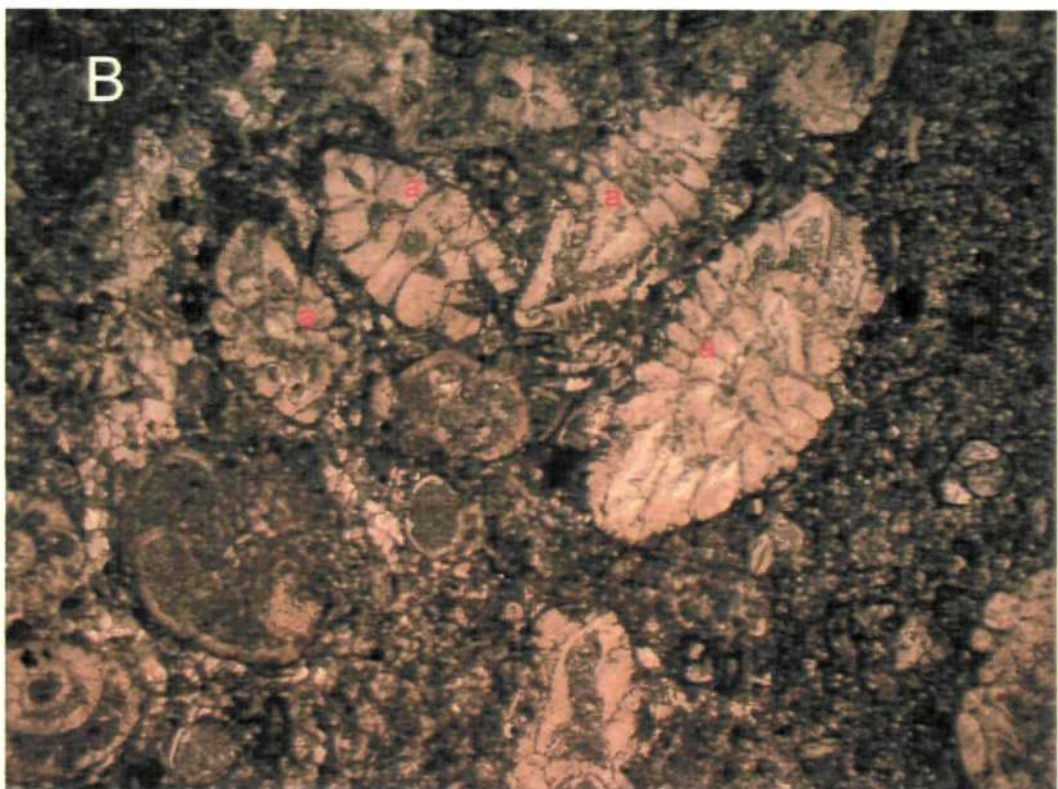
FOV= 5.7 mm



FOV= 2.7 mm



FOV= 5.7 mm



FOV= 5.7 mm

Plate 4.27-4.32

Nummulites peloidal wacke-packstone microfacies from lower Eocene Margala Hill Limestone Formation of the Dalla section, Kala Chitta Range, Upper Indus Basin.

FOV = 5.7 mm.

Fig. 4.27A: *Assilina* spp. (a), *Nummulites* spp. (b), peloid (c), re-crystallised intra-clasts (d).

Fig. 4.27B: *Nummulites* spp. (a), *Assilina* spp. (b), re-crystallised intra-clasts (c).

Fig. 4.28A: *Nummulites* spp. (a), *Assilina* spp. (b), bryozoan (c), peloid (d).

Fig. 4.28B: *Nummulites* spp. (a), *Assilina* spp. (b).

Fig. 4.29A: *Nummulites* spp. (a), bryozoan (b), re-crystallised intra-clast (c).

Fig. 4.29B: *Nummulites* spp. (a), re-crystallised intra-clast (b)

Fig. 4.30A: *Alveolina* spp. partially replaced by spar (a).

Fig. 4.30B: *Alveolina* spp. (a), *Nummulites* spp. (b), peloid (c), dasyclad algae (d).

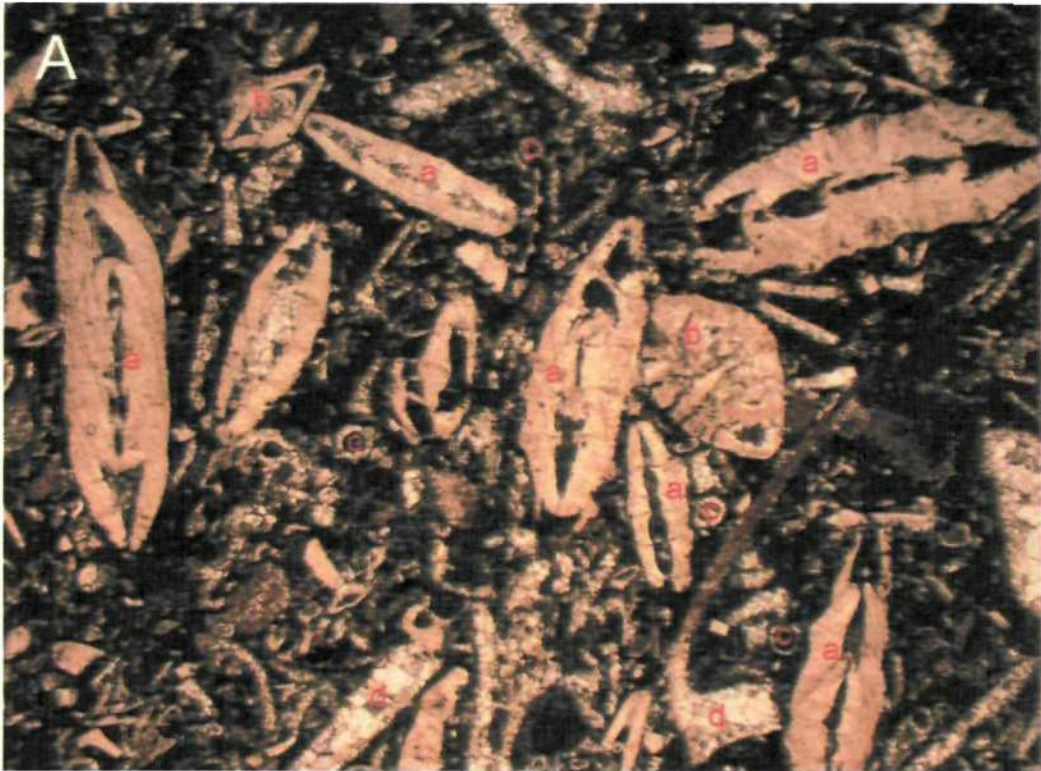
Fig. 4.31A: *Nummulites* spp. (a), calcisphere (b), dasyclad algae (c).

Fig. 4.31B: Calcisphere (a), *Assilina* spp. (b), unidentified foraminiferid (c).

Fig. 4.32A: *Discocyclina* spp. (a), dasyclad algae (b).

Fig. 4.32B: *Assilina* spp. (a), calcite filled micro-fracture (b).

Plate 4.27

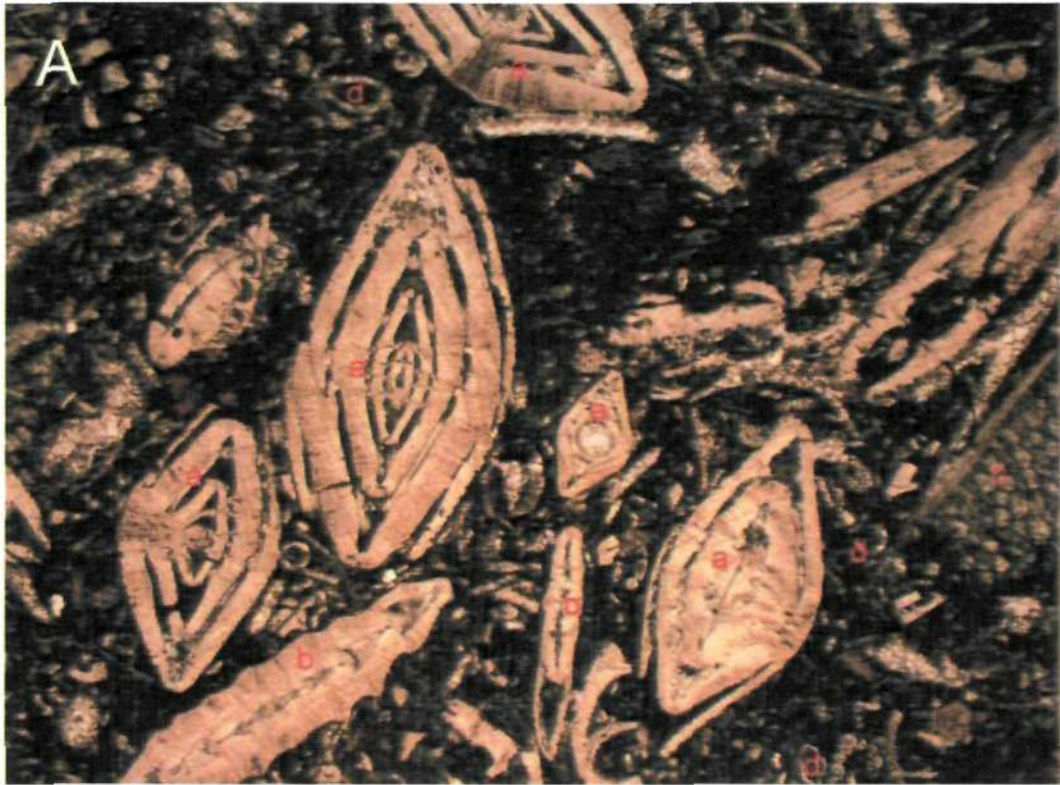


FOV= 5.7 mm



FOV= 5.7 mm

Plate 4.28



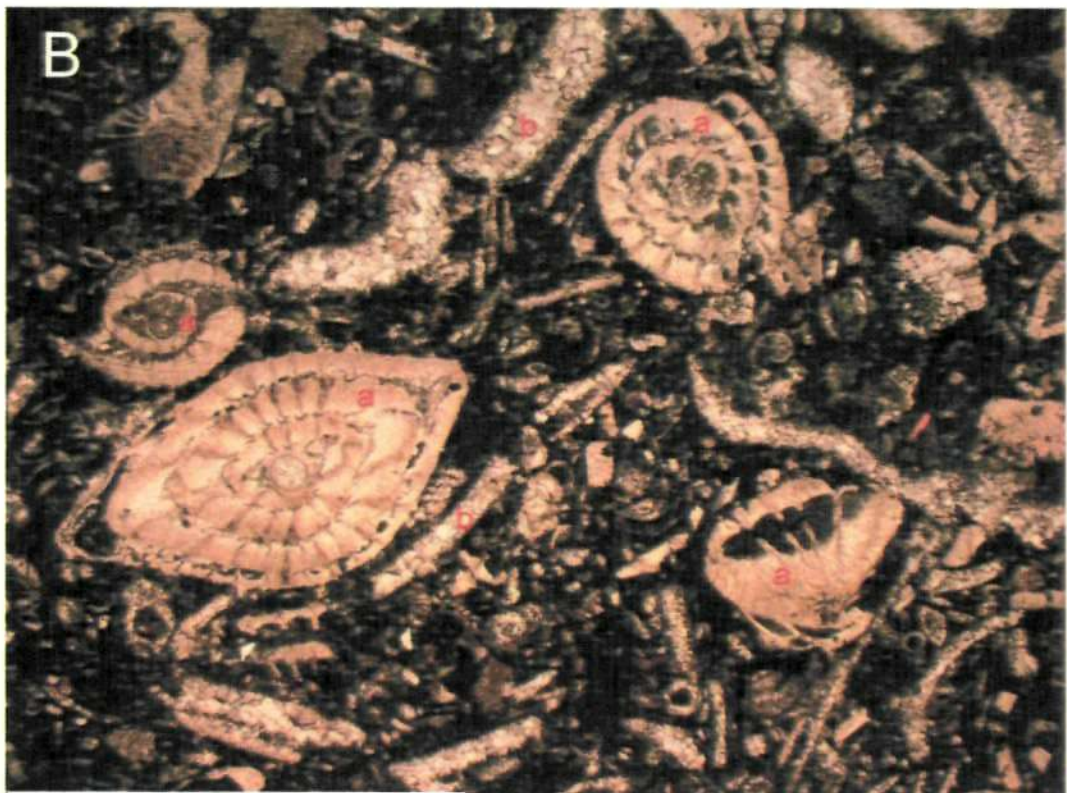
FOV= 5.7 mm



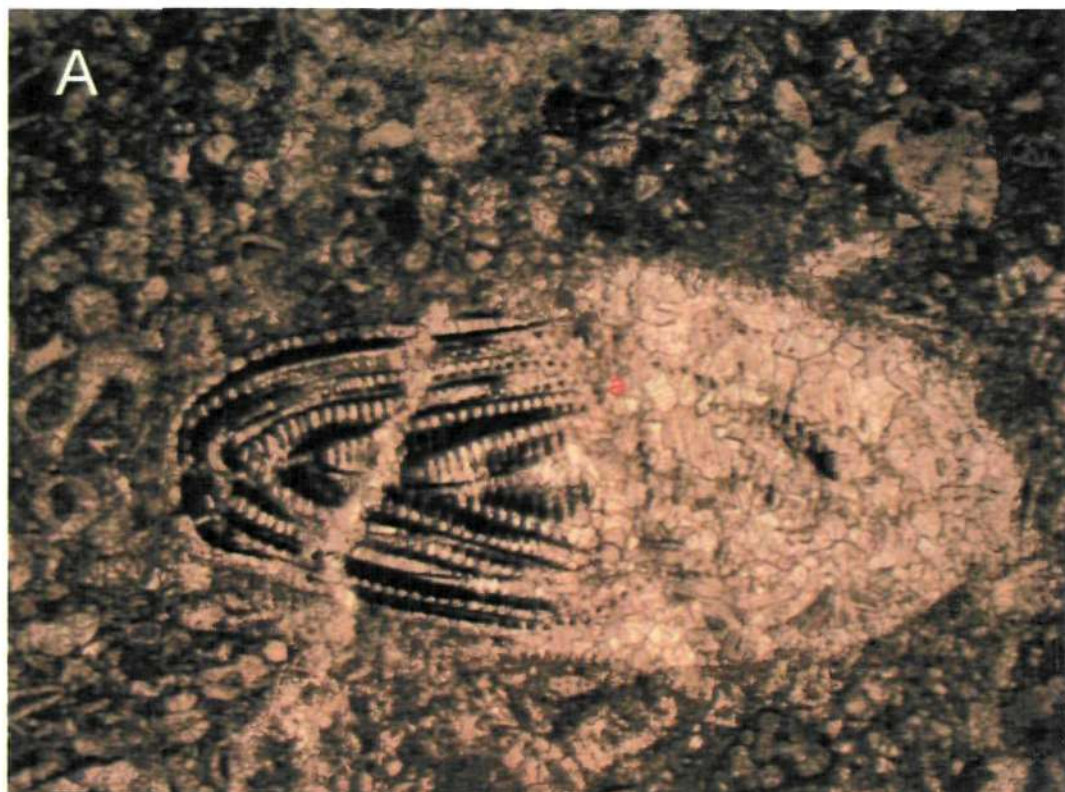
FOV= 5.7 mm



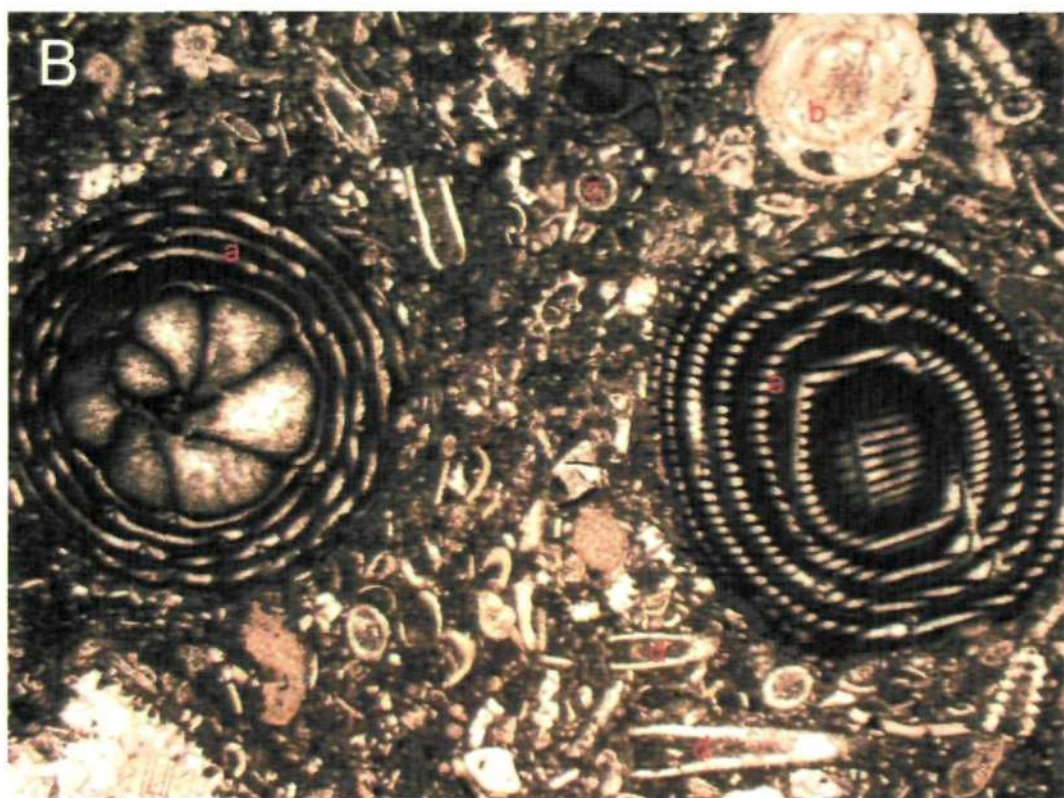
FOV= 5.7 mm



FOV= 5.7 mm



FOV= 5.7 mm



FOV= 5.7 mm

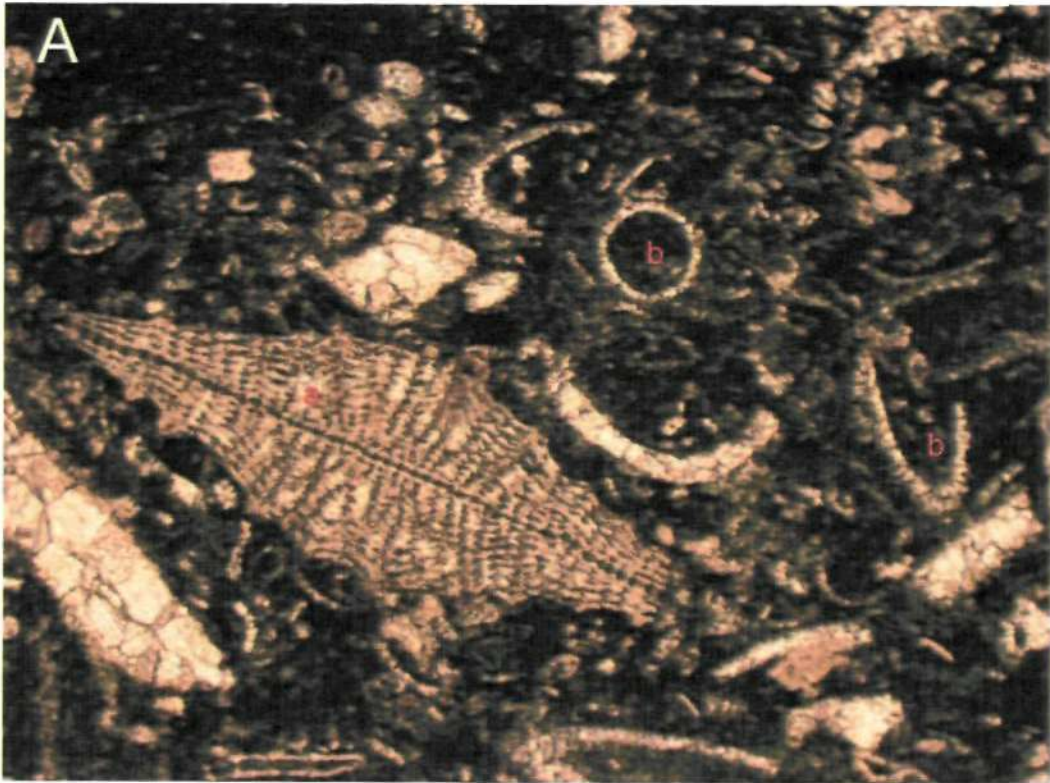
Plate 4.31



FOV= 5.7 mm



FOV= 5.7 mm



FOV= 5.7 mm



FOV= 5.7 mm

Chapter 5: Stratigraphy and palaeoenvironmental assessment of the Paleocene/Eocene boundary interval (Dungan Formation), Indus Basin Pakistan.

5.1 Introduction

Since dinoflagellates are consistently present in Paleogene deposits of northern latitudes (e.g., Iakovleva, 2000) and in the North Sea Basin (e.g., Heilmann-Clausen, 1985; Powell, 1992; Mudge & Bujak, 1994, 1996; Bujak & Mudge, 1994), the organic-walled dinoflagellate cysts (dinocysts) in particular have shown potential for age determination, correlation, and palaeoenvironmental assessment. The organic-walled dinocysts have been increasingly employed as sensitive (palaeo)-environmental indicators (e.g., Sluijs et al., 2005; Sluijs & Brinkhuis, 2009) particularly in carbonate-poor sediments. Other micropalaeontological approaches (e.g., foraminifera, coccolithophorids, diatoms and radiolaria) are highly susceptible to mineralization and chemical dissolution (including diagenesis), which also restricts their use in palaeoenvironmental studies (de Vernal & Mudie, 1992). However, well preserved foraminifera, specifically smaller benthonic foraminifera have been widely used in palaeoenvironmental research (e.g., Van der Zwaan et al., 1990; Speijer et al., 1996 and references herein). The organic-walled dinocysts are neither affected by chemical dissolution or by secondary mineralization, they are only affected by progressive oxidation of the sediments (Versteegh & Zonneveld, 2002; Reichart & Brinkhuis, 2003).

A key outcrop of the Paleocene/Eocene boundary interval is found in the Rakhi Nala section, which is located in the Sulaiman Range near D.G. Khan City, Indus Basin, Pakistan (**Fig. 5.1**). During late Paleocene - early Eocene times this area was located at a low latitude in an equatorial region (**Fig. 5.2**).

Previous work on this section has resulted in a substantial literature base (e.g., Eames, 1952b; Haque, 1956; Latif, 1961, 1964; Samanta, 1973; Kothe et al., 1988; Afzal, 1996; Warraich et al., 1997, 2000). Most of this earlier work has been focused on lithostratigraphy and biostratigraphy. Köthe et al. (1988), as a result of a lack of known dinocyst marker species, proposed a new dinocyst zonation for the Paleogene of the Indus Basin (Pakistan). Their work resulted in the description of 11 dinocyst zones, but they marked the upper Paleocene - lower Eocene Dungan Formation (Rakhi Nala section) as un-zoned. A continuous marine sedimentary section in the Dungan Formation across the Paleocene/Eocene boundary interval is preserved in Rakhi Nala and yields well-preserved and rich dinocyst assemblages. The present study is aimed at a high resolution global and local dinocyst correlation and palaeoenvironmental assessment of the Paleocene/Eocene interval of the Rakhi Nala section. The palaeoenvironmental assessment is based on dinocyst and foraminifera.

5.2. Materials and Methods

Analysis of the dinocyst assemblage has been carried out on a selection of 63 samples collected from the Rakhi Nala section. Sample intervals of 25-50 cm were used for the uppermost part of the Dungan Formation. The 5 m thick *Morozovella velascoensis* Zone of Warraich et al. (2000) yielded 20 samples at a sample interval of <25 cm. All samples for dinocyst examination were processed at *Geotechniques Research* by Jonah Chitolie using a standard palynological processing methodology (hydrochloric acid followed by hydrofluoric acid for demineralisation). A detailed description of the palynological preparation technique used in this study can be found in Chapter-2. The recovered residues, in almost all of the samples, contained well preserved palynomorphs, some of which were transparent.

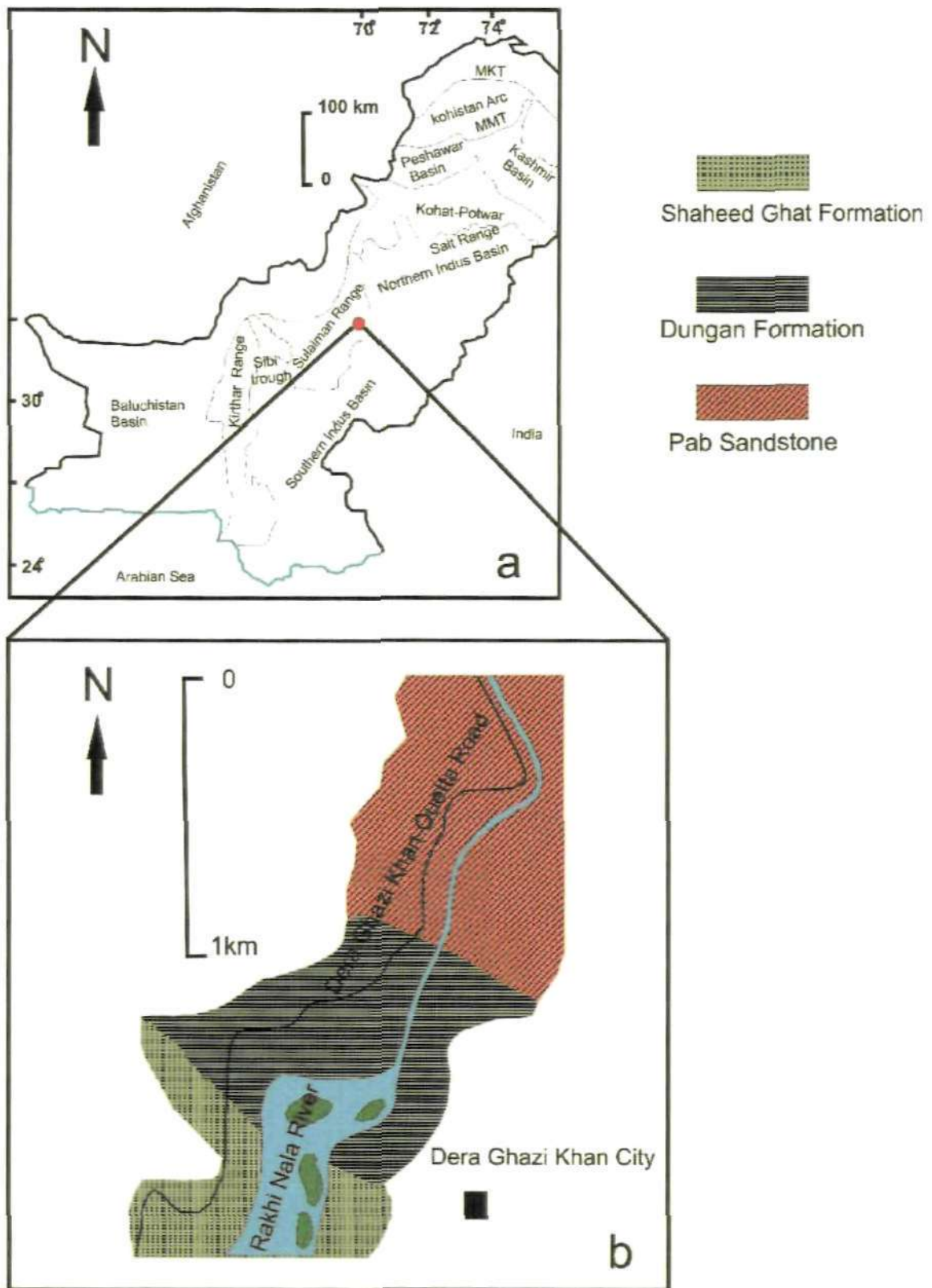


Fig.5.1: Map showing (a) location of the Rakhi Nala section (i.e., red circle) Sulaiman Range, Indus Basin, and (b) detailed map of the Rakhi Nala section. The sky blue coloured line in map (a) shows the coastline.

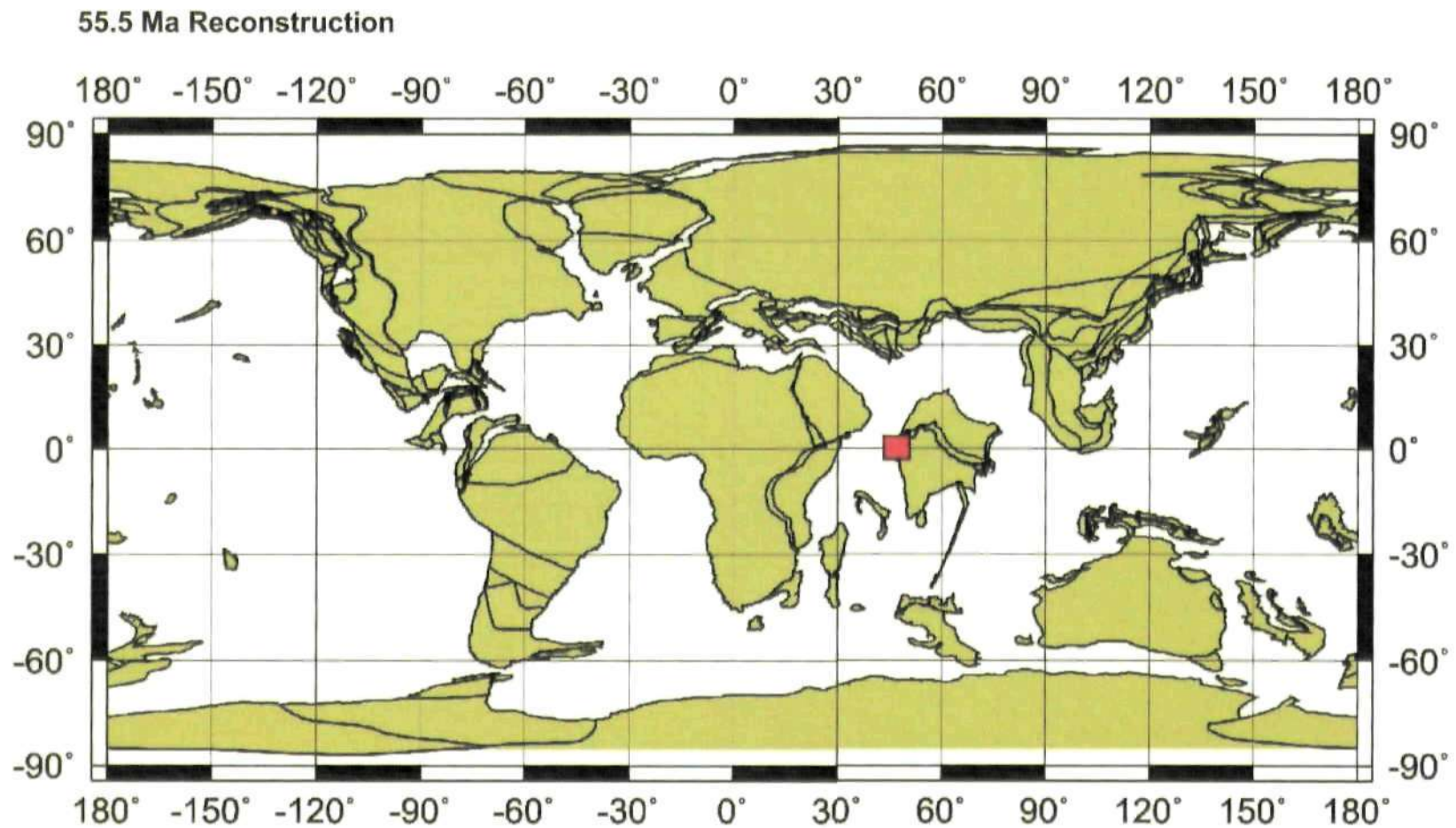


Fig.5.2: Palaeolatitudinal map of the studied area showing the location of the Indus Basin during late Paleocene - early Eocene (ODSN plate tectonic reconstruction service <http://www.odsn.de/odsn/services/paleomap/paleomap.html>).

For all samples, a minimum of 200 dinocysts (where possible) were counted and the entire slide was scanned for the presence of additional age diagnostic taxa. In this chapter, most attention is given to the stratigraphically and palaeoenvironmentally significant dinocyst taxa, the ranges of which have been determined from previous research in lower latitude regions (e.g., Jan du Chêne & Adediran, 1984; Köthe et al., 1988; Bujak & Brinkhuis, 1998; Iakovleva et al., 2001; Iakovleva & Kulkova, 2003). The dinocyst zonation of Köthe et al. (1988) was found to be the most appropriate and used in this study. A list of the recorded species and taxonomic notes on the recorded dinocysts can be found in **Appendix 2**.

Photomicrographs were taken using the digital photomicroscope facilities at the University of Plymouth. For photographed specimens England Finder coordinates are provided (**Plates 5.1, 5.2 & 5.3**).

The total organic carbon and nitrogen content of the samples was measured using a Carlo Erba 1500 elemental analyser at the NERC Isotope Geosciences Laboratories (NIGL) at Keyworth (UK): see detail in Chapter 2. The TOC (%), Nitrogen (%), C/N ratio are given in **Table-3 in Appendix 2**.

5.3. Dinocyst Zonation

As indicated above the dinocyst zones of Köthe et al. (1988) have been applied to the samples from Rakhi Nala and can be identified as follows.

5.3.1. The Pak-DIV Zone

The base of this zone is defined by the Lowest Occurrence (LO) of *Minisphaeridium latirictum* (previously *Cordosphaeridium minimum*) and *Achomosphaera crassipellis*. The top of the zone is marked by the onset of the *Apectodinium* acme. Köthe et al. (1988) correlate this zone with the late NP8

Zone based on *Bomolithus elegans* which has its LO in the early Pak-DIV Zone and ranges to the top of NP8 of Martini (1971). The Pak-DIV Zone can be correlated with the planktonic foraminifera zone P4 of Berggren & Pearson (2005). The chronostratigraphic age of NP8 and late P4 is late Paleocene (Thanetian). Consequently, the Pak-DIV Zone in the Indus Basin can be attributed to the Thanetian.

5.3.2. The Pak-DV Zone

This zone is defined as the interval of the *Apectodinium* acme. It is correlated with the early NP9 of Martini (1971) and with the P5 Zone of Berggren & Pearson (2005). The chronostratigraphic age is, therefore, latest Paleocene (Thanetian).

5.3.3. The Pak-DVI Zone

This zone is defined as the interval from the top of the *Apectodinium* acme to the Lowest Occurrence (LO) of *Wetzeliella astra*. The onset of the Carbon Isotopic Excursion (CIE) is now globally accepted marker for the placement of the P/E boundary (e.g. Aubry & Ouda, 2003). In the present study the onset of the CIE was encountered in Td41 (also see Chapter 6) prior to the LO of *W. astra* (Td42). Therefore, the P/E boundary can be placed in the top-most part of this zone. The top of the *Apectodinium* acme (below) and the lowest occurrence of *W. astra* (above) bracket the P/E boundary in the Indus Basin. This zone can be correlated with the NP9 Zone of Martini (1971) and the late P5 and early E1 zones of Berggren & Pearson (2005). The chronostratigraphic age of the part of this zone before the onset of the CIE is, therefore, latest Thanetian and the part of this zone after the onset of the CIE belongs to the early Ypresian.

5.3.4. The Pak-DVII Zone

This zone is defined as the interval from the lowest occurrence of *W. astra* to the lowest occurrence of *Homotryblium tenuispinosum*. The base of the Eocene approximates to the onset of the CIE instead of the lowest occurrence of *W. astra*. The chronostratigraphic age of this zone in the Indus Basin is, therefore, early Ypresian.

5.4. Local correlation

The Paleocene/Eocene interval dinocyst zones established in the Dungan Formation (part) of the Rakhi Nala section can be correlated locally with the established zones of Köthe et al. (1988) in the Surghar Range and Salt Range, Upper Indus Basin (**Fig. 5.3**). The dinocyst assemblages recovered from the Rakhi Nala section show a close resemblance with those of the Köthe et al. (1988) and Edwards (2007) recorded from the Patala Formation (Upper Indus Basin). The zones Pak-DIV to part of the Pak-DVI are considered to be late Thanetian (late Paleocene) in age while late Pak-DVI & Pak-DVII are early Ypresian (early Eocene) in age and can be correlated with the Pak-DIV to Pak-DVII zones of Köthe et al. (1988) from the Patala Formation of the Upper Indus Basin.

5.5. Global correlation

The Pak-DV Zone, as recognised in the Indus Basin, is the only zone broadly comparable with the corresponding zones in N.W. Europe, United States of America and New Zealand. It is compared with the following zones:

- Zone D5a of Costa & Manum (1988) and of Köthe (1990);
- Zone P6b of Bujak & Mudge (1994) and Mudge & Bujak (1996) in the North Sea Basin;

- The *Apectodinium augustum* (Aau) zone of Powell (1992) and Powell et al. (1996) in South East England;
- The *Muratodinium fimbriatum* Interval Zone of Edwards (1996); and
- The *Apectodinium homomorphum* zone of Wilson (1988) in New Zealand (Fig. 5.4).

This zone is characterized by an acme occurrence of *Apectodinium*. Bujak & Brinkhuis (1998) report that the base of the *Apectodinium* acme occurs near the base of the Tht-5 sequence of Powell et al. (1996), which they equate with sequence Th-5 of Hardenbol (1994). The Th-5 sequence correlates with the carbon isotope excursion (CIE) and oxygen isotope excursion (OIE) of Kennett & Stott (1991). According to Crouch et al. (2001) the *A. augustum* Zone corresponds (worldwide) with the top of the Paleocene-Eocene Thermal Maximum (PETM) which, according to the International Union of Geological Sciences (IUGS), characterizes the P/E boundary (54.93-54.98 Ma). Iakovleva et al. (2001) also report that the *Apectodinium* acme is linked to cycle Tht-5 of Powell et al. (1996) and may be recognized on a global scale. A number of other studies (e.g., Crouch et al., 2000; Heilmann-Clausen & Egger, 2000) confirm that the onset of this *Apectodinium* acme precisely coincides with the CIE based on data from both hemispheres. *A. augustum* is restricted to the *A. augustum* Zone elsewhere but was not encountered in the Rakhi Nala section. However, Edwards (2007) reported the only occurrence of *A. augustum* from the Nammal Gorge, Indus Basin.

The earliest known occurrence of *Apectodinium* is reported from Tethys in the upper part of calcareous nannoplankton Zone NP7/8 (Crouch et al., 2003) and in planktonic foraminifera Zone P3a up to the base of P5 Zone: it has an acme from the base of this zone up to the middle part of nannofossil

Zone NP11 (Bujak & Brinkhuis, 1998). The acme of *Apectodinium* species associated with the CIE (Paleocene/Eocene boundary) is reported worldwide, although Sluijs et al. (2007b) from New Jersey (USA) report the onset of the *Apectodinium* acme ~3000 years prior to the CIE.

5.6. Dinocyst assemblages and palaeoenvironment

The palynological associations at Rakhi Nala show notable changes across the Paleocene/Eocene transition. The palynomorph association is dominantly composed of marine dinocysts and an abundance of *Apectodinium* occurs prior to the onset of CIE (Paleocene/Eocene boundary) and the lowest occurrence of *W. astra* (Paleocene/Eocene boundary of Köthe et al., 1988). The succession is divided into four intervals across the Paleocene/Eocene transition, based on relative changes in dinocyst assemblages and organic matter. These intervals are independent of the dinocyst zones. The main purpose of this analysis is to identify time intervals of change within the dinocyst association and to evaluate these fluctuations in a palaeoecological context (**Fig. 5.5A**).

5.6.1. Interval Td30 - Td33

Description

This interval correlates with the dinocyst zone Pak-DIV and the late nannoplankton zone NP8. This interval is represented by an abundance of *Spiniferites* (*Hystrihosphaera*) up to 53.2% (Td30) which decreases upwards to 42.7% (Td33). *Achmosphaera* comprises 34.6% (Td30) and also decreases upwards. *Operculodinium* is <10% of the assemblage. The percentage of *Apectodinium* increases from 3.2% (Td30) to 13.5% (Td33).

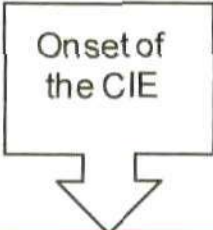

Age	Nanno zones (Martini, 1971)	Dino zone	Surghar Range (Köthe et al., 1988)	Salt Range Nammal Gorge (Köthe et al., 1988)	Sulaiman Range Rakhi Nala (This study)	Dino events
Eocene (part)	NP10	Pak-DVII	Dinoflagellate barren	Dinoflagellate barren	Onset of the CIE 	LO of <i>W. astra</i> 
	Paleocene (part)	NP9	Pak-DVI	Patala Formation (part)		Patala Formation (part)
Pak-DV			<i>Apectodinium</i> acme			
NP8		Pak-DIV				

Fig. 5.3: Dinoflagellate cyst zones intra-basinal correlation of the Indus Basin, **Nanno** = Nannoplankton, **Dino** = Dinocyst, **LO** = lowest occurrence. The red line indicates Paleocene/Eocene boundary, **CIE** = Carbon Isotopic Excursion.

Age	Authors	Paleocene (pars)		Eocene (pars)	
Nanno zones Martini (1971)		NP8	NP9		NP10
USA	Edwards (1996)	Un-zoned	<i>Muratodinium fimbriatum</i>		
Southern former Soviet Union	Andreeva-Grigorovich (1991)	<i>Cerodinium speciosum</i>	<i>Apectodinium homomorphum</i>		
Southern Ural	Vasilieva (1990)	<i>Cerodinium speciosum</i>	<i>Apectodinium homomorphum</i>		
NW Europe	Costa & Manum (1988)	D4	D5a	D5b	D6
New Zealand	Wilson (1988)	<i>P.golzowense</i>	<i>A. homomorphum</i>		various wetzeliellacean zones
SE England	Powell (1992) & Powel et al.(1996)	<i>A. hyperacanthum</i> (Ahy)	<i>A. augustum</i> (Aau)		<i>Glaphyrocysta ordinata</i> (Gor)
North Sea Basin	Bujak & Mudge (1994); Mudge & Bujak (1996)	P6a	P6b		E1a
Pakistan	This study	Pak-DIV	Pak- DV	Pak-DVI	Pak-DVII

Fig. 5.4: Global correlation of the dinocysts zone Pak-DV from Indus Basin, Pakistan, **Nanno**= Nannoplankton. Orange coloured area indicates global correlation of the Zone Pak-DV with D5a and with the bases of *Apectodinium homomorphum*, *A. augustum* and P6b zones.

The P-Cyst (%) increases upward from 3.2% (Td30) to 18.7% (Td33). Other dinocysts present include *Adnatosphaeridium*, *Hystrichokolpma*, *Polysphaeridium*, *Kallosphaeridium*, *Dyphes*, *Kenleyia* complex, *Cordosphaeridium*, *Hystrichosphaeridium*, *Thalassiphora* (dominantly *T. pelagica*), *Delfandrea* and *Glaphyrocysta*. The maximum TOC and C/N values are 0.6% and 10.4 respectively (**Table-3 in Appendix 2**).

Palaeoecological interpretation

The dominance of *Spiniferites* and the presence of *Operculodinium* indicate open marine conditions (Prauss, 2009); also see **Figures 5.5A & 5.5B**). The presence of *Apectodinium*, and its upward increasing numbers, indicates warm surface waters and an increasing trend in nutrient and/or food availability respectively. The low percentage of P-Cyst suggests that the surface water was not sufficiently eutrophic but the upward increasing trend in P-Cyst (%) indicates an upward increase in productivity. The presence of *Glaphyrocysta*, *Polysphaeridium* and *Cordosphaeridium* complexes suggests a pulse of transported coastal elements into an open marine setting. *Thalassiphora* (dominantly *T. pelagica*) appears in the upper part of this interval which may be suggestive of a warm and humid climate in the nearby land area (e.g., Pross & Schmiedl, 2002).

5.6.2. Interval Td33 - Td37

Description

This interval correlates to the top of dinocyst zone Pak-DIV and lower nanoplankton zone NP9. The *Spiniferites* complex decreases upwards from 42.7% (Td33) to 21.6% (Td37). The *Operculodinium* complex shows an overall

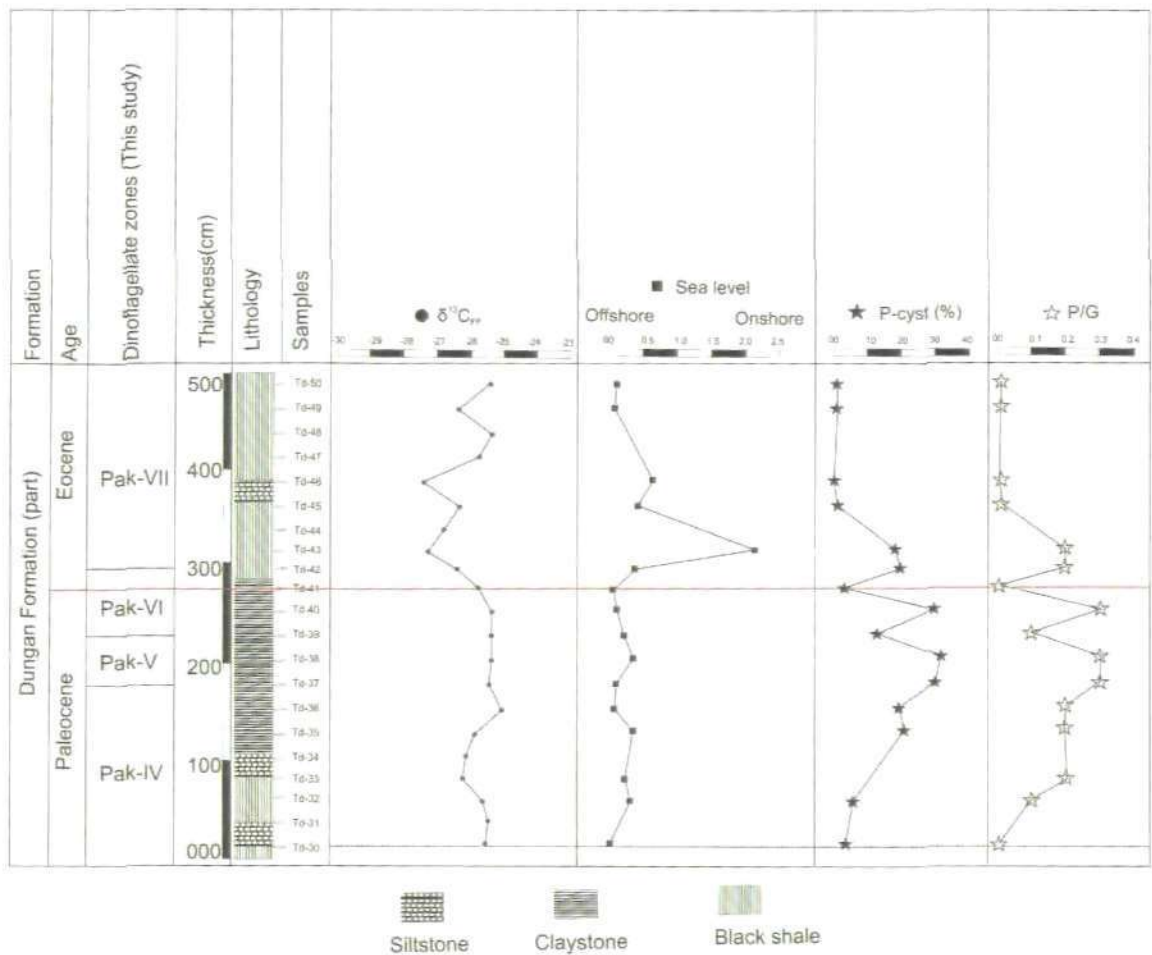


Fig. 5.5B: Dinocyst zones, lithological log, $\delta^{13}C_{FF}$ curve and sea level curve (= Onshore (*Homotryblum*+*Polysphaeridium*)/Offshore (*Spiniferites* association). Sea level curve for Rakhi Nala represents dominantly offshore conditions with minor sea level fluctuations, only sample Td43 shows either a sea level drop (regression) or an increased transportation of the coastal element to an open marine depositional environment. P-cyst (%) indicates changes in sea surface temperature (SST) as well as productivity (e.g., increase in P-cyst (%) shows increase in SST and productivity).

decreasing trend upwards; i.e., 9.9% (Td33) to 7.3% (Td37). *Cordosphaeridium* and *Polysphaeridium* increase upwards; i.e., 1.0% (Td33) to 7.3% (Td37) and 1.6% (Td33) to 3.5% (Td37) respectively. *Glaphyrocysta* is present only in the lower part of the succession and the *Thalassiphora* complex shows an upwards increasing trend; i.e., 2.6% (Td33) to 4.4% (Td37). The *Apectodinium* complex increases upwards from 13.5% (Td33) to 25.7% (Td37). *Deflandrea* is consistently present and disappears in the last sample. The maximum TOC and C/N values are 0.5% and 16.9 respectively (**Table-3 in Appendix 2**).

Palaeoecological interpretation

The high percentage of *Spiniferites* and *Operculodinium* indicates an open marine setting (**Figs 5.5A & 5.5B**). The *Cordosphaeridium*, *Polysphaeridium* and *Glaphyrocysta* complexes suggest an increase in the rate of transported coastal elements up-section. The upward increasing trend of the *Thalassiphora* complex indicates increased terrestrial runoff, possibly as a result of enhanced chemical weathering on land (e.g., Pross & Schmiedl, 2002). The higher percentage of *Apectodinium* is indicative of relatively warmer SSTs. The higher P-Cyst percentage shows further enhancement in the surface water productivity which is reflected by a consistent high TOC. The relatively high C/N ratio also suggests an increase in the proportion of terrestrial organic matter in this interval.

5.6.3. Interval Td37 - Td43

Description

This interval correlates to the dinocyst zones Pak-DV (Td37 to Td 39) and Pak-DVI (Td40 to Td 42) in the middle to upper part of nannoplankton Zone NP9.

The percentage of *Spiniferites (Hystrichosphaera)* is low (8%) in the lower part (Td35) but increases upwards to 63.6% (Td-39) in the middle part and then drops to 5.1% (Td-43) in the uppermost part of this interval. *Achomoshpaera* shows an upward increasing trend; i.e., 12.5% (Td37) to 20.3% (Td43). The *Operculodinium* percentages are also changing in this interval, with low percentages (~10% on average) in the lower part but an increase upwards; i.e., 44.3% (Td43). *Apectodinium* rises to the maximum value 32.5% (Td38) in the middle of the interval and then shows a decreasing trend up-section. The P-Cyst (%) approximately follows the same trend as *Apectodinium*.

Cordosphaeridium is consistently present in this interval. *Thalassiphora* indicates an increasing trend to the middle part (Td38) of the section and then declines upward. *Glaphyrocysta* is present in low percentages only in the lower and upper parts of the succession. *Homotryblium* appears in the middle of the interval and then disappears. The maximum TOC and C/N values are 5.6% and 31.4 respectively (**Table-3 in Appendix 2**).

Palaeoecological Interpretation

The decline in *Spiniferites (Hystrichosphaera)* complex and *Operculodinium* complex, the increase in *Cordosphaeridium* complex, the presence of *Glaphyrocysta* complex and the appearance of *Homotryblium* complex either suggest a relatively proximal setting as a result of a sea level drop or an increased pulse of transported coastal elements into the open marine setting in the upper part of this interval (**Figs 5.5A & 5.5B**).

The highest TOC value and C/N ratio in this interval correspond to the highest absolute concentrations of dinocysts and to the increased percentage of the *Apectodinium* complex. The high percentage of the *Apectodinium* complex

suggests increased nutrient and/or food availability. Variations in the flux, type, and preservation of the organic matter can cause changes in the TOC content of the marine sediments (Wefer et al., 1999). The high percentage of P-cyst suggests an increase in the productivity of the surface waters and the high TOC in this interval may reflect decreased dissolved O₂ in intermediate waters and enhanced preservation of organic carbon. Indeed, benthonic foraminiferal assemblages of the Paleocene/Eocene boundary interval also suggest a change from oxic to suboxic conditions during the PETM worldwide (e.g., Kaiho et al., 1996; Takeda & Kaiho, 2007; Alegret et al., 2005, 2009) and is considered to be a widespread phenomenon in the intermediate waters (Bralower et al., 1997; Thomas, 1998; Katz et al., 1999; Crouch et al., 2003). This O₂ depletion in global intermediate waters may have resulted from a combination of ocean warming and CH₄ oxidation (Dickens, 2000). However, the increased C/N ratio in this interval suggests an increase in the proportion of terrestrial organic matter (Pedersen & Calvert, 1990; Tyson, 1995). The increase in *Thalassiphora* (*T. pelagica*) suggests an increased terrestrial run-off, resulting from enhanced chemical weathering on the land.

5.6.4. Interval Td43-Td50

Description

This interval correlates to dinocyst zone Pak-DVII. The *Spiniferites* (*Hystriosphera*) complex increases upwards from 5.1% (Td-43) to 42.2% (Td-50). The *Operculodinium* complex decreases upward from 44.3% (Td43) to 8.4% (Td-50). *Polysphaeridium* complex, *Cordosphaeridium* complex, *Thalassiphora* complex (dominantly *T. pelagica*) and *Homotryblum* complex are present in low percentages throughout this interval. *Apectodinium* complex and

P-cyst percentages decrease upwards. Other dinocysts present include *Adnatosphaeridium* complex, *Hystrichokolpoma* complex, *Achomosphaera* complex, *Kallosphaeridium* complex, *Dyphes* complex and *Hystrichosphaeridium* complex, the maximum TOC and C/N values are 2.1% and 17.1 respectively in this interval (**Table-3 in Appendix 2**).

Palaeoecological interpretation

The upward increasing trend in *Spiniferites* (*Hystrichosphaera*) complex indicates a trend towards an open marine distal setting or a sea level rise (**Figs 5.5A & 5.5B**). The presence of *Polysphaeridium*, *Cordosphaeridium* and *Homotryblum* complexes indicate a continued supply of coastal elements into an open marine setting. The drop in *Apectodinium* complex and P-cyst (%) suggests a reduction in nutrient and/or food availability and surface water productivity respectively. The presence of *Thalassiphora* indicates that the continued terrestrial supply may be the result of the continuing enhanced chemical weathering on land; the result of the prevailing humid and warm climate. The fairly high, but relatively reduced, maximum TOC value and C/N ratio indicate the presence of prevailing O₂ depleted intermediate waters and slightly reduced proportion of terrestrial organic matter respectively.

5.7. Interpretation of the Peridinioid dinocyst complexes

In the Rakhi Nala section *Apectodinium* is the dominant peridinioid dinocyst. The *Wetzeliella* and *Deflandrea* complexes are present as minor constituents. The dinocyst assemblages suggest that surface waters were eutrophic, the main factor determining the peridinioid complex appears to have been nutrient and/or food availability provided a suitable temperature in the background. As

Apectodinium dominates the peridinioid complex, this indicates both the availability of nutrient and/or food and thermophilic behaviour of *Apectodinium*, while the other peridinioids are indicative of comparatively lower SST (Sluijs et al., 2009). Other studies (e.g., Bujak & Brinkhuis, 1998; Kaiho et al., 1996; Bains et al., 2000; Crouch & Brinkhuis, 2005) report the elevated abundance of the other peridinioids (such as *Deflandrea*) subsequent to the *Apectodinium* acme, which suggests that temperatures cooled after the PETM.

5.8. Discussion

5.8.1. Palaeoproductivity

Harland (1973) introduced the concept of the G/P ratio (G-gonyaulacoid dinocysts, P-peridinioid dinocysts) for dinocyst based productivity reconstruction and suggested that low G/P ratios were associated with significant freshwater input. Since that time this approach has been widely used, but also criticised in a number of studies. Recently Prauss (2009) has highlighted the problems involved with use of the G/P ratio. Powell et al. (1992) suggested that peridinioids are heterotrophic and gonyaulacoids are autotrophic. This suggestion (Powell et al., 1992) was criticized by Dale & Fjellså (1994) who indicated that not all peridinioids are heterotrophic. Heterotrophs indicate eutrophic conditions and, therefore, Dale & Fjellså (1994) and Dale (1996) proposed the term "H-cysts" for heterotrophic dinoflagellates and "A-cysts" for autotrophic dinoflagellates. Heterotrophic dinoflagellates also occur in places other than high productivity areas, such as sea-ice dominated settings and may lead to misidentification of eutrophic areas (Dale & Fjellså, 1994). Despite all these drawbacks, the G/P ratio approach in the identification of Paleogene palaeoproductivity has been successfully applied. Even an unknown portion of

the P-cyst represent autotrophic dinocyst, but the P-cyst still represent the closest approximation to heterotrophic dinoflagellates and can thus be used to reconstruct productivity (e.g., Sluijs et al., 2005).

Other approaches for dinocyst based paleoproductivity reconstruction involve the abundance (specimens) of P-cyst (considered to represent predominantly heterotrophic dinoflagellates feeding on diatoms, other phytoplanktons and organic detritus) (e.g., Crouch, 2001; Crouch et al., 2003; Eshet et al., 1994; Brinkhuis et al., 1998; van Mourik & Brinkhuis, 2000; van Mourik et al., 2001). The acme of the genus *Apectodinium* co-occurring with the prominent PETM negative carbon isotope excursion (CIE) has been recorded from a number of places world-wide;

- New Zealand (Crouch, 2001);
- North Sea Basin (Bujak & Brinkhuis, 1998 and references therein; Steurbaut et al., 2003);
- Greenland, Spitsbergen (e.g., Boulter & Manum, 1989; Nøhr-Hansen, 2003);
- Tethyan Ocean (North Africa, Austria, Tunisia, Uzbekistan, Pakistan, India) (e.g., Köthe et al., 1988; Bujak & Brinkhuis, 1998; Crouch et al., 2003),
- Equatorial Africa (Jan du Chêne & Adediran, 1984); and
- Eastern United States of America (e.g., Edwards, 1989)

This *Apectodinium* acme is considered to be global in nature (e.g., Crouch et al., 2001) and appears to be linked with both high sea surface temperatures and increased availability of nutrients and/or food. A strong increase in nutrient availability in tropical marginal marine settings is considered to be major factor leading to this acme (e.g., Crouch et al., 2001, 2003). Recently, Sluijs &

Brinkhuis (2009) indicate that the genus *Apectodinium* has a systematic resemblance to the extant heterotrophic dinoflagellates (e.g., Evitt, 1985; Lentin & Vozzhennikov, 1989; Fensome et al., 1996b), and that their cyst wall material is also very similar to protoperidinium cysts (mainly diatom feeding, see Buskey, 1997). Despite morphological differences, Sluijs & Brinkhuis (2009) suggest that *Apectodinium* was a heterotrophic dinoflagellate and, if true, then its acme associated with the PETM implies that the global marginal marine ocean became enriched in nutrients and food.

Information about changes in trophic levels of ancient water masses can be obtained from the relative and absolute numbers of peridinioid cysts. However, to distinguish between productivity related to upwelling and runoff-related productivity is not possible from G/P ratios alone. Therefore, Sluijs et al. (2005) suggest that in order to avoid palaeoenvironmental misinterpretations, the dinocyst data set must be considered from multiple perspectives and the interpretations must be based on an inter-disciplinary (i.e., multi-proxy) approach.

In this present work a multi-proxy approach is used to reconstruct palaeoproductivity. This work involves the P-cyst (%) in combination with detailed analysis of other dinocysts, the C/N ratio and TOC (%). The data suggest an upward increasing trend in productivity (**Figs 5.5A & 5.5B**), **Tables 2 & 3 in Appendix 2**) from interval Td30-Td33 up to interval Td37-Td43. The productivity drops in interval Td43-Td50 relative to interval Td37-Td43 but is still fairly high relative to intervals Td30-Td33 and Td33-Td37. The highest productivity is represented by the interval Td37-Td43. With the upward increasing trend in productivity, there is a corresponding increase in the coastal element suggested by the presence of shallow water dinocyst taxa in an open

marine setting. Furthermore, the highest P-cyst (%) values indicate the highest productivity in interval Td37-Td43 corresponding to the highest C/N ratio. This increase in C/N ratio and the presence of coastal elements in an open marine setting suggests that the high abundance of P-cysts is associated with phases of enhanced nutrient availability, probably derived from stronger terrigenous input. Similar approaches have been used by Eshet et al. (1994), Brinkhuis et al. (1998), van Mourik & Brinkhuis (2000), van Mourik et al. (2001), Crouch (2001) and Crouch et al. (2003), .

The C/N ratio shows decreasing trend up-section. The drop in P-cyst (%) values and overall decreasing trend in the C/N ratio in this interval indicate a drop in the probable runoff-related productivity.

5.8.2. Palaeotemperature

A number of proxies (such as oxygen isotopes, Mg/Ca ratios, quantitative analysis of the calcareous microfossils, TEX₈₆ and U^k 37 index) have been used in previous studies to estimate the most important paleoenvironmental parameters (e.g., Sea Surface Temperature (SST)). It is thought that the organic-walled dinocysts are neither affected by chemical dissolution nor by mineralization compared to the calcareous microfossil groups; they are only affected by oxidation. A number of previous studies suggest that compared to other microfossil groups, dinoflagellates are particularly sensitive to temperature changes (see de Vernal et al., 1992, 1994, 1998, 2000, 2001; Versteegh, 1994; Versteegh & Zonneveld, 1994; Rochon et al., 1998; Grøsfjeld et al., 1999; Devillers & de Vernal, 2000; Boessenkool et al., 2001; Sangiorgi et al., 2002, 2003) . Therefore, organic-walled dinoflagellate cysts appear to be a reliable tool in palaeo-SST reconstruction.

Several approaches to dinocyst based paleo-SST reconstruction have been applied. These include;

- Relative contribution of high/mid-latitude (i.e., cool to temperate) versus low-latitude taxa (i.e., warm) (e.g., Brinkhuis & Biffi, 1993; Brinkhuis, 1994; Brinkhuis et al., 1998; Crouch, 2001; Brinkhuis et al., 2003a,b; Sluijs et al., 2003; Huber et al., 2004; Galeotti et al., 2004);
- Detrended correspondence analysis (Brinkhuis et al., 1998);
- Spatial distribution of Antarctic-endemic dinocyst assemblages called the 'Trans-Antarctic Flora' (Wrenn & Beckmann, 1982);
- Diachronous last occurrences (LOs) of the peridinioid taxa (*Wetzeliella gochttii*, *W. symmetrica* and *Rhombodinium draco*) by Pross (2001); and more recently
- Canonical Correspondence Analyses (CCA) by Sluijs & Brinkhuis (2009).

The tropical genus *Apectodinium* shows a global acme associated with the PETM and this acme is synchronous with the CIE (Crouch, 2001; Crouch et al., 2001). Crouch & Brinkhuis (2005) reconstructed the SST based on the percentage of *Apectodinium* species. A similar approach for SST reconstruction is applied in this study. The *Apectodinium* percentage increases up section from interval Td30-Td33 to interval Td37-Td43 and reaches its maximum values in interval Td37-Td43. This up section increase in *Apectodinium* percentage indicates an increasing trend in SST up section which reaches its maximum values in interval Td37-Td43 (**Fig. 5.5B**).

5.8.3. Palaeosalinity

Palaeosalinity reconstruction is important in the understanding of palaeoceanographic changes. It determines the changes in oceanic circulation as salinity is the most important controlling factor of thermohaline circulation. A number of dinocyst based paleo-salinity reconstruction approaches have been applied in previous studies. These include;

- The use of *Spiniferites cruciformis* to reconstruct the brackish water environment (Kouli et al., 2001; Mudie et al., 2002); and
- Morphological changes in dinocysts as a result of low salinity or other environmental stress (Wall et al., 1973; Nehring, 1994a, b; de Vernal et al., 1989; Matthiesen & Brenner, 1996; Dale, 1996; Ellegaard, 2000; Lewis et al., 1999, 2003; Kouli et al., 2001; Brenner, 2001; Lewis & Hallet, 1997).

Salinity and other parameters of environmental stress are the probable factors controlling morphological changes (e.g., Kokinos & Anderson, 1995; Lewis et al., 1999; Mudie et al., 2001; Sluijs et al., 2005). Following the evidence from the literature (e.g., Fensome et al., 1993; Brinkhuis, 1994; Reichert et al., 2004; Pross & Schmiedl, 2002; Köthe, 1990) it is concluded that *Homotryblium* and allied genera can yield information on salinity conditions in the Paleogene (Sluijs et al., 2005).

In this study, following the model of Pross & Schmiedl (2002), the paleo-salinity conditions can be determined. Their model is as follows. They interpreted alternating intervals dominated by *Homotryblium tenuispinosum*/*H. floripes* and *T. pelagica* respectively, to indicate alternations between high- and low- salinity conditions. This distribution pattern was explained through a model invoking repeated environmental changes from relatively dry to relatively humid

conditions and salinity stratification. High abundances of *H. tenuispinosum* and *H. floripes* reflected drier periods where reduced runoff, in combination with strong evaporation, led to increased salinity in near shore settings. Periods of maximum abundances of *T. pelagica* were interpreted as reflecting reduced salinity in the surface waters, increased productivity, salinity stratification and resulting oxygen depletion in the deeper water column.

The continuous presence of *T. pelagica* in the late Paleocene and early Eocene of the Rakhi Nala section indicates low salinity surface waters in the area. The co-occurrence of *Homotryblium* as a minor element in the intervals Td37-Td43 and Td43-Td50 can be interpreted as a probable transported coastal element to open marine setting (Fig. 5.5A).

5.8.4. Other palaeoenvironmental inferences

The depth of deposition, preferential dissolution, surface palaeoproductivity and ecological stress can be determined by using the proportion of planktonic foraminifera, the relationship between diversity and dominance (e.g., Grimsdale & Van Morkhoven, 1955; Adelseck & Berger, 1975; Hart & Bailey, 1979; Berger & Diester-Haass, 1988; Van der Zwaan et al., 1990; Murray, 1991; Herguera, 1992) and the assemblages of planktonic foraminifera. The plankton ratio (p-ratio is expressed by the following formula;

$$\text{p-ratio} = \text{Planktonic (P)} / (\text{Planktonic (P)} + \text{Benthonic (B)}) * 100$$

The p-ratio can be regarded variously as a measure of depth of deposition (e.g., Grimsdale & Van Morkhoven, 1955; Van der Zwaan et al., 1990), a paleoproductivity index (Berger & Diester-Haass, 1988; Herguera, 1992) or as a measure of preferential loss of planktonic foraminifera by dissolution. This preferential loss may occur at or within the sea-bed where

bottom-or pore water is under-saturated in CaCO_3 (e.g., Adelscek (Jr) & Berger, 1975), or due to diagenesis and outcrop weathering (e.g., Murray, 1991). The foraminiferal association in a bathyal setting will be strongly dominated by planktonic foraminifera (>90%) provided that the dissolution is subordinate. However, benthonic foraminifera will predominate towards the basin margins (<20% planktonics). As planktonic foraminifera are generally more susceptible to dissolution, even moderate dissolution will effect the bathyal foraminiferal association. In addition to diagenesis, low oxygen conditions at the seafloor may also inhibit the use of p-ratio for palaeodepth reconstruction (Van der Zwaan et al., 1990).

The p-ratio in Rakhi Nala section is consistently high (>90%) and shows an increasing trend up section. It displays the peak value of 99% in the interval Td43-Td50 (**Fig. 5.6 & Table-1 in Appendix 1**).

The planktonic foraminiferal assemblages are predominantly composed of three genera; *Morozovella*, *Acarinina* and *Subbotina* (**Fig. 5.6**). *Morozovella* is the dominant genus in interval Td30-Td33; this interval is composed of 34-50% *Morozovella*, 23-41% *Subbotina* and 8-16% *Acarinina*. The samples Td34 to Td41 are barren of foraminifera. Only the top two samples of interval Td37-Td43 yielded foraminifera, an assemblage composed of 37-41% *Subbotina*, 28-30% *Morozovella* and 18-20% *Acarinina*. The interval Td43-Td50 contains 37-56% *Subbotina*, 14-43% *Morozovella* and 13-29% *Acarinina*.

The assemblage of benthonic foraminifera comprised 5 agglutinated species and 18 calcareous hyaline species (Warraich, 2000). The agglutinated species are *Ammodiscus turbinatus*, *Gaudryina* sp. cf. *G. laevigata*, *Gaudryina pyramidata*, *Spiroplectamina plummerae* and *Tritaxia globulifera* (Warraich, 2000). The calcareous hyaline species are *Bulimina impendens*, *Bulimina*

midwayensis, *Cibicidoides alleni*, *Cibicidoides hyphalus*, *Cibicidoides pseudoperlucida*, *Corphostoma midwayensis*, *Dentalina* spp., *Angulogavelinella avnimelechi*, *Gloobcassidulina globosa*, *Gyroidnoides globosus*, *Hanzawala ammophila*, *Lenticulina rotulata*, *Nodosaria catenula*, *Oridorsalis plummerae*, *Osangularia plummerae*, *Praebulimina quadrata*, *Silosotmella subspinosa* and *Tritaria herberti* (Warraich, 2000). The benthonic foraminifera encountered in this study are represented in **Plate 5.4** and their distribution is given in **Figure 5.9**.

The extremely high p-ratio in interval Td43-Td50, combined with an overall reduced number of benthonic foraminifera (only 14 species as reported by Warraich (2000)), is either a strong indication that bottom stress: e.g., low O₂ may have played a role in determining the primary foraminiferal composition or represent typical bathyal depositional setting. A distinctly opposite trend in Shannon-Weaver diversity and dominance, as determined by Warraich (2000), displays an ecological stress in the surface water.

The habitat of *Morozovella* and *Acarinina* species is the surface mixed layer and they are indicative of warmer surface water compared to the deep dwellers such as *Subbotina* which have a habitat around the thermocline or even deeper (Shackleton et al., 1985; Lu & Keller, 1993; 1995; Canudo et al., 1995). Therefore, based on the relative abundance of planktonic foraminifera species data of Warraich (2000), some indications of temperature changes or water-mass stratification can be obtained. For example, according to Warraich (2000) the high relative abundance of subbotinids and low relative abundance of morozovellids and *Acarinina* prior to the Benthic Foraminiferal Extinction Event (BFEE) from the Rakhi Nala section, indicate that the surface water was not yet invaded by warmer waters. After the BFEE, morozovellids and

acariniids show an increase in their relative abundance values as warmer water conditions favourable for them prevailed whereas, the relative abundance of cool water subbotinids and globanomalinids decreased (Warraich, 2000). However, no clear interpretation of surface water temperature can be drawn from the relative abundance of planktonic foraminiferal species observed in the present study (**Fig. 5.6 & Table-1 in Appendix 1**).

The benthonic foraminiferal assemblages from the lower Paleocene Velasco Shale Formation, Mexico was named as the Velasco-type fauna (VF) by Berggren & Aubert (1975). The foraminiferal content from this Formation was previously studied by Cushman (1925, 1926) and White (1928, 1929). Many VF species were cosmopolitan and range from the Campanian or Maastrichtian upwards into the Paleocene (Tjalsma & Lohmann, 1983). The benthonic foraminiferal assemblages observed in the lower Paleocene Midway Formation, Texas was named as the Midway-type fauna (MF). The MF and VF are described as two extremes of a range of different assemblages. The VF represent bathyal and abyssal deposits, while the MF represent neritic deposits (e.g., Brotzen, 1948; LeRoy, 1953; Aubert & Berggren, 1976; Salaj et al., 1976; Luger, 1985; Speijer, 1994). The MF species may occur in bathyal and abyssal deposits (Tjalsma & Lohmann, 1983; Van Morkhoven et al., 1986). Most VF species never occur in neritic deposits, indicating that these species have bathyal upper depth limits (Van Morkhoven et al., 1986) (**Fig. 5.7**). The paleobathymetric ranges of the observed species and high p-ratio indicate that the minimum depth of deposition across the Paleocene/Eocene transition should have been not less than 200m (uppermost bathyal), because of the occurrence of VF species such as *Angulogavelinella avnimelechi* and *Gyroidinoides globosus*. The presence of MF species such as *Coryphostoma*

midwayensis (Warracih, 2000) and *Loxostomoides applinae* (Warracih, 2000) are indicative of much shallower depths up to middle neritic (about 30 m) but *Coryphostoma midwayensis* may also be found in bathyal and abyssal deposits (Tjalsma & Lohmann, 1983; Van Morkhoven et al., 1986). Similarly, *Loxostomoides applinae* may occur at bathyal depths as indicated in **Figure 5.7**. The presence of *Nutallides truempyi* (Warracih, 2000) and the absence of any depth-determining MF species later in Zone P7 of Warracih (2000) indicate a much deeper (>500 m) environment of deposition (**Fig. 5.8**).

The occurrence of VF type benthonic foraminiferal species represents bathyal depositional setting for the Paleocene/Eocene interval of the Rakhi Nala. Therefore, the high p-ratio (>90%) may have been less affected or unaffected by any preferential dissolution and reflects a p-ratio of a typical bathyal setting. The benthonic foraminifera occur in low abundance in this bathyal setting and therefore, can only be used to interpret the depth of deposition. The highest occurrence of *Gavelinella beccariiformis* and *Angulogavelinella avnimelechi* coincides with the Paleocene/Eocene boundary (e.g., Speijer, 1995; Speijer et al., 1996). The extinction of *Gavelinella beccariiformis* / *Angulogavelinella avnimelechi* and associated species represents the Benthonic Foraminiferal Extinction Event (BFEE) worldwide, and the top boundary of the latest Paleocene smaller benthonic foraminiferal zone BB1 of Berggren & Miller (1989). The BFEE coincides with the onset of the PETM/CIE and the Paleocene/Eocene boundary worldwide (Kennett & Stott., 1991; Thomas, 1998; Aubry & Ouda, 2003). Therefore, the occurrence of *A. avnimelechi* prior to the onset of the CIE represents BB1, and its highest occurrence may also be used to infer the position of the BFEE, and to place the Paleocene/Eocene boundary

(i.e. the boundary between BB1/BB2 of Berggren & Miller, 1989) in the Rakhi Nala section.

5.9. Conclusions

Four of the dinocyst zones (Pak-DIV to Pak-DVII) of Köthe et al. (1988), established in the Indus Basin, are recognized in the Dungan Formation that is exposed in the Rakhi Nala section, eastern Sulaiman Range. Based on these zones, the Dungan Formation (top) is correlated with the Patala Formation (part) of the Salt Range and the Surghar Range (Upper Indus Basin). The dinocyst assemblages indicate open marine (upper bathyal as inferred from benthic foraminifera and high p-ratio) conditions and a continuous terrestrial supply. A warm and humid climate can be proposed for the adjacent land areas. The *Apectodinium* acme in zone Pak-DV reflects a world-wide high sea surface temperatures reflecting the Paleocene Eocene Thermal Maximum (PETM). This acme in the distribution of *Apectodinium* is recognised globally.

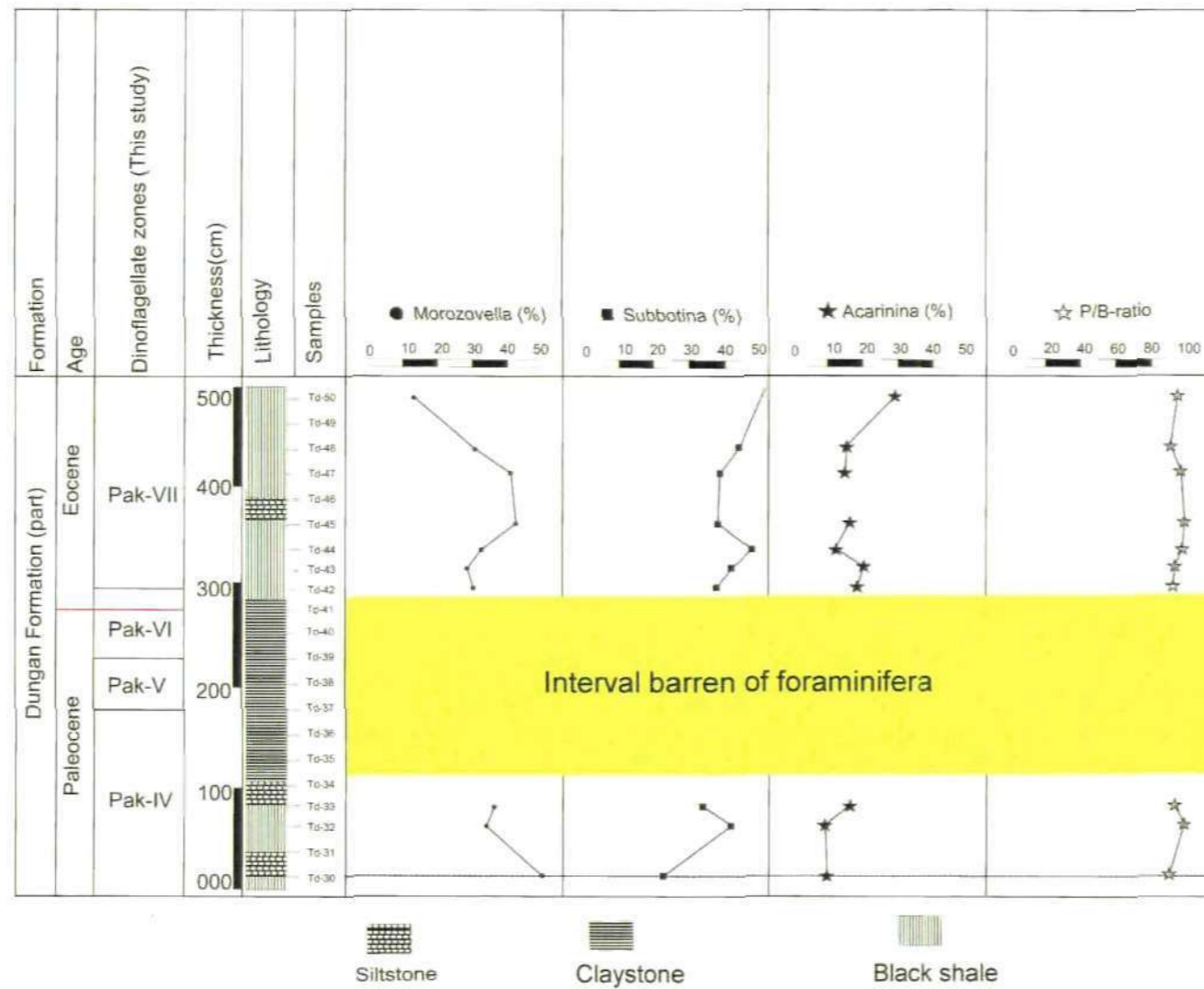


Fig. 5.6: Planktonic foraminiferal composition (in percent) from the Rakhi Nala section, Sulaiman Range, Lower Indus Basin (Pakistan). Yellow coloured area marks an interval barren of foraminifera. Red line indicates the Paleocene/Eocene boundary.

Depth ranges of diagnostic species	Neritic			Bathyal			Abyssal	
	inner 30	middle 100	outer 200	upper 600	middle 1000	lower 2000	upper 3000	lower
<i>Nuttallides truempyi</i>				■	■	■	■	■
<i>Bulimina trinitatensis</i>				■	■	■	■	■
<i>Angulogavelinella avnimelechi</i>				■	■	■		
<i>Aragonia aragonensis</i>				■	■	■	■	■
<i>Gyroidinoides globosus</i>				■	■	■	■	■
<i>Gavelinella beccariiformis</i>				■	■	■	■	■
<i>Coryphostoma midwayensis</i>			■	■	■	■		
<i>Tappanina selmensis</i>			■	■	■	■		
<i>Gavelinella hyphalus</i>			■	■	■	■	■	■
<i>Loxostomoides applinae</i>		■	■	■				
<i>Gavelinella danica/rubiginosa</i>		■	■	■	■	■	■	■

Fig. 5.7: Palaeobathymetric ranges of species modified by Speijer (1994) after Van Morkhoven et al. (1986)

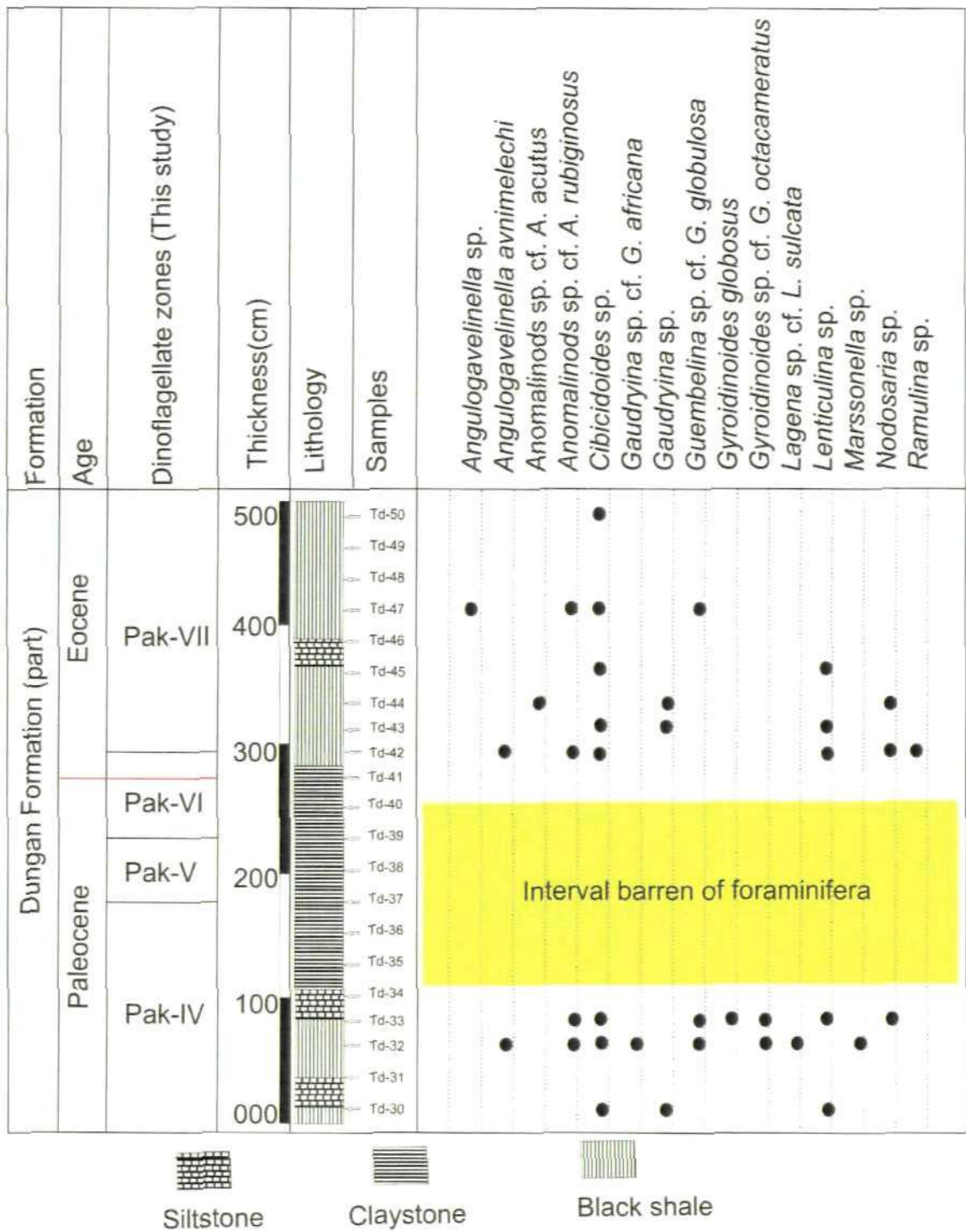
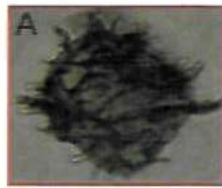
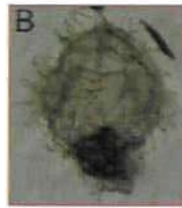


Fig. 5.9: The distribution of benthonic foraminifera recorded in the Paleocene - Eocene interval, Dungan Formation, Rakhi Nala section, Lower Indus Basin (Pakistan). The yellow coloured area indicates interval barren of foraminifera. Red line marks the Paleocene/Eocene boundary.

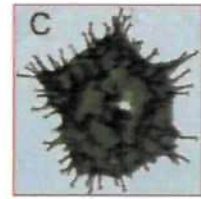
Plate 5.1



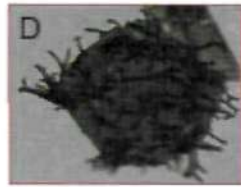
50 μm



50 μm



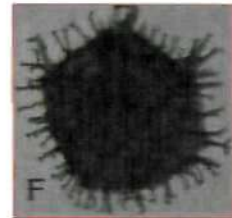
10 μm



50 μm



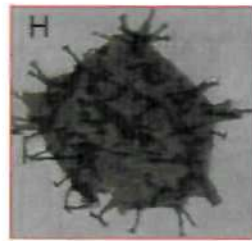
10 μm



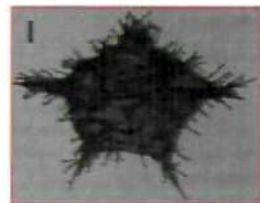
50 μm



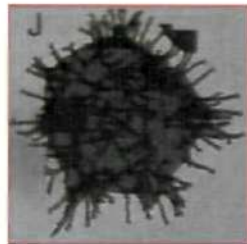
50 μm



50 μm



50 μm



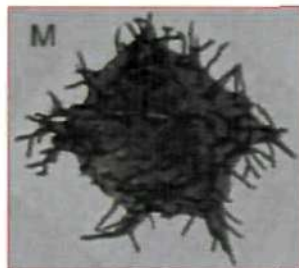
50 μm



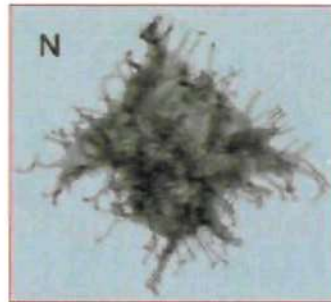
10 μm



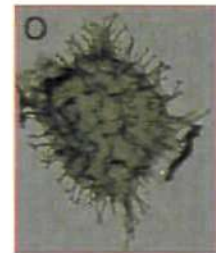
10 μm



50 μm



10 μm



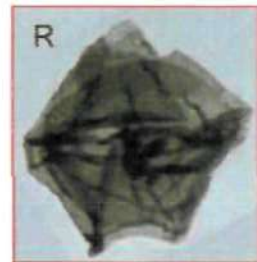
50 μm



10 μm



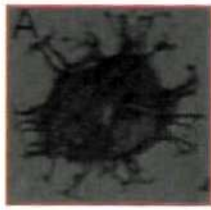
50 μm



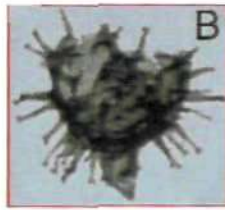
10 μm

Plate 5.1: (A, B, L)-*Apectodinium homomorphum*, sample # and England
Finder coordinates (A-Td42 (2), B-Td42 (2)-J38-1, L-Td35 (1)-V36-3); (E, J, K)-
Apectodinium hyperacanthum, (E-Td40 (1)-C54, J-Td36 (2)-S51-1, K-Td41 (1)-
b39-2); (I, M, N)-*Apectodinium paniculatum*, (I-Td37 (2)-S44-4), M-Td35 (1)-
X50-3, N-Td39 (1)-g38-3); (C, D, F, G, H)-*Apectodinium quinqelatum*, (C-Td38
(1)-m34, D-Td36 (2)-T49-3, F-Td37 (2)-g42-1, G-Td38 (1)-w41-1, H-Td37 (2)-
P44-2); (Q)-*Apectodinium* sp., (Q-Td37(2)-Y48-Z48); (P, R)-*Deflandrea* spp. cf.
D. phosphoritica (P-Td35 (1)-m 37, R-Td36 (2)-E46-1); (O)-*Wetzeliiella astra*,
(O-Td42 (2)-H25-3)

Plate 5.2



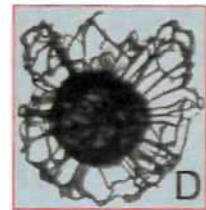
10 μ m



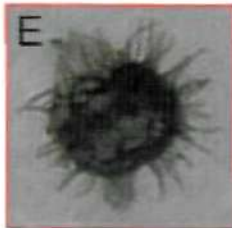
10 μ m



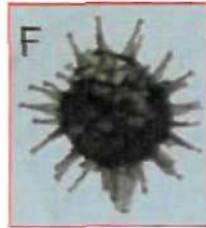
10 μ m



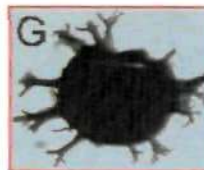
10 μ m



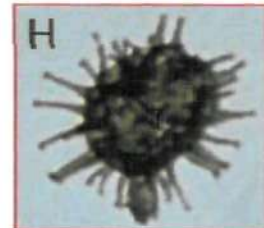
100 μ m



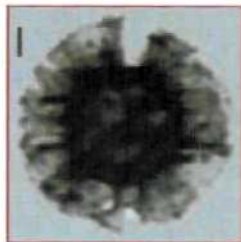
10 μ m



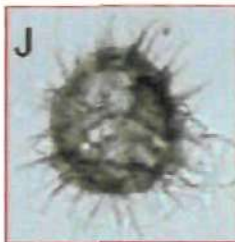
50 μ m



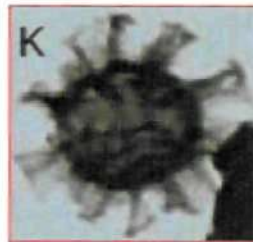
10 μ m



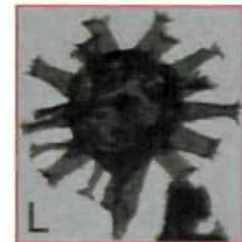
10 μ m



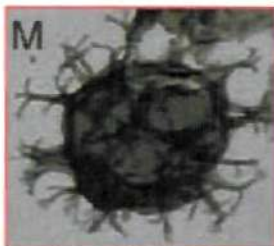
10 μ m



10 μ m



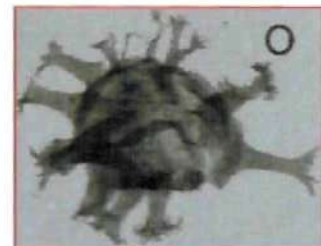
10 μ m



10 μ m



10 μ m



50 μ m

Plate 5.2: (A, M)-*Achomosphaera* spp. cf. *A. ramulifera* sample # and england finder coordinate, (A-(Td30 (1)-O53-1), M-Td32 (1)-V45-3); (B, E, F, H)-*Diphyes* spp. cf. *colligerum*, (B-Td36 (2)-V44, E-Td33 (1)-d35-3, F-Td37 (2)-J40-4, H-Td33 (1)-Q48-1); (C, D)-*Adnatosphaeridium* sp. cf. *A. multispinosum*, (C-Td37 (2)-K43-3, D-Td38 (1)-Q32-3); (G, L)-*Hystrichosphaeridium* spp., (G-Td35 (1)-M35-3, L-Td36 (2)-V55); (N)-*Homotriblyium* sp. cf. *H. tenuispinosum*, (N-Td35 (1)-Q44-4); (I)-*Cordosphaeridium* sp. cf. *C. exilimurum*, (I-Td36 (2)-N47-3); (J)-*Operculodinium* sp., (J-Td33 (1)-Y34); (K)-*Minisphaeridium* sp. cf. *M. latirictum*, (K-Td36 (2)-O47-3); (O)-*Hystrichokolpoma* sp. cf. *H. manipulatum*, (O-Td-32 (1)-U53).

Plate 5.3

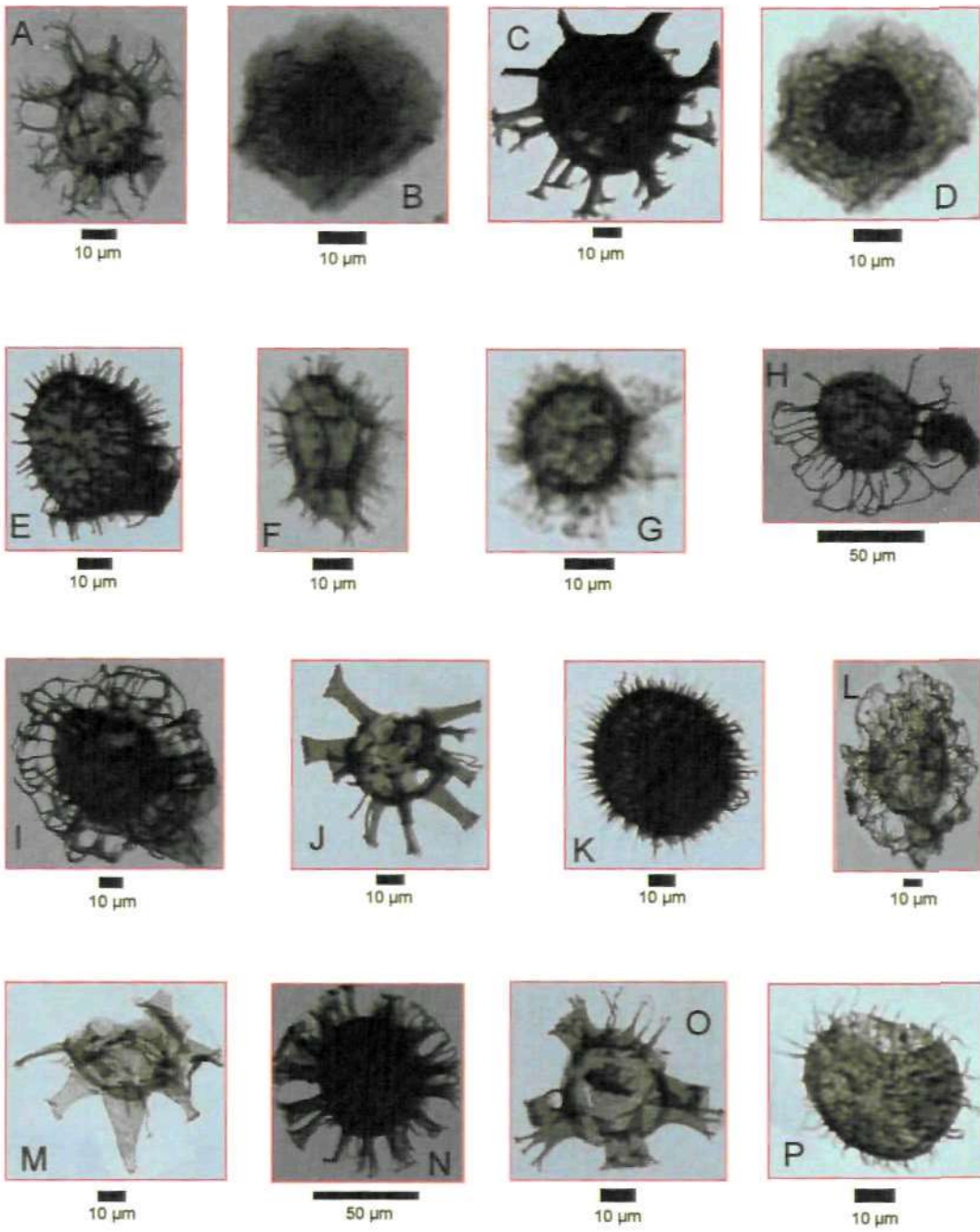


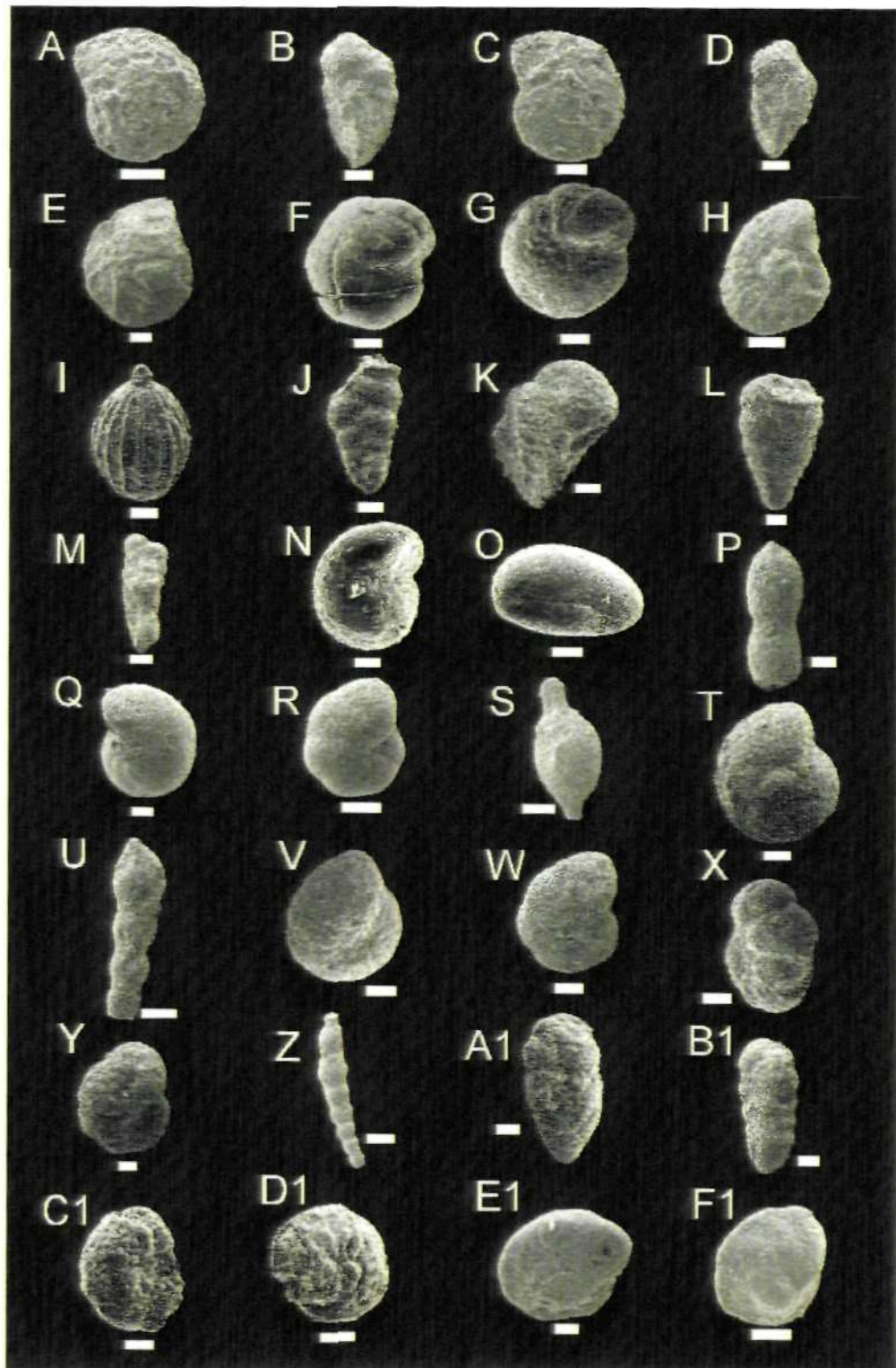
Plate 5.3: (A)-*Spiniferites* sp., (A-Td30 (1)-W50-2); (B, D)-*Thalassiphora* spp. cf. *T. pelagica*, (B-Td35 (1)-N39, D-Td35 (1)-N39 (4)); (C)-*Homotryblium* sp. cf. *H. tenuispinosum*, (C-Td35(1)-N41-4); (E)-*Polysphaeridium* sp., (E-Td36 (2)-P47-1); (K)-Acritarch, (K-Td-38(1)-V39-1); (F)-*Hystrichosphaera* sp. cf. *H. ramose*, (F-Td-33 (1)-U41); (G)-*Muratodinium* sp., (G-Td-33 (1)-V35-3); (N)-*Minisphaeridium* sp. cf. *M. latirictum*, (N-Td-37(2)-T45-2); (O)-*Amphorosphaeridium* sp., (O-Td-36 (2)-I46-4); (M)-*Hystrichokolpoma* sp. cf. *H. unispinum*, (M-Td-30 (1)-E55-4); (H, I)-*Adnatosphaeridium* spp. cf. *A. multispinosum*, (H-Td-35 (1)-N39, I-Td-36 (2)-M56-3); (J)-*Hystrichokolpoma* sp. cf. *H. manipulatum*, (J-Td-38 (1)-U31-4); (L)-*Glaphyrocysta* sp. cf. *G. retiintexta*, (L-Td-41(1)-S45-1); (P)-*Polysphaeridium* sp., (P-Td-30 (1)-V53-3).

Plate 5.4

Benthonic foraminifera from the P/E boundary interval, Dungan Formation, Rakhi Nala, Sulaiman Range, Lower Indus Basin. A, C, E, G, H, J, K, O, P, R, T, U, V, W, X, Y, A1, B1, C1, D1, F1 (Scale bar= 100µm), B, D, M, S, Z (Scale bar= 200µm), F, I, N, Q, E (Scale bar= 50µm).

(A)- *Lenticulina* sp., sample # (Td-30), (C)- *Cibicidoides* sp., sample # (C-Td-30), (E)- *Lenticulina* sp., (E-Td-48), (B, D)- *Gaudryina* sp., (B-Td-43, D-Td-30), (G)- *Angulogavelinella avnimelechi*, (G-Td-32), (H)- *Anomalinoidea* sp. cf. *A. acutus* (Plummer), (H-Td-44), (I)- *Lagena* sp. cf. *L. sulcata* (Walker & Jacob), (I-Td-32), (J, M, B1)- *Guembelina* sp. cf. *G. globulosa* (Ehrenberg), (J-Td-32, M-Td-33, B1-Td-47), (K)- *Gaudryina* sp. cf. *G. africana* (LeRoy), (K-Td-32), (L)- *Marssonella* sp., (L-Td-33), (N)- *Gyroidinoidea globosus*, (N-Td-33), (F, R)- *Gyroidinoidea* sp. cf. *G. octocameratus* (Cushman & Hanna), (F-Td-32, R-Td-33), (O)- *Ostracod* sp., (O-Td-33), (P)- *Nodosaria* fragment, (P-Td-42), (Q)- *Gyroidinoidea globosus*, (Q-Td-33), (S)- *Ramulina* sp., (S-Td-42), (T)- *Cibicidoides* sp., (T-Td-42), (U)- *Nodosaria* sp., (U-Td-42), (V)- *Angulogavelinella avnimelechi*, (Td-42), (W)- *Gyroidinoidea* sp., (Td-42), (X, Y, C1)- *Anomalinoidea* sp. cf. *A. rubiginosus*, (X-Td-42, Y-Td-42, C1-Td-47), (E1)- *Cibicidoides* sp., (Td-50), (Z)- *Nodosaria* sp., (Z-Td-44), (A1)-*Gaudryina* sp., (Cushman), (A1-Td-44), (D1)- *Angulogavelinella* sp., (D1-Td-47), (F1)- *Cibicidoides* sp., (F1-Td-50).

Plate 5.4



Chapter 6: Paleocene-Eocene carbon isotope excursion in organic carbon from Indus Basin, Pakistan.

6.1. Introduction

At the boundary between the Paleocene and Eocene epochs about 55 million years ago, the Earth experienced a strong global warming event. This is widely known as the Paleocene Eocene Thermal Maximum, PETM (Kennett & Stott, 1991; Koch et al., 1992; Norris & Rohl, 1999; Zachos et al., 2001). The PETM corresponds to one of the warmest periods of the whole Phanerozoic, with the exception of the mid-Late Cretaceous (e.g., Zachos et al., 2001). Evidence for the warming is seen in the following:

- In the organic surface ocean paleothermometer TEX₈₆ (Sluijs et al., 2007b);
- A negative oxygen isotope ($\delta^{18}\text{O}$) excursion in marine environments (Kennett & Stott, 1991; Thomas et al., 2002);
- A positive oxygen isotope excursion in terrestrial carbonates (Koch et al., 1995);
- Increased Mg/Ca ratios in planktonic and benthonic foraminifera (Zachos et al., 2003; Tripathi & Elderfield, 2005);
- Poleward migrations of (sub)tropical marine plankton (Kelly et al., 1996; Crouch et al., 2001); and
- Terrestrial plant species (Wing et al., 2005) and mammal migrations across high northern latitudes (Bowen et al., 2002).

The PETM shows a temperature increase of 4°C to 8°C and corresponds to a prominent negative 2.5‰ to 4.0‰ carbon isotopic excursion (CIE) as recorded in marine carbonates (Kennett & Stott, 1991; Bains et al., 1999; Thomas et al.,

2002; Zachos et al., 2003; Tripathi & Elderfield, 2005). Several estimates for the duration of the CIE have been proposed. Detailed earlier studies of the CIE, suggest that $\delta^{13}\text{C}$ steps down within 20 kyrs and returns in a roughly logarithmic pattern to near initial values over ~220 kyrs (e.g., Norris & Rohl, 1999; Rohl et al., 2000). However, relatively recent studies have estimated a duration of ~100kyr for the main body of the CIE (e.g., Farley & Eltgroth, 2003; Rohl et al., 2007; Aziz et al., 2008; Giusberti et al., 2008).

Numerous events in both the marine and terrestrial realms are, somehow, associated with intense warming and excess carbon at the PETM.

These events are;

- Relocation of the sources of oceanic deep waters (e.g., Kennett & Stott, 1991; Nunes & Norris, 2006);
- A decrease in the thermal gradients between pole/equator and surface water/bottom water (e.g., Kennett & Stott, 1991); and
- An acidification of ocean waters (Kennett & Stott, 1991; Thomas, 1998; Wing et al., 2005; Zachos et al., 2005; Zeebe et al., 2008).

Biotic changes include;

- The well-documented benthonic foraminiferal extinction event BFEE (Thomas, 1990a, b; Kennett & Stott, 1991). The simple diversity of benthonic foraminiferal assemblages (>150 μm) averaged ~55-60 species or higher before the extinction event (Thomas, 1990a, b). Benthonic foraminifera (>150 μm) became uncommon to rare (as low as ~30 specimen per sample) during the extinction event (Kennett & Stott, 1991). These large changes in the taxonomic composition and the pattern of decreasing diversity observed by Thomas (1990a, b) were defined as the extinction event. Assemblages containing abundant benthonic

foraminifera include a wide range of morphotypes inferred to be of both infaunal and epifaunal habitat, including trochospiral and other coiled forms (Corliss & Chen, 1988; Thomas, 1990a, b). Many distinctive taxa such as *Gavelinella beccariiformis* and *Neoflabellina* sp. disappeared early and rapidly (<1.5 kyr) during the isotopic shift marking the extinction event (Kennett & Stott, 1991). Most trochospiral forms such as *N. truempyi* had disappeared by the mid-point of the shift (Kennett & Stott, 1991). The interval immediately following the isotope shift is marked by low diversities and abundances of benthonic foraminifera (>150µm fraction) (Kennett & Stott, 1991). Coiled forms are almost completely absent, leaving an assemblage dominated by relatively small and thin-walled uniserial, triserial and other forms typical of an infaunal habitat (Corliss & Chen, 1988; Thomas, 1990a, b). The diversity of benthonic foraminiferal assemblages (>150µm) increased thereafter to an average of ~30 species (>150µm). This increase, in part, resulted from the re-appearance of forms previously present (Thomas, 1990a, b; Kennett & Stott, 1991) ;

- Ostracods decreased markedly in diversity and abundance during the shift, leaving a rare assemblage composed almost exclusively of small, smooth, thin-walled forms (Kennett & Stott, 1991);
- A turnover of the terrestrial mammal faunas is known as the Mammalian Dispersal Event, MDE (Smith, 2000; Gingerich, 2001; Ting et al., 2003; Smith et al., 2006). On land, several events occurred (Clyde & Gingerich, 1998). Some animals that were characteristic of Paleocene faunas, such as the crocodile-like reptile *Champsosaurus* and the pro-primate mammal *Plesiadapis*, became extinct, whereas others, such as the

Artiodactyla (e.g. deer), Perissodactyla (e.g. horses) and Primate taxa appeared for the first time (Gingerich, 1989);

- Acme in the planktonic foraminiferal genus *Acarinina* (Arenillas & Molina, 1996; Kelly et al., 1998), with the dominance of *Morozovella* and the absence of *Subbotina* during the excursion (Petrizzo, 2007); and
- The acme of the dinoflagellate *Apectodinium* (Crouch et al., 2001).

Possible triggering mechanisms for this event include the crossing of a threshold temperature as the Earth warmed gradually (Dickens et al., 1995; Thomas & Shackleton, 1996), cometary impact (Kent et al., 2003; Cramer & Kent, 2005) or explosive volcanism (Bralower et al., 1997; Schmitz et al., 2004). A mechanism involving orbital forcing has been excluded (Cramer et al., 2003). Whatever the mechanism, the magnitude, shape, and global nature of the CIE indicates a massive injection of ^{13}C -depleted carbon into the ocean-atmosphere system followed by sequestering of excess carbon into carbonate and organic matter (Dickens, 2000). While several hypotheses have been proposed for the source responsible for the CIE, the dissociation of seafloor clathrate deposits is now the most widely accepted source for the sudden release of substantial quantities of isotopically light methane (originally proposed by Dickens et al., 1995, 1997).

Mechanisms for the release of the clathrate deposits include, among others, changes in ocean circulation patterns (Nunes & Norris, 2006), a fall in sea level due to up-doming in the North Atlantic Ocean (MacLennan & Jones 2006), a cometary impact (Kent et al., 2003; Cramer & Kent, 2005) and slope failures off the east coast of North America (Katz et al., 2001). In order to explain the CIE, other mechanisms have also been proposed. These include the burning of vast quantities of peat and coal (Kurtz et al., 2003), oxidation of

organic matter due to uplift of epicontinental seas (Higgins & Schrag, 2006), release of thermogenic methane (Svensen et al., 2004) and intense flood basalt magmatism (Storey et al., 2007). Most of these mechanisms have been proposed in isolation to one another, although, most probably a combination of these different mechanisms may have been responsible for the onset of the CIE (Zachos et al., 2008).

Earlier studies carried out on the Dungan Formation, Rakhi Nala section, Indus Basin, focused on biostratigraphy and this provides a framework for the present study (Latif, 1961, 1964; Samanta, 1973; Warraich & Natori, 1997; Warraich et al., 2000). This chapter presents carbon isotopic data from organic matter ($\delta^{13}\text{C}$) both in total organic carbon and in total fine fraction organic carbon (<63 μm - predominantly representing marine dinoflagellates) of the Paleocene/Eocene boundary interval, Dungan Formation, Indus Basin, for the first time. The isotopic data from the Rakhi Nala succession are compared with other Tethyan and global sites.

6.2. Material and Methods

Isotopic analysis has been carried out on 20 samples across the P/E boundary selected from the 63 samples collected from the top Dungan Formation, Rakhi Nala section (**Fig. 6.1**). A relatively higher resolution (<25cm sample intervals) was used for the 5m thick interval across the P/E boundary (*Morozovella velascoensis* Zone of Warraich et al., 2000). A foraminiferal barren and carbonate-poor claystone horizon (**Fig. 6.2A**) about ~170cm thick is described for the first time from the Rakhi Nala section. A similar barren interval associated with the PETM has already been reported from other Tethyan sites (e.g., Kalia & Kinoshita, 2006). Clay or low-carbonate layers coincident with the

PETM have also been identified in several deep sea cores and land-based marine sections (e.g., Bralower et al., 1997; Thomas, 1998; Thomas et al., 1999). However, Zachos et al. (2005) attributed this layer to the consequence of the rapid shoaling of the Carbonate Compensation Depth (CCD). The intervals below, and above, this barren horizon yield abundant planktonic foraminifera but these appear to be highly recrystallized and isotopic analysis would have been extremely unreliable if carried out on such material. For example, isotopic analysis on bulk carbonate and fine fraction carbonate was carried out but failed to yield any significant signal as a result of being diagenetically altered (see **Appendix 3**).

The methods and instrumentation for isotopic, carbonate content and dinoflagellate cyst analyses are given in the chapter on methodology (Chapter-2). Moreover, the presence of a laminated interval, well preserved palynomorphs and a substantial organic matter concentration (TOC= >1%) outside the laminated interval indicates that no severe organic degradation occurred (**Table 6.1**).

6.3. Results

6.3.1. Biostratigraphy

The planktonic foraminiferal biostratigraphy across the P/E boundary interval of the Rakhi Nala section is based on the zonation by Berggren & Pearson (2005). The base of the Zone P5 is characterized by the same criteria as that for the base of the Zone P5 of Warraich et al. (2000); i.e., highest occurrence (HO) of *Globanomalina pseudomenardii*. The lowest occurrence (LO) of PFET (Planktonic Foraminiferal Excursion Taxa) in Tethys coincides with the BFEE (Benthonic Foraminiferal Extinction Event), the negative carbon shift and the

planktonic foraminiferal diversification that characterizes the P-E climatic event (Pardo et al., 1999). The base of the E1 Zone is marked by the LO of PFET as reported by Kalia & Kinsto (2006) from immediately above the barren interval. As the PFET is not observed in the Rakhi Nala section, the placement of the base of E1 Zone (i.e., the Paleocene/Eocene boundary) is here based on the start of the $\delta^{13}\text{C}$ excursion (this study) and the BFEE (Warraich et al., 2000). The LO of *Pseudohastingerina wilcoxensis* marks the base of Zone E2. *P. wilcoxensis* first appears during or just after the PETM, but it is very difficult to distinguish it from the precursor *Globanomalina luxorensis* which is abundant in Lower Eocene Tethyan deposits (Speijer & Samir, 1997; Scheibner & Speijer, 2009). As a result of the sporadic occurrence of *P. wilcoxensis* or *G. luxorensis*, and due to the loss of morphological features because of diagenetic alteration, it is difficult to differentiate between the two species. The top of Zone E1 and the base of the overlying Zone E2 are, therefore, difficult to identify. Zone E3 was not observed, either due to truncation by erosion or because of non-deposition. The upper contact of the Dungan Formation with the overlying Shaheed Ghat Formation is unconformable (Warraich et al., 2000). The absence of the Zone P6 (the lower part is equivalent to E3) of Berggren et al. (1995) is also reported in previous studies (e.g., Warraich & Ogasawara, 2001). This evidence suggests an unconformity at the time of Zone E3 in the Rakhi Nala section.

6.3.2. Stable Isotopes

The co-variance of carbon and oxygen isotopes may be linked through palaeoceanographic cause and effect. However, stratigraphic sample-by-sample covariance of $\delta^{13}\text{C}$ and $\delta^{18}\text{O}$ can often indicate the presence of diagenetic alteration due to recrystallization of carbonate in the presence of

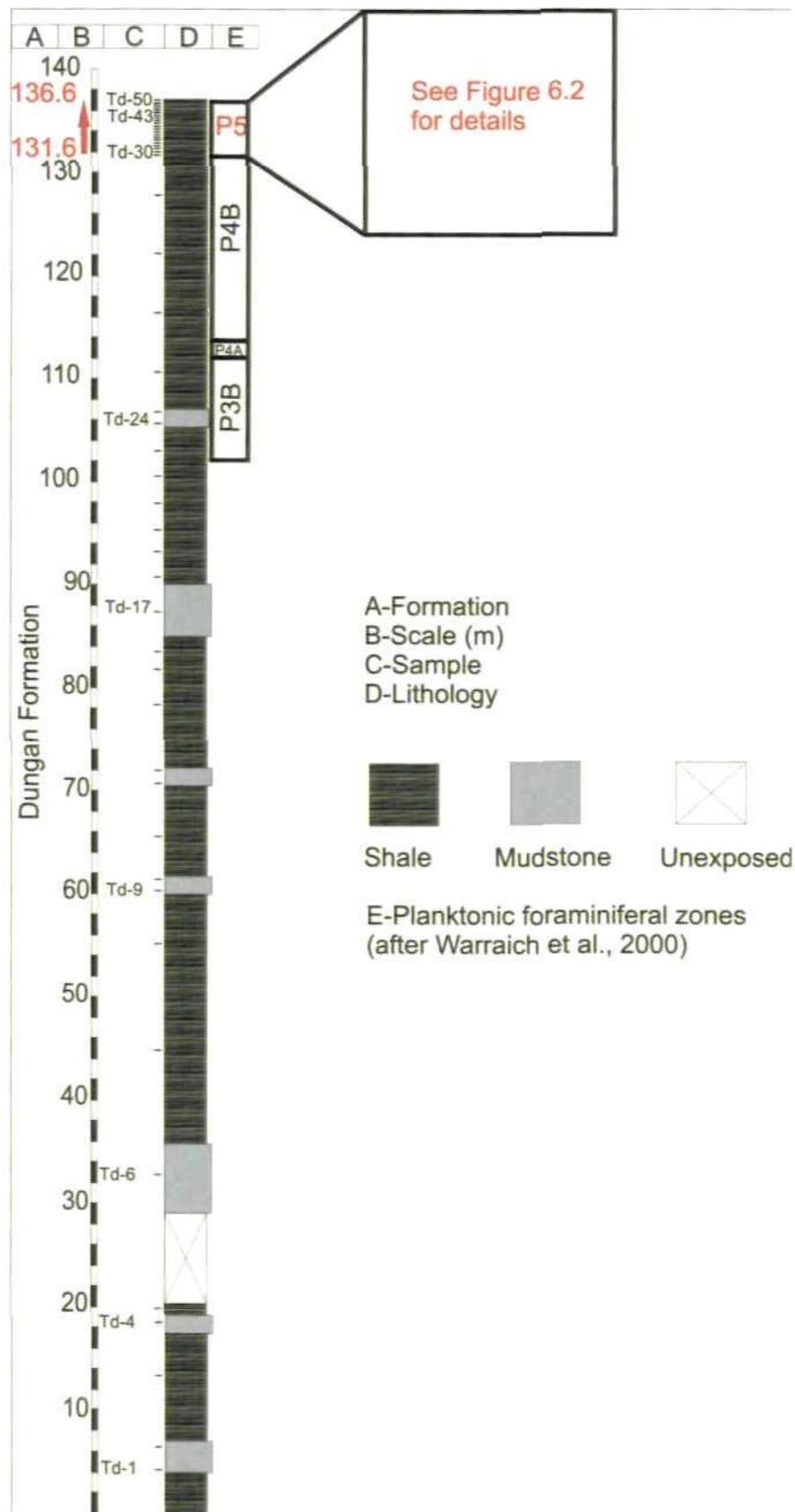


Fig. 6.1: The columnar section of the uppermost 140m of the Dungan Formation in the Rakhi Nala section, Sulaiman Range, Indus Basin (Pakistan).

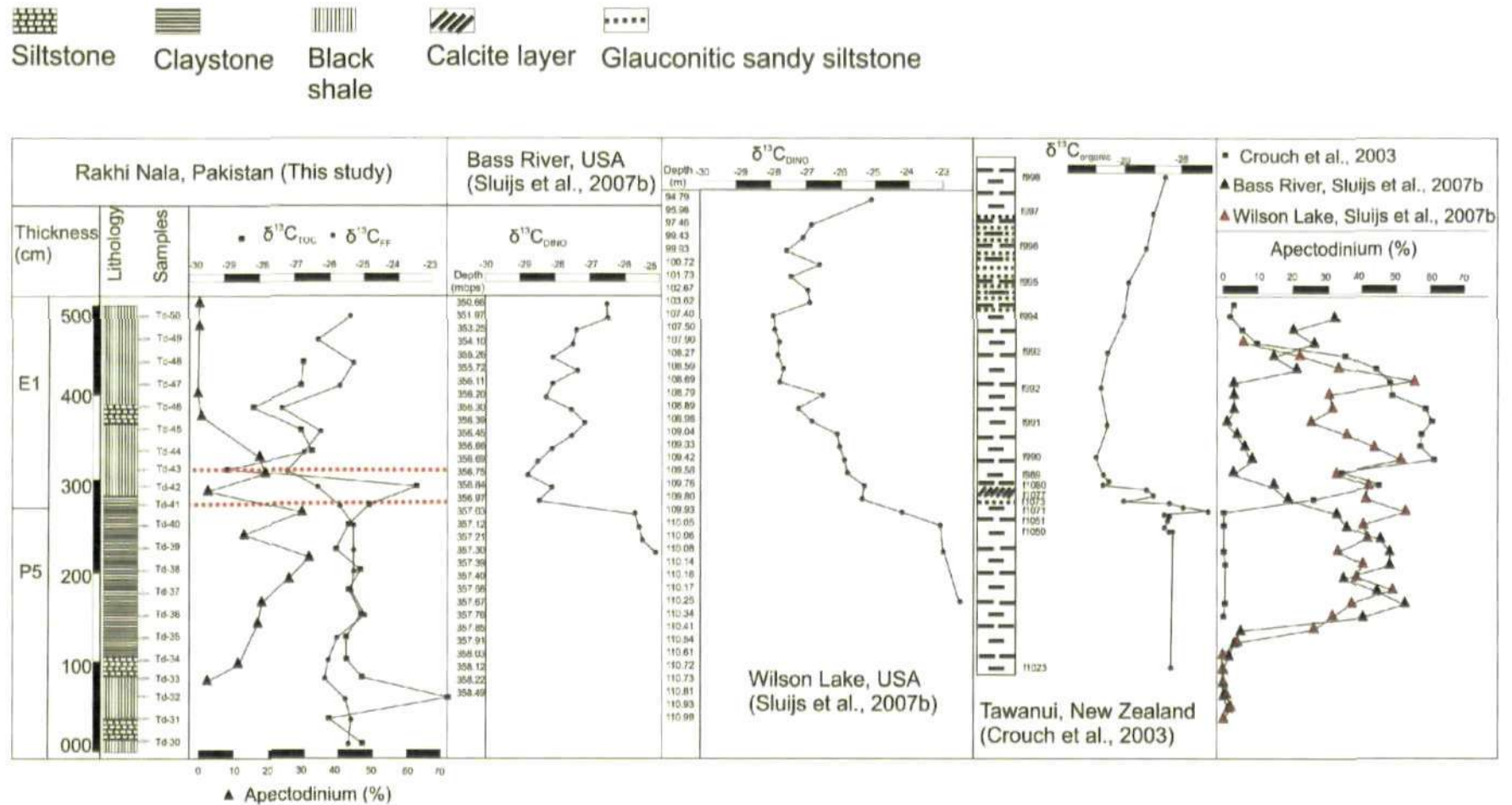


Fig. 6.2A: Lithological, stable isotope and *Apectodinium* data from the Rakhi Nala section and its comparison with other global sections. The area between red dotted lines indicates the onset of CIE in the Rakhi Nala, section, Sulaiman Range, Indus Basin (Pakistan). Curves have been correlated on the basis of the stable isotope data.

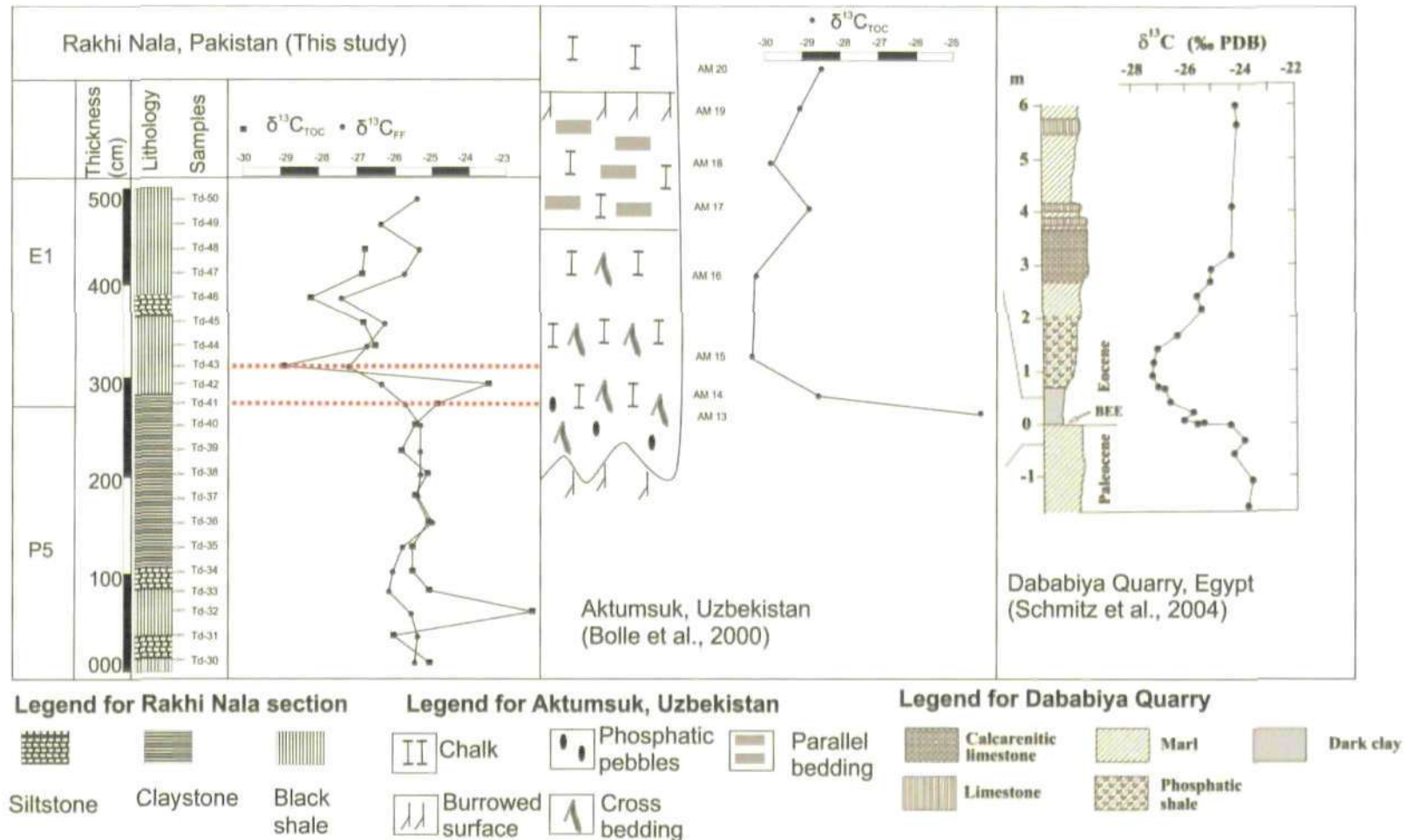


Fig. 6.2B : Lithological and stable isotope data from the Rakhi Nala section and its comparison with other Tethyan sections. Area between dotted red lines shows the onset of CIE in the Rakhi Nala, Indus Basin (Pakistan). Curves have been correlated on the basis of the stable isotope data.

meteoric water (which is depleted in ^{18}O) and which is carrying ^{12}C derived from organic matter (Corfield et al., 1991). The shallow water depositional environments are relatively more susceptible to diagenetic alteration and, therefore, a high correlation coefficient between $\delta^{13}\text{C}$ and $\delta^{18}\text{O}$ may be achieved. Bolle et al. (2000), based on excellent correlation ($R^2=0.94$) from Uzbekistan, reported that the primary stable isotope signal could be partly altered during early diagenesis. The Rakhi Nala section, although a relatively deeper marine depositional environment, shows some correlation ($R^2= 0.50$) between $\delta^{13}\text{C}$ and $\delta^{18}\text{O}$ for the fine fraction carbonate ($<63\mu\text{m}$) isotope data (Fig. 6.4).

The stratigraphical logs and $\delta^{13}\text{C}_{\text{TOC}}$ and $\delta^{13}\text{C}_{\text{FF}}$ (total fine fraction organic carbon) curves for the Rakhi Nala section are shown in **Figure 6.2A**. The reliability of the $\delta^{13}\text{C}_{\text{TOC}}$ values depends upon the organic compounds in the sediment being well mixed as, in such cases, an averaged $\delta^{13}\text{C}_{\text{TOC}}$ signal reliably close to the original one can be obtained (Magioncalda et al., 2004). However, the isotopic signal from the bulk organic carbon values may be biased by factors such as organic matter degradation, bacterial growth, input of allochthonous material, selective preservation and the effect of Rayleigh distillation with depth (Lehmann et al., 2002; Wynn et al., 2005; Smith et al., 2007). The effect of some of these factors cannot be ruled out and, therefore, the isotopic signal from the bulk organic carbon combined with other proxies (e.g., soil nodule carbonate, marine carbonate, biogenic apatite) may serve as a good preservation indicator for the type of material (Jahren et al., 2001; Hasegawa et al., 2003; Magioncalda et al., 2004). The isotopic analysis on the carbonate fraction failed to yield any significant isotopic signal. The isotopic data on the total organic carbon and total fine-fraction organics are, therefore,

presented here. It can be noted that samples Td41 and Td 46 show high C/N_{TOC} value but the overall effect of terrestrial organic input is not very prominent on the isotopic signals, particularly on $\delta^{13}\text{C}_{\text{FF}}$ (see **Figure 6.3**).

In the Rakhi Nala section the maximum $\delta^{13}\text{C}_{\text{TOC}}$ is -22.2‰ with a minimum value of -28.9‰, while the maximum $\delta^{13}\text{C}_{\text{FF}}$ is -25.0‰ with a minimum value of -27.4‰. No significant correlation exists between the organic carbon content (%) and the $\delta^{13}\text{C}$ (‰VPDB) of the samples (i.e., Pre- CIE; $R^2=0.17_{\text{TOC}}$, $R^2=0.14_{\text{FF}}$, CIE; $R^2=0.02_{\text{TOC}}$, $R^2=0.31_{\text{FF}}$). This lack of correlation suggests that the isotope values are not influenced by the amount of organic carbon preserved in the sediments (**Fig. 6.5A & 6.5B**).

Both the bulk organic and fine-fraction organic isotopic signals show the CIE episode (**Fig. 6.2A & 6.2B**). The onset of the CIE occurs immediately above the carbonate-poor, foraminiferal barren interval. The onset of the CIE in the bulk organic ($\delta^{13}\text{C}_{\text{TOC}} = -28.9\text{‰}$) occurs at Td-43 while in the fine fraction organic the CIE ($\delta^{13}\text{C}_{\text{FF}} = -25.7\text{‰}$) begins slightly earlier at Td41. The most negative $\delta^{13}\text{C}_{\text{TOC}}$ and $\delta^{13}\text{C}_{\text{FF}}$ values reach -28.9‰ and -27.4‰ respectively. The pre-CIE $\delta^{13}\text{C}_{\text{TOC}}$ and $\delta^{13}\text{C}_{\text{FF}}$ values are -25.0‰ and -25.0‰ respectively, while the averaged CIE $\delta^{13}\text{C}_{\text{TOC}}$ and $\delta^{13}\text{C}_{\text{FF}}$ values are -27.4‰ and -26.0‰ respectively. It should also be noted that a negative $\delta^{13}\text{C}_{\text{TOC}}$ and $\delta^{13}\text{C}_{\text{FF}}$ peak (< -26.0‰) also occurs at Td-31 and Td-33 respectively before the full onset of the CIE. Finally, a recovery trend towards the pre-excursion isotopic signal (Td-50 = -25.4‰) is seen in only the $\delta^{13}\text{C}_{\text{FF}}$. A full recovery cannot be observed as a result of an incomplete section either because of truncation by erosion or perhaps non-deposition.

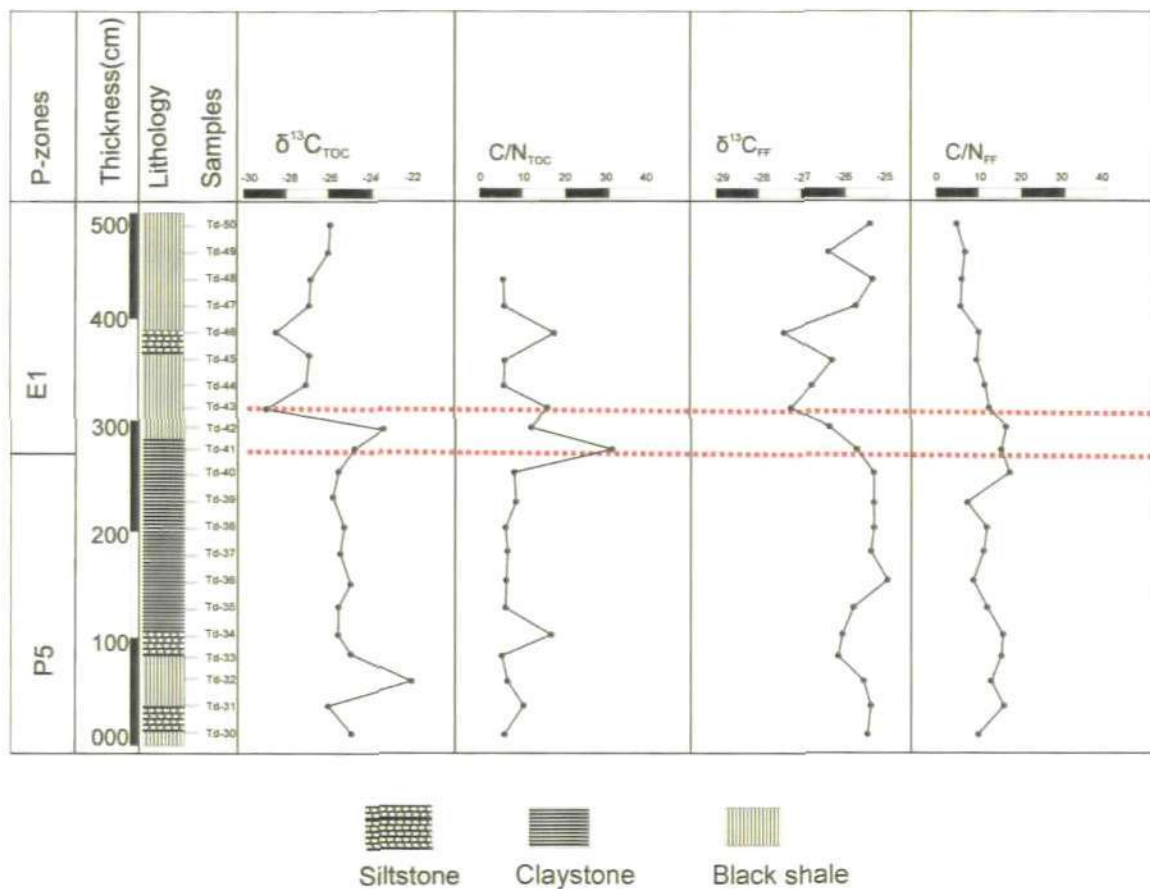


Fig. 6.3: Showing C/N data plotted against isotopic trends. TOC= Total organic carbon, FF= Fine fraction organic. The area between red dotted lines indicate onset of the Carbon Isotopic Excursion (CIE).

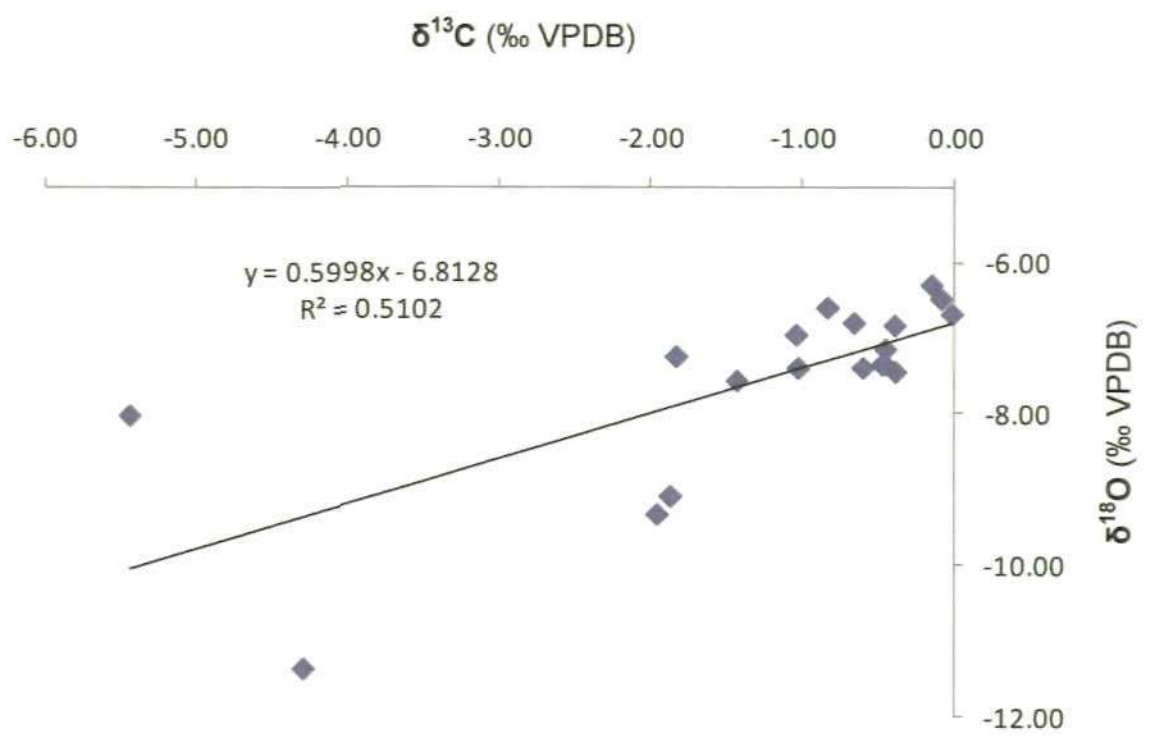


Fig. 6.4: Correlation of $\delta^{18}\text{O}$ (‰ VPDB) and $\delta^{13}\text{C}$ (‰ VPDB) values from the fine fraction carbonate (<63 μm) in the Rakhi Nala section, Pakistan.

Rakhi Nala section							
Sample	Lithology	Colour	TOC (%)	Carbonate (wt %)	<i>Apectodinium</i> (%)	$\delta^{13}\text{C}_{\text{fine fraction}}$ (‰ VPDB)	$\delta^{13}\text{C}_{\text{TOC}}$ (‰ VPDB)
Td-50	Shale	Greenish grey			1.2	-25.4	--
Td-49	Shale	Greenish grey			0.8	-26.4	--
Td-48	Shale	Greenish grey	0.33	4.0	Not processed	-25.3	-26.7
Td-47	Shale	Greenish grey	0.48	13.5	Not processed	-25.7	-26.8
Td-46	Mudstone	Greenish grey	1.63	3.4	0	-27.4	-28.3
Td-45	Shale	Greenish grey	0.41	3.8	1.2	-26.3	-26.8
Td-44	Shale	Blackish grey	0.46	17.8	Not processed	-26.7	-26.6
Td-43	Shale	Black	2.14	7.1	17.7	-27.2	-28.9
Td-42	Shale	Greenish grey	0.86	46.5	19.6	-26.4	-23.5
Td-41	Shale	Greenish grey	5.59	4.4	3.1	-25.7	-24.8
Td-40	Shale	Greenish grey	0.52	4.5	29.5	-25.3	-25.5
Td-39	Shale	Black	0.54	3.4	13.9	-25.3	-25.8
Td-38	Shale	Black	0.40	3.7	32.5	-25.3	-25.2
Td-37	Shale	Brownish black	0.44	3.4	25.7	-25.4	-25.5
Td-36	Shale	Black	0.41	3.4	18.6	-25.0	-25.1
Td-35	Shale	Black	0.41	4.2	18	-25.8	-25.6
Td-34	Mudstone	Black	0.51	3.4	Not processed	-26.1	-25.6
Td-33	Shale	Blackish grey	0.41	4.7	13.5	-26.2	-25.1
Td-32	Shale	Blackish grey	0.56		3.4	-25.6	-22.2
Td-31	Mudstone	Blackish grey	0.47	3.9	Not processed	-25.4	-26.1
Td-30	Shale	Blackish grey	0.43	3.6	3.2	-25.5	-25.1

Table 6.1: Sample numbers, lithology, colour, TOC (%), Carbonate (%), *Apectodinium* (%) and stable isotope results from Rakhi Nala section; **bold** values show the Carbon Isotopic Excursion (CIE).

6.3.3. *Apectodinium*

The percentage of the dinoflagellate *Apectodinium* increases up the section from 3.2% (Td-30) to 13.5% (Td-33) and reaches to the peak percentage of 32.5% (Td-38) and then shows a decreasing trend from Td-39 to Td50. Although some samples show high absolute percentages (e.g., Td-40 (29.5%), Td-42(19.6%) and Td-43 (17.7%)) there is still a declining trend upwards (**Fig. 6.2A**).

6.3.4. Carbonate

The P/E boundary interval is poor in carbonate content with an average value of ~11.0%. The claystone interval (foraminiferal barren) shows the lowest carbonate content with an average percentage of 4.0 with a minimum of 2.1% (Td-36) and a maximum of 8.4% (Td-40). The pre- and post- claystone intervals are relatively high in carbonate content with average values of ~11.7% and ~17.0% respectively (**Table 6.1**).

6.4. Discussion

6.4.1. Comparison with previous studies

Minimum $\delta^{13}\text{C}_{\text{organic}}$ values from the Rakhi Nala section ($\delta^{13}\text{C}_{\text{TOC}} = -28.9\text{‰}$, $\delta^{13}\text{C}_{\text{FF}} = -27.4\text{‰}$) are similar to those reported by Crouch et al., 2003 (-29.4‰), Schmitz et al., 2004 (-27.5‰) and Sluijs et al., 2007b (Bass River = -28.8‰, Wilson Lake = -27.8‰) but slightly more positive than those reported by Bolle et al., 2000 (Aktumsuk, Uzbekistan = -30.4‰) and Sluijs et al., 2007b (North sea = -32.1‰).

A tentative comparison based upon the start of the CIE between the $\delta^{13}\text{C}_{\text{TOC}}$ and $\delta^{13}\text{C}_{\text{FF}}$ (total fine fraction organic carbon) curves from the Rakhi Nala section has been made with those from Dababiya Quarry, Egypt (Schmitz et al., 2004), Tawanui,

New Zealand (Kaiho et al., 1996; Crouch et al., 2003), Aktumsuk, Uzbekistan (Bolle et al., 2000), Bass River and Wilson Lake, New Jersey, USA, (Sluijs et al., 2007b). An early “spike” prior to the full onset of the CIE has been pin-pointed in other studies (e.g., Bowen et al., 2001; Collinson et al., 2003; Bains et al., 2003; Domingo et al., 2009). According to these earlier studies, such an early “spike” may suggest an abrupt thermal event which predates the CIE of the PETM. A gradual trend can be seen at the onset of the CIE in the Rakhi Nala section, Pakistan ($\delta^{13}\text{C}_{\text{FF}}$), Wilson Lake, USA, Tawanui, New Zealand. This trend starts with initial values of -25.3‰ (Td40) at Rakhi Nala, -23.1‰ (110.05 depth (m)) at Wilson Lake, -25.2‰ (357.3 mbs) at Bass River and -27.5‰ (f1073) at Tawanui and progresses to around -26.0‰ from Td41 to Td42 at Rakhi Nala and from 109.93 depth (m) to 109.33 depth (m) at Wilson Lake, from 357.12mbs to 357.03 mbs at Bass River and to around -29.0‰ from f1074 to f1076 at Tawanui, New Zealand. An abrupt onset of the CIE can be seen in Rakhi Nala, Pakistan ($\delta^{13}\text{C}_{\text{TOC}}$) from -23.5‰ (Td42) to -28.9‰ (Td-43) and from -24.3‰ (AM13) to -28.6‰ (AM14) in Aktumsuk, Uzbekistan and from -24.4‰ to -26.0‰ (over 10cm vertical distance across the GSSP horizon) in Dababiya, Egypt. All sections show typical $\delta^{13}\text{C}$ CIE values with some variabilities; e.g., Rakhi Nala (~-2.1‰ -total fine fraction organic, ~-2.3‰ -TOC), Wilson Lake (~-3.5‰), Tawanui (~-1.5‰), Bass River (~-3.5‰) and Aktumsuk (~-1.8‰).

6.4.2. Environmental precursors to CIE

The prominent negative CIE of the PETM reflects a massive input of ^{13}C depleted (light) carbon to the ocean-atmosphere system (Dickens et al., 1995). This massive injection of light carbon is considered to be responsible for the rapid increase in global surface temperatures and environmental change that characterize the

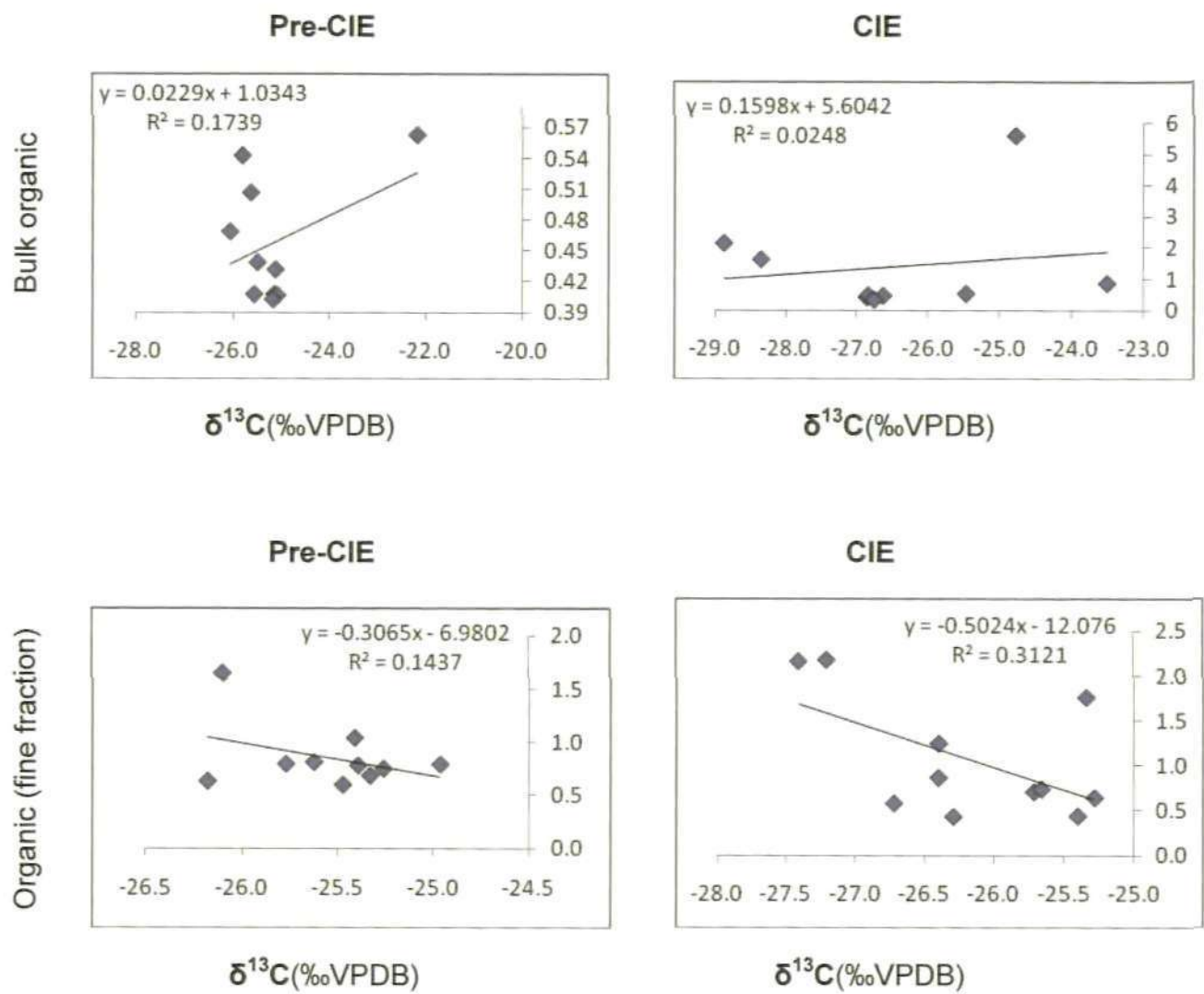


Fig.6.5A: $\delta^{13}\text{C}$ (‰ VPDB) versus total organic carbon (TOC % wt) for the Rakhi Nala section. Pre- CIE and CIE values have been separated.

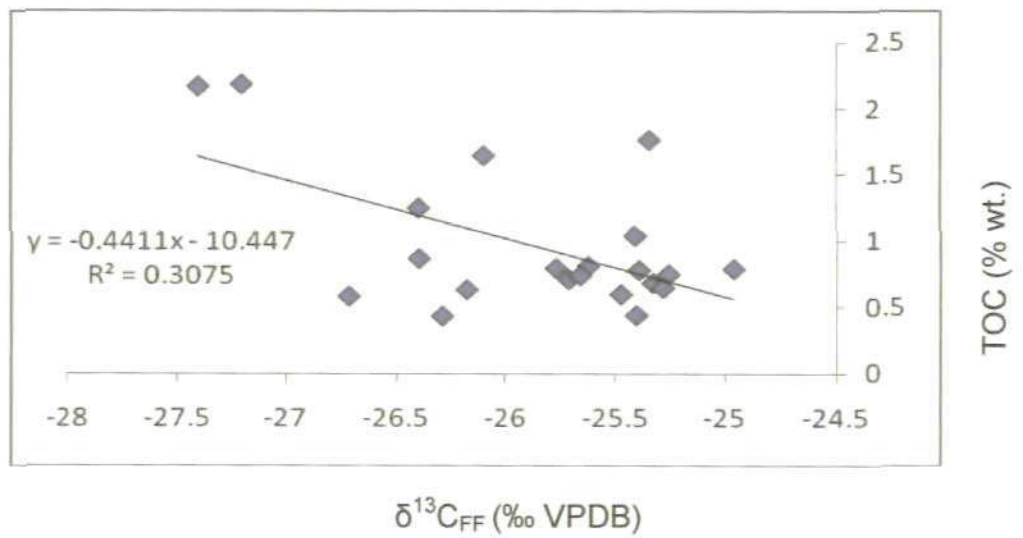
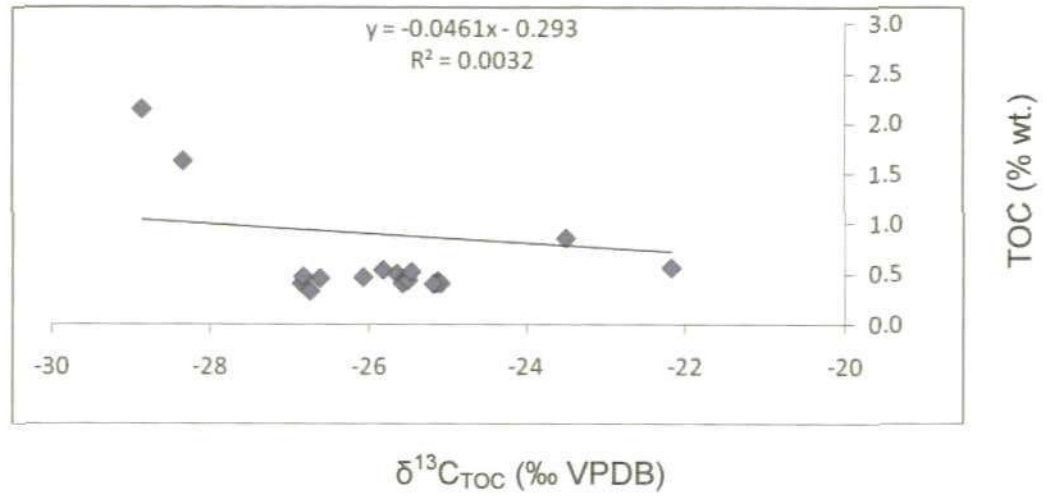


Fig. 6.5B: $\delta^{13}\text{C}$ (‰ VPDB) versus total organic carbon (TOC % wt.) for the Rakhi Nala section, pre-CIE and CIE values are collated.

climate perturbation (Kennett & Stott, 1991; Zachos et al., 2003; Tripathi & Elderfield, 2005; Sluijs et al., 2006). One prominent example of biotic change associated with the onset of the CIE is recorded along continental margins where sediment sequences from all latitudes contain high abundances of dinoflagellate cysts belonging to the subtropical genus *Apectodinium* (Crouch et al., 2001; Sluijs et al., 2006; Sluijs et al., 2007a, b). This is known as the *Apectodinium* acme.

In the Rakhi Nala section the onset of the CIE ($\delta^{13}\text{C}_{\text{FF}}$) is at Td41. The onset of the *Apectodinium* acme is at Td-33, clearly lying below the CIE. This is not an artefact of bioturbation because the CIE is identified at the same level in the $\delta^{13}\text{C}_{\text{FF}}$ record, which is predominantly derived from the dinoflagellates (dominantly *Apectodinium*) in this interval (**Fig. 6.2A**). This early onset of the *Apectodinium* acme has been pin-pointed in a study from the USA and North Sea Basin by Sluijs et al. (2007b). This increase in *Apectodinium*, combined with a negative "spike" in $\delta^{13}\text{C}_{\text{TOC}}$ and $\delta^{13}\text{C}_{\text{FF}}$ and the occurrence of a carbonate-poor, foraminiferal barren laminated black shale interval, prior to the onset of the CIE, are the earliest signs of anomalous environmental change associated with the PETM. Some climate proxy records in earlier studies (Thomas et al., 2002; Tripathi & Elderfield, 2005) also suggest that the onset of warming slightly preceded the CIE. This record from the Rakhi Nala section is in agreement with that of Sluijs et al. (2007b), that there is 'warming before the CIE' but in this tropical section another factor i.e., nutrient availability is considered to be the dominant controlling factor for this palaeoenvironmental change. According to them, their observation is consistent with the hypothesis of Dickens et al. (1995) which states that the thermal dissociation of submarine gas hydrates caused the CIE. In order to reconstruct the palaeotemperature,

the palaeothermometer proxy analysis i.e., TEX₈₆ was carried by Dr Richard Pancost at University of Bristol but the analysis failed to yield any useful information about warming prior to the CIE in the Rakhi Nala section. According to Dr Richard Pancost the material from the Rakhi Nala section (Indus Basin) is too mature not only for TEX₈₆ but also for n-alkane isotope analysis.

6.4.3. $\delta^{13}\text{C}$ gradient and palaeoceanographic inferences

Surface Productivity, Eutrophication and Anoxia

The CIE interval is a period of environmental stress on the Tethyan sea floor and water column; i.e., prevailing eutrophic and oxygen depleted conditions. The increased trophic conditions and reduced ventilation (O₂-depletion) is probably the result of enhanced surface productivity (Speijer & van der Zwaan, 1994; Speijer et al., 1996; Speijer et al., 1997; Alegret et al., 2005).

There is always a $\delta^{13}\text{C}$ gradient from the sea surface to the sea floor through the water column. This gradient is controlled by the ocean productivity. The organic matter is predominantly composed of light carbon ¹²C and very little amount of ¹³C. During increased productivity the organic matter sinks to the bottom and as a result of the removal of organic carbon surface waters become relatively enriched in ¹³C. On the sea floor the breakdown of the organic matter takes place as a result of oxidation. This breakdown results in the release of light carbon and the bottom water is, therefore, depleted in $\delta^{13}\text{C}$. The surface waters often show more positive $\delta^{13}\text{C}$ values than deeper in the water column and at the sea floor. The more enhanced the productivity, the more pronounced this difference in surface water and deep water $\delta^{13}\text{C}$ values becomes (Berger & Vincent, 1986).

Dinoflagellate cysts inhabited the surface waters of the oceans, and by controlling the source of the coarser organic material as much as possible (by using <math> < 63\mu\text{m}</math> fraction), we should find the results from the fine fraction organic to represent the isotopic composition of these surface waters.

In the Rakhi Nala section there is a lack of a clear gradient between $\delta^{13}\text{C}_{\text{FF}}$ (dominated by surface water component) and $\delta^{13}\text{C}_{\text{TOC}}$ (representing both surface and sea floor components) prior to the onset of the CIE. A gradient starts to develop after the full onset of the CIE which indicates an increase in surface productivity leading to eutrophic conditions. Such eutrophic conditions may lead to anoxia at the bottom and the same can be seen in the Rakhi Nala section as is indicated by the increasing TOC (%) values at the same level (Fig. 6.2A).

Oceanic circulation

Young deep waters close to their source of formation are rich in dissolved oxygen and depleted with respect to CO_2 . As a result, they have relatively high $\delta^{13}\text{C}$ values (Kroopnick, 1985). As deep waters move away from their source areas, they become progressively depleted with respect to $\delta^{13}\text{C}$ due to the oxidation of ^{12}C -rich organic matter. For instance, modern North Atlantic Deep Water (NADW) is approximately 1.0‰ enriched in $\delta^{13}\text{C}$ relative to Pacific Deep Water (Kroopnick, 1985). Previous palaeoceanographical work on the PETM suggests that global warming in the earliest Eocene may have contributed to large scale changes in deep-ocean circulation (e.g., Kennett & Stott, 1991; Nunes & Norris, 2006).

At the discovery of the PETM, Kennett & Stott (1991) described a change in the oceanic circulation from a Southern Ocean source to a Warm Saline

Deep Water (WSDW) system and they considered the Tethys to be the site of formation. They claimed that this change in circulation was a primary cause of the BEE (Benthic Extinction Event) and the same cause is also confirmed by Pak & Miller (1992). Following the pre-existing work on the palaeoceanography of the PETM, Nunes & Norris (2006) suggested that before, and after, the CIE (PETM) the site of deep water formation was in the Southern Hemisphere. During the CIE this site shifted to the Northern Hemisphere. Prior to the work of Kennet & Stott (1991), this change in oceanic circulation and consequent episodes of extinction were considered to be induced by tectonics (e.g., Rea et al., 1990). However, the following work of Speijer & van der Zwaan (1994) linked this change in oceanic circulation to a rapid global warming. Schmitz et al. (1996) partially agreed with the previously held belief of Kennett & Stott (1991) by relating the deep sea benthic extinction to the spreading of warm saline bottom water. However, their data indicate that the Egyptian part of the southern Tethyan shelf did not supply the world ocean with deep waters during the BEE. They did not rule out other Tethyan areas as possible sites for deep water production. They also support the hypothesis of Rea et al. (1990) and suggested that the changes in ocean circulation may be related to a sudden large scale tectonic event affecting an important sill or gateway. Galeotti et al. (2004) observed a bathymetric migration of agglutinated foraminifera species from outer neritic-bathyal to lower bathyal-abyssal settings and they argued that the distribution of modern benthonic foraminifera is controlled by flux rates of organic matter, dissolved oxygen concentration in the bottom water and pore water temperature. These parameters display a depth dependent gradient. Similarly this bathymetric migration during the PETM was caused by fluctuations of any one or a combination of these parameters. Their data further

support temperature as a predominant controlling factor and they agreed with Kennett & Stott (1991) and Kaminski et al. (1996) and attributed the increase in temperature to the WSDW formation at this site.

6.5. Conclusions

Organic matter enclosed in the sediments from a land section, namely Rakhi Nala (Indus Basin, Pakistan), have been analysed with the aim of detecting the negative CIE associated with the PETM. The onset of the $\delta^{13}\text{C}$ excursion has been pin-pointed immediately above the foraminiferal barren and carbonate-poor interval of laminated black shale coincident with the Benthonic Foraminiferal Extinction Event of Warraich et al. (2000). The complete recovery of $\delta^{13}\text{C}$ may not be detected due to the presence of an unconformity. Typical $\delta^{13}\text{C}$ excursion values are -28.9‰ and -26.4‰ in $\delta^{13}\text{C}_{\text{TOC}}$ and $\delta^{13}\text{C}_{\text{FF}}$ respectively. The $\delta^{13}\text{C}$ excursion cannot be detected in the carbonate fraction as it is diagenetically altered.

The peak abundance of *Apectodinium* combined with the occurrence of foraminiferal barren and carbonate-poor interval of black laminated shale, prior to the onset of the $\delta^{13}\text{C}$ excursion indicate that an environmental change may have preceded the $\delta^{13}\text{C}$ excursion. This is in agreement with the work of Sluijs et al. (2007b) but nutrient and/or food availability in already warm tropical waters is considered to be the overriding factor for this change. The establishment of a $\delta^{13}\text{C}$ gradient between the surface and bottom water after the onset of the CIE shows increased productivity.

Chapter 7: Synthesis

7.1. Introduction

In the previous chapters, various aspects of biostratigraphy and palaeoenvironmental changes during the Paleocene-Eocene (P/E) interval along the Tethyan margin from the Indus Basin (Pakistan) have been discussed. The response of the marine system to the climatic perturbation during the Paleocene-Eocene transition is investigated by combined analyses of foraminifera, organic-walled dinocysts, stable isotopes and other geochemical proxies such as C/N ratio, TOC (%) and carbonate content (%). To extract a robust biostratigraphical and palaeoenvironmental signal and avoid any misinterpretations, a multiproxy approach is applied in the present study.

This final chapter attempts to integrate different biostratigraphical schemes from shallow to deep water environments and to develop an integrated picture of the palaeoenvironment across the P/E transition from the Indus Basin both in a Tethyan and a global context.

7.2. Chemo- and biostratigraphical calibration of the P/E boundary

The bio-chronostratigraphical calibration between shallow and open marine deposits at a regional and global scale is, generally, a difficult task. The organisms living in different depth domains, generally occupy disparate habitats. In the past, attempts have been made to inter-calibrate the characteristic fossil groups of different depth regimes (e.g., Luterbacher, 1970; Kapellos & Schaub, 1973; von Hillebrandth, 1975; Bolli et al., 1985; Serra-Kiel et al., 1996). More recently Scheibner & Speijer (2009) reported an inter-calibration of larger foraminifera to the more widely used pelagic zonation schemes (planktonic

foraminifera and calcareous nannofossils) across the Paleocene/Eocene boundary interval (**Fig. 7.1**).

The Global Stratotype Section and Point (GSSP) for the basal Eocene has now been established in the Dababiya section in the Nile Valley of Egypt (Aubry & Ouda, 2003). The onset of the Carbon Isotope Excursion (CIE) associated with the Paleocene Eocene Thermal Maximum (PETM) acts as a prime criterion for delineating the Paleocene/Eocene boundary in marine and non-marine sequences in sections around the world. In pelagic sediments the CIE is placed between the planktonic foraminiferal zones P5 and E1 (Berggren & Pearson, 2005) and between calcareous nannofossil subzones NP9a and NP9b (Aubry, 1995). Prior to the establishment of the GSSP, this boundary was considered to coincide with the boundary between SBZ5 and SBZ6 in shallow marine deposits (Serra-Kiel et al., 1998) (**Fig. 7.1**). However, later, it was observed that an important event called the Larger Foraminiferal Turnover (LFT) coincides with the CIE (Orue-Etxebarria et al., 2001; Pujalte et al., 2003 and Scheibner et al., 2005). Therefore, using the LFT as a biomarker, the pragmatic placement of the P/E boundary between SBZ4 and SBZ5 by Hottinger (1998) in the shallow water domain has now been confirmed by Scheibner et al. (2005) and Scheibner & Speijer (2009) (**Fig. 7.1**).

The Indus Basin contains sections where the interfingering of the shallow marine shelf and open marine deposits across the Paleocene/Eocene interval (discussed in Chapters-3 & 4) provide an excellent opportunity to establish shallow to deep marine correlation. The foraminifera and dinoflagellate cysts investigated and reported in the previous chapters, along with those from the previous studies, and the stable isotope analysis from this study provides the basis for this correlation.

	Series	Age			P Zone		NP Zone		B Zone	SB Zone	
		Berggren et al. (1995/2000)	Serra-Kiel et al. (1998)	Scheibner et al. (2005)	Berggren and Pearson (2005)	Berggren et al. (1995)	Martini (1971) Okada and Bukry (1980) Aubry (1995) Aubry et al. (2000)	Berggren and Miller (1989)	Serra-Kiel et al. (1998)	Scheibner et al. (2005)	
LFT PETM CIE	Early Eocene	Ypresian	Ilerdian	Ilerdian	E4	P6b	NP10	d	BB1	SBZ8	SBZ8
					E3	P6a		c		SBZ7	SBZ7
		E2			P5	b		SBZ6		SBZ6	
		E1				a	SBZ6	SBZ5			
		Late Paleocene			Thanetian	Selandian	P5			NP9	b
	P4c		P4c	a			SBZ4	SBZ4			
	P4b		P4b	NP7/8			BB2	SBZ3	SBZ3		
	P4a			NP6				SBZ3	SBZ3		

Fig. 7.1: Paleocene - Eocene correlation of deep and shallow waters biostratigraphical schemes in the Tethyan Realm; **LFT**- Larger Foraminiferal Turnover, **PETM** - Paleocene Eocene Thermal Maximum, **CIE**-Carbon Isotopic Excursion, **P Zone** – Planktonic foraminiferal zones, **NP Zone** - Nannoplankton zones, **B Zone** - Bathyal benthonic foraminiferal zones, **SB Zone** - Shallow benthonic foraminiferal zones (after Scheibner & Speijer, 2009).

7.2.1. Stable isotope stratigraphy

The CIE is the agreed marker for the placement of the Paleocene/Eocene boundary in marine and non-marine sequences worldwide. In this study, therefore, $\delta^{13}\text{C}$ analyses were carried out on different fractions of the same samples as mentioned in Chapter-6. The CIE is recognised in both the total organic carbon ($\delta^{13}\text{C}_{\text{TOC}}$) and also in the total fine fraction organic ($\delta^{13}\text{C}_{\text{FF}}$, representing dominantly marine dinoflagellates). The base of the CIE is characterized by a negative $\delta^{13}\text{C}$ shift between samples Td41 and Td43 in the Rakhi Nala section, Sulaiman Range (Lower Indus Basin), which is followed by a further decrease until it reaches its lowest values. This shift marks the onset of the CIE and hence the Paleocene/Eocene boundary (**Fig. 7.2**). The Paleocene part of the $\delta^{13}\text{C}$ curve is characterized by relatively high values. The Lower Eocene values are generally lower than the Upper Paleocene values (see **Table 6.1** in Chapter 6).

7.2.2. Calcareous nannofossils

The Paleocene/Eocene boundary is conventionally correlated with the NP9/NP10 boundary (Martini, 1971). Aubry et al. (2000) now place it at NP9a/b boundary by the simultaneous lowest occurrences (LO's) of several calcareous nannofossils taxa: i.e., *Rhomboaster calcitrapa*, *R. spineus*, *Discoaster araneus* and *D. anartios*. According to Dupuis et al. (2003) the lower part of the CIE (Paleocene/Eocene boundary) closely correlates with the NP9a/b boundary (**Fig. 7.1**). In addition to the above species the highest occurrence (HO) of *Fasciculithus alanii*, which is restricted to NP9a occurs close to the onset of the CIE (e.g., Aubry, 1998; von Salis et al., 1998; Galeotti et al., 2000 and Monechi et al., 2000).

In the Indus Basin Köthe et al. (1988) applied the zonal scheme of Martini (1971) and also reported additional markers. Following Martini, they placed the Paleocene/Eocene boundary at the boundary between NP9 and NP10. The marker species for the P/E boundary interval (mentioned earlier), used by Okada & Bukry (1980), Aubry (1995) and Aubry et al. (2000) in the modification and subdivisions of the Martini (1971) zonal scheme, are not reported in the earlier studies from the Indus Basin. The absence of these species may partly be due to the coarse sampling resolution used in previous research or may be due to the carbonate-poor interval across the Paleocene/Eocene boundary as observed in the Rakhi Nala section. Therefore, the newly available calcareous nannofossil zonal scheme (e.g., Aubry et al., 2000) cannot be adopted in the Indus Basin for the Paleocene/Eocene boundary interval. Further studies on the calcareous nannofossils in the Indus Basin may be required to update the calcareous nannofossil zonation. However, the Paleocene/Eocene boundary is assumed to be within the NP-9 Zone.

7.2.3. Dinoflagellates

A definition for the base of the Eocene using a dinoflagellate cyst zonation by way of a nannoplankton correlation was proposed by Costa & Muller (1978) as equivalent to the base of the *Wetzeliella astra* Zone (D6a). However, Harland (1979), Morton et al. (1983), Knox et al. (1983) and Powell (1988) questioned this interpretation (i.e., that the base of the *W. astra* Zone is equivalent to the base of the Eocene). They found it difficult, not only to delineate the *W. astra* Zone in southern England, but they were also unable to differentiate the index species from *Apectodinium hyperacanthum* (e.g., Harland, 1979; Knox et al., 1983). Following the work of Morton et al. (1983) later investigations on the

Rockall Plateau (DSDP, Site 555) show that the base of the *W. astra* Zone lies in an undated sequence between zones NP9 and NP10. In the light of the above evidence, the *W. astra* appearance is a weak candidate for the definition of the Paleocene/Eocene boundary. In the Indus Basin, however, Köthe et al. (1988) used the first appearance of *W. astra* to place the Paleocene/Eocene boundary coincident with NP9/NP10 boundary.

Four dinoflagellate zones of the late Paleocene-early Eocene are recognized in this study, the details being given in Chapter-5. These zones, in ascending order, are; Pak-DIV, Pak-DV, Pak-DVI and Pak-DVII. The lowest occurrence (LO) of *W. astra* is not a very reliable marker for the placement of the Paleocene/Eocene boundary, and its LO (i.e., Td42) occurs after the onset of the CIE (i.e., Td41) in this study, and therefore, the LO of *W. astra* cannot be used to mark the Paleocene/Eocene boundary (**Fig. 7.2**). However, the calibration of the Paleocene/Eocene boundary with the NP9/NP10 zonal boundary or with the NP9a/NP9b subzonal boundary requires further investigation. The highest occurrence of *Apectodinium augustum* is the marker for the Paleocene/Eocene boundary in the central North Sea Basin (Powell, 1988) and it is also considered to be marker specie of the CIE (e.g., Sluijs & Brinkhuis, 2009). This species was not observed in the present study but its only occurrence is recorded from the Upper Indus Basin by Edwards (2007). The *Apectodinium* acme is also considered to coincide with the Paleocene/Eocene boundary in a number of other studies (e.g., Boulter & Manum, 1989; Bujak & Brinkhuis, 1998; Crouch, 2001; Crouch et al., 2001; Nøhr-Hansen, 2003; Steurbaut et al., 2003; Sluijs et al., 2006). The existing tropical marine waters and the increased availability of nutrients and/or food prior to the CIE in marginal Tethyan basins provided suitable conditions for the

Apectodinium acme. The decrease in *Apectodinium* during the CIE suggests a decrease in nutrient and/or food availability. Therefore, in this study, and some other Tethyan and global sections (e.g. Crouch et al., 2003; Sluijs et al., 2007b), this acme occurs prior to the CIE and cannot be used to place the Paleocene/Eocene boundary. Therefore, the zones Pak-DIV to Pak-DVI (part) of the upper Indus Basin belong to the Upper Paleocene and Zone Pak-VI (part) and Pak-DVII belong to the Lower Eocene.

7.2.4. Planktonic foraminifera

The deep marine deposits present in the Indus Basin generally contain abundant planktonic foraminiferal assemblages (up to >90% in, for example, the Rakhi Nala section). These assemblages allow the application of the standard tropical biozonation of Berggren et al. (1995) and Berggren & Pearson (2005) with the limitations discussed in Chapter-4.

The P5 Zone of Berggren et al. (1995) (the host zone for the Paleocene/Eocene boundary) is modified by Berggren & Pearson (2005) into a further three zones; P5, E1 and E2. This new zonal scheme retains the P-notation for Paleocene and adopts an E-notation for the Eocene zones. This modification of the previous P5 is based on the lowest occurrence (LO) of the Planktonic Foraminiferal Excursion Taxa (PFET) marking the P5 and E1 boundary and on the lowest occurrence of *Pseudohastingerina wilcoxensis* marking the E1 and E2 boundary. However, the top boundary of E2 is the same as that of the top boundary of previous P5 Zone. The LO of the PFET is coincident with the CIE and its occurrence is restricted to the E1 Zone. Recently the use of the LO of the *Acarinina sibaiaensis* as the marker species for the base of E1 and the PETM has been questioned and *Acarinina multicamerata*

introduced as a new marker species for the PETM (e.g., Guasti & Speijer, 2008; Scheibner & Speijer, 2009).

The PFET was not observed in the present or previous studies of the Indus Basin, Pakistan. However, the PFET taxa (i.e., *Acarinina africana* and *Acarinina sibaiaensis*) are described by Kalia & Kinoshita (2006) from the Indian part of the Indus Basin (i.e., the eastern extension of Indus Basin to Rajasthan, India). They observed the LO of the PFET taxa from just above the barren interval which is coincident with the onset of the CIE in the Rakhi Nala section. Therefore, the base of E1 (i.e., Paleocene/Eocene boundary) is placed just above the barren interval in the Rakhi Nala section based on the Benthonic Foraminiferal Extinction Event of Warraich et al. (2000) and the onset of the CIE (this study)(Fig. 7.2). The boundary between E1 and E2 cannot be confidently placed in the Rakhi Nala succession as it is difficult to distinguish between *P. wilcoxensis* and *G. luxorensis*. However, this boundary has been identified using the LO of *P. wilcoxensis* in the upper Indus Basin following the work of Afzal (1997).

7.2.5. Smaller benthonic foraminifera

Berggren & Miller (1989), using the extinctions of *Gavelinella beccariiformis* and associated deep-sea benthonic taxa, defined a zonal boundary between benthic foraminiferal zones BB1 and BB2. This extinction of the deep-sea benthic foraminifera has previously been recognized by Beckmann (1960), von Hillebrandt (1962), Tjalsma & Lohmann (1983) and Thomas (1998). Zone BB1 spans the entire Paleocene and is distinguished from BB2 (Lower Eocene) by the extinction of *Angulogavelinella avnimelechi*, *G. beccariiformis* and *Neoflabellina jarvisi*. The BB2 taxa are represented by *Nuttallides truempyi*,

Turrilina brevispira, *Bulimina callahani* and *B. trinitatensis* (e.g., Speijer et al., 2000).

In the Indus Basin (Pakistan), in a study by Dr Nomura reported by Warraich (2000), *G. beccariiformis* was not observed but the extinction of other Velasco-type species such as *A. avnimelechi*, *Gyroidinoides globosus* and *Cibicidoides hyphalus* was reported (Fig. 5.7 in Chapter 5). Similar extinction patterns have been reported from other Tethyan sections (e.g., Speijer, 1994; Speijer et al., 1995; Speijer & Schmitz, 1998; Dupuis et al., 2003; Alegret et al., 2005; Ernst et al., 2006). This extinction level of deep sea benthic foraminifera coincides with the Paleocene/Eocene boundary (i.e., the onset of the CIE) worldwide (Kennett & Stott, 1991; Thomas, 1998). Using this faunal turnover, the Paleocene/Eocene boundary can be located in the outer neritic to upper bathyal deposits of the Indus Basin such as that typified by the Rakhi Nala section (Fig. 7.2).

7.2.6. Larger benthonic foraminifera

The larger foraminifera are the most common constituents of the late Paleocene-early Eocene carbonate platforms. According to Hottinger (1998), the larger foraminifera show a diversification at a specific level (i.e., adult dimorphism and large test size within the Paleocene/Eocene transition). The Paleocene/Eocene transition represents two out of the five important phases in the global community maturation cycle. Phase-2 (late Paleocene) represents an increase in generic diversity and Phase-3 (lower Eocene) represents an abrupt diversification of different species (Hottinger, 2001). The post K/Pg boundary interval time of long term and short term palaeoenvironmental change such as increasing oligotrophy and higher sea surface temperature led to the demise of

corals in low latitudes and created new niches for many groups including larger foraminifera (Scheibner et al., 2005). Recent observations have shown that this evolutionary change, the Larger Foraminiferal Turnover (LFT), correlates with the PETM in the deeper parts of the Tethyan basins (e.g., Orue-Etxebarria et al., 2001; Pujalte et al., 2003). The LFT coincides with the SBZ4-SBZ5 zonal boundary of Scheibner & Speijer (2009).

The larger foraminifera of the carbonate platform deposits developed in the Indus Basin (e.g., Salt Range (**Fig. 7.3**), Dungan hill (**Fig. 7.4**)) have previously been studied by Haque (1956), White (1989), Afzal (1997), Sameeni (1998) and Shafique (2001): for a full account see Chapter 4 (this study). This earlier work identified a number of biostratigraphically important taxa of larger foraminifera. The characteristic larger foraminifera of the late Paleocene-early Eocene (SBZ4 to SBZ5 of Serra-Kiel et al., 1998) encountered in this and previous studies are discussed below. The late appearance of *Nummulites* in the Indus Basin (e.g., in **Figures 7.3 & 7.4**) has recently been attributed to biogeographical barriers between east and west Tethys, these barriers are thought to have been caused by the initial stages of India-Asia collision (Afzal et al., 2010).

The *Alveolina levis* Zone of Hottinger (1960), SBZ4 of Serra-Kiel et al. (1998) and the *Alveolina cucumiformis* Zone of Hottinger (1960), SBZ5 Zone of Serra-Kiel et al. (1998) in the Indus Basin contain of the following larger foraminifera; **SBZ4**-*Miscellanea miscella*, *M. stampi*, *Lockhartia* spp., *L. haimei*, *L. conditi roeae*, *Ranikothalia sindensis*, *R. nuttalli*, *Rotalia* spp., *Operculina jiwani*, *Op. subgranulosa*, *Op. Salsa*, *Op. sindensis*, *Op. canalifera*, *Broekinella* sp. cf. *B. arabica*, *Daviesina* sp. aff. *D. langhami*, "*Orbitolina*" *daviesi*, *Actinosiphon punjabensis*, *Assilina dandotica*, *Discocyclina ranikotensis*,

Fasciolites spp. (including *F. vredenburgi*), *Saudia labyrinthica*; **SBZ5**-
Nummulites spp., *Nummulites deserti*, *N. thalicus*, *Assilina dandotica*, *A.*
spinosa, *A. prisca*, *A. leymerie*, *A. granulosa*, *Alveolina vredenburgi* (= *Al.*
cucumiformis), *Miscellanea miscella*, *M. stampi*, *Lockhartia* spp. *L. haimei*,
Ranikothalia sindensis, *R. nuttalli*, *Operculina salsa*, *Op. subgranulosa*, *Op.*
jiwani, *Opertorbitolites douvillei*, *Orbitolites complanatus*, *Somalina* sp.,
Discocycline douvillei, *Rotalia* spp., *Fasciolites* (Ta1-Ta2 stage boundary of
Adams (1970); White, (1989); SRX1-SRX3 Zones of Afzal (1997) and Chapter-
4, this study). The Larger Foraminiferal Turnover, such as the replacement of
typical Paleocene taxa by Eocene taxa (i.e., replacement of *Ranikothalia* and
Miscellanea dominated assemblages by *Nummulites* and *Alveolina*), in the
Indus Basin can be seen at the SBZ4-SBZ5 zonal boundary and hence the
Paleocene/Eocene boundary can be identified and correlated with the deeper
water sections such as the Rakhi Nala section of the Sulaiman Range.

7.3. Integrated stratigraphy

The Indus Basin was tectonically active during the Paleocene/Eocene transition.
The basin was topographically composed of many lows and highs as can be
observed from the variable lithologies. As a result of the variable water depths,
larger foraminiferal-dominated carbonate platforms were developed in some
areas (e.g., Kohat-Potwar sub-basin and Salt Range - Upper Indus Basin,
Dungan Hill - Lower Indus Basin) (**Figs 7.3 & 7.4**), while in other areas
planktonic foraminiferal-dominated outer neritic to upper bathyal conditions
prevailed (e.g., Sulaiman Range - Lower Indus Basin) (**Fig. 7.2**). This
palaeobathymetric range in the Indus Basin provides the opportunity to calibrate
the various deep to shallow water biostratigraphical schemes. These different

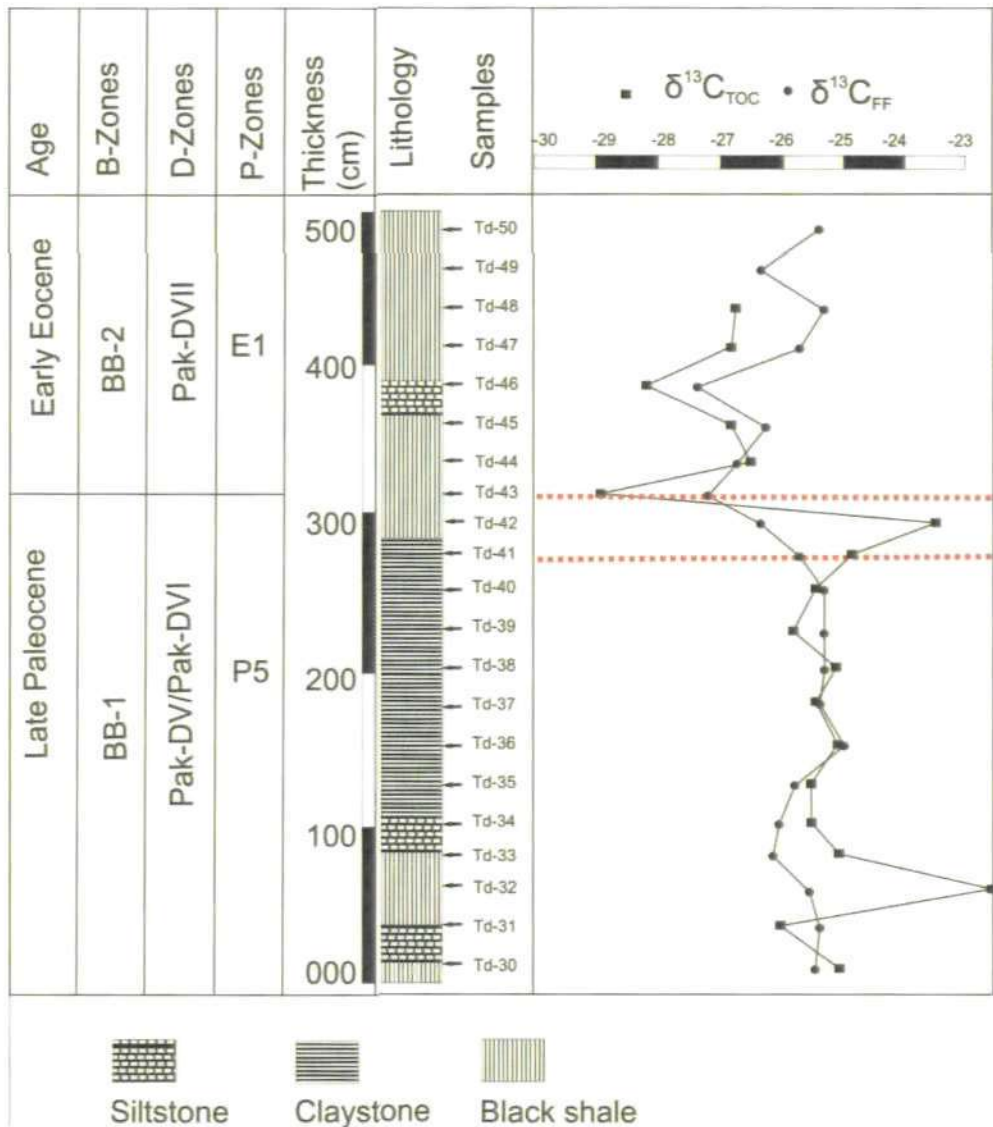


Fig. 7.2: The different biostratigraphical schemes, lithology and carbon isotope data of the Dungan Formation, Rakhi Nala section, Sulaiman Range, Lower Indus Basin. **B- zones** = Bathyal benthonic zones of Berggren & Miller (1989), **D- Zone** = Dinoflagellate zones (This study) and **P- Zones** = Planktonic foraminifera zones of Berggren & Pearson (2005). The area between the red dotted lines shows the onset of the CIE.

biostratigraphical schemes together with the litho-and chemostratigraphy across the Paleocene/Eocene transition are integrated below.

In carbonate platform deposits (e.g. Upper Indus Basin) the late Paleocene is represented by SBZ4 and lower Eocene by SBZ5. Both zones can be separated by the typical SBZ4 (Paleocene) taxa (i.e., *Ranikothalia* spp. and *Miscellanea* spp.) and typical SBZ5 (Eocene) taxa (i.e., *Nummulites* spp. and *Alveolina* spp.). In deeper marine deposits (e.g., Sulaiman Range, Lower Indus Basin) the base of the CIE coincides with the LO of PFET (i.e., the base of E1), with the smaller benthonic zones BB1/BB2 boundary (based on the Benthonic Foraminiferal Extinction Event (BFEE) of Warraich et al., 2000), and is bracketed between the top of the *Apectodinium* acme (below) and the LO of *W. astra* (above) in the upper most part of the Pak-DVI. Uncertainty may arise on the question of the precise correlation of the CIE with the shallow benthic zonation, as stable isotope data from any of the carbonate platform deposits in the basin are not available. Therefore, larger foraminifera together with a well-defined CIE from a continuous carbonate platform section can further improve the deep to shallow water correlation across the Paleocene/Eocene transition in the Indus Basin (Pakistan).

7.4. Palaeoenvironment of the P/E boundary interval

The presence of larger foraminifera, carbonate platform deposits together with smaller benthonic foraminiferal species of Midway-type fauna (e.g., *Cibicidoides*, anomalinids) are indicative of neritic and shelf environments in parts of the Indus Basin (e.g., Kohat-Potwar sub-basins and Salt Range - Upper Indus Basin, Dungan Hill Range - Lower Indus Basin). The presence of dominantly

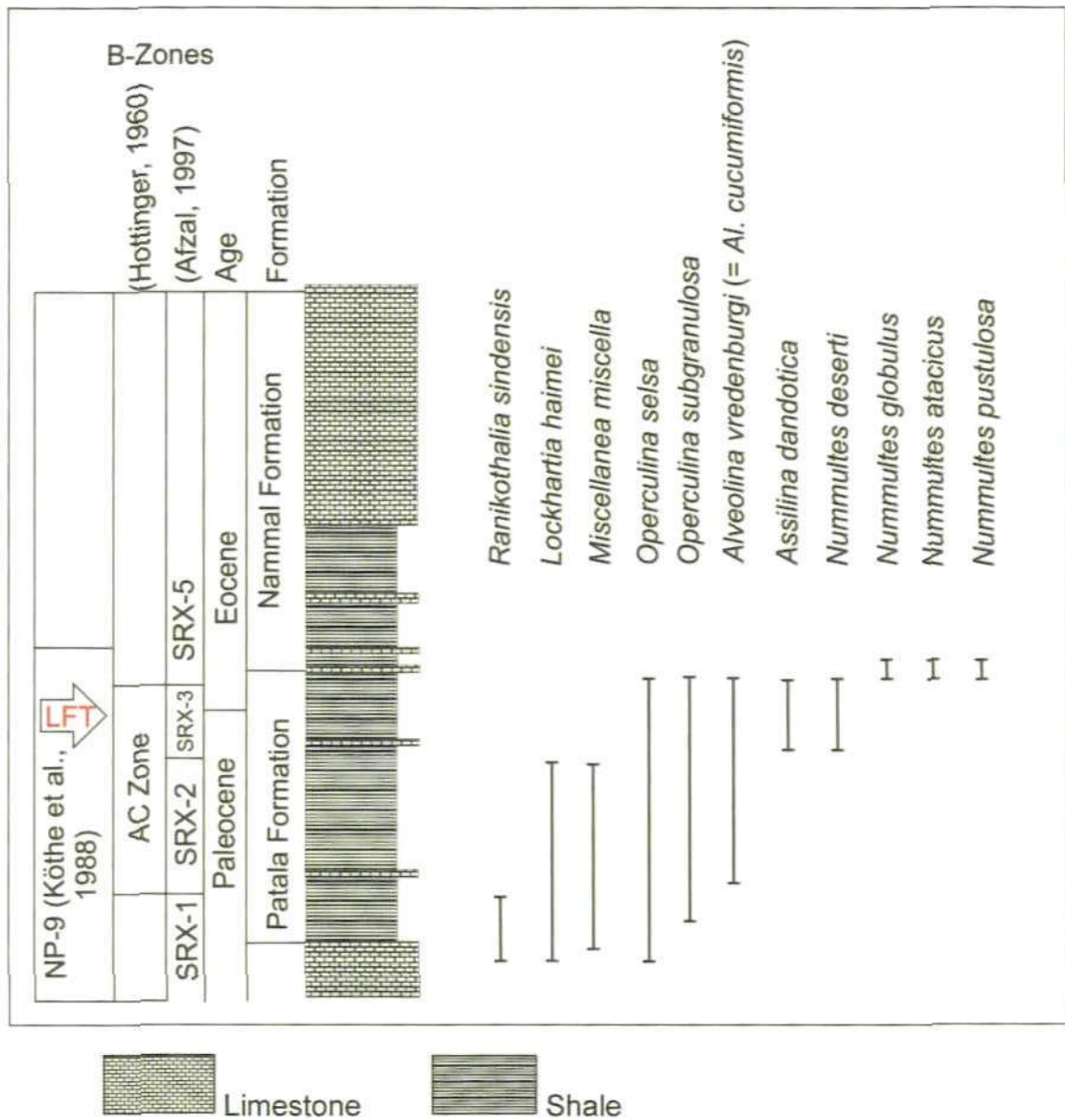


Fig. 7.3: The Larger Foraminiferal Turnover (LFT) in the Chichali Pass section (i.e., replacement of Paleocene taxa such as *Ranikothalia* and *Lockhartia* by Eocene taxa such as *Nummulites*), SRX-4 is missing due to absence of larger foraminifera in interval between SRX-3 and SRX-5 (Modified after Afzal, 1997); **B-Zones** = Larger foraminiferal zones, **AC Zone** = *Alveolina cucumiformis* Zone.

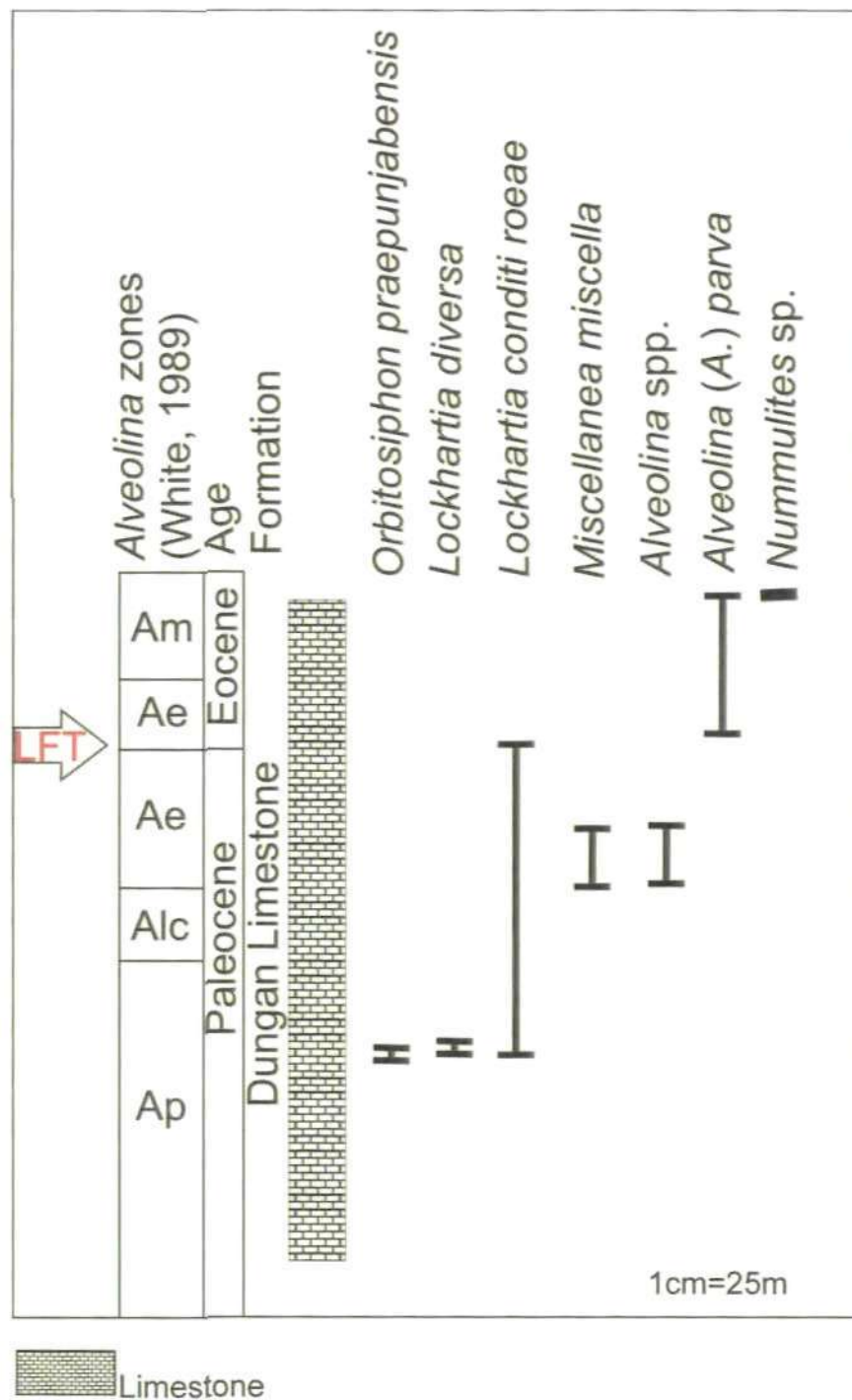


Fig. 7.4: Lithological log and biostratigraphical subdivision of the succession at Dungan Hill, together with the stratigraphical distribution of selected larger foraminiferal taxa (modified after White, 1989); **Ap** (*Alveolina primaeva* Zone), **Alc** (*Alveolina levis*-*Alveolina cucumiformis* Zone), **Ae** (*Alveolina ellipsodalls* Zone), **Am** (*Alveolina moussoulensis* Zone). LFT = Larger Foraminiferal Turnover.

endemic smaller benthonic foraminiferal taxa in the upper Indus Basin, as reported by Afzal (1997), indicates limited connection of the bottom water with the world oceans. However, other parts in the Indus Basin (e.g., Rakhi Nala, Sulaiman Range - Lower Indus Basin) which is composed of deep marine shale facies with a high p-ratio (i.e., >90%), Velasco-type smaller benthonic foraminifera such as *Angulogavelinella avnimelechi* and *Gyroidinoides globosus* and abundant open marine dinoflagellates such as *Spiniferites* indicate a deeper outer neritic to upper bathyal environment of deposition. The presence of cosmopolitan smaller benthonic foraminifera and open marine dinoflagellates in the Sulaiman Range (Lower Indus Basin) also indicate that the entire water column is well connected with the world oceans.

The most important palaeoenvironmental parameters such as palaeoproductivity and palaeotemperature have been reconstructed by a combination of proxies (Chapters 5 & 6). The high number of peridinioid cysts together with the presence of dominant tropical planktonic foraminiferal taxa (i.e., *Morozovella* and *Acarinina*) are indicators of increased surface water productivity in tropical marine waters. The increased abundance of the dinoflagellate cyst *Apectodinium* prior to the onset of the CIE (Chapter 6) indicates increased availability of the food and/or nutrients prior to the $\delta^{13}\text{C}$ shift, suggesting that the palaeoenvironmental change may have been preceded this shift. In some other studies it have been suggested that warming preceded the CIE (e.g., Thomas et al., 2002; Tripathi & Elderfield, 2005), and this early warming is considered to have been responsible for the release of isotopically light carbon from the methane hydrates. Initially suggested by Dickens et al. (1995), this is considered to be the most likely explanation for the CIE. The high TOC (%) values and the presence of benthonic foraminiferal species such as

anomalinids indicate stress on the Tethyan floor: i.e., oxygen deficiency at the sediment/water interface caused by high surface water productivity. This high productivity can be partly linked with the increased terrigenous input as indicated by high C/N ratios and the presence of dinoflagellate species like *Thalassiphora pelagica*. Such an O₂ deficiency and a change from oxic to suboxic conditions in the intermediate waters during the PETM is considered to be a widespread phenomenon (e.g., Kaiho et al., 1996; Bralower et al., 1997; Thomas, 1998; Katz et al., 1999; Crouch et al., 2003; Takeda & Kaiho, 2007; Alegret et al., 2005, 2009). This O₂ depletion in global intermediate waters may have resulted from a combination of ocean warming and CH₄ oxidation (Dickens, 2000).

7.5. Conclusions

The Paleocene-Eocene boundary interval successions of the Indus Basin (Pakistan) have provided an excellent opportunity for the placement of the Paleocene/Eocene boundary and for the calibration of platform and pelagic stratigraphic schemes. The base of the CIE, which is a global marker for the placement of the Paleocene/Eocene boundary, is used for the first time in the Indus Basin to delineate the Paleocene/Eocene boundary. The Paleocene/Eocene boundary coincides with the following pelagic and platform biostratigraphical boundaries;

- Planktonic foraminiferal zonal boundary between P5 and E1 (based on the onset of the CIE and BFEE of Warraich et al., 2000);
- In the top most part of the dinocyst Zone Pak-DVI prior to the lowest occurrence of *W. astra*; and
- Larger foraminiferal zonal boundary between SBZ4 and SBZ5.

The CIE allows the correlation of various evolutionary events in pelagic (i.e., Benthonic Foraminiferal Extinction Event, Planktonic Foraminiferal Excursion Taxa and *Apectodinium* acme) and platform biota (i.e., Larger Foraminiferal Turnover).

An outer neritic to upper bathyal environment of deposition is proposed for the Rakhi Nala section, Suliaman Range (Lower Indus Basin). The presence of dominantly open marine dinoflagellates and cosmopolitan smaller benthonic foraminifera indicate that the entire water column of the Tethyan Ocean at this site was well connected with world oceans. The presence of *Apectodinium* abundance before the onset of the CIE (P/E boundary) propose increased availability of nutrient and/or food in already warm tropical waters, and this increase in nutrients may have been responsible for the acme of *Apectodinium* prior to the CIE (P/E boundary) in tropical marginal basins.

This investigation of the Paleocene/Eocene succession in the Indus Basin (Pakistan) raises a number of further questions that could be investigated. These are:

- As it is evident from the literature (e.g., Beck et al., 1995) that during the Paleocene/Eocene interval time the Indus Basin was tectonically active as a result of the northward movement of the Indian Plate. This tectonic activity results in sea level fluctuations which are reflected by variable lithologies across the Paleocene/Eocene interval in the Indus Basin. This suggests that local factors (i.e., dominantly tectonic movement in this case) may be influencing the palaeoenvironment of the Paleocene/Eocene interval time in the Indus Basin. It is important to identify the local factors when investigating a global phenomenon (such as PETM).

- Further investigations of more field sections for the Paleocene/Eocene interval will provide a detail configuration of the Indus Basin, which may form a basis for the determination of the differential effect (i.e., to investigate the palaeoenvironmental change along a palaeobathymetric gradient) of the Paleocene/Eocene boundary event. Therefore, such an assessment of the palaeoenvironment may help to identify the local factors.
- The palaeoenvironmental assessment on a palaeobathymetric gradient may also result into more biostratigraphical data which can be used to improve the shallow waters to deep waters correlation of different biostratigraphical schemes in the Indus Basin.
- Investigation of the stable isotopes particularly on unaltered carbonate fraction is required to determine the shape, duration and magnitude of the Carbon Isotope Excursion from the Indus Basin. Such data may also improve the palaeoceanographic (e.g., ocean circulation changes during Paleocene/Eocene interval) and palaeoclimatic interpretations.
- Investigation of the palaeothermometer proxies (e.g., TEX₈₆) may provide information on warming before the Carbon Isotope Excursion.
- Quantitative analysis of the clay minerals (e.g., kaolinite, illite and smectite) may provide information on climate change (e.g., temperature and rainfall). For example, the kaolinite percentage and the ratio of kaolinite to illite and smectite in marine sediments

are good indices for the estimation of climate changes (e.g., Robert & Kennett, 1994).

References

- Abbas, G. 1999. *Microfacies, depositional environments, diagenesis and porosity development in limestone horizons of Kirthar Formation (Middle-Late Eocene) in frontal parts of Sulaiman Fold-Belt and adjoining areas, Pakistan*. Unpublished PhD Thesis, Institute of Geology, University of Punjab, Lahore, Pakistan.
- Abrard, D. 1956. Une Operculine cordelée de l'Éocène inférieur de la Côte-d'Ivoire. *Operculina (Nummulitoides) tessieri*, n. subgen., n. sp. *Bulletin de la Société géologique de France* **5**, 489-493.
- Adams, C. G. 1970. A reconstruction of the East Indian Letter Classification of the Tertiary. *Bulletin of the British Museum (Natural History), Geology* **19**, 87-137.
- Adams, C. G. 1988. Septa, septal traces and septal filaments in the foraminiferal genus *Nummulites* Lamarck. *Journal of Micropalaeontology* **7**, 89-102.
- Adelseck (Jr.), C. G. & Berger, W. H. 1975. On the dissolution of planktonic foraminifera and associated microfossils during settling and on the sea floor. *Cushman Foundation for Foraminiferal Research, Special Publication* **13**, 70-81.
- Afzal, J. 1996. Late Cretaceous to early Eocene foraminiferal biostratigraphy of the Rakhi Nala area Sulaiman Range, Pakistan. *Pakistan Journal of Hydrocarbon Research* **8**, 1-24.
- Afzal, J. 1997. *Foraminiferal Biostratigraphy and Paleoenvironments of the Patala and Nammal Formations at the Paleocene/Eocene boundary in Salt Range and Sughar Range, Pakistan*. Unpublished PhD Thesis, University of Punjab, Lahore, Pakistan.

- Afzal, J. & Von Daniels, C. H. 1991. Foraminiferal biostratigraphy and Paleoenvironmental interpretation of the Paleocene to Eocene Patala and Nammal formations from Khairabad East, Western Salt Range, Pakistan. *Pakistan Journal of Hydrocarbon Research* **3**, 61-79.
- Afzal, J., Khan, A. M., & Shafique, N. A. 1997. Biostratigraphy of Kirthar Formation (Middle to Late Eocene), Sulaiman Basin, Pakistan. *Pakistan Journal of Hydrocarbon Research* **9**, 15-33.
- Afzal, J., Williams, M. & Aldridge, R. J. 2009. Revised stratigraphy of the lower Cenozoic succession of the Greater Indus Basin in Pakistan. *Journal of Micropaleontology* **28**, 7-23.
- Afzal, J., Williams, M., Leng, M. J., Aldridge, R. J. & Stephenson, M. H. 2010. Evolution of Paleocene to Early Eocene larger benthic foraminifer assemblages of the Indus Basin, Pakistan. *Lethaia*, DOI: 10.1111/j.1502-3931.2010.00247.x.
- Alegret, L., Ortiz, S., Arenillas, I. & Molina, E. 2005. Palaeoenvironmental turnover across the Palaeocene/Eocene boundary at the Stratotype section Dababiya (Egypt) based on benthic foraminifera. *Terra Nova* **17**, 526-536.
- Alegret, L., Ortiz, S., Orue-Etxebarria, X., Bernaola, G., Baceta, J. I., Monechi, S., Apellaniz, E. & Pujalte, V. 2009. The Paleocene-Eocene Thermal Maximum: New Data on Microfossil Turnover at the Zumaia Section, Spain. *Palaios* **24**, 318-328.
- Alimarina, V. P. 1962. Nekotorye osobennosti razvitiya planktonnykh foraminifer v rannem Paleogene Severnogo Kavkaza: *Biulletin Moskovskogo obschestvo isputatel'ny prirody, otdel geologiya* **37**, 128-129.

- Alimarina, V. P. 1963. Nekotorye osobennosti razvitiya planktonnykh foraminifer v svyazi s zonalny ras'cheleniem nizhnogo paleogene severnogo Kavkaza: Akademiya Nauk SSSR, *Voprosy Mikropaleontologii* **7**, 158-195.
- Almoghi-Labin, A., Bein, A. & Sass, E. 1993. Late Cretaceous upwelling system along the southern Tethys margin (Israel): Interrelationship between productivity, bottom water environments, and organic matter preservation. *Paleoceanography* **8**, 671-690.
- Al-Sayigh, A. R. S. 1998. *Lower Tertiary foraminifera from South East Oman*. Unpublished PhD Thesis, University of Wales, Aberystwyth, United Kingdom.
- Archangelsky, S. 1969. Sobre el paleomicroplancton del Terciario Inferior de Rio Turbio, Provincia de Santa Cruz. *Ameghiniana* **5**, 406-416.
- Arenillas, I. & Molina, E. 1996. Biostratigrafia y evolucion de las asociaciones de foraminiferos planctonicos del transito Palaeoceno-Eoceno en Alamedilla (Cordilleras Beticas). *Revista Española de Micropaleontología* **18**, 85-98.
- Ashraf, M. & Bhatti, M. 1991. *Nannofossil biostratigraphy of the Patala and Nammal Formations from Khairabad East, western Salt Range, Pakistan*. Hydrocarbon Development Institute, Islamabad, Pakistan, Unpublished Report.
- Aubert, J. & Berggren, W. A. 1976. Paleocene benthic foraminiferal biostratigraphy and paleoecology of Tunisia. *Bulletin du Centre de Recherches Pau-SPNA* **10**, 379-469.
- Aubry, M. -P. 1995. From chronology to stratigraphy: interpreting the lower and middle Eocene stratigraphic record in the Atlantic Ocean. In: Berggren, W. A., Kent, D. V., Aubry, M. -P. and Hardenbol, J. (Eds), *Geology, Time Scales and Global Stratigraphic Correlation*. Society of Economic

Paleontologists and Mineralogists (Society for Sedimentary Geology),
Special Publication **54**, 213-274.

- Aubry, M. -P. 1998. Early Paleogene calcareous nannoplankton evolution, a tale of climatic amelioration. *In*: Aubry, M. -P., Lucas, S. G., Berggren, W. A. (Eds), *Late Paleocene-early Eocene climatic and biotic events in the marine and terrestrial records*. New York, Columbia University Press, 158-203.
- Aubry, M. -P., Cramer, B. S., Miller, K. G., Wright, J. D., Kent, D. V. and Olsson, R. K. 2000. Late Paleocene event chronology: unconformities, not diachrony. *Bulletin de la Société géologique de France* **171**, 367-378.
- Aubry, M. -P. & Ouda, K. 2003. Introduction. *In*: Ouda, K. & Aubry, M. -P. (Eds), *The upper Paleocene-lower Eocene of the Upper Nile Valley: Part 1, Stratigraphy*. *Micropaleontology* **49**, Supplement 1, ii-iv.
- Ayres, M. G., Bilal, M., Jones, R. W., Slentz, L. W., Tartir, M. & Wilson, A. O. 1982. Hydrocarbon habitat in main producing areas, Saudi Arabia. *American Association of Petroleum Geologists, Bulletin* **66**, 1-9.
- Aziz, H. A., Hilgen, F. J., Van Luijk, G. M., Sluijs, A., Kraus, M. J., Pares, J. M. & Gingerich, P. D. 2008. Astronomical climate control on paleosol stacking patterns in the upper Paleocene-lower Eocene Willwood Formation, Bighorn Basin, Wyoming. *Geology* **36**, 531-534.
- Bains, S., Corfield, R. M. & Norris, R. D. 1999. Mechanisms of climate warming at the end of the Paleocene. *Science* **285**, 724-727.
- Bains, S., Norris, R. D., Corfield, R. M. & Faul, K. L. 2000. Termination of global warmth at the Palaeocene/Eocene boundary through productivity feedback. *Nature* **407**, 171-174.
- Bains, S., Norris, R. D., Corfield, R. M., Bowen, G. J., Gingerich, P. D. & Koch,

- P. L. 2003. Marine-terrestrial linkages at the Paleocene-Eocene boundary. *In*: Wing, S., Gingerich, P. D., Schmitz, B., Thomas, E. (Eds), *Causes and Consequences of Globally Warm Climates in the Early Paleogene*. Geological Society of America, Boulder (CO), Special Paper **369**, 1-9.
- Ball, D. F. 1964. Loss-on-ignition as an estimate of organic matter and organic carbon in non-calcareous soils. *European Journal of Soil Science* **15**, 84-92.
- Banks, C. J. & Warburton, J. 1986. Passive roof duplex geometry in the frontal structure of the Kirthar and Sulaiman mountain belts, Pakistan. *Journal of Structural Geology* **8**, 229-237.
- Bé, A. W. H. & Hutson, W. H. 1977. Ecology of planktonic foraminifera and biogeographic patterns of life and fossil assemblages in the Indian Ocean. *Micropaleontology* **23**, 369-414.
- Beck, R. A., Burbank, D. W., Sercombe, W. J., Riley, G. W., Barndt, J. K., Berry, J. R., Afzal, J., Khan, A. M., Jurgen, H., Metje, J., Cheema, A., Shafique, N. A., Lawrence, R. D. & Khan, M. A. 1995. Stratigraphic evidence for an early collision between northwest India and Asia. *Nature* **373**, 55-58.
- Beckmann, J. P. 1960. Distribution of benthonic foraminifera at the Cretaceous-Tertiary boundary of Trinidad (West-Indies). *In*: Rosenkrantz, A., Brotzen, F. (Eds), *International Geological Congress. Report of the Twenty-First Session Norden. Part V: the Cretaceous-Tertiary Boundary*. Copenhagen, Det Berlingske Bogtrykkeri, 57-69.
- Bender, F. K. 1995. Tectonics and structure. *In*: Bender, F. K., Raza, H. A. & Bannert, D. (Eds), *Geology of Pakistan*. Gebruder Borntraeger, Berlin, 414 pp.

- Benedek, P. N. 1972. Phytoplanktonen aus dem Mittel- und oberoligozän von Tönisberg (Niederrheingebiet). *Palaeontographica Abteilung B* **137**, 1-71.
- Bengtsson, L. & Enell, M. 1986. Chemical analysis. In: Berglund, B. E. (Ed.), *Handbook of Holocene palaeoecology and palaeohydrology*. John Wiley and Sons, Chichester, 423-451.
- Berger, W. H. & Vincent, E. 1986. Deep-sea carbonates: reading the carbon-isotope signal. *Geologische Rundschau* **75**, 249-269.
- Berger, W. H. & Diester-Haass, L. 1988. Paleoproductivity: the benthic/planktonic ratio in foraminifera as a productivity index. *Marine Geology* **81**, 15-25.
- Berggren, W. A. 1960. Paleogene biostratigraphy and planktonic foraminifera of SW Soviet Union: an analysis of recent Soviet investigations: *Stockholm Contributions in Geology* **6**, 63-125.
- Berggren, W. A. 1969. Rates of evolution in some Cenozoic planktonic foraminifera. *Micropaleontology* **15**, 351-365.
- Berggren, W. A. 1992. Paleogene planktonic foraminiferal Magnetobiostratigraphy of the Southern Kergulen Plateau (Sites 747-749). *Proceedings of the Ocean Drilling Program, Scientific Results* **120**, 551-569.
- Berggren, W. A. & Aubert, J. 1975. Paleocene benthonic foraminiferal biostratigraphy, paleobiogeography and paleoecology of Atlantic-Tethyan regions; Midway-type fauna. *Palaeogeography, Palaeoclimatology, Palaeoecology* **18**, 73-192.
- Berggren, W. A. & Miller, K. G. 1989. Cenozoic bathyal and abyssal calcareous benthic foraminiferal zonation. *Micropaleontology* **35**, 308-320.
- Berggren, W. A., Kent, D. V., Swisher III, C. C. & Aubry, M. -P. 1995. A revised

- Cenozoic geochronology and chronostratigraphy. *In*: Berggren, W. A., Kent, D. V., Aubry, M. -P. & Hardenbol, J. (Eds), *Geochronology, Time Scales and Global Stratigraphic Correlation*. Society of Economic Paleontologists and Mineralogists, Special Publication, **54**, 129-212.
- Berggren, W. A. & Norris, R. 1997. Biostratigraphy, Phylogeny, and systematic of Paleocene planktic foraminifera. *Micropaleontology* **43** (supplement 1), 1-116.
- Berggren, W. A., Aubry, M. -P., Van Fossen, M., Kent, D. V., Norris, R. D. & Quillevere, F. 2000. Integrated Paleocene calcareous plankton magnetobiochronology and stable isotope stratigraphy: DSDP Site 384 (NW Atlantic Ocean). *Palaeogeography, Palaeoclimatology, Palaeoecology* **159**, 1-51.
- Berggren, W. A. & Ouda, K. 2003. Upper Paleocene-lower Eocene planktonic foraminiferal biostratigraphy of the dababiya section, Upper Nile Valley (Egypt). *Micropaleontology* **49** (Suppl-1), 61-92.
- Berggren, W. A., Ouda, K., Ahmed, E. A., Obaidalla, N. & Saad, K. 2003. Upper Paleocene-lower Eocene planktonic foraminiferal biostratigraphy of the Wadi Abu Ghurra section, Upper Nile Valley (Egypt). *Micropaleontology* **49** (Suppl-1), 167-178.
- Berggren, W. A. & Pearson, P. N. 2005. A revised tropical to subtropical Paleogene planktonic foraminiferal zonation. *Journal of Foraminiferal Research* **35**, 279-298.
- Bhandari, A. 2008. Ostracode biostratigraphy and carbon and oxygen isotopic studies across the Paleocene/Eocene boundary in the subsurface of Jaisalmer Basin, Rajasthan, India. *Palaeobiodiversity and Palaeoenvironments* **88**, 67-76.

- Blandford, W. T. 1876. Note on the geology of the neighbourhood of Lyngan and Runneekot, northwestern Kotrree in Sind. *Memoir of the Geological Survey of India* **20**, 229-237.
- Blandford, W. T. 1880. The geology of western Sind. *Memoir of the Geological Survey of India* **17**, 1-210.
- Blandford, W. T. 1883. Geological note on the hills in the neighbourhood of Sind and Punjab frontier between Quetta and Dera Ghazi Khan. *Memoir of the Geological Survey of India* **20**, 229-237.
- Blondeau, A. 1972. *Les Nummulites*. Vuibert, Paris, 254pp.
- Blow, W. H. 1979. *The Cainozoic Globigerinida: A Study of the Morphology, Taxonomy, Evolutionary Relationships and the Stratigraphical Distribution of Some Globigerinida (mainly Globigerinacae)*, E. J. Brill, Leiden, 3 vols, 1452pp.
- Boessenkool, K. P., Vand Gelder, M. -J., Brinkhuis, H. & Troelstra, S. R. 2001. Distribution of organic-walled dinoflagellate cysts in surface sediments from transects across the Polar Front offshore southeast Greenland. *Journal of Quaternary Science* **16**, 661-666.
- Bold, H. C. 1973. *Morphology of Plants*, Harper, New York, 668pp.
- Bolli, H. M. 1957a. The genera *Globigerina* and *Globorotalia* in the Paleocene-Lower Eocene Lizard Springs formation of Trinidad, B.W.I. *In*: Loeblich, A. R. Jr, & collaborators (Eds), *Studies in foraminifera*: Bulletin of the United States National Museum **215**, 61-82.
- Bolli, H. M. 1957b. Planktonic foraminifera from the Eocene Navet Formation and San Fernando Formations in Trinidad, B. W. I. *In*: Loeblich, A. R. Jr, & collaborators (Eds), *Studies in foraminifera*: Bulletin of the United States National Museum **215**, 155-172.

- Bolli, H. M. & Cita, M. B. 1960. Globigerine e Globorotalie del Paleocene de Paderno d'Ada (Italia). *Revista Italiana Paleontologia* **66**, 361-402.
- Bolli, H. M. 1966. Zonation of Cretaceous to Pliocene marine sediments based on planktonic foraminifera. *Boletino Informativo Association Venezolana de Geologia, Minearias Petroleo* **9**, 1-34.
- Bolli, H. M., Saunders, J. B. & Perch-Nielson, K. 1985. *Plankton Stratigraphy*. Cambridge University Press, Cambridge 1031pp.
- Bolle, M. -P., Pardo, A., Hinrichs, K. -U., Adatte, T., Von Salis, K., Burns, S., Keller, G. & Muzylev, N. 2000. The Paleocene-Eocene transition in the marginal northeastern Tethys (Kazakhstan and Uzbekistan). *International Journal of Earth Sciences* **89**, 390-414.
- Bowen, G. J., Koch, P. L., Gingerich, P. D., Norris, R. D., Bains, S. & Corfield, R. M. 2001. Refined isotope stratigraphy across the continental Paleocene-Eocene boundary on Polecat Bench in the Northern Bighorn Basin. *In: Gingerich, P. D. (Ed.), Paleocene-Eocene stratigraphy and Biotic change in the Bighorn and Clarks Fork basins, Wyoming*, The University of Michigan Papers on Paleontology **33**, 73-88.
- Bowen, G. J., Clyde, W. C., Koch, P. L., Ting, S., Alroy, J., Tsubamoto, T., Wang, Y. & Wang, Y. 2002. Mammalian dispersal at the Paleocene/Eocene boundary. *Science* **295**, 2062-2065.
- Boulter, M. C. & Manum, S. B. 1989. The Brito-Arctic Igneous Province flora around the Palaeocene/Eocene boundary. *In: Eldholm, O., Thiede, J. & Taylor, E. (Eds), Proceedings of the Ocean Drilling Program, Scientific Results*, Ocean Drilling Program, College Station, Texas, 663-680.
- Bralower, T. J. 2002. Evidence of surface water oligotrophy during the Paleocene-Eocene thermal maximum: nannofossil assemblage data from

Ocean Drilling Program Site 690, Maud Rise, Weddell Sea.

Paleoceanography **17**, 13-1—13-12.

- Bralower, T. J., Thomas, D. J., Zachos, J. C., Hirschmann, M., Röhl, U., Sigurdsson, H., Thomas, E. & Whitney, D. L. 1997. High-resolution records of the late Paleocene thermal maximum and circum-Caribbean volcanism: Is there a causal link? *Geology* **25**, 963-966.
- Brasier, M. D. 1980. *Microfossils*. George Allen & Unwin Ltd, London, 193pp.
- Brasier, M. D. 1985. Fossil indicators of nutrient levels. 1: Eutrophication and climate change. In: Bosence, D. W. J. & Allison, P. A. (Eds), *Marine Palaeoenvironmental Analysis from Fossils*, Geological Society, London, Special Publications **83**, 113-132.
- Brenner, W. 2001. Organic-walled microfossils from the central Baltic Sea, indicators of environmental change and base for ecostratigraphic correlation. *Baltica* **14**, 40-51.
- Brinkhuis, H. 1994. Late Eocene to Early Oligocene dinoflagellate cysts from the Priabonian type-area (Northeast Italy): biostratigraphy and paleoenvironmental interpretation. *Palaeogeography, Palaeoclimatology, Palaeoecology* **107**, 121-163.
- Brinkhuis, H. & Biffi, U. 1993. Dinoflagellate cyst stratigraphy of the Eocene/Oligocene transition in central Italy. *Marine Micropaleontology* **22**, 131-183.
- Brinkhuis, H., Bujak, J. P., Smit, J., Versteegh, G. J. M. & Visscher, H. 1998. Dinoflagellate-based sea surface temperature reconstructions across the Cretaceous-Tertiary boundary. *Palaeogeography, Palaeoclimatology, Palaeoecology* **141**, 67-83.
- Brinkhuis, H., Huber, M., Sluijs, A., Zachos, J. C. & Warnaar, J. 2003a. The end

of the Early Eocene Climatic Optimum: Evidence for Concomitant Cooling of Southern Ocean Surface Waters and Global Deep Waters From Dinoflagellate Endemism. *American Geophysical Union, Fall Conference, San Francisco, Abstract volume F887.*

- Brinkhuis, H., Munsterman, D. K., Sengers, S., Sluijs, A., Warnaar, J. & Williams, G. L. 2003b. Late Eocene to Quaternary dinoflagellate cysts from ODP Site 1168, off western Tasmania. *In: Exon, N. F., Kennett, J. P. & Malone, M. (Eds), Proceedings Ocean Drilling Program, Scientific Results.* Available from World Wide Web: http://www-odp.tamu.edu/publications/189_SR/105/105.htm, College Station, Texas, 1-36.
- Brotzen, F. 1948. The Swedish Paleocene and its foraminiferal fauna. *Sveriges geologiska Undersökning, Avh, Ser. C. No. 493*, 1-140, Stockholm.
- Brotzen, F. & Pozaryska, K. 1961. Foraminifères du Paléocène et de l'Éocène inférieur en Pologne septentrionalee remarques paléogéographiques. *Revue de Micropaléontologie* **4**, 155-166.
- Bujak, J. P. & Mudge, D. C. 1994. A high-resolution North Sea Eocene dinocyst zonation. *Journal of the Geological Society, London* **151**, 449-462.
- Bujak, J. P. & Brinkhuis, H. 1998. Global warming and dinocyst changes across the Paleocene/Eocene Epoch boundary. *In: Aubry, M. -P., Lucas, S. G. & Berggren, W. A. (Eds), Late Paleocene-early Eocene Climatic and Biotic Events in the Marine and Terrestrial Records.* Columbia University Press, New York, 277-295.
- Busky, E. J. 1997. Behavioral components of feeding selectivity of the heterotrophic dinoflagellate *Protoperidinium pellucidum*. *Marine Ecology Progress Series* **153**, 77-89.

- Butt, A. F. 1989. The Paleogene stratigraphy of the Kala Chitta Range, Northern Pakistan. *Acta Mineralogica Pakistanica* **3**, 97-110.
- Butt, A. F. 1991. *Ranikothalia sindensis* Zone in late Paleocene biostratigraphy. *Micropaleontology* **37**, 77-85.
- Bybell, L. M. & Self-Trail, J. M. 1993. *Calcareous Nannofossils from Paleogene deposits in the Salt Range, Pakistan*. Geological Survey of Pakistan, Project Report (IR) PK-109.2B, Unpublished.
- Canudo, J. I. & Molina, E. 1992. Planktic foraminiferal faunal turnover and bio-chronostratigraphy of the Paleocene-Eocene boundary at Zumaya (northern Spain). *Revista de la Sociedad Geológica de España* **5**, 145-157.
- Canudo, J. I., Keller, G., Molina, E. & Ortiz, N. 1995. Planktic foraminiferal turnover and $\delta^{13}\text{C}$ isotopes across the Paleocene-Eocene transition at Caravaca and Zumaya, Spain. *Palaeogeography, Palaeoclimatology, Palaeoecology* **114**, 75-100.
- Carpenter, W. B. 1850. On the microscopic structure of *Nummulina*, *Orbitolites* and *Orbitoides*. *Quarterly Journal of the Geological Society, London* **6**, 21-38.
- Carpenter, W. B., Parker, W. K. & Jones, T. R. 1862. *Introduction to the study of the foraminifera*. London, Ray Society, 319 pp., 22pls.
- Carter, H. J. 1853. Descriptions of some of the larger forms of fossilised foraminifera in Scinde: with observations on their internal structure. *Annals and Magazine of Natural History* **11**, 161-177.
- Caudri, C. M. B. 1944. The larger foraminifera from San Juan de los Morros, State of Guarico, Venezuela. *Bulletins of American Paleontology* **28**, 5-43.
- Caudri, C. M. B. 1975. Geology and paleontology of Soldado Rock, Trinidad

- (West Indies). Part 2: The larger foraminifera. *Eclogae Geologicae Helvetiae* **68**, 533-589.
- Caudri, C. M. B. 1996. The larger foraminifera of Trinidad (West Indies). *Eclogae Geologicae Helvetiae* **89**, 1137-1309.
- Charisi, S. D. & Schmitz, B. 1995. Stable ($\delta^{13}\text{C}$, $\delta^{18}\text{O}$) and strontium ($^{87}\text{Sr}/^{86}\text{Sr}$) isotopes through the Paleocene at Gebel Aweina, eastern Tethyan region. *Palaeogeography, Palaeoclimatology, Palaeoecology* **116**, 103-129.
- Charisi, S. D. & Schmitz, B. 1998. Paleocene to early Eocene paleoceanography of the Middle East: The $\delta^{13}\text{C}$ and $\delta^{18}\text{O}$ isotopes from foraminiferal calcite. *Paleoceanography* **13**, 106-118.
- de Cizancourt, M. 1938. Nummulites et Assilines du Flysch de Gardez et du Khost, Afghanistan Oriental. In: de Cizancourt, M. & Cox, L. R. (Eds), *Contribution a l'étude des faunes Tertiaires de l'Afghanistan*, Mémoires de la Société Géologique de France **39**, 1-28.
- Clyde, W. C. & Gingerich, P. D. 1998. Mammalian community response to the latest Paleocene thermal maximum: an isotaphonomic study in the northern Bighorn Basin, Wyoming. *Geology* **26**, 1011-1014.
- Coccioni, R., Angori, E., Galeotti, S., Giusberti, L., Guasti, E., Monechi, S., Sprovieri, M. & Tateo, F. 2004. The Paleocene/Eocene boundary in the Contessa Road Section (Gubbio, Central Italy): new high-resolution integrated data from a classical pelagic Tethyan setting. In: Bice, K., Aubry, M. -P. & Ouda, K. (Eds), *Climate and Biota of the Early Paleogene CBEP V*, Fifth International Conference on Global Events and reorganisation of the biosphere in the Paleocene-Eocene transition, February 8-12, Luxor, Egypt, Abstract and Program Book, C-10.

- Coccioni, R. & Luciani, V. 2004. Planktonic foraminifera and environmental changes across the Bonarelli Event (OAE2, latest Cenomanian) in its type area: a high-resolution study from the Tethyan reference Bottaccione section (Gubbio, Central Italy). *Journal of Foraminiferal Research* **34**, 109-129.
- Cole, W. S. & Herrick, S. M. 1953. Two species of larger foraminifera from Paleocene beds of Georgia. *Bulletins of American Paleontology* **35**, 6-9.
- Collinson, M. E., Hooker, J. J. & Grocke, D. R. 2003. Cobham lignite bed and penecontemporaneous macrofloras of southern England: A record of vegetation and fire across the Paleocene-Eocene Thermal Maximum. In: Wing, S., Gingerich, P. D., Schmitz, B., & Thomas, E. (Eds), *Causes and consequences of globally warm climates in the Early Paleogene*, Geological Society of America, Boulder (CO), Special Paper **369**, 333-349.
- Conrad, W. 1941. Notes protistologiques xix. Quelques microfossiles des silex crétacé. *Bulletin de Musée Royal d'Histoire Naturelle de Belgique*, Bruxelles **17**, 1-10.
- Cookson, I. C. 1953. Records of the occurrence of *Botryococcus braunii*, *Pediastrum* and the Hystrichosphaerideae in Cainozoic deposits of Australia. *Memoirs of the National Museum, Melbourne* **18**, 107-123.
- Cookson, I. C. 1965. Cretaceous and Tertiary microplankton from southeastern Australia. *Proceedings of the Royal Society of Victoria* **78**, 85-93.
- Cookson, I. C. & Eisenack, A. 1961. Tertiary microplankton from the Rottneest Island bore, Western Australia. *Journal of the Royal Society of Western Australia* **44**, 39-47.
- Cookson, I. C. & Hughes, N. F. 1964. Microplankton from the Cambridge

- Greensand (mid-Cretaceous). *Palaeontology* **7**, 37-59.
- Cookson, I. C. & Eisenack, A. 1965. Microplankton from the Dartmoor Formation, SW Victoria. *Proceedings of the Royal Society of Victoria* **79**, 133-137.
- Copeland, P. 1997. The when and where of the growth of the Himalaya and the Tibetan Plateau. In: Ruddiman, W. F. (Ed.), *Tectonic Uplift and Climate Change*, Plenum, New York, 20-40.
- Corfield, R. M., Cartlidge, J. E., Premoli-Silva, I. & Housley, R. A. 1991. Oxygen and carbon isotope stratigraphy of the Palaeogene and Cretaceous limestones in the Bottacione Gorge and the Contessa Highway sections, Umbria, Italy. *Terra Nova* **3**, 414-422.
- Corliss, B. H. & Chen, C. 1988. Morphotype patterns of Norwegian Sea deep-sea benthic foraminifera and ecological implications. *Geology* **16**, 716-719.
- Costa, L. I. & Downie, C. 1976. The distribution of the dinoflagellate *Wetzeliella* in the Palaeogene of northwestern Europe. *Palaeontology* **19**, 591-614.
- Costa, L. I. & Downie, C. 1979. The Wetzeliellaceae; Palaeogene dinoflagellates. *Proceedings of the IV international Palynological Conference*, Lucknow, (1976-77) **2**, 34-46.
- Costa, L. I. & Muller, C. 1978. Correlation of Cenozoic dinoflagellate and nannoplankton zones from the NE Atlantic and NW Europe. *Newsletters on Stratigraphy* **7**, 65-72.
- Costa, L. I., Denison, C. & Downie, C. 1978. The Paleocene/Eocene boundary in the Anglo-Paris Basin. *Journal of Geological Society, London* **135**, 261-264.
- Costa, L. I. & Manum, S. B. 1988. The description of the interregional zonation

- of the Paleogene (D1-D15) and the Miocene (D16-D20). In: Vinken, R. (Ed.), *The Northwest European Tertiary Basin*. Results of the International Geological Correlation Programme, Project No.124. Geologisches Jahrbuch, A **100**, 321-330.
- Cotter, G. D. P. 1933. The geology of the part of the Attock District west of longitude 72° 45' E. *Memoir of the Geological Survey of India* **55**, 63-161.
- Cramer, B. S., Wright, J. D., Kent, D. V. & Aubry, M. -P. 2003. Orbital climate forcing of $\delta^{13}\text{C}$ excursions in the late Paleocene-early Eocene (chrons C24n-C25n). *Paleoceanography*, **18**(4), 1097, doi: 10.1029/2003PA000909
- Cramer, B. S. & Kent, D. 2005. Bolide summer: The Paleocene/Eocene thermal maximum as a response to an extraterrestrial trigger. *Palaeogeography, Palaeoclimatology, Palaeoecology* **224**, 144-166.
- Crouch, E. M. 2001. Environmental change at the time of the Paleocene-Eocene biotic turnover. *Laboratory of Palaeobotany and Palynology Contribution Series* **14**, 216 pp.
- Crouch, E. M., Bujak, J. P. & Brinkhuis, H. 2000. Southern and Northern Hemisphere dinoflagellate cyst assemblage changes in association with the Late Paleocene thermal maximum. *Geologiska Föreningen: Stockholm, Förhandlingar* **122**, 40-41.
- Crouch, E. M., Heilmann-Clausen, C., Brinkhuis, H., Morgans, H. E. G., Rogers, K. M., Egger, H. & Schmitz, B. 2001. Global dinoflagellate event associated with the late Paleocene thermal maximum. *Geology* **29**, 315-318.
- Crouch, E. M., Dickens, G. R., Brinkhuis, H., Aubry, M. -P., Hollis, C. J., Rogers, K. M. & Visscher, H. 2003. The *Apectodinium* acme and terrestrial

- discharge during the Paleocene-Eocene thermal maximum: new palynological, geochemical and calcareous nannoplankton observations at Tawanui, New Zealand. *Palaeogeography, Palaeoclimatology, Palaeoecology* **194**, 387-403.
- Crouch, E. M. & Brinkhuis, H. 2005. Environmental change across the Paleocene-Eocene transition from eastern New Zealand: A marine palynological approach. *Marine Micropaleontology* **56**, 138-160.
- Cushman, J. A. 1925. Some new foraminifera from the Velasco Shale of Mexico. *Contributions from the Cushman Laboratory for Foraminiferal Research* **1**, 18-23.
- Cushman, J. A. 1926. The Foraminifera of the Velasco shale of the Tampico embayment San Luis Potosi, Mexico. *American Association of Petroleum Geologists, Bulletin* **10**, 581-612.
- Cushman, J. A. 1927. New and interesting foraminifera from Mexico and Texas. *Contributions from the Cushman Laboratory for Foraminiferal Research* **3**, 111-117.
- Cushman, J. A. & Renz, H. H. 1942. Eocene, Midway, foraminifera from Soldado Rock, Trinidad. *Contributions from the Cushman Laboratory for Foraminiferal Research* **18**, 1-20.
- Dale, B. 1996. Dinoflagellate cyst ecology: Modeling and geological applications. *In: Jansonius, J. & McGregor, D. C. (Eds), Palynology: Principles and Applications*, American Association of Stratigraphic Palynologists Foundation, Dallas, 1249-1276.
- Dale, B. 2001. The sedimentary record of dinoflagellate cysts: looking back into the future of phytoplankton blooms. *Scientia Marina* **65**, 257-272.
- Dale, B. & Fjellså, A. 1994. Dinoflagellate cysts as paleoproductivity indicators:

- state of the art, potential and limits. *In*: Zahn, R., Pedersen, T. F., Kaminski, M. A. & Labeyrie, L. (Eds), *Carbon Cycling in the Glacial Ocean: Constraints on the Ocean's Role in Global Change*. Springer-Verlag, Berlin, 521-537.
- Danilchik, W. & Shah, S. M. I. 1987. Stratigraphy and coal resources of the Makarwal area, Trans-Indus Mountains, Mianwali District, Pakistan. *United States Geological Survey, Professional Paper 1341*, 1-38.
- D' Archiac, A. & Haime, J. 1853. *Description des animaux fossiles du groupe nummulitique de l'Inde, Précédé d'une résumé géologique et d'une monographie des Nummulites*. Gide & J. Baudry, Paris.
- Davey, R. J., Downie, C., Sarjeant, W. A. S. & Williams, G. L. 1966. Studies on Mesozoic and Cainozoic dinoflagellate cysts. *Bulletin of the British Museum of Natural History, London (Geology Supplement) 3*, 248pp.
- Davey, R. J. & Williams, G. L. 1966. The genus *Hystrichosphaeridium* and its allies. *In*: Davey, R. J., Downie, C., Sarjeant, W. A. S. & Williams, G. L. Studies on Mesozoic and Cainozoic dinoflagellate cysts. *Bulletin of the British Museum of Natural History, London (Geology Supplement) 3*, 53-106.
- Davey, R. J. & Williams, G. L. 1969. Generic reallocations. *In*: Davey, R. J., Downie, C., Sarjeant, W. A. S. & Williams G. L. (Eds), *Appendix to "Studies on Mesozoic and Cainozoic dinoflagellate cysts"* Bulletin of the British Museum of Natural History, London (Geology Supplement) 3, Appendix: 4-7.
- Davies, L. M. 1927. The Ranikot beds at Thal (North-West Frontier Ranges of India). *Quarterly Journal of the Geological Society, London 83*, 260-290.
- Davies, L. M. 1930. The fossil fauna of the Samana Range and some

- neighbouring areas, the Paleocene foraminifera. *Memoirs of the Geological Survey of India, Palaeontologia Indica* **15**, 67-79.
- Davies, L. M. 1932. The genera *Dictyoconoides* Nuttall, *Lockhartia* nov. and *Rotalia* Lamarck, Their type species, generic differences and fundamental distinction from the *Dictyoconus* group of Forams. *Transactions of the Royal Society of Edinburgh* **57**, 397-428.
- Davies, L. M. 1935. The Eocene Beds of Punjab Salt Range. *Nature* **135**, 188-188.
- Davies, L. M. 1939. Geographical changes in the northwestern India during late Cretaceous and early Tertiary times. *Proceedings of the Sixth Pacific Science Congress of the Pacific Science Association*, 483-501.
- Davies, L. M. & Pinfold, E. S. 1937. The Eocene beds of the Punjab Salt Range. *Memoir of the Geological Survey of India* **24**, 1-79.
- Davis, D. M. & Lillie, R. J. 1994. Changing mechanical response during continental collision: active examples from the foreland thrust belts of Pakistan. *Journal of Structure Geology* **16**, 21-34.
- Dean, W. E. 1974. Determination of carbonate and organic matter in calcareous sediments and sedimentary rocks by loss on ignition: comparison with other methods. *Journal of Sedimentary Petrology* **44**, 242-248.
- Deflandre, G. 1935. Considérations biologiques sur les microorganismes d'origine planctonique conservés dans les silex de la craie. *Bulletin Biologique de la France et de la Belgique, Paris* **69**, 213-244.
- Deflandre, G. 1937. Microfossiles des silex Crétacés. II. Flagellés incertae sedis Hystrichosphaeridés. Sarcodinés. Organismes divers. *Annals Paléontologie* **26**, 51-103.
- Deflandre, G. 1947. Sur quelques microorganismes planctoniques des silex

- Jurassiques. *Bulletin de l'Institut Océanographique de Monaco* **921**, 1-10.
- Deflandre, G. 1952. Protozoes. Généralités. In: Piveteau, J. (Ed.), *Traité de Paléontologie*, Masson, Paris, 89-130.
- Deflandre, G. & Cookson, I. C. 1955. Fossil microplankton from Australian Late Mesozoic and Tertiary sediments. *Australian Journal of Marine and Freshwater Research*, Melbourne **6**, 242-313.
- De Graciansky, P. -C., Hardenbo, J., Jacquin, T. & Vail, P. R. (Eds). 1998. Mesozoic and Cenozoic stratigraphy of European basins. *Society of Economy Paleontologists and Mineralogists (Society of Sedimentary Geology) Special Publication* **60**, 1-786.
- Devillers, R. & DeVernal, A. 2000. Distribution of dinoflagellate cysts in surface sediments of the northern North Atlantic in relation to nutrient content and productivity in surface waters. *Marine Geology* **166**, 103-124.
- Dickens, G. R. 2000. Methane oxidation during the late Palaeocene thermal maximum. *Bulletin de la Société géologique de France* **171**, 37-49.
- Dickens, G. R., O'Neil, J. R., Rea, D. K. & Owen, R. M. 1995. Dissociation of oceanic methane hydrate as a cause of the carbon isotope excursion at the end of the Paleocene. *Paleoceanography* **10**, 965-971.
- Domingo, L., López-Martínez, N., Leng, M. J. & Grimes, S. T. 2009. The Paleocene-Eocene Thermal Maximum record in the organic matter of the Claret and Tendryu continental sections (South-central Pyrenees, Lleida, Spain). *Earth and Planetary Science Letters* **281**, 226-237.
- D'Orbigny, A. 1826. Tableau méthodique de la classe des Céphalopodes. *Annals des Sciences Naturelles* **7**, 245-314.
- Dorreen, J. M. 1974. The Western Gaj River section, Pakistan and Cretaceous-Tertiary boundary. *Micropaleontology* **20**, 178-193.

- Downie, C., Hussain, M. A. & Williams, G. L. 1971. Dinoflagellate cyst and acritarch associations in the Palaeogene of southeast England. *Geoscience and Man* **3**, 29-35.
- Downie, C. & Sarjeant, W. A. S. 1963. On the interpretation and status of some hystichosphere genera. *Palaeontology*, London **6**, 83-96.
- Drobne, K. 1975. *Hottingerina lukasi* n. gen., n. sp. (Foraminiferida) iz srednjega paleocena v severozahodni jugoslaviji. *Radzprave* **18**, 242-253.
- Drooger, C. W. 1960. Some early rotaliid foraminifera. *Proceedings, Koninklijke Nederlandse Akademie van Wetenschappen (Section B)* **63**, 287-334.
- Dunham, R. J. 1962. Classification of carbonate rocks according to depositional texture. *Memoirs of the American Association of Petroleum Geologists* **1**, 108-121, pls 1-7.
- Dupuis, C., Aubry, M. -P., Steurbaut, E., Berggren, W. A., Ouda, K., Magioncalda, R., Cramer, B. S., Kent, D. V., Speijer, R. P. & Heilmann-Clausen, C. 2003. The Dababiya Quarry Section: Lithostratigraphy, clay mineralogy, geochemistry and Paleontology. *Micropaleontology* **49**, Suppl. 1, 41-59.
- Eames, F. E. 1952a. A contribution to the study of the Eocene in western Pakistan and western India: A. The geology of standard sections in the western Punjab and in the Kohat District. *Quarterly Journal of the Geological Society, London* **107**, 159-171.
- Eames, F. E. 1952b. A contribution to the study of the Eocene in western Pakistan and western India: D. Discussion of the faunas of certain standard sections, and their bearing on the classification and correlation of the Eocene in western Pakistan and western India. *Quarterly Journal*

of the Geological Society, London **107**, 173-200.

- Edwards, L. E. 1989. Dinoflagellate Cysts from the Lower Tertiary Formations, Haynesville Cores, Richmond County, Virginia, Geology and Paleontology of the Haynesville Cores-Northeastern Virginia Coastal Plain. *United States Geological Survey, Professional Paper 1489-C*, 23 pp.
- Edwards, L.E. 1996. Graphic correlation of the Marlboro Clay and Nanjemoy Formation (Uppermost Paleocene and Lower Eocene) of Virginia and Maryland. In: Jansonius, J. & McGregor, D.C. (Eds), *Palynology: Principles and Applications: Salt Lake City*, American Association of Stratigraphic Palynologists Foundation, **3**, 989-999 and Appendix 1, 1004-1005.
- Edwards, L.E. 2007. Paleocene and Eocene dinocysts from the Salt Range, Punjab, northern Pakistan. In: Warwick, P.D. & Wardlaw, B.R. (Eds), *Regional studies of the Potwar Plateau area, northern Pakistan*, United States Geological Survey Bulletin **2078**, p. C1-C10, fossil pls. C1, C2.
- Ehrenberg, C. G. 1838. Über das Massenverhältniss der jetzt lebenden kiesel-Infusorien und über ein neues Infusorien-Conglomerat als Polirschiefer von Jastraba in Ungarn. *Abhandlungen der königlichen Akademie der Wissenschaften zu Berlin* **1836**, 109-135.
- Eisenack, A. 1954. Mikrofossilien aus Phosphoriten des sàmlandischen Unteroligozàns und über die Einheitlichkeit der Hystrichospaerideen. *Palaeontographica*, Stuttgart, (A) **105**, 49-95.
- Eisenack, A. 1961. Einige Erörterungen über fossile Dinoflagellaten nebst Übersicht über die zur Zeit bekannten Gattungen. *Neues Jahrbuch für Geologie und Paläontologie, Abhandlungen* **112**, 281-324.

- Eisenack, A. & Gocht, H. 1960. Neue Namen für einige Hytrichosphären der Bernsteinformation Ostpreussens. *Neues Jahrbuch für Geologie und Paläontologie, Monatshefte*, 511-518.
- El-Dawy, M. H. 2001. Paleocene benthic foraminiferal biostratigraphy and paleobathymetry in the sections between El Sheikh Fadl and Ras Gharib, Eastern Desert, Egypt. *Micropaleontology* **41**, 23-46.
- El Kammar, A. M. & El Kammar (Jr), M. M. 1996. Potentiality of chemical weathering under arid conditions of black shales from Egypt. *Journal of Arid Environments* **33**, 179-199.
- Ellegaard, M. 2000. Variations in dinoflagellate cyst morphology under conditions of changing salinity during the last 2000 years in the Limfjord, Denmark. *Review of Palaeobotany and Palynology* **109**, 65-81.
- Ernst, S. R., Guasti, E., Dupuis, C. & Speijer, R. P. 2006. Environmental perturbation in the southern Tethys across the Paleocene/Eocene boundary (Dababiya, Egypt): Foraminiferal and clay mineral records. *Marine Micropaleontology* **60**, 89-111.
- Eshet, Y., Almogi-Labin, A. & Bein, A. 1994. Dinoflagellate cysts, paleoproductivity and upwelling systems: A Late Cretaceous example from Israel. *Marine Micropaleontology* **23**, 231-240.
- Evitt, W. R. 1963. A discussion and proposals concerning fossil dinoflagellates, hystichospheres, and acritarchs, I. *Proceedings of the National Academy of Sciences of the United States of America* **49**, 158-164.
- Evitt, W. R. 1985. Sporopollenin dinoflagellate cysts: their morphology and interpretation. *American Association of Stratigraphic Palynologists Foundation*, Dallas, USA, 333pp.
- Fairbanks, R. G., Wiebe, P. H. & Be, A. W. H. 1980. Vertical distribution and

- isotope composition of living planktonic foraminifera in the western North Atlantic. *Science* **207**, 61-63.
- Farley, K. A. & Eltgroth, S. F. 2003. An alternative age model for the Paleocene-Eocene thermal maximum using extraterrestrial (super 3) He. *Earth and Planetary Science Letters* **208**, 135-148.
- Fatmi, A. N. 1974. Lithostratigraphic units of the Kohat-Potwar Range, Indus Basin, Pakistan. *Memoirs of the Geological Survey of Pakistan* **10**, 1-80.
- Fensome, R. A., Taylor, F. J. R., Norris, G., Sarjeant, W. A. S., Wharton, D. I. & Williams, G. L. 1993. A Classification of Fossil and Living Dinoflagellates. *Micropaleontology, Special Publication* **7**, 351 pp.
- Fensome, R. A., Gocht, H. & Williams, G. L. 1996a. *The Eisenack Catalog of Fossil Dinoflagellates Volume 4*. E. Schweizerbart'sche Verlagsbuchhandlung, Stuttgart, Germany, 2009-2548.
- Fensome, R. A., Riding, J. B. & Taylor, F. J. R. 1996b. Dinoflagellates. In: Jansonius, J. & McGregor, D. C. (Eds), *Palynology: principles and applications*. American Association of Stratigraphic Palynologists Foundation, 107-169.
- Fermor, L. L. 1935. General Report of the Geological Survey of India for the year 1934. *Records of the Geological Survey of India* **69**, 1-108.
- Fisher, J. K. 2006. *A foraminiferal and stable isotope investigation of the Cenomanian-Turonian extinction and oceanic anoxic event*. Unpublished PhD Thesis, University of Plymouth, UK.
- Folk, R. L. 1959. Practical petrographic classification of limestones. *American Association of Petroleum Geologists, Bulletin* **43**, 1-38.
- Fornaciari, E., Giusberti, L., Luciani, V., Tateo, F., Agnini, C., Backman, J., Oddone, M. & Rio, D. 2007. An expanded Cretaceous/Tertiary transition

- in a pelagic setting of the Southern Alps (central-western Tethys).
Palaeogeography, Palaeoclimatology, Palaeoecology **255**, 98-131.
- Galeotti, S., Angori, E., Coccioni, R., Ferrari, G., Galbrun, B., Monechi, S.,
Premoli-Silva, I., Speijer, R. P. & Turf, B. 2000. Intergrated stratigraphy
across the Paleocene/Eocene boundary in the Contessa Road section,
Gubbio (central Italy). *Bulletin de la Société géologique de France* **171**,
355-365.
- Galeotti, S., Kaminski, M. A., Coccioni, R. & Speijer, R. P. 2004. High resolution
deep water Agglutinated Foraminiferal record across the
Paleocene/Eocene transition in the Contessa Road section (Central Italy).
*In: Bubik, M. & Kaminski, M. A. (Eds), Proceedings of the Sixth
International Workshop on Agglutinated Foraminifera*, Grzybowski
Foundation, Special Publication **8**, 83-103.
- Galloway, J. J. 1928. A revision of the Family Orbitoididae. *Journal of
Paleontology* **2**, 45-69.
- Gavrilov, Y. O., Kodina, L. A., Lubchenko, I. Y. & Muzylev, N. G. 1997. The late
Paleocene anoxic event in epicontinental seas of peri-Tethys and
formation of the sapropelite unit: Sedimentology and geochemistry.
Lithology and Mineral Resources **32**, 427-514.
- Gee, E. R. & Gee, D. G. 1989. Overview of the geology and structure of the Salt
Range, with observations on related areas of northern Pakistan, *In:*
Malinconico, L. L. & Lille, R. J. (Eds), *Tectonics of the Western
Himalayas*, Geological Society of America, Special Publication **232**, 95-
112.
- Gerlach, E. 1961. Mikrofossilien aus dem Oligozän und Miozän
Nordwestdeutschlands, unter besonderer Berücksichtigung der

- Hystriosphærideen und Dinoflagellaten. *Neues Jahrbuch für Geologie und Paläontologie, Abhandlungen* **112**, 143-228.
- Gibson, T. G. 1989. Planktonic benthonic foraminiferal ratios: Modern pattern and Tertiary applicability. *Marine Micropaleontology* **15**, 29-52.
- Gibson, T. G. 1990. Upper Paleocene foraminiferal biostratigraphy and paleoenvironments of the Salt Range, Punjab, Pakistan. *United States Geological Survey, Bulletin* **2078**, 1-13.
- Gill, W. D. 1952. Facies and fauna in the Bhadar Beds of the Punjab Salt Range, Pakistan. *Journal of Paleontology* **27**, 824-844.
- Gill, W. D. 1953. The genus *Assilina* in Laki Series (Lower Eocene) of the Kohat-Potwar Basin, Northwest Pakistan. *Contributions from the Cushman Foundation for Foraminiferal Research* **4**, 76-84.
- Gingerich, P. D. 1989. New earliest Wasatchian mammalian fauna from the Eocene of northwestern Wyoming: composition and diversity in a rarely sampled high-floodplain assemblage. *Museum of Paleontology, the University of Michigan, Papers in Paleontology* **28**, 1-97.
- Gingerich, P. D. 2001. Biostratigraphy of the continental Paleocene-Eocene boundary interval on Polecat Bench in the northern Bighorn Basin. In: Gingerich, P. D. (Ed.), *Paleocene-Eocene Stratigraphy and Biotic Change in the Bighorn and Clarks Fork Basins, Wyoming*, University of Michigan Papers on Paleontology **33**, 37-72.
- Giresbach, C. L. 1893. On the geology of the country between the Chappar Rift and Harnai in Baluchistan. *Records of the Geological Survey of India* **26**, 113-147.
- Giusberti, L., Coccioni, R., Sprovieri, M. & Tateo, F. 2008. Perturbation at the sea floor during the Paleocene-Eocene Thermal Maximum: Evidence

- from benthic foraminifera at Contessa Road, Italy. *Marine Micropaleontology* **70**, 102-119.
- Glaessner, M. F. 1934. Stratigraphy of the Lower Palaeogene of the northern and eastern Caucasus in the light of microfossil studies: *Trudy Inf. sbornik neftyanogo geologo-razvedochnogo instituta (NIGRI)* **4**, 110-129 (In Russian).
- Glaessner, M. F. 1937a. Planktonische Foraminiferen aus der Kreide und dem Eozan und ihre stratigraphische Bedeutung: Studies in Micropaleontology, *Publications of the Laboratory of Paleontology, Moscow University* **1**, 27-52.
- Glaessner, M. F. 1937b. Studien über Foraminiferen aus der Kreide und dem Tertiär des Kaukasus: Problems in Paleontology, *Publications of the Laboratory of Paleontology, University of Moscow* **2**, 349-408.
- Gradstein, F. M., Kristiansen, I. L., Loemo, L. & Kaminski, M. A. 1992. Cenozoic foraminiferal and dinoflagellate cyst biostratigraphy of the central North Sea. *Micropaleontology* **38**, 101-137.
- Gradstein, F. M. and Ogg, J. G. 2004. Geologic Time Scale 2004 why, how, and where next! *Lethaia* **37**, 175-181.
- Gradstein, F., Ogg, J. G. & Smith, A. G. (Eds). 2004. *A Geologic Time Scale*. Cambridge University Press, Cambridge, 610pp.
- Grimsdale, T. F & Van Morkhoven, F. P. C. M. 1955. The ratio between pelagic and benthonic foraminifera as a means of estimating depth of deposition of sedimentary rocks. *Proceedings of the 4th World Petroleum Congress, 1955, Rome, sec. I/D* **4**, 473-491.
- Grøsfjeld, K., Larsen, E., Sejrup, H. -P., de Vernal, A., Flatebf, T., Vestbf, M., Hafliðason, H. & Aarseth, I. 1999. Dinoflagellate cysts reflecting surface-

- water conditions in Voldafjorden, western Norway during the last 11 300 years. *Boreas* **28**, 403-415.
- Guasti, E. & Speijer, R. P. 2007. The Paleocene-Eocene Thermal Maximum in Egypt and Jordan: An overview of the planktic foraminiferal record. *In*: Monechi, S., Coccioni, R. & Rampino, M. R. (Eds), *Large Ecosystem Perturbations: Causes and Consequences*, Geological Society of America, Special Paper **424**, 53-67.
- Guasti, E. & Speijer, R. P. 2008. *Acarinina muticamerata* n. sp. (Foraminifera): a new marker for the Paleocene-Eocene thermal maximum. *Journal of Micropaleontology* **27**, 5-12.
- Gümbel, C. W. 1870. Beiträge zur foraminiferenfauna der nordalpinen, älteren Eocängebilde oder den kressenberger Nummulitenschichte. *Abhandlungen des königlichen, Bayerischen, Akademik der Wissenschaften.*, (1868) 10(2), 581-730.
- Haque, A. F. M. M. 1956. The smaller foraminifera of the Ranikot and the Laki of the Nammal Gorge, Salt Range. *Memoirs of the Geological Survey of Pakistan, Paleontologia Pakistanica* **1**, 1-300.
- Haque, A. F. M. 1959. The smaller foraminifera of the Meting Limestone (Lower Eocene) Meting, Hyderabad Division, West Pakistan. *Memoirs of the Geological Survey of Pakistan, Paleontologia Pakistanica* **2**, 1-43.
- Hardenbol, J. 1994. Sequence stratigraphic calibration of Paleocene and lower Eocene continental margin deposits in NW Europe and the US Gulf Coast with the oceanic chronostratigraphic record. *Geologiska Föreningens Förhandlingar*, Meeting Proceedings "Stratigraphy of the Paleocene" **116**, 49-51.
- Harland, R. 1973. Dinoflagellate cysts and acritarchs from the Bearpaw

Formation (Upper Campanian) of southern Alberta, Canada.

Palaeontology **16**, 665-706.

Harland, R. 1983. Distribution maps of recent dinoflagellate in bottom sediments from the North Atlantic Ocean and adjacent seas. *Palaeontology* **26**, 321-387.

Harland, R. & Long, D. 1996. A Holocene dinoflagellate cyst record from offshore North-east England. *Proceedings of the Yorkshire Geological Society* **51**, 65-74.

Hart, M. B. 1999. The evolution and biodiversity of Cretaceous planktonic Foraminifera. Evolution et diversité des Foraminifera planctoniques du Crétacé. *Geobios* **32**, 247-255.

Hart, M. B. & Bailey, H. M. 1979. The distribution of planktonic Foraminifera in the mid-Cretaceous of N. W. Europe, *Aspekte der Kreie Europas, IUGS., Ser. A* **6**, 527-542.

Hasegawa, T., Pratt, L. M., Maeda, H., Shigeta, Y., Okamoto, T., Kase, T. & Uemura, K. 2004. Upper Cretaceous stable carbon-isotope stratigraphy of terrestrial organic matter from Sakhalin, Russian Far East: a proxy for the isotopic composition of paleoatmospheric CO₂. *Palaeogeography, Palaeoclimatology, Palaeoecology* **189**, 97-115.

Haynes, J. R. 1988. Massively cordate nummulitids (Foraminifera) at the Paleocene/Eocene boundary in Tethys. *Indian Journal of Geology* **60**, 215-230.

Haynes, J. R., Racey, A. & Whittaker, J. E. 2010. A revision of the early Palaeogene *nummulitids* (Foraminifera) from northern Oman, with implications for their classification. In: Whittaker, J. E. & Hart, M. B. (Eds), *Micropalaeontology, Sedimentary Environments and Stratigraphy: A*

- tribute to Dennis Curry (1912-2001)*. The Micropalaeontological Society, Special Publications, 29-89. DOI: 10.1144/TMS004.4.
- Heilmann-Clausen, C. 1985. Dinoflagellate stratigraphy of the uppermost Danian to Ypresian in the Viborg 1 borehole, central Jylland, Denmark. *Denmarks Geologiske Undersøgelse II.Række* **7**, 1-69.
- Heilmann-Clausen, C. & Egger, H. 2000. The Anthering outcrop (Austria), a key-section for correlation between Tethys and Northwestern Europe near the Paleocene/Eocene boundary. *In*: Schmitz, B., Sundquist, B. & Andreasson, F. P. (Eds), *Early Paleogene Warm Climates and Biosphere Dynamics*. GFF (Geologiska Föreningen: Stockholm, Förhandlingar), Geological Society of Sweden, Uppsala **122**, 69pp.
- Hemleben, C., Spindler, M. & Anderson, O. R. 1989. *Modern planktonic foraminifera*, Springer-Verlag, Berlin, 363pp.
- Hemphil, W. R. & Kidwai, A. H. 1973. Stratigraphy of the Banu and Dera Ismail Khan areas, Pakistan. *United States Geological Survey Professional Paper* **716-B**, 1-36.
- Herguera, J. C. 1992. Deep-sea benthic foraminifera and biogenic opal; glacial to postglacial productivity changes in the western Equatorial Pacific. *Marine Micropaleontology* **19**, 79-98.
- Higgins, J. A. & Schrag, D. P. 2006. Beyond methane: towards a theory for the Paleocene-Eocene thermal maximum. *Earth and Planetary Science Letters* **245**, 523-537.
- von Hillebrandt, A. 1962. Das Paläozän und seine Foraminiferenfauna im Becken von Reichenhall und Salzburg. *Bayerischen Akademie der Wissenschaften, Mathematisch-Naturwissenschaftliche Klasse, Abhandlungen* **108**, 1-182.

- von Hillebrandt, A. 1975. Correlation entre les biozones de grands foraminifères planctoniques de l'Ilerdien. *Bulletin de la Société géologique de France* **17**, 162-167.
- Horner, R. A. 1985. *Sea ice biota*. CRC Press, Boca Raton, Florida (USA), 215pp.
- Hottinger, L. 1960. Recherches sur les Alveolines du Paleocene et de l'Eocene. *Schwizerische Palaeontologische Abhandlungen* **75/76**, 1-243.
- Hottinger, L. 1982. Larger Foraminifera, giant cells with a historical background. *Naturwissenschaften* **69**, 361-371.
- Hottinger, L. 1983. Processes determining the distribution of larger foraminifera in space and time. *Utrecht Micropaleontological Bulletins* **30**, 239-253.
- Hottinger, L. 1998. Shallow benthic foraminifera at the Paleocene-Eocene boundary. *Strata* **9**, 61-64.
- Hottinger, L. 2001. Learning from the Past? In: Box, E. & Pignati, J. (Eds), *The living world, Part Two: Discovery and Spoliation of the Biosphere*, San Diego, Academic Press **4**, 449-477.
- Hottinger, L. 2009. The Paleocene and earliest Eocene foraminiferal Family Miscellaneidae: neither nummulitids nor rotaliids. Carnets de Géologie/Notebooks on Geology, Brest, Article 2009/06 (CG2009_a06).
- Hottinger, L. & Schaub, H. 1960. Zur Stufeneinteilung des Paleocaens und des Eocaens. Einführung der Stufen Ilerdian und Biarritzien. *Eclogae Geologicae Helveticae, Basel* **53**, 453-480.
- Huber, B. T. 1991. Paleocene and early Neogene planktonic foraminifer biostratigraphy of Sites 738 and 744, Kerguelen Plateau (Southern Indian Ocean). *Proceedings of the Ocean Drilling Program, Scientific Results* **114**, 281-298.

- Huber, M., Brinkhuis, H., Stickley, C. E., Döös, K., Sluijs, A., Warnaar, J., Schellenberg, S. A. & Williams, G. L. 2004. Eocene circulation of the Southern Ocean: Was Antarctica kept warm by subtropical waters? *Paleoceanography* **19**(4), doi: 10.1029/2004PA001014.
- Humayon, M., Lillie, R. J. & Lawrence, R. D. 1991. Structural interpretations of the eastern Sulaiman fold belt and foredeep, Pakistan. *Tectonics* **10**, 299-324.
- Hunting Survey Corporation Ltd. 1961. *Reconnaissance geology of part of west Pakistan, a Colombo Plan Cooperative Project*. A report published for Government of Pakistan by Government of Canada. Maracle Press, Toronto, 1-550.
- Iakovleva, A. I., Oreshkina, T. V., Alekseev, A. S. & Rousseau, D. -D. 2000. A new Paleogene micropaleontological and palaeogeographical data in the Petchora Depression, northeastern European Russia. *Comptes Rendus de l'Académie des Sciences-Séries IIA. Earth and Planetary Science* **330**, 485-491.
- Iakovleva, A. I., Brinkhuis, H. & Cavagnetto, C. 2001. Late Palaeocene-Early Eocene dinoflagellate cysts from the Turgay Strait, Kazakhstan; correlations across ancient seaways. *Palaeogeography, Palaeoclimatology, Palaeoecology* **172**, 243-268.
- Iakovleva, A. I. & Kulkova, I. A. 2003. Paleocene-Eocene dinoflagellate zonation of Western Siberia. *Review of Palaeobotany and Palynology* **123**, 185-197.
- Ingle (Jr.), J. C. 1980. Cenozoic paleobathymetry and depositional history of selected sequences within the southern California continental borderland. *Cushman Foundation for Foraminiferal Research, Special Publication* **19**, 163-195.

- Islam, M. A. 1983. Dinoflagellate cyst taxonomy and biostratigraphy of the Eocene Bracklesham Group in southern England. *Micropaleontology* **29**, 328-353.
- Jadoon, I. A. K. 1991. The style and evolution of foreland structures: An example from Sulaiman lobe, Pakistan. *Pakistan Journal of Hydrocarbon Resources* **3**, 1-17.
- Jadoon, I. A. K. 1992. Oceanic/Continental transitional crust underneath the Sulaiman thrust lobe and evolutionary tectonic model for the Indian/Afghan collision zone. *Pakistan Journal of Hydrocarbon Resources* **4**, 33-44.
- Jadoon, I. A. K., Lawrence, R. D. & Lillie, R. J. 1992. Balanced and retrodeformed geological cross-section from the frontal Sulaiman Lobe, Pakistan: Duplex development in thick strata along the western margin of the Indian Plate. In: McClay, K. (Ed.), *Thrust Tectonics*, Chapman and Hall, London, 343-357.
- Jadoon, I. A. K., Lawrence, R. D. & Khan, S. H. 1993. Mari-Bugti pop-up zone in the central Sulaiman fold belt, Pakistan. *Journal of Structural Geology* **16**, 147-158.
- Jahren, A. H., Arens, N. C., Sarmiento, G., Guerrero, J. & Amundson, R. 2001. Terrestrial record of methane hydrate dissociation in the Early Cretaceous. *Geology* **29**, 159-162.
- Jamilddin, A., Hussain, T. & Memon, A. R. 1971. Geological map of Sind 35 1/1; Khuzdar district, Baluchistan, Sheet No. 251, Scale 1: 50, 000. *Geological Survey of Pakistan Map Series*, Quetta, **2**.
- Jan du Chêne, R. E. & Adediran, S. A. 1984. Late Paleocene to early Eocene dinoflagellates from Nigeria. *Cahiers de Micropaléontologie* **3**, 1-88.

- Jones, R. W. 1997. Aspect of the Cenozoic stratigraphy of the Northern Sulaiman Ranges, Pakistan. *Journal of Micropaleontology* **16**, 51-58.
- Kadri, I. B. 1995. *Petroleum Geology of Pakistan*. Pakistan Petroleum Limited, Karachi, 275pp.
- Kaiho, K., Arinobu, T., Ishiwatari, R., Morgans, H. E. G., Okada, H., Takeda, N., Tazaki, K., Zhou, G., Kajiwara, Y., Matsumoto, R., Hirai, A., Niitsuma, N. & Wada, H. 1996. Latest Paleocene benthic foraminiferal extinction and environmental change at Tawanui, New Zealand. *Paleoceanography* **11**, 447-465.
- Kalia, P. & Kintso, R. 2006. Planktonic foraminifera at the Paleocene/Eocene boundary in the Jaisalmer Basin, Rajasthan, India. *Micropaleontology* **52**, 521-536.
- Kaminski, M. A., Gradstein, F. M. & Berggren, W. A. 1989. Paleogene benthic foraminiferal stratigraphy and paleoecology at Site 647, southern Labrador Sea. *Proceedings of the Ocean Drilling Program, Scientific Results* **105**, 705-730.
- Kaminski, M. A., Kuhnt, W. & Radley, J. D. 1996. Palaeocene-Eocene deep water agglutinated foraminifera from the Numidian Flysch (Rif, Northern Morocco): their significance for the Palaeoceanography of the Gibraltar Gateway. *Journal of Micropalaeontology* **15**, 1-19.
- Kapellos, C. & Schaub, H. 1973. Zur Korrelation von Biozonierungen mit Gross foraminifera und Nannoplankton im Paläogen der Pyrenäen. *Eclogae Geologicae Helveticae, Basel* **53**, 454-479.
- Katz, M. E., Pak, D. K., Dickens, G. R. & Miller, K. G. 1999. The source and fate of massive carbon input during the latest Paleocene thermal maximum. *Science* **286**, 1531-1533.

- Katz, M. E., Cramer, B. S., Mountain, G. S., Katz, S. & Miller, K. G. 2001. Uncorking the bottle: What triggered the Paleocene/Eocene thermal maximum methane release? *Paleoceanography* **16**, 549-562.
- Kazmi, A. H. 1988. Stratigraphy of the Dungan Group in Kach-Ziarat area, northeast Baluchistan. *Geological Bulletin University of Peshawar* **21**, 117-130.
- Kazmi, A. H. 1995. Sedimentary sequence. In: Bender, F. K. & Raza, H. A. (Eds), *Geology of Pakistan*, Gebruder Borntraeger, Berlin, 414pp.
- Keijzer, F. G. 1945. *Outline of the geology of the eastern part of the province of Oriente, Cuba with notes on the geology of other parts of the Island*. Unpublished PhD Thesis, University of Utrecht, Netherlands, 1-239.
- Keller, G. 2002. *Guembelitra*-dominated late Maastrichtian planktic foraminiferal assemblages mimic early Danian in central Egypt. *Marine Micropaleontology* **47**, 71-100.
- Keller, G. & Pardo, A. 2004. Age and paleoenvironment of the Cenomanian-Turonian global stratotype section and point at Pueblo, Colorado. *Marine Micropaleontology* **51**, 95-128.
- Kelly, D. C., Bralower, T. J., Zachos, J. C., Premoli-Silva, I. & Thomas, E. 1996. Rapid diversification of planktonic foraminifera in the tropical Pacific (ODP Site 865) during the late Paleocene thermal maximum. *Geology* **24**, 423-426.
- Kennett, J. P. & Stott, L. D. 1990. Proteus and Proto-oceanus: Ancestral Paleogene oceans as revealed from Antarctic stable isotopic results; ODP leg 1131. In: Barker, P. F., Kennett, J. P., et al. (Eds), *Proceedings of the Ocean Drilling Program, Scientific Results* **113**, 865-880.
- Kennett, J. P. & Stott, L. D. 1991. Abrupt deep-sea warming,

- palaeoceanographic changes and benthic extinctions at the end of the Palaeocene. *Nature* **353**, 225-229.
- Kent, D. V., Cramer, B. S., Lanci, L., Wang, D., Wright, J. D. & Van der Voo, R. 2003. A case for a comet impact trigger for the Paleocene/Eocene thermal maximum and carbon isotope excursion. *Earth and Planetary Science Letters* **211**, 13-26.
- Klump, B. 1953. Beitrag zur Kenntnis der Mikrofossilien des mittleren und oberen Eozän. *Palaeontographica Abteilung A* **103**, 377-406.
- Knox, R. W. O.'B., Harland, R. & King, C. 1983. Dinoflagellate cyst analysis of the basal London Clay of southern England. *Newsletters on Stratigraphy* **12**, 71-74.
- Koch, P. L., Zachos, J. C. & Gingerich, P. D. 1992. Correlation between isotope records in marine and continental carbon reservoirs near the Palaeocene-Eocene boundary. *Nature* **358**, 319-322.
- Koch, P. L., Zachos, J. C. & Dettman, D. L. 1995. Stable isotope stratigraphy and paleoclimatology of the Paleogene Bighorn Basin (Wyoming, USA). *Palaeogeography, Palaeoclimatology, Palaeoecology* **115**, 61-89.
- Kokinos, J. P. & Anderson, D. M. 1995. Morphological development of resting cysts in cultures of the marine dinoflagellate *Lingulodinium poyedrum* (= *L. machaerophorum*). *Palynology* **19**, 143-166.
- Köthe, A. 1990. Paleogene dinoflagellates from Northwest Germany. *Geologisches Jahrbuch* **118**, 1-111.
- Köthe, A., Khan, M. A. & Ashraf, M. 1988. Biostratigraphy of the Surghar Range, Salt Range, Sulaiman Range and the Kohat area, Pakistan, according to Jurassic through Paleogene Calcareous Nannofossils and Paleogene Dinoflagellates. *Geologischen Landesämtern in der*

Bundesrepublik Deutschland, Hannover **71**, 1-87.

- Kouli, K., Brinkhuis, H. & Dale, B. 2001. *Spiniferites cruciformis*: a fresh water dinoflagellate cyst? *Review of Palaeobotany and Palynology* **113**, 273-286.
- Kouwenhoven, T. J., Speijer, R. P., van Oosterhout, C. W. M. & van der Zwaan, G. J. 1997. Benthic foraminiferal assemblages between two major extinction events: the Paleocene El Kef section, Tunisia. *Marine Micropaleontology* **29**, 105-127.
- Krashennikov, V. A. 1965. Zonal'naya stratigrafiya paleogena vostochnogo srednizemnomor'ya in Stratigrafiya paleogenovykh otlozhenii Sirii: *Akademiya Nauk SSSR, Geologicheskaya Institut, Trudy* **133**, 28-75.
- Krashennikov, V. A. 1965. Geograficheskoe i stratigraficheskoe raspredelenie planktonnykh foraminifer v otlozhenyakh Paleogena tropicheskoi oblasti [Geographical and Stratigraphical Distribution of Planktonic Foraminifers in Paleogene Deposits of Tropical and Subtropical Areas]: *Izdatelstvo "Nauka", Moscow, Akademiya Nauka SSSR*, 184p.
- Krashennikov, V. A. & Hoskins, R. S. 1973. Late Cretaceous, Paleocene and Eocene planktonic foraminifera. *Initial Reports of the Deep Sea Drilling Project* **20**, 105-203.
- Krashennikov, V. A. & Muzylev, N. G. 1975. Sootnoshenie zonal'nykh shkal po planktonnym foraminiferam i nannoplanktony v razrezakh paleogena Severnogo Kavkaza [Correlation of planktonic foraminiferal and calcareous nannoplankton. Zones in Paleogene sections of the west Caucasus]: *Voprosy Mikropaleontologii* **18**, 212-224.
- Kroopnick, P. M. 1985. The distribution of ^{13}C of TCO_2 in the world oceans. *Deep-Sea Research* **32**, 57-84.

- Kureshi, A. A. 1978. Tertiary larger foraminiferal zones of Pakistan. *Revista Española de Micropaleontología* **10**, 467-483.
- Kurtz, A. C., Kump, L. R., Arthur, M. A., Zachos, J. C. & Paytan, A. 2003. Early Cenozoic decoupling of the global carbon and sulfur cycles. *Paleoceanography* **18**, 14-1-14-4.
- Lamarck, J. B. 1801. *Système des animaux sans vertèbres*. The Author, Paris, 1-432.
- Latif, M. A. 1961. The use of the pelagic foraminifera in the subdivision of the Paleocene-Eocene of the Rakhi Nala, West Pakistan. *Geological Bulletin of the Punjab University, Lahore* **1**, 31-45.
- Latif, M. A. 1964. Variation in the abundance and morphology of pelagic foraminifera in the Paleocene-Eocene of the Rakhi Nala, West Pakistan. *Geological Bulletin of Punjab University, Lahore* **4**, 29-109.
- Latif, M. A. 1970. Explanatory notes on the geology of southeastern Hazara to accompany the revised geological map. *Jahrbuch der Geologischen Bundesanstalt, Sonderband* **15**, 5-20.
- La Touch, T. D. 1893. Report on the oil springs at Mughal Kot in the Shirani Hills. *Records of the Geological Survey of India* **25**, 171-175.
- Lawver, L. A. Gahagan, L. M. 1998. Opening of Drake Passage and its impact on Cenozoic ocean circulation. In: Crowley, T. J. & Burke, K. G. (Eds), *Tectonic Boundary Conditions for climate Reconstructions*, Oxford Monographs on Geology and Geophysics. Oxford University Press, New York **39**, 212-226.
- Leckie, R. M., Yuretich, R. F., West, O. L. O., Finkelstein, D. & Schmidt, M. 1998. Paleooceanography of the southwestern Western Interior Sea during the time of the Cenomanian-Turonian boundary (Late Cretaceous).

- In: Dean, W. E. & Arthur, M. A. (Eds), *Stratigraphy and Palaeoenvironments of the Cretaceous Western Interior Seaway, USA*, Society of Economic Paleontologists and Mineralogists, Concepts in Sedimentology and Paleontology **6**, 101-126.
- Lehmann, M. F., Bernasconi, S. M., Barbieri, A. & McKenzie, J. A. 2002. Preservation of organic matter and alteration of its carbon and nitrogen isotope composition during simulated and in situ early sedimentary diagenesis. *Geochimica et Cosmochimica Acta* **66**, 3573-3584.
- Lejeune-Carpentier, M. 1937. L'étude microscopique des silex. Un fossile anciennement connu et pourtant méconnu: *Hystriosphæra ramosa* Ehrbg. (Deuxième note). *Annales de la Société géologique de Belgique* **60**, 239-260.
- Lentin, J. K. & Williams, G. L. 1977. *Fossil dinoflagellates: index to genera and species, 1977 edition*. Bedford Institute of Oceanography Report **BI-R-77-8**, 1-209.
- Lentin, J. K. & Vozzhennikova, T. F. 1989. The fossil dinoflagellate cysts *Kisselovia* emend. and *Charlesdowniea* gen. nov., *Review of Palaeobotany and Palynology* **58**, 215-229.
- Leonov, V. P. & Alimarina, G. P. 1964. *Stratigraphical problems of the Paleogene deposits of the northwestern Caucasus*: Moscow University Press, Moscow, 204 p.
- LeRoy, L. W. 1953. Biostratigraphy of the Maqfi Section, Egypt. *Geological Society of America, Memoir* **54**, 60-71.
- Lewis, J. & Hallet, R. 1997. *Lingulodinium polyedrum* (*Gonayaulax polyedra*), a blooming dinoflagellate. *Oceanography and Marine Biology Annual Review* **35**, 97-161.

- Lewis, J., Rochon, A. & Harding, I. 1999. Preliminary observations of cyst-theca relationships in *Spiniferites ramosus* and *Spiniferites membranaceus* (Dinophyceae). *Grana* **38**, 113-124.
- Lewis, J., Ellegaard, M., Hallett, R. I., Harding, I. & Rochon, A. 2003. Environmental control of cyst morphology in gonyaulacoid dinoflagellates. *In: Matsuoka, K., Yoshida, M. & Iwataki, M. (Eds), Seventh International Conference on Modern and fossil Dinoflagellates, Dino7, Nagasaki, Japan, September 21-25; Program, Abstracts, and Participants Volume, Additional Abstract.*
- Leymerie, A. 1846. Mémoire sur le terrain à *Nummulites* (épicrotécé) des Corbières et de la Montagne Noire. *Mémoires de la Société géologique de France* (série 2) **1**, 337-373.
- Lillie, R. J., Lawrence, R. D., Humayun, M. & Jadoon, I. A. K. 1989. The Sulaiman thrust lobe of Pakistan: early stage under thrusting of the Mesozoic rifted margin of the Indian subcontinent (abstract). *Geological Society of America, Abstract with Programs* **21**, A318.
- Lipps, J. H. 1979. The ecology and paleoecology of planktic foraminifera. *In: Lipps, J. H., Berger, W. H., Buzas, M. A., Douglas, R. G. & Ross, C. A. (Eds), Foraminiferal ecology and paleoecology, Society of Economic Paleontologists and Mineralogists, Short Course, Houston 6*, 62-104.
- Lirer, F. 2000. A new technique for retrieving calcareous microfossils from lithified lime deposits. *Micropaleontology* **46**, 365-356.
- Loeblich, A. R. & Tappan, H. 1957. Planktonic foraminifera of Paleocene and early Eocene age from the Gulf and Atlantic coastal Plains. *Bulletin of United States National Museum* **215**, 173-198.
- Loeblich, A. R. & Tappan, H. 1988. *Foraminiferal genera and their classification.*

- Van Nostrand Reinhold Company Incorporation, New York, USA vol. **1**, 1-970 & vol. **2**, 1-212.
- Luciani, V., Giusberti, L., Agnini, C., Backman, J., Fornaciari, E. & Rio, D. 2007. The Paleocene-Eocene Thermal Maximum as recorded by Tethyan planktonic foraminifera in the Forada section (northern Italy). *Marine Micropaleontology* **64**, 189-214.
- Lu, G. & Keller, G. 1993. The Paleocene-Eocene transition in the Antarctic Indian Ocean: Inference from planktic foraminifera. *Marine Micropaleontology* **21**, 101-142.
- Lu, G. & Keller, G. 1995. Planktic foraminiferal faunal turnovers in the subtropical Pacific during the late Paleocene to early Eocene. *Journal of Foraminiferal Research* **25**, 97-116.
- Luger, P. 1985. Stratigraphie der marinen Oberkreide und des Alttertiärs im südwestlichen Oberrhin-Becken (SW-Ägypten) unter besonderer Berücksichtigung der Mikropaläontologie, Palökologie und Paläogeographie. *Berliner Geowissenschaftliche Abhandlungen, Reihe A: Geologie und Paläontologie*, **63**, 151 pp.
- Luterbacher, H. P. 1964. Studies in some Globorotalia from the Palaeocene and Lower Eocene of the central Apennines. *Ecologiae Geologicae Helvetiae* **57**, 631-730.
- Luterbacher, H. P. 1970. *Environmental distribution of Early Tertiary microfossils, Tremp basin, Northeastern Spain*. Esso Production Research, European Laboratories, Houston, Texas **47**.
- MacArthur, R. H. & Wilson, E. O. 1967. *The theory of island biogeography*. Princeton University Press, Princeton, 167pp.
- MacLennan, J. & Jones, S. M. 2006. Regional uplift, gas hydrate dissociation

- and the origins of the Paleocene-Eocene Thermal Maximum. *Earth and Planetary Science Letters* **245**, 65-80.
- MacRae, R. A., Fensome, R. A. & Williams, G. L. 1996. Fossil dinoflagellate diversity, originations, and extinctions and their significance. *Canadian Journal of Botany* **74**, 1687-1694.
- Magioncalda, R., Dupuis, C., Smith, T., Steurbaut, E. & Gingerich, P. D. 2004. Paleocene-Eocene carbon isotope excursion in organic carbon and pedogenic carbonate: direct comparison in a continental stratigraphic section. *Geology* **32**, 553-556.
- Maier, D. 1959. Planktonuntersuchungen in tertiären und quartären marinen Sedimenten. *Neues Jahrbuch für Geologie und Paläontologie, Abhandlungen* **107**, 278-340.
- Mantell, G. A. 1850. *A pictorial atlas of fossil remains consisting of coloured illustrations selected from Parkinson's "Organic remains of a former world", and Artis's "Antediluvian phytology"*. Henry G. Bohn, London xii, 207p.
- Marret, F. & Scourse, J. 2002. Control of modern dinoflagellate cyst distribution in the Irish and Celtic seas by seasonal stratification dynamics. *Marine Micropaleontology* **47**, 101-116.
- Marshall, J. D. 1992. Climatic and oceanographic isotopic signals from the carbonate rock record and their preservation. *Geological Magazine* **192**, 143-160.
- Martini, E. 1971. Standard Tertiary and Quaternary calcareous nannoplankton zonation. In: Farinacci, A. (Ed.), *Proceedings of the Second Planktonic Conference, Roma 1970, Volume 2*, Edizioni Tecnoscienza, Rome, 739-785.

- Matthiessen, J. & Brenner, W. 1996. Chlorococcalalgen und dinoflagellaten-
zysten in rezenten sedimenten des Greifswalder Boddens (südliche
Ostsee). *Senckenbergiana Maritima* **27**, 33-48.
- Matthiessen, J., Zonneveld, K. A. F., de Vernal, A., Head, M. J. & Harland, R.
2005. Recent and Quaternary organic-walled dinoflagellate cysts in Arctic
marine environments and their paleoenvironmental significance.
Paläontologische Zeitschrift **79**, 3-51.
- McCrea, J. M. 1950. On the isotopic chemistry of carbonates and a
paleotemperature scale. *The Journal of Chemical Physics* **18**, 849-857.
- Meissner, C. R. A. M., Master, J. M., Rashid, M. A. & Hussain, M. 1974.
Stratigraphy of the Kohat Quadrangle, Pakistan. *United States
Geological Survey, Professional Paper 716D*, 1-30.
- Meissner, C. R. A. M., Rashid, M. A. & Sethi, U. B. 1975. Geology of the
Parachinar Quadrangle, Pakistan. *United States Geological Survey,
Professional Paper 716-F*, 1-24.
- Middlemiss, C. S. 1896. The geology of Hazara and the Black Mountains.
Memoirs of the Geological Survey of India **26**, 302pp.
- Molina, E., Arenillas, I. & Pardo, A. 1999. High resolution planktic foraminiferal
biostratigraphy and correlation across the Paleocene/Eocene boundary
in the Tethys. *Bulletin de la Société géologique de France* **170**, 521-530.
- Monechi, S., Angori, E. & Speijer, R. P. 2000. Upper Paleocene biostratigraphy
in the Mediterranean region: Zonal markers, diachronism, and
preservational problems. *Geologiska Föreningens i Stockholm
Förhandlingar* **122**, 108-110.
- Morgenroth, P. 1966. Mikrofossilien und Konkretionen des
nordwesteuropäischen Untereozäns. *Palaeontographica*, Stuttgart, (B)

- Morozova, V. G. 1939. K stratigrafii vekhnogo mela i paleogena Embenskoj oblasti po faune foraminifera [Stratigraphy of the Upper Cretaceous and paleogene of the Emba area based on foraminiferal faunas]: *Moskovski Obschchii. Ispytateley Prirody Byulletin, otdel Geologiya* **17**, 59-96 (in Russian includes an English Summary).
- Morozova, V. G. 1961. Datsko-Montskie planktonnye foraminifery Yuga SSSR (Danian Mountain planktonic foraminifera of the southern USSR). *Paleontologicheskij zhurnal* **2**, 8-19.
- Morton, A. C., Backman, J. & Harland, R. 1983. A reassessment of the stratigraphy of DSDP Hole 117 A, Rockall Plateau: implications for the Palaeocene-Eocene boundary in N.W. Europe. *Newsletters on Stratigraphy* **12**, 104-111.
- van Mourik, C. A. & Brinkhuis, H. 2000. Data Report: Organic Walled Dinoflagellate Cyst Biostratigraphy of the Latest Middle to Late Eocene at Hole 1053A (Subtropical Atlantic Ocean). In: Kroon, D., Norris, R. D. & Klaus, A. (Eds.), *Proceedings of the Ocean Drilling Program, Scientific Results, 171B*. Available from World Wide Web: http://www-odp.tamu.edu/publications/171B_SR/chap_06.htm. College Station, Texas.
- van Mourik, C. A., Brinkhuis, H. & Williams, G. L. 2001. Mid-to Late Eocene organic-walled dinoflagellate cysts from ODP Leg 171B, offshore Florida. In: Kroon, D., Norris, R. D. & Klaus, A. (Eds), *Western North Atlantic Palaeogene and Cretaceous Palaeoceanography*. Geological Society, London, Special Publications **183**, 225-251.
- Mudge, D. C. & Bujak, J. P. 1994. Eocene stratigraphy of the North Sea Basin.

Marine and Petroleum Geology **11**, 166-181.

- Mudge, D. C. & Bujak, J. P. 1996. Palaeocene biostratigraphy and sequence stratigraphy of the UK central North Sea. *Marine and Petroleum Geology* **13**, 295-312.
- Mudie, P. J. & Harland, R. 1996. Aquatic Quaternary. *In*: Jansonius, J. & McGregor, D. C. (Eds), *Palynology: Principles and Applications*, American Association of Stratigraphic Palynologists Foundation, Dallas, 843-877.
- Mudie, P. J., Rochon, A., Aksu, A. E. & Gillespie, H. 2002. Dinoflagellate cysts, freshwater algae and fungal spores as salinity indicators in Late Quaternary cores from Marmara and Black Seas. *In*: Aksu, A. E. & Yaltirak, C. (Eds), *Quaternary paleoclimatic-paleoceanographic and tectonic evolution of the Marmara Sea and environs; a collection of papers dedicated to the memory of Dr. Ihsan Ketin*. *Marine Geology* **190**, 203-232.
- Müller, P. J., Erlenkeuser, H. & von Grafenstein, R. 1983. Glacial-interglacial cycles in oceanic productivity inferred from organic carbon contents in eastern North Atlantic sediment cores. *In*: Thiede, J. & Suess, E. (Eds), *Coastal upwelling: Its sediment Record (Part B)*, Plenum Press, New York, 365-398.
- Müller, P. J., Schneider, R. R. & Ruhland, G. 1994. Late Quaternary PCO₂ variations in the Angola current: evidence from organic carbon $\delta^{13}\text{C}$ and alkenon temperatures. *In*: Zahn, R., Pedersen, T. F., Kaminski, M. A. & Labeyrie, L. (Eds), *Carbon Cycling in the Glacial Ocean: Constraints on the Ocean's Role in Global Climate Change*. NATO ASI Series, Springer, Berlin **17**, 343-366.

- Murray, J. W. 1973. *Distribution and ecology of living benthic foraminiferids*. Heinemann, London, 274 pp.
- Murray, J. W. 1991. *Ecology and palaeoecology of benthic foraminifera*, Longman Scientific and Technical (John Wiley), Harlow, 365 pp.
- Murray, J. W. 2006. *Ecology and applications of benthic foraminifera*. University Press, Cambridge, 426 pp.
- Nagappa, Y. 1959. Foraminiferal biostratigraphy of the Cretaceous-Eocene succession in the India-Pakistan-Burma region. *Micropaleontology* **5**, 145-192.
- Nehring, S. 1994a. Dinoflagellaten-Dauercysten in deutschen Küstengewässern: Vorkommen, Verbreitung und Bedeutung als Rekrutierungspotential. *Berichte des Instituts für Meereskunde der Christian-Albrechts-Universität Kiel* **259**, 1-231.
- Nehring, S. 1994b. Spatial distribution of dinoflagellate resting cysts in recent sediments of Kiel Bight, Germany (Baltic sea). *Ophelia* **39**, 137-158.
- Noetling, F. 1903. Übergang zwischen Kreide und Eocän in Baluchistan. *Centralbl. Mineralogie und Paläontologie, Jahrbuch* **4**, 514-523.
- Nøhr-Hansen, H. 2003. Dinoflagellate cyst stratigraphy of the Palaeogene strata from the Hellefisk-1, Ikermiut-1, Kangamiut-1, Nukik-1, Nukik-2 and Qulleq-1 wells, offshore West Greenland. *Marine and Petroleum Geology* **20**, 987-1016.
- Norris, D. R. & Röhl, U. 1999. Carbon cycling and chronology of climate warming during the Palaeocene/Eocene transition. *Nature* **401**, 775-778.
- Norris, D. R. & Röhl, U. 2000. Astronomically tuned chronostratigraphy for the Palaeocene-Eocene transition. *In*: Schmitz, B., Sundquist, B. & Andreasson, F. P. (Eds), *Early Paleogene Warm Climates and Biosphere*

- Dynamics*. Geologiska Föreningen: Stockholm, Förhandlingar **122**, 117-118.
- Nunes, F. & Norris, R. D. 2006. Abrupt reversal in ocean overturning during the Palaeocene/Eocene warm period. *Nature* **439**, 60-63.
- Nuttall, W. L. F. 1925. The stratigraphy of the Laki Series (Lower Eocene) of parts of Sind and Baluchistan (India); with a description of the larger foraminifera contained in those beds. *Quarterly Journal of the Geological Society, London* **81**, 417-452.
- Nuttall, W. L. F. 1926. The larger Foraminifera of the Upper Ranikot Series (Lower Eocene) of Sind, India. *Geological Magazine, London* **63**, 112-121.
- Nuttall, W. L. F. 1931. The stratigraphy of the upper Ranikot Series of Sind. *Records of the Geological Survey of India* **65**, 306-313.
- Okada, H. & Bukry, D. 1980. Supplementary modification and introduction of code numbers to the low-latitude coccolith biostratigraphic zonation (Bukry, 1973; 1975). *Marine Micropaleontology* **5**, 321-325.
- Oldham, R. D. 1890. Report on the geology and economic resources of the country adjoining the Sind-Pishin railway between Sharigh and Spintagi, and of the country between it and Khattan. *Records of the Geological Survey of India* **23**, 93-109.
- Olsson, R. K., Hemleben, C., William, A. B., Berggren, W. A. & Huber, B. T. 1999. Atlas of Paleocene planktonic foraminifera. *Smithsonian Contributions to Paleobiology* **85**, 1-25.
- Ortiz, N. 1995. Differential patterns of benthic foraminiferal extinctions near the Paleocene/Eocene boundary in the North Atlantic and the western Tethys. *Marine Micropaleontology* **26**, 341-359.

- Orue-Etxebarria, X., Pujalte, V., Bernaola, G., Apellaniz, E., Baceta, J. I., Payros, A., Nuñez-Betelu, K., Serra-Kiel, J. & Tosquella, J. 2001. Did the Late Paleocene thermal maximum affect the evolution of larger foraminifers? Evidence from calcareous plankton of the Campo Section (Pyrenees, Spain). *Marine Micropaleontology* **41**, 45-71.
- Pak, D. K. & Miller, K. G. 1992. Paleocene to Eocene Benthic Foraminiferal Isotopes and Assemblages: Implications for Deepwater Circulation. *Paleoceanography* **7**, 405-422.
- Pancost, R. D., Steart, D. S., Handley, L., Collinson, M. E., Hooker, J. J., Scott, A. C., Grassineau, N. V. & Glasspool, I. J. 2007. Increased terrestrial methane cycling at the Palaeocene-Eocene thermal maximum. *Nature* **449**, 332-335.
- Pardo, A., Keller, G. & Oberhänsli, H. 1999. Paleoecologic and paleoceanographic evolution of the Tethyan realm during the Paleocene-Eocene transition. *Journal of Foraminiferal Research* **29**, 37-57.
- Pastels, A. 1948. Contributions à l'étude des microfossiles de l' Eocène belge. *Mémoires du Musée royal d' Histoire naturelle de Belgique, Bruxelles* **109**, 1-77.
- Pedersen, T. F. & Calvert, S. E. 1990. Anoxia versus productivity: what controls the formation of organic carbon-rich sediments and sedimentary rocks. *American Association of Petroleum Geologists, Bulletin* **74**, 454-466.
- Petrizzo, M. R. 2007. The onset of the Paleocene-Eocene Thermal Maximum (PETM) at Sites 1209 and 1210 (Shatsky Rise, Pacific Ocean) as recorded by planktonic foraminifera. *Marine Micropaleontology* **63**, 187-200.
- Pfender, J. 1935. À propos du Siderolites vidali Douvillé, et de quelques autres.

Bulletin de la Société géologique de France **4**, 225-236.

- Phleger, F. B. 1960. *Ecology and Distribution of Recent Foraminifera*. John Hopkins University Press, Baltimore, 297pp.
- Pinfold, E. S. 1939. The Dunghan Limestone and the Cretaceous unconformity in northwest India. *Records of the Geological Survey of India* **74**, 189-198.
- Pivnik, D. A. 1992. *Depositional Response to Encroachment of Himalayan compressional and Transpressional Deformation on the northern Pakistan Foreland*. Unpublished PhD Thesis, Dartmouth College, Hanover, New Hampshire, U.S.A.
- Plummer, H. J. 1926. Foraminifera of the Midway Formation in Texas: *University of Texas Bulletin, Austin* **2644**, 1-206.
- Porth, H. & Raza, H. A. 1990. *On the geology and hydrocarbon prospects of Sulaiman province, Indus Basin, Pakistan*. Unpublished Technical report, Bundesanstalt für Geowissenschaften und Rohstoffe, Hannover/Hydrocarbon Development Institute, Pakistan, 127pp.
- Postuma, J. A. 1971. *Manual of planktonic foraminifera*. Elsevier Publishing Company, Amsterdam, 1-420.
- Powell, A. J. 1988. A modified dinoflagellate biozonation for the latest Palaeocene and earliest Eocene sediments from the central North Sea. *Review of Palaeobotany and Palynology* **56**, 327-344.
- Powell, A. J. 1992. Dinoflagellate cysts of the Tertiary System. *In*: Powell, A. J. (Ed.), *A stratigraphic index of dinoflagellate cysts*. British Micropaleontological Society, Special Publication, Chapman and Hall, London, 155-251.
- Powell, A. J., Brinkhuis, H. & Bujak, J. P. 1996. Upper Paleocene-Lower

- Eocene dinoflagellate cyst sequence biostratigraphy of southeast England. *In: Knox, R.W.O'B., Corfield, R. M. & Dunay, R. E. (Eds), Correlation of the early Paleogene in Northwest Europe*, Geological Society, London, Special Publications **101**, 145-183.
- Prauss, M. L. 2009. The K/Pg boundary at Brazos-River, Texas, USA - An approach by marine palynology. *Palaeogeography, Palaeoclimatology, Palaeoecology* **283**, 195-215.
- Premoli Silva, I. & Bolli, H. M. 1973. Late Cretaceous to Eocene planktonic foraminifera and stratigraphy of Leg 15 Sites in the Caribbean Sea, *Initial Reports of the Deep Sea Drilling Project* **15**, 499-547.
- Price, G. D. & Hart, M. B. 2002. Isotopic evidence for Early to mid-Cretaceous ocean temperature variability. *Marine Micropaleontology* **46**, 45-58.
- Pross, J. 2001. Dinoflagellate cyst biogeography and biostratigraphy as a tool for palaeoceanographic reconstructions: An example from the Oligocene of western and northwestern Europe. *In: Luterbacher, H., Pross, J. & Wille, W. (Eds), Studies in Dinoflagellate Cysts in Honour of Hans Gocht, Neues Jahrbuch für Geologie und Paläontologie-Abhandlungen* **219**, 207-220.
- Pross, J. & Schmiedl, G. 2002. Early Oligocene dinoflagellate cysts from the Upper Rhine Graben (SW Germany): Paleoenvironmental and paleoclimatic implications. *Marine Micropaleontology* **45**, 1-24.
- Pross, J., Kotthoff, U. & Zonneveld, K. A. F. 2004. Die Anwendung organischwandiger Dinoflagellatenzysten zur Rekonstruktion von Paläoumwelt, Paläoklima und Paläozeanographie: Möglichkeiten and Grenzen. *Paläontologische Zeitschrift* **78**, 5-39.
- Pujalte, V., Orue-Etxebarria, X., Schmitz, B., Tosquella, J., Baceta, J.I., Payros,

- A., Bernaola, G., Caballero, F. & Apellaniz, E. 2003. Basal Ilerdian (earliest Eocene) turnover of larger Foraminifera: Age constraints based on calcareous plankton and delta $\delta^{13}\text{C}$ isotopic profiles from new southern Pyrenean sections (Spain). *In*: Wing, S. L., Gingerich, P. D., Schmitz, B. & Thomas, E. (Eds), *Causes and consequences of globally warm climates in the early Paleogene*, Geological Society of America, Boulder, Special Papers **369**, 205-221.
- Rabha, S. & Kalia, P. 2007. The case study of Paleocene-Eocene planktonic foraminifera in a near shore environment (Jaisalmer Basin, Rajasthan, India). *Geological Society of America, Abstracts with Programs* **39** (6).
- Racey, A. 1995. Lithostratigraphy and larger foraminiferal (nummulitid) biostratigraphy of the Tertiary of Northern Oman. *Micropaleontology* **41**, 1-123.
- Raza, H. A., Ahmad, R. & Ali, S. M. 1989. Petroleum zones of Pakistan. *Pakistan Journal of Hydrocarbon Research* **2**, 1-20.
- Rea, D. K., Zachos, J. C., Owen, R. M. & Gingerich, P. D. 1990. Global change at the Paleocene-Eocene boundary: climatic and evolutionary consequences of tectonic events. *Palaeogeography, Palaeoclimatology, Palaeoecology* **79**, 117-128.
- Reichart, G. -J. & Brinkhuis, H. 2003. Later Quaternary *Protoperidinium* cysts as indicators of paleoproductivity in the northern Arabian Sea, *Marine Micropaleontology* **49**, 303-370.
- Reichart, G. -J., Brinkhuis, H., Huiskamp, F. & Zachariasse, W. J. 2004. Hyperstratification following glacial overturning events in the northern Arabian Sea. *Paleoceanography* **19**(2), PA2013. 10. 1029/2003PA000900.
- Robert, C. & Kennett, J. P. 1994. Antarctic subtropical humid episode at the

- Paleocene-Eocene boundary: Clay-mineral evidence, *Geology* **22**, 211-214.
- Robinson, J., Beck, R., Gnos, E. & Vincent, R. K. 2000. New structural and stratigraphic insights for northwestern Pakistan from field and Landsat Thematic Mapper data, *Geological Society of America, Bulletin* **112**, 364-374.
- Rochon, A., de Vernal, A., Sejrup, H. -P. & Hafliðason, H. 1998. Palynological evidence of climatic and oceanographic changes in the North Sea during the last deglaciation. *Quaternary Research* **49**, 197-207.
- Rochon, A., de Vernal, A., Turon, J.-L., Mathiessen, J. & Head, M. J. 1999. Distribution of recent dinoflagellate cysts in surface sediments for the North Atlantic Ocean and adjacent seas in relation to sea-surface parameters. *American Association of Stratigraphic Palynologists Foundation, Contribution Series* **35**, 1-146.
- Röhl, U., Bralower, T. J., Norris, R. D. & Wefer, G. 2000. New chronology for the late Paleocene Thermal Maximum and its environmental implications. *Geology* **28**, 927-930.
- Röhl, U., Brinkhuis, H., Sluijs, A. & Fuller, M. 2004a. On the search for the Paleocene/Eocene Boundary in the Southern Ocean: Exploring ODP Leg 189 Holes 1171D and 1172D, Tasman Sea. *In*: Exon, N. F., Malone, M. & Kennett, J. P. (Eds), *The Cenozoic Southern Ocean: Tectonics, Sedimentation, and Climate Change Between Australia and Antarctica*, American Geophysical Union, Geophysical Monograph Series **151**, 113-125.
- Röhl, U., Brinkhuis, H., Stickley, C. E., Fuller, M., Schellenberg, S. A., Wefer, G. & Williams, G. L. 2004b. Sea level and astronomically induced

- environmental changes in Middle and Late Eocene sediments from the East Tasman Plateau. *In: Exon, N. F., Malone, M. & Kennett, J. P. (Eds), The Cenozoic Southern Ocean: Tectonics, Sedimentation, and Climate Change Between Australia and Antarctica*. American Geophysical Union, Geophysical Monograph Series **151**, 127-151.
- Röhl, U., Westerhold, T., Bralower, T. J. & Zachos, J. C. 2007. On the duration of the Paleocene-Eocene thermal maximum (PETM). *Geochemistry, Geophysics, Geosystems* **8**, 1-13.
- Rühlemann, C., Müller, P. J., & Schneider, R. R. 1999. Organic carbon and carbonate as paleoproductivity proxies: Examples from high and low productivity areas of the tropical Atlantic. *In: Fischer, G. & Wefer, G. (Eds), Use of Proxies in paleoceanography: examples from the South Atlantic*, Springer-Verlag, Berlin, 315-344.
- Salaj, J., Pozaryska, K. & Szczechura, J. 1976. Foraminiferida, zonation and subzonation of the Palaeocene of Tunisia. *Acta Palaeontologica Polonica* **21**, 127-190.
- von Salis, K., Ouda, K., Saad, E. D. M., Tantawy, A. A. & Bernasconi, S. 1998. Calcareous nannofossils, foraminifera and stable isotope studies from the P/E boundary sections in Egypt. *Strata* **9**, 113-115.
- Samanta, B. K. 1970. Middle Eocene planktonic foraminifera from the Lakhpat, Cutch, Western India. *Micropaleontology* **16**, 185-215.
- Samanta, B. K. 1973. Planktonic foraminifera from the Paleocene-Eocene succession in the Rakhi Nala, Sulaiman Range, Pakistan. *Bulletin of the British Museum (Natural History), Geology* **22**, 421-482.
- Sameeni, S. J. 1998. *Biostratigraphy of the Eocene succession of the Salt Range, Northern Pakistan*. Unpublished PhD Thesis, Institute of Geology,

University of the Punjab, Lahore, Pakistan.

- Sangiorgi, F., Capotondi, L. & Brinkhuis, H. 2002. A centennial scale organic-walled dinoflagellate cyst record of the last deglaciation in the South Adriatic Sea (central Mediterranean). *Palaeogeography, Palaeoclimatology, Palaeoecology* **186**, 199-216.
- Sangiorgi, F., Capotondi, L., Combourieu Nebout, N., Vigliotti, L., Brinkhuis, H., Giunta, S., Lotter, A. F., Morigi, C., Negri, A. & Reichert, G. J. 2003. Holocene seasonal sea surface temperature variations in the South Adriatic sea inferred from a multi-proxy approach. *Journal of Quaternary Science* **18**, 723-732.
- Sarjeant, W. A. S. 1970. The genus *Spiniferites* Mantell, 1850 (Dinophyceae). *Grana* **10**, 74-78.
- Sarnthein, M., Pflaumann, U., Ross, R., Tiedemann, R. & Winn, K. 1992. Transfer functions to reconstruct ocean productivity: a comparison. In: Summerhayes, C. P., Prell, W. L. & Emeis, K. -C. (Eds), *Upwelling systems: Evolution since the early Miocene*. Geological Society, London, Special Publications **64**, 411-427.
- Sarwar, G. & Dejong, K. A. 1979. Arcs, oroclines, syntaxes: The curvatures of the mountain belts in Pakistan. In: Farah, A. & Dejong, K. A. (Eds), *Geodynamics of Pakistan*. Geological Survey of Pakistan, Quetta, 341-349.
- Savin, S. M., Abel, L., Barrera, E., Hodell, D., Keller, G., Kennett, J. P., Killingley, J. & Berger, W. H. 1985. The evolution of Miocene surface and near-surface marine temperatures: Oxygen isotopic evidence. *Memoirs of the Geology Society of America* **163**, 49-79.
- Schaub, H. 1981. Nummulites et Assilines de la Téthys Paléogène. Taxinomie,

phylogénèse et biostratigraphie. *Schweizerische Paläontologische Abhandlungen* **104-106**, 1-236 (+ Atlas).

- Scheibner, C., Speijer, R. P. & Marzouk, A. M. 2005. Turnover of larger foraminifera during the Paleocene-Eocene Thermal Maximum and Paleoclimatic control on the evolution of platform ecosystems. *Geology* **33**, 493-496.
- Scheibner, C. & Speijer, R. P. 2009. Recalibration of the Tethyan shallow-benthic zonation across the Paleocene-Eocene boundary: the Egyptian record. *Geologica Acta* **7**, 195-214.
- Schellenberg, S. A., Brinkhuis, H., Stickley, C. E., Fuller, M., Kyte, F. T. & Williams, G. L. 2004. The Cretaceous/Paleogene transition on East Tasman Plateau, southwestern Pacific. In: Exon, N. F., Malone, M. & Kennett, J. P. (Eds), *The Cenozoic Southern Ocean: Tectonics, Sedimentation, and Climate Change Between Australia and Antarctica*. American Geophysical Union, Geophysical Monograph Series **151**, 93-112.
- Schmitz, B., Speijer, R. P. & Aubry, M. -P. 1996. Latest Paleocene benthic extinction event on the southern Tethyan shelf (Egypt): Foraminiferal stable isotopic ($\delta^{13}\text{C}$, $\delta^{18}\text{O}$) records. *Geology* **24**, 347-350.
- Schmitz, B., Peucker-Ehrenbrink, B., Heilmann-Clausen, C., Åberg, G., Asaro, F. & Lee, C. -T. A. 2004. Basaltic explosive volcanism, but no comet impact, at the Paleocene-Eocene boundary: high-resolution chemical and isotopic records from Egypt, Spain and Denmark. *Earth and Planetary Science Letters* **225**, 1-17.
- Schubert, R. J. 1908. Beiträge zu einer natürlichen Systematik der Foraminiferen. *Neues Jahrbuch für Mineralogie, Geologie und*

Paläontologie, Beilage-Band 25, 232-260.

- Serra-Kiel, J., Tosquella, J., Ferrandez & Samsó, J. M. 1996. Larger foraminiferal biostratigraphy. *In: Early Eocene Stage Boundaries, International meeting and field conference, Zaragoza (Spain)*, 48-49.
- Serra-Kiel, J., Hottinger, L., Caus, E., Drobne, K., Ferrandez, C., Jauhri, A. K., Less, G., Pavlovec, R., Pignatti, J., Samsó, J. M., Schaub, H., Sirel, E., Strougo, A., Tambareau, Y., Tosquella, J. & Zakrevskaya, E. 1998. Larger foraminiferal biostratigraphy of the Tethyan Paleocene and Eocene. *Bulletin de la Société géologique de France* **169**, 281-300.
- Shackleton, N. J., Corfield, R. M. & Hall, M. A. 1985. Stable isotope data and the ontogeny of Paleogene planktonic foraminifera. *Journal of Foraminiferal Research* **15**, 321-336.
- Shafique, N. A. 2001. *Spatial biostratigraphy of NW Pakistan*. Unpublished PhD Thesis, Miami University, USA.
- Shah, S. M. I. 1977. Stratigraphy of Pakistan. *Memoirs of the Geological Survey of Pakistan* **12**, 1-138.
- Shah, S. M. I. 1987. Lithostratigraphic units of the Sulaiman and Kirthar Provinces, Lower Indus Basin, Pakistan. *Geological Survey of Pakistan Memoirs, Quetta* **17**(I-III).
- Shah, S. M. I. 1990. Coal resources of Baluchistan. *In: Kazmi, A. H. & Siddiqui, R. A. (Eds), Significance of the coal resources of Pakistan*. Geological Survey of Pakistan/United States Geological Survey, 63-93.
- Shutskaya, E. K. 1956. Stratigrafiya nizhnikh gorizontov paleogena tsentral'nogo predkavkaz'ya po foraminiferam: *Trudy instituta geologicheskikh nauk* **164**, 3-119.
- Shutskaya, E. K. 1958. Izmenchivosti nekotorikh nizhnepaleogenovikh

- plannktonikh foraminifer severnogo Kavkaza: *Akademiya Nauk SSSR, Voprosyi Mikropaleontologii* **2**, 84-90.
- Shutskaya, E. K. 1960a. Stratigrafiya i fatsii nizhnego paleogena Predkavkazya: *Vsesoyuznyi nauchno-issledovatel'skii geologo-razvedochnyi neftyanoi institut (VNIGNI)*, GOSTOPTEKHIZDAT, Moscow, 104p.
- Shutskaya, E. K. 1960b. Stratigrafiya i fatsii nizhnego paleogena severnogo Prekavkaza i Kryma. *In: Yanshin, A. L et al., (Eds), Paleogenovye otlozhenii yuga evropeiskoi chasti SSSR: Akaemiya Nauk SSSR, Izdatels'tvo Moscow*, 207-229.
- Shutskaya, E. K. 1970. Stratigrafiya, foraminifery i paleogeografiya nizhnego paleogena Kryma, predkavkaz'ya i zapadnoi chadsti srednei azii: *Vsesoyuznyi nauchno-issledovadatel'skii geologo-razvedochniy nefyanoi institute (VNIGRI), Trudy* **70**, 256p.
- Shutskaya, E. K., Schwemberger, Y. N. & Khasina, G. I. 1965. Uploshschenkhyia globorotalii iz verkhnepaleotsenovykh i nizhneeotsenovykh otlozhenii Kryma, Predkavkaz'ya i Zakaspiya. *In: Sazonova, N. T. & Shutskaya, E. K. (Eds), Fauna Mesozoya i Kainzoya Evropeiskoi chasti SSSR i Srednei Azii: Vsesoyuznyi nauchnoissledovatel'skii geolorazvedochnyi nef'tyanoi institut (VNIGNI), Trudy* **44**, 192-211, Izdatel'stvo "NEDRA", Moskva.
- Sinclair, H. D., Sayer, Z. R. & Tucker, M. E. 1998. Carbonate sedimentation during early foreland basin subsidence: the Eocene succession of the French Alps. *In: Wright, V. P. & Burchette, T. P. (Eds), Carbonate Ramps, Geological Society, London, Special Publications* **149**, 205-227.
- Sirel, E. 1976. Systematic study of some species of the genera *Alveolina*, *Nummulites*, *Ranikothalia* and *Assilina* in the south Polath (S.W.

Ankara), *Türkiye Jeoloji Kurumu Bülteni* **19**, 89-102.

- Sluijs, A. 2006. *Global change during the Paleocene – Eocene thermal maximum*. PhD Thesis, Utrecht University, Netherlands.
- Sluijs, A., Brinkhuis, H., Stickley, C. E., Warnaar, J., Williams, G. L. & Fuller, M. 2003. Dinoflagellate cysts from the Eocene/Oligocene transition in the Southern Ocean; results from ODP Leg 189. *In: Exon, N. F., Kennett, J. P. & Malone, M. J. (Eds), Proceedings Ocean Drilling Program, Scientific Results*. Available from World Wide Web: http://www-odp.tamu.edu/publications/189_SR/104/104.htm, College Station, Texas, 1-42.
- Sluijs, A., Pross, J. & Brinkhuis, H. 2005. From greenhouse to icehouse; organic-walled dinoflagellate cysts as paleoenvironmental indicators in the Paleogene. *Earth Science Reviews* **68**, 281-315.
- Sluijs, A., Schouten, S., Pagani, M., Woltering, M., Brinkhuis, H., Sinninghe Damste, J. S., Dickens, G. R., Huber, M., Reichert, G.-J., Stein, R., Matthiessen, J., Lourens, L. J., Pedentchouk, N., Backman, J., Moran, K. & the Expedition 302 Scientists. 2006. Subtropical Arctic Ocean temperatures during the Palaeocene/Eocene thermal maximum. *Nature* **441**, 610-613.
- Sluijs, A., Bowen, G. J., Brinkhuis, H., Lourens, L. J. & Thomas, E. 2007a. The Palaeocene-Eocene Thermal Maximum super greenhouse: biotic and geochemical signatures, age models and mechanisms of global change. *In: Williams, M., Haywood, A. M., Gregory, F. J. & Schmidt, D. N. (Eds), Deep Time Perspectives on Climate Change: Marrying the Signal From Computer Models and Biological Proxies*. The Micropalaeontological Society, Special Publications, The Geological Society, London, **2**, 323-

- Sluijs, A., Brinkhuis, H., Schouten, S., Bohaty, S. M., John, C. M., Zachos, J. C., Reichart, G. -J, Damsté, J. S. S., Crouch, E. M. & Dickens, G. R. 2007b. Environmental precursors to rapid light carbon injection at the Palaeocene/Eocene boundary. *Nature* **450**, 1218-1221.
- Sluijs, A. & Brinkhuis, H. 2009. A dynamic climate and ecosystem state during the Paleocene-Eocene Thermal Maximum: inferences from dinoflagellate cyst assemblages at the New Jersey Shelf. *Biogeosciences* **6**, 1-27.
- Smith, F. G. 1955. Planktonic foraminifera as indicators of depositional environment. *Micropaleontology* **1**, 147-151.
- Smith, F. A., Wing, S. L. & Freeman, K. H. 2007. Magnitude of the carbon isotope excursion at the Paleocene-Eocene thermal maximum: the role of plant community change. *Earth and Planetary Science Letters* **262**, 50-65.
- Smith, T. 2000. Mammals from the Paleocene-Eocene transition in Belgium (Tienen Formation, MP7): Palaeobiogeographical and biostratigraphical implications. *Geologiska Föreningens Förhandlingar* **122**, 148-149.
- Smith, T., Rose, K. D. & Gingerich, P. D. 2006. Rapid Asia-Europe-North America geographic dispersal of earliest Eocene primate *Teilhardina* during the Paleocene-Eocene Thermal Maximum. *Proceedings of the National Academy of Sciences* **103**, 11223-11227.
- Smout, A. H. 1954. *Lower Tertiary foraminifera from the Qatar Peninsula*. British Museum (Natural History), London, 96pp.
- Smout, A. H. & Haque, A. F. M. M. 1956. A note on the larger foraminifera and Ostrocooda of the Ranikot from the Nammal Gorge, Salt Range, West Pakistan. *Geological Survey of Pakistan* **8**, 49-60.

- Snyder, S. W. & Waters, V. J. 1985. Cenozoic planktonic foraminiferal biostratigraphy of the Goban Spur region. *Initial Reports of the Deep Sea Drilling Project* **80**, 439-472.
- Speijer, R. P. 1994. The late Paleocene benthic foraminiferal extinction as observed in the Middle East. In: Laga, P. (Ed.), *Paleocene-Eocene Boundary Events*, Bulletin de la Société belge de Géologie **103**, 267-280.
- Speijer, R. P. & van der Zwaan, G. J. 1994. The differential effect of the Paleocene/Eocene boundary event: extinction and survivorship in shallow to deep water Egyptian benthic foraminiferal assemblages. In: Speijer, R.P. (Ed.), *Extinction and Recovery Patterns in Benthic Foraminiferal Paleocommunities across the Cretaceous/Paleogene and Paleocene/Eocene Boundaries*. Ph.D. Thesis, Facultiet Aardwetenschappen, Utrecht Universiteit. *Geologica. Ultraiectina* **124**, 121-168.
- Speijer, R. P., Schmitz, B., Aubry, M. -P. & Charisi, S. D. 1995. The latest Paleocene benthic extinction event: Punctuated turnover in outer neritic foraminiferal faunas from Gebel Aweina, Egypt. *Israel Journal of Earth Sciences* **44**, 207-222.
- Speijer, R. P., van der Zwaan, G. J. & Schmitz, B. 1996. The impact of Paleocene/Eocene boundary events on middle neritic benthic foraminiferal assemblages from Egypt. *Marine Micropaleontology* **28**, 99-132.
- Speijer, R. P. & Samir, A. M. 1997. *Globanomalina luxorensis*, a Tethyan biostratigraphic marker of latest Paleocene global events. *Micropaleontology* **43**, 51-62
- Speijer, R. P., Schmitz, B. & van der Zwaan, G. J. 1997. Benthic foraminiferal

- repopulation in response to latest Paleocene Tethyan anoxia. *Geology* **25**, 683-686.
- Speijer, R. P. & Schmitz, B. 1998. A benthic foraminiferal record of Paleocene sea level and trophic/redox conditions at Gebel Aweina, Egypt. *Palaeogeography, Palaeoclimatology, Palaeoecology* **137**, 79-101.
- Speijer, R. P., Schmitz, B. & Luger, P. 2000. Stratigraphy of late Palaeocene events in the Middle East: Implications for low to middle-latitude successions and correlations. *Journal of the Geological Society, London* **157**, 37-47.
- Speijer, R. P. & Wagner, T. 2002. Sea-level changes and black shales associated with the late Paleocene thermal maximum: Organic-geochemical and micropaleontologic evidence from the southern Tethyan margin (Egypt-Israel). *Geological Society of America, Bulletin* **356**, 533-549.
- Spero, H. J. 1987. Symbioses in the planktonic foraminifer, *Orbulina universa*, and the isolation of its symbiotic dinoflagellate, *Gymnodinium beii* sp. nov. *Journal of Phycology* **23**, 307-317.
- Stainforth, R. M., Lamb, J. L., Luterbacher, H., Beard, J. H. & Jeffords, R. M. 1975. Cenozoic planktonic foraminiferal zonation and characteristics of index forms. *University of Kansas, Paleontological Contributions, Article* **62**, 1-425 (in two parts).
- Sturbaut, E., Magioncalda, R., Dupuis, C., Van Simaey, S., Roche, E. & Roche, M. 2003. Palynology, paleoenvironments, and organic carbon isotope evolution in lagoonal Paleocene-Eocene boundary settings in North Belgium. In: Wing, S. L., Gingerich, P. D., Schmitz, B. & Thomas, E. (Eds), *Causes and Consequences of Globally Warm Climates in the*

Early Paleogene, Geological Society of America, Special Paper **369**, 291-317.

- Stickley, C. E., Brinkhuis, H., Schellenberg, S. A., Sluijs, A., Röhl, U., Fuller, M., Grauert, M., Huber, M., Warnaar, J. & Williams, G. L. 2004. Timing and nature of the deepening of the Tasmanian Gateway. *Paleoceanography* **19**(4), doi: 10.1029/2004PA001022.
- Storey, M., Duncan, R. A & Swisher III, C. C. 2007. Paleocene-Eocene Thermal Maximum and the opening of the Northeast Atlantic. *Science* **316**, 587-589.
- Stover, L. E., Brinkhuis, H., Damassa, S. P., de Verteuil, L., Helby, R. J., Monteil, E., Partridge, A., Powell, A. J., Riding, J. B., Smelror, M. & Williams, G. L. 1996. Mesozoic-Tertiary dinoflagellates, acritarchs and prasinophytes. In: Jansonius, J. & McGregor, D. C. (Eds), *Palynology: Principles and Applications*, American Association of Stratigraphic Palynologists Foundation, Dallas, 641-750.
- Stover, L. E. & Evitt, W. R. 1978. *Analyses of pre-Pleistocene organic-walled dinoflagellates*. Stanford University Publications, Geological Sciences 15, 300p.
- Subbotina, N. N. 1934. Raspredelenie mikrofauny v foraminiferovykh sloyakh raiona goroda Nal'chik i Chernykh Gor (Severnyi Kavkaz): *Inf. sbornik neftyannogo geologo-razvedochnogo instituta (NIGRI) za 1933-1934*, 97p.
- Subbotina, N. N. 1936. Stratigrafiya nizhnego paleogena i verkhnego mela Severnaya Kavkaza po fauna foraminifer: *Trudy neftyannogo geologo-razvedochnogo instituta (NIGRI)* **96**, 3-32 (French summary, p. 29, 30).
- Subbotina, N. N. 1939. Foraminifery nizhnetretichnykh otlozhenii Severnogo

- Kavkaza SSSR. Sbornik statei po mikrofauna: *Trudy neftyanogo geologo-razvedochnogo instituta (NIGRI)* **105**, 31-69 (English summary, p. 64, 65).
- Subbotina, N. N. 1947. Foraminifery datskikh i paleogenovykh otlozhenii severnogo Kavkaza [Foraminifera of the Danian and Paleogene deposits of the Northern Caucasus]. in *Mikrofauna neftnykh mestorozhdenii Kavkaza, Emby I Srednei Azii. Trudy Neftianogo razvedochnogo Instituta. Novaia seriia, Leningard, Moscow*, 39-160.
- Subbotina, N. N. 1953. Iskopaemye foraminifery SSSR (Globigerinidy, khantkeninidy i Globorotaliidy): *Trudy Vsesoyznogo Nauchno-Issledvatel'skogo Geologo-razvedochnogo Instituta (VNIGRI)* **76** GOSTOPETEKHIZDAT, Leningrad, 1-296. Translated into English by E. Lees, 1971, Fossil Foraminifera of the USSR; Globigerinidae, Hantkeninidae and Globorotaliidae: Collet's Ltd., London and Wellingborough, 321 pp.
- Svensen, H., Planke, S., Malthé-Sørensen, A., Jamtveit, B., Myklebust, R., Rasmussen-Eidem, T. & Rey, S. S. 2004. Release of methane from a volcanic basin as a mechanism for initial Eocene global warming. *Nature* **429**, 542-545.
- Tahirkheli, R. A. K., Mattauer, M., Proust, R. & Tapponnier, P. 1979. The India Eurasia suture zone in northern Pakistan: Synthesis and interpretation of recent data at Plate scale. In: Farah, A. & Dejong, K. A. (Eds), *Geodynamics of Pakistan*. Geological Survey of Pakistan, Quetta, 125-130.
- Takeda, K. & Kaiho, K. 2007. Faunal turnovers in central Pacific benthic foraminifera during the Paleocene-Eocene thermal maximum.

- Palaeogeography, Palaeoclimatology, Palaeoecology* **251**, 175-197.
- Targarona, J., Warnaar, J., Boessenkool, K. P., Brinkhuis, H. & Canals, M. 2000. Recent dinoflagellate cyst distribution in the north Canary Basin, NW Africa. *Grana* **38**, 170-178.
- Taylor, F. J. R. (Ed.), 1987. *The biology of dinoflagellate*. Botanical Monographs **21**. Blackwell Scientific Publications, London, 785 pp.
- Thomas, E. 1990a. Late Cretaceous-Early Eocene mass extinctions in the deep sea. *In*: Sharpton, V. L. & Ward, P. D. (Eds), *Global catastrophes in Earth History*, Geological Society of America, Special Publication **247**, 481-495.
- Thomas, E. 1990b. Late Cretaceous through Neogene deep-sea benthic foraminifers (Maud Rise, Weddall Sea, Antarctica). *In*: Proceedings of the Ocean Drilling Program, Scientific Results. College Station, Texas, Ocean Drilling Program 113, 571-594.
- Thomas, E. & Shackleton, N. J. 1996. The Palaeocene-Eocene benthic foraminiferal extinction and stable isotope anomalies. *In*: Knox, R. W. O'B., Corfield, R. M. & Dunay, R. E. (Eds), *Correlation of the Early Paleogene in Northwest Europe*. Geological Society, London, Special Publications **101**, 401-441.
- Thomas, E. 1998. Biogeography of the late Paleocene benthic foraminiferal extinction. *In*: Aubry, M. -P., Lucas, S. G. & Berggren, W. A., (Eds), *Late Paleocene-early Eocene Climatic and Biotic Events in the marine and Terrestrial Records*. Columbia University Press, New York, 214-243.
- Thomas, D. J., Bralower, T. J. & Zachos, J. C. 1999. New evidence for subtropical warming during the late Paleocene thermal maximum: Stable isotopes from Deep Sea Drilling Project Site 527, Walvis Ridge. *Paleoceanography* **14**, 561-570.

- Thomas, D. J., Zachos, J. C., Bralower, T. J., Thomas, E. & Bohaty, S. 2002. Warming the fuel for the fire: Evidence for the thermal dissociation of methane hydrate during the Palaeocene-Eocene thermal maximum. *Geology* **30**, 1067-1070.
- Ting, S., Bowen, G. J., Koch, P. L., Clyde, W.C., Wang, Y., Wang, Y. & McKenna, M. C. 2003. Biostratigraphic, chemostratigraphic, and magnetostratigraphic study across the Paleocene-Eocene boundary in the Hengyang Basin, Hunan, China. *In*: Wing, S., Gingerich, P. D., Schmitz, B. & Thomas, E. (Eds), *Causes and Consequences of Globally Warm Climates in the Early Paleogene*. Geological Society of America, Boulder (CO), Special Papers **369**, 521-536.
- Tjalsma, R. C. & Lohmann, G. P. 1983. Paleocene-Eocene Bathyal and Abyssal Benthic Foraminifera from the Atlantic Ocean. *Micropaleontology, Special Publication*, Number **4**, 1-90.
- Todd, R. & Kniker, H. T. 1952. An Eocene foraminiferal fauna from the Agua Fresca shale of Magallanes province, southernmost Chile. *Cushman Foundation for Foraminiferal Research, Special Publication* **1**, 1-28.
- Toulmin, L. D. 1941. Eocene smaller foraminifera from the salt Mountain limeston of Alabama. *Journal of Paleontology* **15**, 567-611.
- Toumarkine, M. & Luterbacher, H. 1985. Paleocene and Eocene planktonic foraminifera. *In*: Bolli, H. M., Saunders, J. B. & Perch-Nielsen, K. (Eds), *Plankton Stratigraphy*, Cambridge University Press, Cambridge **1**, 87-154.
- Trench, R. K. 1987. Non-parasitic symbioses. *In*: Taylor, F. J. R. (Ed.), *The biology of dinoflagellates*. Botanical Monographs, 530-570.
- Tripathi, A. K. & Elderfield, H. 2005. Deep-sea temperatures and circulation changes at the Paleocene-Eocene Thermal Maximum. *Science* **308**,

1894-1898.

- Turon, J. -L. 1981. *Le palynoplancton dans l'environnement actuel de l'Atlantique Nord oriental. Evolution climatique et hydrologique depuis le Dernier Maximum Glaciaire*. Unpublished PhD Thesis, Université de Bordeaux, 313 pp.
- Tyson, R. V. 1995. *Sedimentary Organic Matter: Organic Facies and Palynofacies*. Chapman and Hall, London, 615 pp.
- van der Zwaan, G. J., Jorriksen, F. J. and De Stigter, H. C. 1990. The depth dependency of planktonic/benthic foraminiferal ratios; constraints and applications. *Marine Geology* **95**, 1-16.
- van Morkhoven, F. P. C. M., Berggren, W. A. & Edwards, A. S. 1986. Cenozoic cosmopolitan deep-water benthic foraminifera. *Bulletin Centre Research Exploration et Production, Elf-Aquitaine, Memoire* **11**, 421pp.
- van Simaeys, S., Brinkhuis, H., Pross, J., Williams, G. L. & Zachos, J. C. 2005. Arctic dinoflagellate migrations mark the strongest Oligocene glaciations. *Geology* **33**, 709-712.
- Vaughan, T. W. & Cole, W. S. 1941. Preliminary report on the Cretaceous and Tertiary larger foraminifera of Trinidad, British West Indies. *Geological Society of America, Special Papers* **30**, 1-137.
- de Vernal, A., Goyette, C. & Rodrigues, C. G. 1989. Contribution palynostratigraphique (dinokystes, pollen et spores) à la connaissance de la mer de Champlain: coupe de Saint-Césaire, Québec. *Canadian Journal of Earth Sciences* **26**, 2450-2464.
- de Vernal, A. & Mudie, P. J. 1992. Pliocene and Quaternary dinoflagellate cyst stratigraphy in the Labrador Sea: Paleoenvironmental implications. In: Head, M. J. & Wrenn, J. H. (Eds), *Neogene and Quaternary Dinoflagellate*

Cysts and Acritarchs. American Association of Stratigraphic

Palynologists Foundation, Dallas, 329-436.

de Vernal, A., Turon, J. L. & Guiot, J. 1994. Dinoflagellate distribution in high-latitude marine environments and quantitative reconstruction of sea-surface salinity, temperature and seasonality. *Canadian Journal of Earth Sciences* **31**, 48-62.

de Vernal, A., Rochon, A., Turon, J. L. & Matthiessen, J. 1998. Organic-walled dinoflagellate cysts: Palynological tracers of sea-surface conditions in middle to high latitude marine environments. *Geobios* **30**, 905-920.

de Vernal, A., Hillaire-Marcel, C., Turon, J. & Matthiessen, J. 2000.

Reconstruction of sea-surface temperature, salinity, and sea-ice cover in the northern North Atlantic during the last glacial maximum based on dinocyst assemblages. *Canadian Journal of Earth Sciences* **37**, 725-750.

de Vernal, A., Matthiessen, J., Mudie, P. J., Rochon, A., Boessenkool, K. P., Eynaud, F., Grøsfjeld, K., Guiot, J., Hamel, D., Harland, R., Head, M. J., Kunz-Pirrung, M., Loucheur, V., Peyron, O., Pospelova, V., Radi, T., Turon, J. -L. & Voronina, E. 2001. Dinoflagellat cyst assemblages as tracers of sea-surface conditions in the northern North Atlantic, Arctic and sub-Arctic seas: the new "n-677" data base and its application for quantitative paleoceanographic reconstruction. *Journal of Quaternary Science* **16**, 681-698.

Versteegh, G. J. M. 1994. Recognition of cyclic and non-cyclic environmental changes in the Mediterranean Pliocene: A palynological approach. *Marine Micropaleontology* **23**, 147-183.

Versteegh, G. J. M. & Zonneveld, K. A. F. 1994. Determination of (palaeo-) ecological preferences of dinoflagellates by applying Detrended and

- Canonical Correspondence analysis to Late Pliocene dinoflagellate cyst assemblages of the south Italian Singha section. *Review of Palaeobotany and Palynology* **84**, 181-199.
- Versteegh, G. J. M. & Zonneveld, K. A. F. 2002. Use of selective degradation to separate preservation from productivity, *Geology* **30**, 615-618.
- Vredenburg, E. W. 1906. A geological sketch of the Baluchistan desert and part of the Eastern Perisa. *Memoirs of the Geological Survey of India* **31**, 179-302.
- Waagen, W. & Wynne, A. B. 1872. The Geology of Mount Sirban in the Upper Punjab. *Memoirs of the Geological Survey of India* **9**, 331-350.
- Wall, D., Dale, B. & Harada, K. 1973. Descriptions of new fossil dinoflagellates from the Late Quaternary of the Black Sea. *Micropaleontology* **19**, 18-31.
- Wall, D., Dale, B., Lohmann, G. P. & Smith, W. K. 1977. The environmental and climatic distribution of dinoflagellate cysts in the North and South Atlantic and adjacent seas. *Marine Micropaleontology* **30**, 319-343.
- Warraich, M. Y. 2000. *Paleogene Planktonic Foraminiferal Biostratigraphy of the Sulaiman Range, Southern Indus Basin, Pakistan*. Unpublished PhD Thesis, University of Tsukuba.
- Warraich, M. Y., Ali, M., Ahmad, M. A., Siddiqui, R. H. & Hirayama, J. 1995. Geology and structure of calcareous zone in Muslim Bagh and Kila Saifullah Area, Pakistan. *Geologica, Geological Survey of Pakistan, Geoscience Laboratory, Islamabad* **1**, 61-77.
- Warraich, M. Y. & Natori, H. 1997. Geology and planktonic foraminiferal biostratigraphy of the Paleocene-Eocene succession of the Zinda Pir section, Sulaiman Range, southern Indus Basin, Pakistan. *Bulletin of the Geological Survey of Japan* **48**, 595-630.

- Warraich, M. Y., Ogasawara, K. & Nishi, H. 2000. Late Paleocene to early Eocene planktic foraminiferal biostratigraphy of the Dungan Formation, Sulaiman Range, central Pakistan. *Paleontological Research* **4**, 275-301.
- Warraich, M. Y. & Ogasawara, K. 2001. Tethyan Paleocene-Eocene planktic foraminifera from the Rakhi Nala and Zinda Pir land sections of the Sulaiman Range, Pakistan: *Science Reports of the Institute of Geoscience, University of Tsukuba, Section B*, **22**, 1-59.
- Warwick, P.D., Johnson, E. A. & Khan, I. H. 1998. Collision-induced tectonism along the northwestern margin of the Indian subcontinent as recorded in the Upper Paleocene to Middle Eocene strata of central Pakistan (Kirthar and Sulaiman Ranges). *Paleogeography, Palaeoclimatology, Palaeoecology* **142**, 201-216.
- Wefer, G., Berger, W. H, Bijma, J. & Fischer, G. 1999. Clues to ocean history: a Brief overview of proxies. In: Fischer, G. & Wefer, G. (Eds), *Use of Proxies in Paleoceanography: Examples from the South Atlantic*, Springer-Verlag, Berlin, 1-68.
- Weiss, W. 1988. *Larger and planktonic foraminiferal biostratigraphy of the Cretaceous and the paleogene in the Salt Range, the Kohat area and the Sulaiman range, Pakistan*. Unpublished Technical Report, Bundesanstalt für Geowissenschaften und Rohstoffe, Hannover, 57pp .
- Weiss, W. 1993. Age assignments of larger foraminiferal assemblages of Maastrichtian to Eocene age in northern Pakistan. *Zitteliana* **20**, 223-252.
- Wells, N. A. 1984. *Marine and continental sedimentation in the Early Cenozoic Kohat basin and adjacent northern Indo-Pakistan*. Unpublished PhD Thesis, University of Michigan, USA.
- Wetzel, W. 1933. Die in organischer Substanz erhaltenen Mikrofossilien des

- baltischen Kreide-Feuersteins mit einem sediment-petrographischen und stratigraphischen Anhang. *Palaeontographica Abteilung A* **78**, 1-110.
- White, M. P. 1928. Some index foraminifera of the Tampico Embayment area of Mexico (Part I). *Journal of Paleontology* **2**, 177-215.
- White, M. P. 1929. Some index foraminifera of the Tampico Embayment area of Mexico (Part 3). *Journal of Paleontology* **3**, 30-58.
- White, M. R. 1989. *Foraminiferal biostratigraphy of Tertiary limestones in Northern Oman and Western Pakistan*. Unpublished PhD Thesis, Royal Holloway and Bedford New College, University of London.
- Williams, M. D. 1959. Stratigraphy of Lower Indus Basin, West Pakistan. *In: Proceedings of the 5th World Petroleum Congress, New York, Section 1*, Paper 19, 377-390.
- Williams, G. L., Brinkhuis, H., Pearce, M. A., Fensome, R. A. & Weegink, J. W. 2004. Southern Ocean and global dinoflagellate cyst events compared; index events for the Late Cretaceous-Neogene. *In: Exon, N. F., Kennett, J. P. & Malone, M. J. (Eds), Proceedings Ocean Drilling Program, Scientific Results*. Available from World Wide Web: http://www-odp.tamu.edu/publications/189_SR/107/107.htm, College Station, Texas, 1-98.
- Williams, G. L. & Downie, C. 1966. Further dinoflagellate cysts from the London Clay. *In: Davey, R. J., Downie, C., Sarjeant, W. A. S. & Williams, G. L. Studies on Mesozoic and Cainozoic dinoflagellate cysts*. Bulletin of the British Museum Natural History, London, (Geol. Suppl.) **3**, 215-235.
- Wilson, G. J. 1988. Paleocene and Eocene dinoflagellate cysts from Waipawa, Hawkes Bay, New Zealand. *New Zealand Geological Survey, Paleontological Bulletin* **57**, 96pp.

- Wilson, G. J. & Clowes, C. D. 1980. *A concise catalogue of organic-walled fossil dinoflagellate genera*. New Zealand Geological Survey, Department of Scientific and Industrial Research, New Zealand, 199 pp.
- Wing, S. L., Harrington, G. J., Smith, F. A., Bloch, J. I., Boyer, D. M. & Freeman, K. H. 2005. Transient floral change and rapid global warming at the Paleocene-Eocene boundary. *Science* **310**, 993-996.
- Wrenn, J. H. & Beckman, S. W. 1982. Maceral, total organic carbon, and palynological analyses of Ross Ice Shelf Project site J9 cores. *Science* **216**, 187-189.
- Wynne, A. 1872. Memoir on the geology of Kutch. *Memoirs of the Geological Survey of India* **9**, 1-289.
- Wynne, A. B. 1874. Notes on the geology of the neighborhood of Mari hill station in the Punjab. *Records of the Geological Survey of India* **7**, 64-74.
- Wynn, J. G., Bird, M. I. & Wong, V. N. L. 2005. Rayleigh distillation and the depth profile of $^{13}\text{C}/^{12}\text{C}$ ratios of soil organic carbon from soils of disparate texture in Iron Range National Park, Far North Queensland, Australia. *Geochimica et Cosmochimica Acta* **69**, 1961-1973.
- Yeats, R. S. & Lawrence, R. D. 1984. Tectonics of the Himalayan thrust belt in northern Pakistan. *In*: Haq, B. U. & Milliman, J. D. (Eds), *Marine Geology and Oceanography of Arabian Sea and Coastal Pakistan*, Van Nostrand Reinhold, New York, 177-198.
- Yeats, R. S. & Hussain, A. 1987. Timing of structural events in the Himalayan foothills of northwestern Pakistan. *Geological Society of America, Bulletin* **99**, 161-176.
- Zachos, J. C., Lohmann, K. C., Walker, J. C. G. & Wise, S. W. 1993. Abrupt climate change and transient climates during the Paleogene: a marine

- perspective. *Journal of Geology* **101**, 191-213.
- Zachos, J., Pagani, M., Sloan, L., Thomas, E. & Billups, K. 2001. Trends, rhythms, and aberrations in global climate 65 Ma to present. *Science* **292**, 686-693.
- Zachos, J. C., Wara, M. W., Bohaty, S., Delaney, M. L., Petrizzo, M. R., Brill, A., Bralower, T. J. & Premoli-Silva, I. 2003. A transient rise in tropical sea surface temperature during the Paleocene-Eocene Thermal Maximum. *Science* **302**, 1551-1554.
- Zachos, J. C., Röhl, U., Schellenberg, S. A., Sluijs, A., Hodell, D. A., Kelly, D. C., Thomas, E., Nicolo, M., Raffi, I., Lourens, L. J., McCarren, H. & Kroon, D. 2005. Rapid Acidification of the Ocean During the Paleocene-Eocene Thermal Maximum. *Science* **308**, 1611-1615.
- Zachos, J. C., Dickens, G. R. & Zeebe, R. E. 2008. An early Cenozoic perspective on greenhouse warming and carbon-cycle dynamics. *Nature* **451**, 279-283.

Appendix 1

Taxonomic notes on foraminifera and
table of foraminiferal composition
(in percent)

Taxonomic notes on planktonic foraminifera

This research work does not include a full taxonomic account but a list of the taxa used and references consulted to check species determination is provided.

Some of the references mentioned here are not given in the list of references.

Class **FORAMINIFERA** Lee (1990)

Order **GLOBIGERINIDA** Lankester (1885)

Family **GLOBOROTALIDAE** Cushman (1927)

Genus ***Acarinina*** Subbotina (1953)

Acarinina pseudotopilensis (Subbotina),

Acarinina pseudotopilensis; Subbotina (1953), Krasheninnikov & Hoskins (1973), Huber (1991)

Globorotalia pseudotopilensis (Subbotina); Stainforth et al. (1975)

Globorotalia (Acarinina) pseudotopilensis (Subbotina); Blow (1979)

Acarinina wilcoxensis (Cushman & Ponton)

Globorotalia wilcoxensis; Cushman & Ponton (1932), Bolli (1957), Samanta (1973), Stainforth et al. (1975)

Genus ***Globanomalina*** Haque (1956)

Globanomalina chapmani (Parr)

Globorotalia chapmani; Parr (1938), Berggren et al. (1967)

Globorotalia membranacea (Ehrenberg); LeRoy (1953)

Globorotalia elongata Glaessner; Bolli (1957)

Globorotalia elongata Glaessner; Loeblich & Tappan (1957)

Globorotalia troelseni; Loeblich & Tappan (1957)

Globorotalia emilei; El-Naggar (1966)

Globorotalia troelseni (Loeblich & Tappan); El-Naggar (1966)

Globorotalia chapmani (Parr); Berggren et al. (1967)

Globorotalia chapmani (Parr); Stainforth et al. (1976)

Globorotalia (Turborotalia) chapmani (Parr); Berggren et al. (1967), Blow (1979)

Globorotalia troelseni (Loeblich & Tappan); Blow (1979)

Planorotalites chapmani (Parr); Luger (1985), Toumarkine & Luterbacher (1985), Huber (1991)

Globorotalia chapmani (Parr); Haig et al. (1993)

Globanomalina chapmani (Parr); Olsson et al. (1999)

Globanomalina luxorensis (Nakkady)

Anomalina luxorensis; Nakkady (1950)

Anomalina luxorensis (Nakkady); LeRoy (1953)

Globanomalina ovalis; Haque (1956)

Globigerina pseudoiota; Hornibrook (1958)

Anomalina luxorensis (Nakkady); Nakkady (1959)

Globorotalia chapmani (Parr); Berggren et al. (1967)

Pseudohastigerina wilcoxensis (Cushman & Ponton); Berggren et al. (1967)

Pseudohastigerina pseudoiota (Hornibrook); Samanta (1973)

Pseudohastigerina wilcoxensis (Cushman & Ponton); Stainforth et al. (1975)

Globorotalia (Turborotalia) chapmani (Parr); Berggren et al. (1967), Blow (1979)

Globanomalina ovalis (Haque); Banner (1989)

Pseudohastigerina wilcoxensis (Cushman & Ponton); Stott & Kennett (1990)

Genus ***Pseudohastigerina*** Banner & Blow (1959)

Pseudohastigerina wilcoxensis (Cushman & Ponton)

Nonion wilcoxensis; Cushman & Ponton (1932)

Hastigerina eocaenica; Berggren (1960)

Pseudohastigerina wilcoxensis (Cushman & Ponton); Berggren et al. (1967),
Stainforth et al. (1975), Blow (1979), Luger (1985) Toumarkine & Luterbacher
(1985)

Genus ***Morozovella*** McGowran in Luterbacher (1964)

Morozovella acutispira (Bolli & Cita)

Globorotalia acutispira; Bolli & Cita (1960)

Globorotalia kolchidica; Morozova (1961), Stainforth et al. (1975), Snyder &
Waters (1985)

Morozovella acutispira (Bolli & Cita); Berggren & Norris (1997), Olsson et al.
(1999)

Morozovella acuta (Toulmin)

Globorotalia wilcoxensis; Cushman & Ponton var. *acuta* Toulmin (1941)

Globorotalia acuta (Toulmin); Loeblich & Tappan (1957), Stainforth et al. (1975)

Globorotalia parva (Ray); Samanta (1970), Samanta (1973)

Morozovella acuta (Toulmin); Samanta (1973), Toumarkine & Luterbacher
(1985), Berggren & Norris (1997), Olsson et al. (1999)

Globorotalia (Morozovella) velascoensis parva (Rey); Blow (1979)

Morozovella aragonensis (Nuttall)

Globorotalia aragonensis; Nuttall (1930), Subbotina (1953), Postuma (1971),
Samanta (1973), Stainforth et al. (1975)

Morozovella aragonensis (Nuttall); Toumarkine & Luterbacher (1985)

Globorotalia (Morozovella) aragonensis (Nuttall); Blow (1979)

Morozovella conicotruncata (Subbotina)

Globorotalia conicotruncata; Subbotina (1947), Samanta (1973), Stainforth et al.
(1975)

Globorotalia angulata abundcamerata; Bolli (1957), Bolli & Cita (1960)

Globorotalia abundcamerata (Bolli); Postuma (1971)

Globorotalia (Morozovella) angulata conicotruncata (Subbotina); Blow (1979)

Morozovella conicotruncata (Subbotina); Toumarkine & Luterbacher (1985),

Berggren & Norris (1997), Olsson et al. (1999)

Morozovella occlusa (Loeblich & Tappan)

Globorotalia occlusa; Loeblich & Tappan (1957), Stainforth et al. (1975)

Globorotalia (Morozovella) occlusa (Loeblich & Tappan); Blow (1979)

Morozovella occlusa (Loeblich & Tappan); Berggren & Norris (1997), Olsson et al. (1999)

Morozovella subbotinae (Morozova)

Globorotalia subbotinae; Morozova (1939), Samanta (1973), Stainforth et al. (1975)

Globorotalia rex (Martin); Postuma (1971)

Globorotalia (Morozovella) subbotinae subbotinae (Morozova); Blow (1979)

Morozovella subbotinae (Morozova); Toumarkine & Luterbacher (1985), Snyder & Waters (1985), Berggren & Norris (1997), Olsson et al. (1999)

Morozovella aequa (Cushman & Renz)

Globorotalia crassata (Cushman) var. *aequa*; Cushman & Renz (1942)

Globorotalia aequa (Cushman & Renz); Bolli (1957), Postuma (1971), Samanta (1973), Stainforth et al. (1975)

Globorotalia (Morozovella) aequa aequa (Cushman & Renz); Blow (1979)

Morozovella aequa (Cushman & Renz); Snyder & Waters (1985), Toumarkine & Luterbacher (1985)

Globorotalia (Morozovella) aequa lacerti (Cushman & Renz); Blow (1979)

Globorotalia (Morozovella) aequa tholiformis; Blow (1979)

Morozovella formosa formosa (Bolli)

Globorotalia formosa formosa ; Bolli (1957), Samanta (1973), Stainforth et al. (1975)

Globorotalia formosa (Bolli); Postuma (1971)

Morozovella formosa formosa (Bolli); Toumarkine & Luterbacher (1985)

Family **GLOBIGERINIDAE** Carpenter et al. (1862)

Genus ***Subbotina*** Brotzen & Pozaryska (1961)

Subbotina trangularis (White)

Globigerina trangularis; White (1928), Bolli (1957), Samanta (1973)

Subbotina trangularis trangularis (White); Blow (1979)

Subbotina tiangularis (White); Berggren & Norris (1997), Olsson et al. (1999)

Subbotina patagonica (Todd & Kniker)

Globigrina patagonica; Todd & Kniker (1952)

Subbotina patagonica (Todd & Kniker); Huber (1991), Berggren & Norris (1997)

Subbotina triloculinoides (Plummer)

Globigerina triloculinoides; Plummer (1926), Loeblich & Tappan (1957),

Stainforth et al. (1975), Toumarkine & Luterbacher (1985)

Subbotina triloculinoides triloculinoides (Plummer); Blow (1979)

Subbotina triloculinoides (Plummer); Berggren & Norris (1997), Olsson et al. (1999)

Subbotina velascoensis (Cushman)

Globigerina velascoensis; Cushman (1925), Bolli (1957), Samanta (1973),

Stainforth et al. (1975), Toumarkine & Luterbacher (1985)

Subbotina velascoensis (Cushman); Snyder & Waters (1985), Berggren & Norris (1997), Olsson et al. (1999)

Parasubbotina varianta (Subbotina)

Globigerina varianta; Subbotina (1953)

Subbotina varianta (Subbotina); Berggren (1992)

Parasubbotina varianta (Subbotina); Olsson et al. (1999)

Taxonomic notes on larger benthonic foraminifera

This research work does not include a full taxonomic account but a list of the taxa used and references consulted to check species determination is provided. Some of the references mentioned here are not given in the list of references.

Class **FORAMINIFERA** Lee (1990)

Order **ROTALIIDA** Lankester (1885)

Superfamily **NUMMULITACEAE** de Blainville (1825)

Family **NUMMULITIDAE** de Blainville (1825)

Subfamily **NUMMULITINAE** Carpenter (1850)

Genus ***Nummulites*** Lamarck (1801)

Nummulites sp. cf. ***N. atacicus*** Leymerie (1846)

Nummulites sp. cf. ***N. globulus*** Leymerie (1846).

Subfamily **PALAEONUMMULITINAE** Haynes et al. (2010)

Genus ***Assilina*** d'Orbigny (1826)

Assilina sp. cf. ***A. ranikoti*** (Nuttall)

Assilina ranikoti; Nuttall (1926)

Assilina ranikoti (Nuttall); Davies (1927)

Assilina ranikotensis (Nuttall); Nuttall (1931)

Assilina ranikoti (Nuttall); Schaub (1981)

Genus **Caudrina** Haynes et al. (2010)

Caudrina sp. cf. soldadensis Vaughan & Cole (1941)

Miscellanea soldadensis; Vaughan & Cole (1941)

Ranikothalia soldadensis (Vaughan & Cole); Caudri (1944)

Operculinoides georgianus; Cole & Herrick (1953)

Ranikothalia soldadensis (Vaughan & Cole); Drooger (1960)

Ranikothalia soldadensis (Vaughan & Cole); Caudri (1975)

Ranikothalia soldadensis (Vaughan & Cole); Caudri (1996)

Genus **Nummulitoides** Abrard (1956)

Nummulitoides sp. cf. N. inaequilateralis (Carter)

Nummulitoides inaequilateralis; Carter (1853)

Operculina inaequilateralis; Carter (1853)

Genus **Operculina** d'Orbigny (1826)

Operculina sp. cf. O. hardiei (d'Archiac & Haime)

Operculina hardiei; d'Archiac & Haime (1853)

Operculina hardiei (d'Archiac & Haime); Racey (1995)

Genus **Paleonummulites** Schubert (1908)

Genus **Ranikothalia** Caudri (1944)

Ranikothalia sp. cf. R. nuttalli kohatica (Davies)

Ranikothalia nuttalli kohatica; Davies (1927)

Nummulites nuttalli var. *kohaticus*; Davies (1927)

Nummulites nuttalli; sensu Sirel (1976)

Ranikothalia nuttalli; sensu Haynes (1988)

Ranikothalia nuttalli; sensu Racey (1995)

Suborder **ROTALIINA** Delage & Hérouard (1896)

Superfamily **NUMMULITACEAE** de Blainville (1825)

Family **DISCOCYCLINIDAE** Galloway (1928)

Genus ***Discocyclina*** Gümbel (1870)

Orbitoides (*Discocyclina*); Gümbel (1870)

Discocyclina (Gumbel); Loeblich & Tappan (1988)

Actinocyclina (Gumbel); Loeblich & Tappan (1988)

Family **PELLATISPIRIDAE** Hanzawa (1937)

Genus ***Miscellanea*** Pfender (1935)

Suborder **MILIOLINA** Delage & Hérouard (1896)

Superfamily **ALVEOLINACEAE** Ehrenberg (1839)

Family **RHAPYDIONINIDAE** Keijzer (1945)

Subfamily **RHAPYDIONININAE** Keijzer (1945)

Genus ***Alveolina*** d'Orbigny (1826)

Family **SORITIDAE** Ehrenberg (1839)

Subfamily **SORITINAE** Ehrenberg (1839)

Genus ***Orbitolites*** Lamarck (1801)

Suborder **ROTALIINA** Delage & Hérouard (1896)

Superfamily **ORBITOIDACEA** Schwager (1876)

Family **ROTALIIDAE** Ehrenberg (1839)

Subfamily **ROTALIINAE** Ehrenberg (1839)

Genus ***Lockhartia*** Davies (1932)

Taxonomic notes on smaller benthonic foraminifera

This research work does not include a full taxonomic account but a list of the taxa used and references consulted to check species determination is provided. Some of the references mentioned here are not given in the list of references.

Anomalinoids* sp. cf. *A. acutus (Plummer)

Anomalina ammonoides (Reuss) var. *acuta*; Plummer (1926)

Anomalina acuta (Plummer); Cushman (1951)

Gyroidinoides* sp. cf. *G. octocameratus (Cushman & Hanna)

Gyroidina soldanii (d'Orbigny) *octocamerata*; Cushman & Hanna (1927)

Gyroidina octocamerata (Cushman & Hanna); Kuhn (1992)

Cibicidoides* sp. cf. *C. decoratus (LeRoy)

Cibicidoides decoratus; LeRoy (1953)

Gaudryina* sp. cf. *G. ellisorae (Cushman)

Gaudryina (*Pseudogaudryina*) *ellisorae*; Cushman (1936)

Gaudryina (*Pseudogaudryina*) *ellisorae* (Cushman); Cushman (1946)

Lagena* sp. cf. *L. sulcata (Walker & Jacob); LeRoy (1953)

Gaudryina* sp. cf. *G. africana (LeRoy)

Gaudryina africana; LeRoy (1953)

Marssonella* sp. cf. *M. oxyconus (Reuss); LeRoy (1953)

Coryphostoma* sp. cf. *C. midwayensis (Cushman); Tjalsma & Lohmann (1983)

Siphogenerinoides* sp. cf. *S. eleganta (Plummer)

Siphogenerina eleganta; Plummer (1926)

Siphogenerinoides eleganta (Plummer); LeRoy (1953)

Siphogenerinoides eleganta (Plummer); Aubert & Berggren (1976)

Gavelinella* sp. cf. *G. beccariiformis (White)

Rotalia beccariiformis; White (1928)

Gavelinella beccariiformis (White); Aubert & Berggren (1976)

Stensioeina beccariiformis (White); Salaj et al. (1976)

Gavelinella beccariiformis (White); Dailey (1983)

Gavelinella beccariiformis (White); Tjalsma & Lohmann (1983)

Stensioina beccariiformis (White); Van Morkhoven (1986)

Gavelinella beccariiformis (White); Thomas (1990)

Stensioeina beccariiformis (White); Nomura (1991)

Stensioina beccariiformis (White); Katz & Miller (1991)

Valvulineria beccariiformis (White); Kuhn (1992)

Gavelinella beccariiformis (White); Widmark & Malmgren (1992)

Genera	Samples >125µm														
	Td-30	Td-31	Td-32	Td-33	Td-35-Td-41	Td-34	Td-42	Td-43	Td-44	Td-45	Td-46	Td-47	Td-48	Td-49	Td-50
Subbotina	70.0		135.0	100.0	Interval barren of foraminifera		113.0	119.0	160.0	117.0		120.0	132.0		173.0
Acarinina	29.0		27.0	49.0			56.0	57.0	46.0	52.0		47.0	47.0		89.0
Morozovella	151.0		110.0	106.0			92.0	82.0	112.0	135.0		131.0	93.0		44.0
Globanomalina	3.0		3.0	2.0			14.0	4.0	8.0	3.0		2.0	3.0		0.0
others	36.0		4.0	32.0			18.0	14.0	4.0	2.0		12.0	12.0		0.0
Benthics	31.0		22.0	21.0			22.0	15.0	9.0	3.0		12.0	20.0		7.0
Total count	302.0		323.0	294.0			303.0	284.0	337.0	311.0		316.0	301.0		306.0
Subbotina (%)	23.2		41.8	34.0			37.3	41.9	47.5	37.6		38.0	43.9		56.5
Acarinina (%)	9.6		8.4	16.7			18.5	20.1	13.6	16.7		14.9	15.6		29.1
Morozovella (%)	50.0		34.1	36.1			30.4	28.9	33.2	43.4		41.5	30.9		14.4
P-ratio	90.3		97.8	93.2		93.0	94.8	97.3	99.0		96.3	93.5		97.8	

Table-1: Foraminiferal composition (in percent) from the Rakhi Nala section, Sulaiman Range, Lower Indus Basin (Pakistan). Blue bars= samples which were thin sectioned only. Orange coloured row= sample names, Yellow coloured row= total foraminiferal count.

Appendix 2

List of dinocyst species, taxonomic
notes on dinocysts and geochemical
data

Dinocyst complexes	Td-30	Td-32	Td-33	Td-35	Td-36	Td-37	Td-38	Td-39	Td-40	Td-41	Td-42	td43	td45	td46	td49	td50
<i>Apectodinium</i>	6	6	26	59	61	88	123	45	74	9	44	14	3	0	1	3
<i>Spiniferites</i> (<i>hystrichosphaera</i>) association	100	80	82	26	86	74	55	206	88	141	41	4	96	4	64	105
<i>Adnatosphaeridium</i>	2	6	0	32	40	14	7	8	3	15	2	0	2	3	3	22
<i>Hystrichokolpoma</i>	0	3	1	0	0	0	1	4	0	1	3	0	0	0	2	2
<i>Achomosphaera</i>	65	39	32	26	19	43	16	13	11	41	71	16	64	5	39	37
<i>Polysphaeridium</i>	0	5	3	18	8	12	32	7	20	16	16	9	9	3	2	14
<i>Kallosphaeridium</i>	3	1	2	2	1	11	0	0	1	6	0	0	0	0	0	2
<i>Dyphyes</i>	0	5	4	0	13	5	6	2	2	5	0	1	1	1	0	3
<i>Wetzelialla</i>	0	6	9	3	2	14	1	0	0	2	0	0	0	0	0	0
<i>Operculodinium</i>	0	9	19	68	21	25	43	9	32	27	36	35	12	8	7	21
<i>Cordosphaeridium</i>	4	5	2	38	38	25	34	20	15	13	10	0	16	1	4	20
<i>Hystrichospharedium</i>	7	9	6	17	17	17	15	5	2	2	0	0	15	0	8	6
<i>Thalassiphora</i>	0	0	5	28	27	15	40	4	3	13	0	0	4	0	0	14
<i>Deflandrea</i>	0	0	1	5	2	0	0	0	0	0	0	0	0	0	0	0
<i>Glaphyrocysta</i>	1	0	0	5	0	0	0	0	0	2	1	0	0	0	0	0
<i>Homotryblum</i>	0	0	0	0	0	0	5	1	0	0	0	0	30	0	1	0
Total	188	174	192	327	335	343	378	324	251	293	224	79	252	25	131	249

Table-2: Dinocyst composition (actual counts) from Rakhi Nala section, Sulaiman Range Pakistan.

Dinocyst complexes	Td30	Td32	Td33	Td35	Td36	Td37	Td38	Td39	Td40	Td41	Td42	Td43	Td45	Td46	Td49	Td50
<i>Apectodinium</i>	3.2	3.4	13.5	18.0	18.2	25.7	32.5	13.9	29.5	3.1	19.6	17.7	1.2	0.0	0.8	1.2
<i>Spiniferites</i> (<i>hystrichosphaera</i>) association	53.2	46.0	42.7	8.0	25.7	21.6	14.6	63.6	35.1	48.1	18.3	5.1	38.1	16.0	48.9	42.2
<i>Adnatosphaeridium</i>	1.1	3.4	0.0	9.8	11.9	4.1	1.9	2.5	1.2	5.1	0.9	0.0	0.8	12.0	2.3	8.8
<i>Hystrichokolpoma</i>	0.0	1.7	0.5	0.0	0.0	0.0	0.3	1.2	0.0	0.3	1.3	0.0	0.0	0.0	1.5	0.8
<i>Achomosphaera</i>	34.6	22.4	16.7	8.0	5.7	12.5	4.2	4.0	4.4	14.0	31.7	20.3	25.4	20.0	29.8	14.9
<i>Polysphaeridium</i>	0.0	2.9	1.6	5.5	2.4	3.5	8.5	2.2	8.0	5.5	7.1	11.4	3.6	12.0	1.5	5.6
<i>Kallosphaeridium</i>	1.6	0.6	1.0	0.6	0.3	3.2	0.0	0.0	0.4	2.0	0.0	0.0	0.0	0.0	0.0	0.8
<i>Dyphyes</i>	0.0	2.9	2.1	0.0	3.9	1.5	1.6	0.6	0.8	1.7	0.0	1.3	0.4	4.0	0.0	1.2
<i>Wetzeliella</i>	0.0	3.4	4.7	0.9	0.6	4.1	0.3	0.0	0.0	0.7	0.0	0.0	0.0	0.0	0.0	0.0
<i>Operculodinium</i>	0.0	5.2	9.9	20.8	6.3	7.3	11.4	2.8	12.7	9.2	16.1	44.3	4.8	32.0	5.3	8.4
<i>Cordosphaeridium</i>	2.1	2.9	1.0	11.6	11.3	7.3	9.0	6.2	6.0	4.4	4.5	0.0	6.3	4.0	3.1	8.0
<i>Hystrichospheredium</i>	3.7	5.2	3.1	5.2	5.1	5.0	4.0	1.5	0.8	0.7	0.0	0.0	6.0	0.0	6.1	2.4
<i>Thalassiphora</i>	0.0	0.0	2.6	8.6	8.1	4.4	10.6	1.2	1.2	4.4	0.0	0.0	1.6	0.0	0.0	5.6
<i>Deflandrea</i>	0.0	0.0	0.5	1.5	0.6	0.0	0.0	0.0	0.0	0.0	0.0	0.0	0.0	0.0	0.0	0.0
<i>Glaphyrocysta</i>	0.5	0.0	0.0	1.5	0.0	0.0	0.0	0.0	0.0	0.7	0.4	0.0	0.0	0.0	0.0	0.0
<i>Homotryblum</i>	0.0	0.0	0.0	0.0	0.0	0.0	1.3	0.3	0.0	0.0	0.0	0.0	11.9	0.0	0.8	0.0
P-Cyst (%)	3.19	6.90	18.75	20.49	19.40	29.74	32.80	13.89	29.48	3.75	19.64	17.72	1.19	0.00	0.76	1.20
P-Cyst	6.0	12.0	36.0	67.0	65.0	102.0	124.0	45.0	74.0	11.0	44.0	14.0	3.0	0.0	1.0	3.0
G-Cyst	182.0	162.0	156.0	260.0	270.0	241.0	254.0	279.0	177.0	282.0	180.0	65.0	249.0	25.0	130.0	246.0
P/G ratio	0.03	0.07	0.19	0.20	0.19	0.30	0.33	0.14	0.29	0.04	0.20	0.18	0.01	0.00	0.01	0.01

Table-2(continued): Dinocyst composition (in percent), peridinioid cyst (P-cyst) in percent and P/G ratio from Rakhi Nala section, Sulaiman Range Pakistan.

Td Sample number	% TOC	%N	C/N _{TOC}
30	0.4	0.1	6.4
31	0.5	0.0	10.4
32	0.6	0.1	7.4
33	0.4	0.1	5.2
34	0.5	0.0	16.9
35	0.4	0.1	6.6
36	0.4	0.1	6.9
37	0.4	0.1	7.2
38	0.4	0.1	6.9
39	0.5	0.1	8.0
40	0.5	0.1	7.7
41	5.6	0.2	31.4
42	0.9	0.1	13.4
43	2.1	0.1	16.7
44	0.5	0.1	6.8
45	0.4	0.1	7.0
46	1.6	0.1	17.1
47	0.5	0.1	6.9
48	0.3	0.0	6.8

Table-3: TOC (%), Nitrogen (%), C/N_{TOC} ratio from Rakhi Nala Section, Sulaiman Range, Lower Indus Basin, Pakistan.

Dinocysts assemblage from Rakhi Nala section

This research work does not include a full taxonomic account but a list of the taxa used and references consulted to check species determination is provided.

Achomosphaera* sp. cf. *A. ramulifera

Hystrichosphaera cf. *ramosa* (Ehrenberg); Deflandre (1935)

Hystrichosphaeridium ramuliferum; Deflandre (1937)

Baltisphaeridium ramuliferum (Deflandre); Downie & Sarjeant (1963)

Achomosphaera ramulifera (Deflandre); Evitt (1963)

Adnatosphaeridium* sp. cf. *A. multispinosum

Williams & Downie *in* Davey et al. (1966)

Apectodinium* *homomorphum

Hystrichosphaeridium geometricum; Pastsiels (1948)

Wetzeliella homomorpha; Deflandre & Cookson (1955)

Apectodinium homomorphum; Lentin & Williams (1977)

Apectodinium hyperacanthum

Cookson & Eisenack (1965), Lentin & Williams (1977)

Apectodinium paniculatum

Costa & Downie (1976), Lentin & Williams (1977)

Apectodinium quinquelatum

Hystrichosphaeridium geometricum; Pastsiels (1948)

Wetzeliella cf. *ovalis*; Eisenack (1961)

Apectodinium quinquelatum; Williams & Downie (1966), Costa & Downie (1979)

Minisphaeridium latirictum

Cordosphaeridium minimum; Morgenroth (1966), Davey & Williams (1969),

Benedek (1972)

Minisphaeridium latirictum; Fensome et al. (2009)

Cordosphaeridium* sp. cf. *C. exilimum

Davey & Williams (1966)

Deflandrea* sp. cf. *D. phosphoritica

Cookson & Eisenack (1961)

Diphyes* sp. cf. *D. colligerum

Hystrichosphaeridium sp.; Cookson (1953)

Hystrichosphaeridium colligerum; Deflandre & Cookson (1955)

Hystrichosphaeridium colligerum; Deflandre & Cookson (1962)

Baltisphaeridium colligerum (Deflandre & Cookson); Downie & Sarjeant (1963)

Diphyes colligerum (Deflandre & Cookson); Cookson (1965)

Glaphyrocysta* sp. cf. *G. retiintexta

Cookson (1965), Stover & Evitt (1978)

Homotryblium* sp. cf. *H. tenuispinosum

Davey & Williams (1966)

Hystrichokolpoma* sp. cf. *H. manipulatum

Islam (1983)

Hystrichokolpoma* sp. cf. *H. unispinum

Klump (1953)

***Hystrichosphaera* sp. cf. *H. ramosa* (Ehrenberg)**

Xanthidium ramosum; Ehrenberg (1838)

Xanthidium furcatum; Ehrenberg (1838)

Xanthidium ramosum; Ehrenberg (1854)

Xanthidium furcatum; Ehrenberg (1854)

Hystrichosphaera furcata (Ehrenberg); Wetzel (1932)

Hystrichosphaera ramosa (Ehrenberg); Wetzel (1932)

Hystrichosphaera furcata (Ehrenberg); Deflandre (1935)

Hystrichosphaera ramosa (Ehrenberg); Deflandre (1937)
Hystrichosphaera ramosa (Ehrenberg); Lejeune (1937)
Hystrichosphaera furcata (Ehrenberg); Conrad (1941)
Hystrichosphaera furcata (Ehrenberg); Deflandre (1947)
Hystrichosphaera ramosa (Ehrenberg); Deflandre (1947)
Hystrichosphaera furcata (Ehrenberg); Deflandre (1952)
Hystrichosphaera ramosa (Ehrenberg); Deflandre (1952)
Hystrichosphaera furcata (Ehrenberg); Cookson & Hughes (1964)

Hystrichosphaeridium (Deflandre)
Hystrichosphaeridium; Deflandre (1937)
Hystrichosphaeridium (Deflandre); Eisenack (1958)

Muratodinium (Drugg)
Muratodinium; Drugg (1970)

Operculodinium* sp. cf. *O. bergmannii
Archangelsky (1969), Stover & Evitt (1978)

Polysphaeridium* sp. cf. *P. asperum
Maier (1959), Davey & Williams (1969)

***Spiniferites* sp.** Mantell (1850), Sarjeant (1970)
Hystrichosphaera; Wetzel (1933)
Hystrichokibotium; Klump (1953)

Thalassiphora* sp. cf. *T. pelagica (Eisenack)
Bion pelagicum; Eisenack (1938)
Pterospermopsis pelagica (Eisenack); Eisenack (1954)
Thalassiphora pelagica (Eisenack); Eisenack & Gocht (1960)
Pterospermopsis pelagica (Eisenack); Gerlach (1961)
Thalassiphora pelagica (Eisenack); Gerlach (1963)

Thalassiphora pelagica (Eisenack); Brosius (1963)

Wetziella astra

Costa et al. (1978)

Appendix 3

Stable isotope data of the carbonate
fraction (bulk and fine fraction) from the
Rakhi Nala section, Indus Basin
(Pakistan)

Sample Number	Name	$\delta^{13}\text{C}$	$\delta^{18}\text{O}$
Sample No/s	Data file name/s	final	final
17	260409 TD50 203.raw	0.50	-6.84
18	260409 TD49 233.raw	0.63	-6.62
19	260409 TD48 122.raw	-0.40	-7.58
20	260409 TD47 112.raw	0.12	-7.83
21	260409 TD46 096.raw	-1.08	-8.38
22	260409 TD45 129.raw	-0.11	-8.08
23	260409 TD44 124.raw	0.00	-7.44
24	260409 TD43 124.raw	-1.41	-7.80
25	260409 TD42 151.raw	0.30	-6.26
26	260409 TD41 186.raw	0.04	-6.51
27	260409 TD40 240.raw	0.07	-7.45
29	260409 TD39 335.raw	-0.38	-8.21
32	260409 TD36 958.raw	-4.13	-8.02
35	260409 TD34 142.raw	-0.92	-7.50
36	260409 TD33 186.raw	-0.33	-6.78
37	260409 TD32 216.raw	-0.41	-7.21
38	260409 TD31 198.raw	-0.62	-7.46
39	260409 TD30 232.raw	-1.03	-7.49

Table-4: Stable isotope data of the carbonate fraction (in bulk) from the Rakhi Nala section, Sulaiman Range, Indus Basin (Pakistan).

Name	Sample Number	$\delta^{13}\text{C}$ Final	average C	std	$\delta^{18}\text{O}$ final	average O	std
080609 TD30.raw	Td30.00	-0.66	-0.60	0.28	-7.55	-7.40	0.46
080609TD30B.raw	Td30.00	-0.95			-7.34		
230609 TD30.raw	Td30.00	-0.45			-7.90		
240609 TD30.raw	Td30.00	-0.32			-6.80		
230609 TD31.raw	Td31.00	-1.14	-1.01	0.25	-7.77	-7.40	0.51
240609 TD31.raw	Td31.00	-1.04			-7.60		
290609 TD31.raw	Td31.00	-0.65			-6.64		
290609 D31B.raw	Td31.00	-1.23			-7.59		
230609 TD32.raw	Td32.00	-0.93	-0.83	0.07	-6.59	-6.60	0.14
240609 TD32.raw	Td32.00	-0.79			-6.70		
290609 TD32.raw	Td32.00	-0.79			-6.40		
290609 D32B.raw	Td32.00	-0.80			-6.71		
080609 TD33.raw	Td33.00	-0.70	-0.66	0.05	-6.91	-6.80	0.08
080609 D33B.raw	Td33.00	-0.59			-6.80		
230609 TD33.raw	Td33.00	-0.67			-6.76		
240609 TD33.raw	Td33.00	-0.67			-6.73		
230609 TD34.raw	Td34.00	-1.12	-1.03	0.09	-7.32	-6.96	0.36
240609 TD34.raw	Td34.00	-1.01			-7.15		
290609 TD34.raw	Td34.00	-1.06			-6.86		
290609 D34B.raw	Td34.00	-0.92			-6.51		
080609 TD35.raw	Td35.00	-1.12	-1.95	0.56	-7.92	-9.34	1.46
080609 D35B.raw	Td35.00	-2.30			-8.61		
230609 TD35.raw	Td35.00	-2.23			-11.29		
240609 TD35.raw	Td35.00	-2.14			-9.55		
230609 TD36.raw	Td36.00	-4.58	-4.28	0.23	-8.65	-11.38	2.39

Table-5: Stable Isotope data of the carbonate fine fraction from the Rakhi Nala section, Indus Basin (Pakistan).

Name	Sample Number	$\delta^{13}\text{C}$ Final	average C	std	$\delta^{18}\text{O}$ final	average O	std
240609 TD36.raw	Td36.00	-4.14			-13.10		
290609 D36B.raw	Td36.00	-4.33			-12.40		
300609 TD36.raw	Td36.00	-4.06			-11.45		
300609TD36B.raw	Td36.00	-4.52			-10.32		
230609 TD37.raw	Td37.00	-7.66			-9.39		
290609 TD37.raw	Td37.00	-7.49			-11.18		
290609TD37B.raw	Td37.00	-5.16	-5.43	0.62	-8.71	-8.03	0.86
290609TD37C.raw	Td37.00	-4.71			-6.87		
290609TD37D.raw	Td37.00	-5.74			-8.72		
300609 TD37.raw	Td37.00	-6.11			-8.50		
300609TD37B.raw	Td37.00	-5.03			-7.35		
080609 TD38.raw	Td38.00	-1.72	-1.86	0.16	-10.01	-9.10	0.62
080609TD38B.raw	Td38.00	-1.88			-8.95		
300609 TD38.raw	Td38.00	-1.77			-8.78		
300609TD38B.raw	Td38.00	-2.09			-8.66		
230609 TD39.raw	Td39.00	-0.66	-0.47	0.29	-7.75	-7.35	0.45
240609 TD39.raw	Td39.00	-0.66			-7.47		
290609 TD39.raw	Td39.00	-0.04			-6.70		
290609TD39B.raw	Td39.00	-0.53			-7.50		
230609 TD40.raw	Td40.00	-0.18	0.01	0.14	-7.03	-6.85	0.14
240609 TD40.raw	Td40.00	0.15			-6.86		
290609 TD40.raw	Td40.00	0.01			-6.81		
290609TD40B.raw	Td40.00	0.06			-6.70		
080609TD41B.raw	Td41.00	0.02	-0.07	0.14	-6.55	-6.48	0.14
230609 TD41.raw	Td41.00	-0.14			-6.30		

Table-5 (continued): Stable isotope data of the carbonate fine fraction from the Rakhi Nala section, Indus Basin (Pakistan).

Name	Sample Number	$\delta^{13}\text{C}$ Final	average C	std	$\delta^{18}\text{O}$ final	average O	std
240609 TD41.raw	Td41.00	0.06			-6.43		
290609 TD41.raw	Td41.00	-0.23			-6.64		
080609 TD42.raw	Td42.00	-0.16	-0.14	0.13	-6.36	-6.30	0.15
080609TD42B.raw	Td42.00	-0.22			-6.48		
230609 TD42.raw	Td42.00	-0.23			-6.20		
240609 TD42.raw	Td42.00	0.06			-6.15		
080609 TD43.raw	Td43.00	-1.71	-1.82	0.09	-7.31	-7.25	0.15
080609TD43B.raw	Td43.00	-1.80			-7.41		
230609 TD43.raw	Td43.00	-1.86			-7.23		
290609 TD43.raw	Td43.00	-1.93			-7.05		
080609 TD44.raw	Td44.00	-0.64	-0.45	0.28	-7.14	-7.15	0.05
080609TD44B.raw	Td44.00	-0.49			-7.22		
230609 TD44.raw	Td44.00	-0.62			-7.15		
240609 TD44.raw	Td44.00	-0.04			-7.10		
080609 TD45.raw	Td45.00	-0.40	-0.38	0.16	-7.47	-7.45	0.06
080609TD45B.raw	Td45.00	-0.40			-7.36		
230609 TD45.raw	Td45.00	-0.56			-7.47		
240609 TD45.raw	Td45.00	-0.17			-7.49		
230609 TD46.raw	Td46.00	-1.31	-1.42	0.66	-7.53	-7.57	1.06
240609 TD46.raw	Td46.00	-1.17			-7.81		
290609 TD46.raw	Td46.00	-2.37			-8.75		
290609TD46B.raw	Td46.00	-0.84			-6.18		
080609 TD47.raw	Td47.00	-0.33	-0.45	0.14	-7.50	-7.35	0.11
080609TD47B.raw	Td47.00	-0.33			-7.25		
230609 TD47.raw	Td47.00	-0.56			-7.36		

Table-5 (continued): Stable isotope data of the carbonate fine fraction from the Rakhi Nala section, Indus Basin (Pakistan).

Name	Sample Number	$\delta^{13}\text{C}$ Final	average C	std	$\delta^{18}\text{O}$ final	average O	std
240609 TD47.raw	Td47.00	-0.59			-7.28		
230609 TD48.raw	Td48.00	-1.12	-0.39	0.53	-9.23	-6.83	1.86
240609 TD48.raw	Td48.00	-0.31			-7.10		
290609 TD48.raw	Td48.00	-0.27			-6.20		
290609TD48B.raw	Td48.00	0.16			-4.80		
240609 TD49.raw	Td49.00	-0.64	0.15	0.53	-8.23	-6.64	1.08
290609 TD49.raw	Td49.00	0.34			-5.99		
290609TD49B.raw	Td49.00	0.48			-6.38		
290609TD49C.raw	Td49.00	0.43			-5.96		
230609 TD50.raw	Td50.00	-0.11	0.00	0.08	-6.74	-6.68	0.09
240609 TD50.raw	Td50.00	0.06			-6.77		
290609 TD50.raw	Td50.00	0.00			-6.57		
290609TD50B.raw	Td50.00	0.04			-6.65		

Table-5 (continued): Stable isotope data of the carbonate fine fraction from the Rakhi Nala section, Indus Basin (Pakistan).

Present work	Sluijs et al., 2007b		Present work	Bolle et al., 2000	Crouch et al., 2003	Sluijs et al., 2007b
Rakhi Nala	Bass River	Wilson lake	Rakhi Nala	Aktumsuk, Uzbekistan	Tawanui, Newzealand	North sea
Dinoflagellate isotope record			Total organic carbon isotopic record			
$\delta^{13}C_{FF}$ (‰ VPDB)	$\delta^{13}C_{DINO}$ (‰ VPDB)	$\delta^{13}C_{DINO}$ (‰ VPDB)	$\delta^{13}C_{TOC}$ (‰ VPDB)	$\delta^{13}C_{TOC}$ (‰ VPDB)	$\delta^{13}C_{TOC}$ (‰ VPDB)	$\delta^{13}C_{TOC}$ (‰ VPDB)
-25.5	-22.61	-19.96	-25.1	-24.3	-28.2	-25.44
-25.4	-23	-21.17	-26.1	-28.64	-28.2	-26.31
-25.6	-21.62	-21.64	-22.2	-30.35	-28.2	-26.33
-26.2	-23.86	-23.28	-25.1	-30.22	-28.3	-26.09
-26.1	-24.04	-22.84	-25.6	-28.84	-28.3	-26.25
-25.8	-23.81	-23.34	-25.6	-29.83	-28.2	-26.11
-25.0	-23.76	-22.8	-25.1	-29.05	-28.3	-26.67
-25.4	-24.1	-23.25	-25.5	-28.55	-27.5	-27.28
-25.3	-24.21	-23.18	-25.2		-28.0	-28.38
-25.3	-23.8	-23.82	-25.8		-28.2	-28.25
-25.3	-23.84	-22.94	-25.5		-29.0	-29.13
-25.7	-24.16	-22.09	-24.8		-28.5	-28.92
-26.4	-24.24	-22.35	-23.5		-28.6	-29.59
-27.2	-25.27	-22.49	-28.9		-29.4	-29.76
-26.7	-25.61	-21.69	-26.6		-29.3	-28.58
-26.3	-25.73	-20.89	-26.8		-29.4	-29.63
-27.4	-25.79	-21.55	-28.3		-29.5	-29.57
-25.7	-28.45	-20.82	-26.8		-29.3	-28.28
-25.3	-28.12	-23.07	-26.7		-29.4	-31.45
-26.4	-28.8	-23.33			-29.3	-31.70
-25.4	-28.52	-23.85			-29.0	-30.56
	-28.14	-22.45			-28.9	-31.76
	-27.63	-23.44			-28.6	-32.11
	-28.26	-23.48				-31.26
	-28.64	-24.37				-31.79
	-28.3	-23.02				-30.53
	-28.14	-22.56				-31.49
	-27.43	-23.13				-31.73
	-28.09	-24.39				-31.68
	-27.66	-25.46				-31.21
	-27.49	-25.31				-28.62
	-26.64	-25.85				-29.16
	-26.67	-25.99				26.89
		-26.19				
		-26.29				
		-26.89				
		-27.7				
		-27.64				
		-27.77				
		-27.72				
		-27.87				
		-27.89				
		-26.87				
		-26.91				
		-27.45				
		-26.69				
		-27.61				
		-27.16				
		-26.82				
		-24.67				
		-25.19				
		-22.96				

Table 6: Comparison of $\delta^{13}C$ (organic) values from Rakhi Nala with other global sections, **bold** values show the CIE.

Appendix 4

Samples collected from Indus Basin,
Pakistan.

Sample	Field section	Remarks	Sample	Field section	Remarks
DS0	Dalla	Used	DS24	Dalla	Used for larger foraminifera and microfacies
DS1	Dalla	Used	DS25	Dalla	Used
DS2	Dalla	Used	DS26	Dalla	Used for larger foraminifera and microfacies
DS3	Dalla	Used	DS27	Dalla	Used
DS4	Dalla	Used	DS28	Dalla	Used for larger foraminifera and microfacies
DS5	Dalla	Used	DS29	Dalla	Used for larger foraminifera and microfacies
DS6	Dalla	Used	DS30	Dalla	Used for larger foraminifera and microfacies
DS7	Dalla	Used	DS31	Dalla	Used for larger foraminifera and microfacies
DS8	Dalla	Used	DS32	Dalla	Used for larger foraminifera and microfacies
DS9	Dalla	Used	DS33	Dalla	Used
DS10	Dalla	Used	DS34	Dalla	Used
DS11	Dalla	Used	DS35	Dalla	Used
DS12	Dalla	Used	DS36	Dalla	Used
DS13	Dalla	Used	DS37	Dalla	Used for larger foraminifera and microfacies
DS14	Dalla	Used	DS38	Dalla	Used for larger foraminifera and microfacies
DS15	Dalla	Used	DS39	Dalla	Used for larger foraminifera and microfacies
DS16	Dalla	Used	DS40	Dalla	Used
DS17	Dalla	Used			
DS18	Dalla	Used			
DS19	Dalla	Used			
DS20	Dalla	Used for larger foraminifera and microfacies			
DS21	Dalla				
DS22	Dalla	Used for larger foraminifera and microfacies			
DS23	Dalla	Used for larger foraminifera and microfacies			

Sample	Field section	Remarks	Sample	Field section	Remarks
KD1	Kali Dilli	Used for larger foraminifera and microfacies	KD25	Kali Dilli	Used for larger foraminifera and microfacies
KD2	Kali Dilli	Used	KD26	Kali Dilli	Used
KD3	Kali Dilli	Used	KD27	Kali Dilli	Used
KD4	Kali Dilli	Used for larger foraminifera and microfacies	KD28	Kali Dilli	Used
KD5	Kali Dilli	Used	KD29	Kali Dilli	Used
KD6	Kali Dilli	Used	KD30	Kali Dilli	Used for larger foraminifera and microfacies
KD7	Kali Dilli	Used	KD31	Kali Dilli	Used for larger foraminifera and microfacies
KD8	Kali Dilli	Used	KD32	Kali Dilli	Used
KD9	Kali Dilli	Used	KD33	Kali Dilli	Used
KD10	Kali Dilli	Used	KD34	Kali Dilli	Used
KD11	Kali Dilli	Used	KD35	Kali Dilli	Used for larger foraminifera and microfacies
KD12	Kali Dilli	Used for larger foraminifera and microfacies	NS1	Neka	Not used
KD13	Kali Dilli		NS2	Neka	Not used
KD14	Kali Dilli	Used for larger foraminifera and microfacies	NS3	Neka	Not used
KD15	Kali Dilli	Used for larger foraminifera and microfacies	NS4	Neka	Not used
KD16	Kali Dilli	Used for larger foraminifera and microfacies	NS5	Neka	Not used
KD17	Kali Dilli	Used	NS6	Neka	Not used
KD18	Kali Dilli	Used for larger foraminifera and microfacies	NS7	Neka	Not used
KD19	Kali Dilli	Used for larger foraminifera and microfacies	NS8	Neka	Not used
KD20	Kali Dilli	Used	NS9	Neka	Not used
KD21	Kali Dilli	Used	NS10	Neka	Not used
KD22	Kali Dilli	Used	NS11	Neka	Not used
KD23	Kali Dilli	Used	NS12	Neka	Not used
KD24	Kali Dilli	Used	NS13	Neka	Not used

Sample	Field section	Remarks	Sample	Field section	Remarks
NS14	Neka	Not used	Tp26	Nammal gorge	Not used
NS15	Neka	Not used	Tp27	Nammal gorge	Not used
NS16	Neka	Not used	Tp28	Nammal gorge	Not used
NS17	Neka	Not used	Tp29	Nammal gorge	Not used
NS18	Neka	Not used	Tp30	Nammal gorge	Not used
NS19	Neka	Not used	Tp31	Nammal gorge	Not used
NS20	Neka	Not used	Tp32	Nammal gorge	Not used
NS21	Neka	Not used	Tp33	Nammal gorge	Not used
NS22	Neka	Not used	Tp34	Nammal gorge	Not used
NS23	Neka	Not used	Tp35	Nammal gorge	Not used
NS24	Neka	Not used	Tp36	Nammal gorge	Not used
NS25	Neka	Not used	Tp37	Nammal gorge	Not used
NS26	Neka	Not used	Tp38	Nammal gorge	Not used
NS27	Neka	Not used	Tp39	Nammal gorge	Not used
NS28	Neka	Not used	Tp40	Nammal gorge	Not used
NS29	Neka	Not used	Tp41	Nammal gorge	Not used
Tp1	Nammal gorge	Not used	Tp42	Nammal gorge	Not used
Tp2	Nammal gorge	Not used	Tp43	Nammal gorge	Not used
Tp3	Nammal gorge	Not used	Tp44	Nammal gorge	Not used
Tp4	Nammal gorge	Not used	Tp45	Nammal gorge	Not used
Tp5	Nammal gorge	Not used	Tp46	Nammal gorge	Not used
Tp6	Nammal gorge	Not used	Tp47	Nammal gorge	Not used
Tp7	Nammal gorge	Not used	Tp48	Nammal gorge	Not used
Tp8	Nammal gorge	Not used	Tp49	Nammal gorge	Not used
Tp9	Nammal gorge	Not used	Tp50	Nammal gorge	Not used
Tp10	Nammal gorge	Not used	Tp51	Nammal gorge	Not used
Tp11	Nammal gorge	Not used	Tp52	Nammal gorge	Not used
Tp12	Nammal gorge	Not used	En1	Nammal gorge	Not used
Tp13	Nammal gorge	Not used	ZTd1	Zinda Pir	Not used
Tp14	Nammal gorge	Not used	ZTd2	Zinda Pir	Not used
Tp15	Nammal gorge	Not used	ZTd3	Zinda Pir	Not used
Tp16	Nammal gorge	Not used	ZTd4	Zinda Pir	Not used
Tp17	Nammal gorge	Not used	ZTd5	Zinda Pir	Not used
Tp18	Nammal gorge	Not used	ZTd6	Zinda Pir	Not used
Tp19	Nammal gorge	Not used	ZTd7	Zinda Pir	Not used
Tp20	Nammal gorge	Not used	ZTd8	Zinda Pir	Not used
Tp21	Nammal gorge	Not used	ZTd9	Zinda Pir	Not used
Tp22	Nammal gorge	Not used	ZTd10	Zinda Pir	Not used
Tp23	Nammal gorge	Not used	ZTd11	Zinda Pir	Not used
Tp24	Nammal gorge	Not used	ZTd12	Zinda Pir	Not used
Tp25	Nammal gorge	Not used	ZTd13	Zinda Pir	Not used

Sample	Field section	Remarks	Sample	Field section	Remarks
ZTd14	Zinda Pir	Not used	ZTd42	Zinda Pir	Not used
ZTd15	Zinda Pir	Not used	ZTd43	Zinda Pir	Not used
ZTd16	Zinda Pir	Not used	ZTd44	Zinda Pir	Not used
ZTd17	Zinda Pir	Not used	ZTd45	Zinda Pir	Not used
ZTd18	Zinda Pir	Not used	ZTd46	Zinda Pir	Not used
ZTd19	Zinda Pir	Not used	ZTd47	Zinda Pir	Not used
ZTd20	Zinda Pir	Not used	ZTd48	Zinda Pir	Not used
ZTd21	Zinda Pir	Not used	ZTd49	Zinda Pir	Not used
ZTd22	Zinda Pir	Not used	ZTd50	Zinda Pir	Not used
ZTd23	Zinda Pir	Not used	Kps1	Rakhi Nala	Used
ZTd24	Zinda Pir	Not used	Td1	Rakhi Nala	Used
ZTd25	Zinda Pir	Not used	Td2	Rakhi Nala	Used
ZTd26	Zinda Pir	Not used	Td3	Rakhi Nala	Used
ZTd27	Zinda Pir	Not used	Td4	Rakhi Nala	Used
ZTd28	Zinda Pir	Not used	Td5	Rakhi Nala	Used
ZTd29	Zinda Pir	Not used	Td6	Rakhi Nala	Used
ZTd30	Zinda Pir	Not used	Td7	Rakhi Nala	Used
ZTd31	Zinda Pir	Not used	Td8	Rakhi Nala	Used
ZTd32	Zinda Pir	Not used	Td9	Rakhi Nala	Used
ZTd33	Zinda Pir	Not used	Td10	Rakhi Nala	Used
ZTd34	Zinda Pir	Not used	Td11	Rakhi Nala	Used
ZTd35	Zinda Pir	Not used	Td12	Rakhi Nala	Used
ZTd36	Zinda Pir	Not used	Td13	Rakhi Nala	Used
ZTd37	Zinda Pir	Not used	Td14	Rakhi Nala	Used
ZTd38	Zinda Pir	Not used	Td15	Rakhi Nala	Used
ZTd39	Zinda Pir	Not used	Td16	Rakhi Nala	Used
ZTd40	Zinda Pir	Not used	Td17	Rakhi Nala	Used
ZTd41	Zinda Pir	Not used	Td18	Rakhi Nala	Used

Sample	Field section	Remarks	Sample	Field section	Remarks
Td19	Rakhi Nala	Used	Td33	Rakhi Nala	Used for dinocysts and foraminifera
Td20	Rakhi Nala	Used	Td34	Rakhi Nala	Used for dinocysts and foraminifera
Td21	Rakhi Nala	Used	Td35	Rakhi Nala	Used for dinocysts and foraminifera
Td22	Rakhi Nala	Used	Td36	Rakhi Nala	Used for dinocysts and foraminifera
Td23	Rakhi Nala	Used	Td37	Rakhi Nala	Used for dinocysts and foraminifera
Td24	Rakhi Nala	Used	Td38	Rakhi Nala	Used for dinocysts and foraminifera
Td25	Rakhi Nala	Used	Td39	Rakhi Nala	Used for dinocysts and foraminifera
Td26	Rakhi Nala	Used	Td40	Rakhi Nala	Used for dinocysts and foraminifera
Td27	Rakhi Nala	Used	Td41	Rakhi Nala	Used for dinocysts and foraminifera
Td28	Rakhi Nala	Used	Td42	Rakhi Nala	Used for dinocysts and foraminifera
Td29	Rakhi Nala	Used	Td43	Rakhi Nala	Used for dinocysts and foraminifera
Td30	Rakhi Nala	Used for dinocysts and foraminifera	Td44	Rakhi Nala	Used for dinocysts and foraminifera
Td31	Rakhi Nala	Used for dinocysts and foraminifera	Td45	Rakhi Nala	Used for dinocysts and foraminifera
Td32	Rakhi Nala	Used for dinocysts and foraminifera	Td46	Rakhi Nala	Used for dinocysts and foraminifera

Sample	Field section	Remarks	Sample	Field section	Remarks
Td47	Rakhi Nala	Used for dinocysts and foraminifera	Td59	Rakhi Nala	Used
Td48	Rakhi Nala	Used for dinocysts and foraminifera	Td60	Rakhi Nala	Used
Td49	Rakhi Nala	Used for dinocysts and foraminifera			
Td50	Rakhi Nala	Used for dinocysts and foraminifera			
Td51	Rakhi Nala	Used			
Td52	Rakhi Nala	Used			
Td53	Rakhi Nala	Used			
Td54	Rakhi Nala	Used			
Td55	Rakhi Nala	Used			
Td56	Rakhi Nala	Used			
Td57	Rakhi Nala	Used			
Td58	Rakhi Nala	Used			